CHROMATOGRAPHIC METHODS OF ANALYSIS APPLIED TO COUMARINS AND CELL ORGANELLES

A thesis submitted for the degree of Ph.D.

By

Ciarán F. Duffy, B.Sc.

December 1999

School of Biotechnology

Dublin City University

Under the supervision of

Prof. Richard O'Kennedy

Twice Touched

A method passing, an idea living,
The details put into a line.
The thoughts too busy, nothing thinking,
A journey prepared detached, sublime.

Goodbyes and promises, you follow with me,
We take the road, to stop at the cross.
Too long to look, too long to think,
The final start and then be lost.

Stop and turn, a profound goodbye
The rush, the loss, the crying pain.
Not to look and then, to see it all
Never, always, different again

Deeply touched, I shake your hand,
A gentle nod, you shaked mine.
A chasm of sorrow, always carved,
To guide a tear with passing time.

You continued on, I couldn't move,
Confusion, loss, I had to leave.
You slowed and stopped to look and wave,
The road was blurred, felt, believed.

To remember is beauty, caught in tears,
To forget impossible, a desperate fear.

Brian R. Duffy
18 December 1994

DECLARATION

I hereby certify that the material, which I now submit for assessment on the programme of study leading to the award of Ph.D., is entirely my own work, and has not been taken from the work of others, save and to the extent that such work has been cited and acknowledged within the text of my work.

Signed: _____ Date: 30/3/00

ACKNOWLEDGEMENTS

The beginning of a Ph.D. starts not when in third level, but in your whole approach to life, education and your vision of the future. For my vision and outlook I thank my parents, Richard and Geraldine, for their constant love and support, the perfect balance to life, the perfect upbringing and for providing what, for me, were the best opportunities enabling me to achieve this goal. To Brian, Pamela and Gavan, the best family one could get.

To Professor Richard O'Kennedy for granting me the opportunity to embark on this road, the wonderful opportunities he supported me in during my four years of work which made my time so rich in experiences, learning both in and outside the lab, and for his patience, friendship and advice. To my friends in the lab; Tony, an encyclopaedia of knowledge and great source of humour, Declan, for his help and support in getting started, Gary, for conversations relating to the more sensitive side of life, to Brian, Deirdre, John, Mike, Paul and Stephen and Bernie.

For my time spent at the University of Alberta, I thank Prof. D. Jed Harrison for allowing me the opportunity to carry out the microchip based CE work. To Said Attiya for his never-ending patience and help with the microchips, Dr. Nicolas Bings, for help with microchip software and some great stories, Gregor Ocvirk, for mind bending conversations on the social and intellectual differences between Europeans and North Americans, Cameron Skinner, for a great ice fishing trip and Thompson Tang, who provided yet more advice on the chip and controlling software.

For my time working in the University of Minnesota I thank Prof. Edgar Arriaga for allowing me the opportunity to travel to the University of Minnesota, for his constant support, advice and never-ending patience, and most of all, friendship, of which I have come to value most highly. Prof. Sean C. Garrick, for his friendship and support during my stay in Minneapolis. For invaluable help in data analysis and discussion for chapter 7, I would also like to extend a special thank-you to Megan Wolgamot (U of M).

To Mick, for everything and more that one could ask of a best friend during undergrad and postgrad together, and also to his parents, Michael and Alice for their friendship and support, and to Sarah, a big thank-you. Thanks also to Gina.

Finally, there is one person who has been alongside me through my whole life, good times and bad, and who saw it almost through my own eyes, so close is our relationship. Words cannot convey my gratitude for the friendship, love and support that my brother Brian has given to me in my life so far, and for the help and advice throughout my Ph.D., for great times both gone and to come.

ABSTRACT

The clinical use of any drug requires a complete understanding of its biotransformation properties. The drug coumarin has for years been used in clinical applications. High performance liquid chromatography (HPLC) and capillary electrophoresis (CE) were applied to the study of coumarin metabolism, in particular the phase I and phase II metabolites, 7-hydroxycoumarin and 7-hydroxycoumarin glucuronide. Glucuronidation is the principal pathway for detoxification of many drugs and is catalysed by the enzyme uridine diphosphate glucuronyl transferase (UDPGT). Both chromatographic methods were applied to the analysis of the UDPGT activity in rabbit tissue samples. CE was applied to the study of β-glucuronidase activity for the same samples.

Microchip-based capillary electrophoresis with laser induced fluorescence detection was used to investigate antibody based detection methods for the anticoagulant, warfarin, and the pesticide parathion. A novel approach for the assay used an easily labelled drug-protein conjugate as tracer, rather than the conventional free drug with fluorescent tag. However, problems associated with heterogeneity of the antibody preparation and also with the labelled drug protein, did not allow complete resolution of antibody-drug-protein from free drug-protein to be effected.

Knowledge of what happens on a sub-cellular level is also required for a complete understanding of drug disposition. The use of capillary electrophoresis for the analysis of cell organelles was examined. Liposomes were chosen as a model as they could be tailored to mimic certain characteristics of different organelles (size, membrane composition), and are also manufactured industrially for use in drug delivery/targeting. The method developed provides critical information on size and membrane composition on a single liposome basis that can be used to monitor liposome preparations for use in clinical applications. Having successfully established this method, CE was then applied to the analysis of mitochondria, isolated from Chinese hamster ovary cells. Two specific organelle probes were used, i.e. nonyl acridine orange (NAO) for mitochondrial mass analysis, and rhodamine 123 (Rh123)

for membrane potential studies. NAO is a membrane specific probe and its uptake is independent on the energetic state of the mitochondria, binding to the cardiolipin content in a 2:1 ratio, while rhodamine 123 requires a membrane potential for its uptake. Measurement of fluorophore content of each individual mitochondrion gives information on membrane size and activity. A preliminary analysis of the mitochondrial proteome was carried out by capillary gel electrophoresis following the purification of protein from isolated mitochondria and labelling with a fluorescent tag.

ABBREVIATIONS

AAP	Acryloyl amino propanol
Ab	Antibody
Ag	Antigen
ATP	Adenosine triphosphate
APS	Adenosine-5-phosphosulphate
BSA	Bovine serum albumin
CE	Capillary electrophoresis
CGE	Capillary gel electrophoresis
CMC	Critical micelle concentration
DMSO	Dimethyl sulphoxide
DNA	Deoxyribonucleic acid
ER	Endoplasmic reticulum
FACS	Fluorescence activated cell sorter
FFE	Free flow electrophoresis
FITC	Flourescein isothiocyanate
FID	Flame ionisation detection
FTIR	Fourier transform infra-red
GC	Gas chromatography
GLC	Gas liquid chromatography
GSC	Gas solid chromatography
2HPAA	2-Hydroxyphenylacetic acid
7-HC	7-Hydroxycoumarin
7-HCG	7-Hydroxycoumarin glucuronide
7-HS	7-Hydroxycoumarin sulphate
cITP	Capillary isotachophoresis
cIEF	Capillary isoelectric focusing
JC-1	5,5',6,6'-tetrachloro-1,1',3,3' tetraethylbenzimidazolylcarbocyanine iodide

LIF	Laser-induced fluorescence
MECC	Micellar electrokinetic capillary chromatography
MMP	Mitochondrial membrane potential
MS	Mass spectrometry
NA	Numerical aperture
NAO	Nonyl acridine orange
NCI	National Cancer Institute
NMDA	N-methyl-D-aspartate
OA	Osteoarthritis
OHP	Outer Helmholtz Plane
PAPS	3'-Phosphoadenosine-5'-phosphosulphate
PAGE	Polyacrylamide gel electrophoresis
PBS	Phosphate-buffered saline
PC	Phosphatidyl choline
PEA	Phosphatidyl ethanolamine
PS	Phosphatidyl serine
PMT	Photomultiplier tube
PNS	Postnuclear supernatant
PUVA	Psoralen ultraviolet A
PSI	Pounds per square inch
ROS	Reactive oxygen species
Rh123	Rhodamine 123
mRNA	Messenger ribonucleic acid
SDS	Sodium dodecyl sulphate
SIC	Sample introduction channel
hSI	Human sterol isomerase
ST	Sulphotransferase
THF	Tetrahydrofuran
TMRM	Tetramethylrhodamine methylester perchlorate
TMRE	Tetramethylrhodamine ethylester perchlorate
UDP	Uridine diphosphate
UDPGT	Uridine diphosphate glucuronyl transferase

AWARDS/FELLOWSHIPS

Award Type: **Wood-Whelan Research Fellowship**

Awarding Body: International Union of Biochemistry and Molecular Biology.

Date: April 1999.

Award: Travel and living expenses during research carried out at the University of Minnesota.

Research area: Development of capillary electrophoresis methods for analysis of liposomes and cell organelles.

Award Type: **Travel bursary.**

Awarding Body: Royal Irish Academy

Date: February 1998.

Award: Travel bursary to the University of Alberta, Edmonton, Alberta, Canada.

Research area: Micro-chip capillary electrophoresis-based immunoassays.

PUBLICATIONS

Duffy, Ciarán F., O'Kennedy, Richard. (1998).

Determination of 7-hydroxycoumarin and its glucuronide and sulphate conjugates in liver slice incubates by capillary zone electrophoresis.

Journal of Pharmaceutical and Biomedical Analysis, ***17:*** *1279-1284.*

Bogan, Declan P., **Duffy, Ciarán F.**, O'Kennedy, Richard. (1997).

In vitro glucuronidation of 7-hydroxycoumarin and determination of 7-hydroxycoumarin and 7-hydroxycoumarin glucuronide by capillary electrophoresis.

Journal of Chromatography A, 772: 321-326.

Duffy, C. F., Bogan, D. P., O'Kennedy, R. (1997)

Determination by HPLC of the UDP-glucuronyl transferase activity for 7-hydroxycoumarin in rabbit tissues samples.

Journal of Liquid Chromatography and Related Technologies, ***20(2):*** *217-226.*

Bogan, Declan P., Keating, Gary J., Reinartz, Heiko, **Duffy, Ciarán F.**, Smyth, Malcom R., O'Kennedy, Richard and Thornes, R. Douglas. (1997)

In "Coumarins: Biology, Applications and Mode of action". Edited by O'Kennedy, R., Thornes, R.D., John Wiley and Sons Ltd., Chichester, Sussex, England, *pp 267-302.*

Bogan, D. P., Cooke, D., **Duffy, C. F.**, Byrden, T., O'Kenedy, R. (1996)

Studies on the analysis, metabolism and mode of action of coumarin.

Abstract for the *Biochemical Society Meeting, No. 658, Liverpool, 59.*

Duffy, C. F., O'Kennedy R. (1997)

Review on *Preparative Gel Chromatography on Sephadex LH-20.* Hans Henke. Translated by Anthony J. Rackstraw, Chromatographic Methods Series. Pp. xx + 618. Huthig 1995.

Analyst, 122, 20N.

PRESENTATIONS

Ciarán Duffy, Hongjun Shu*, Edgar Arriaga.

Functional classification of proteins using organelle analysers.

16th American Peptide Symposium, Minneapolis, MN, USA, July 4th – 9th, 1999

Ciarán F. Duffy,* Paul. Dillon, Said Attiya, D. Jed Harrison, Richard O'Kennedy.

Microchip Capillary Electrophoresis – Development of an immunoassay for Parathion.

Biochemical Society Meeting, Dublin City University, Glasnevin, Dublin 9, September 9 –12, 1998.

Bogan, D. P., **Duffy, C. F.***, and O'Kennedy, R.

In vitro glucuronidation of 7-hydroxycoumarin and determination of 7-hydroxycoumarin and 7-hydroxycoumarin glucuronide by capillary electrophoresis.

Tenth International Symposium on Capillary Electrophoresis and Isotachophoresis, Prague, Czech Republic, September 17 - 20, 1996.

Bogan, D. P., Cooke, D., **Duffy, C. F.**, Bryden, T. and O'Kennedy, R.*

Studies on the analysis, metabolism and mode of action of coumarins

The Biochemical Society Meeting No. 685, University of Liverpool, April 16-19, 1996.

CONTENTS

Declaration ii

Acknowledgements iii

Abstract iv

Abbreviations vi

Awards/Fellowships vii

Publications ix

Presentations xi

1. Introduction

1.1 Chromatographic analysis in biotechnology 2

1.2 Coumarins and analysis 4

1.2.1 Coumarins 4

1.2.2 Occurrence 4

1.2.3 Human exposure 6

1.2.4 Metabolism of coumarin 6

1.2.4.1 Glucuronidation of coumarins 7

1.2.4.2 Sulphation of coumarins 7

1.2.4.3 Deconjugation of coumarins 8

1.2.5 Clinical applications of coumarins 9

1.2.6 Toxicology 10

1.2.7 Coumarin analysis 11

1.2.7.1 Thin layer chromatography 11

1.2.7.2 High performance liquid chromatography 12

1.2.7.3 Gas chromatography 16

1.2.7.4 Voltametric and polarographic methods 17

1.2.7.5 Capillary electrophoresis 18

1.3 Chip-based microcolumn separation systems 19

1.3.1 Immunoassays on chip 21

1.4 Organelles and chromatographic analysis 21
1.4.1 Analysis of cell organelles 22
1.4.1.1 Gradients 22
1.4.1.2 Immunoisolation 23
1.4.1.3 Free flow electrophoresis 24
1.4.1.4 Flow cytometry and organelle analysis 25
1.4.1.5 Microscopy 27
1.4.2 Limitations involved in analysis of whole cells and organelles 28
1.4.3 Proteomics 29
1.4.3.1 2-D Gel electrophoresis 31

2. Materials and Methods

2.1 Materials 34
2.2 Equipment 36
2.3 Methods 38
2.3.1 General methods 38
2.3.1.1 Bicinchoninic acid (BCA) assay 38
2.3.1.2 Preparation of buffers for capillary electrophoresis 38
2.3.1.3 Preparation of mobile phases for HPLC 39
2.3.2 Determination by HPLC of the UDP-Glucuronyl transferase activity for 7-hydroxycoumarin in rabbit tissue samples 40
2.3.2.1 Tissue preparation 40
2.3.2.2 Preparation of standards for HPLC UDPGT assay 41
2.3.2.3 HPLC separation 41
2.3.3 In vitro glucuronidation of 7-hydroxycoumarin and determination of 7-hydroxycoumarin and 7-hydroxycoumarin glucuronide by capillary electrophoresis 42
2.3.3.1 Uridine diphosphate glucuronyl transferase assay 42
2.3.3.2 β-Glucuronidase assay 42
2.3.3.3 Reaction solution for β-Glucuronidase activity 43
2.3.3.4 Controls 43
2.3.3.5 Standard curve preparation 44
2.3.3.6 CE separation 45
2.3.4 Determination of 7-hydroxycoumarin and its glucuronide and sulphate conjugates by capillary zone electrophoresis 46
2.3.4.1 Synthesis of 7-hydroxycoumarin sulphate 46
2.3.4.2 NMR analysis of 7-hydroxycoumarin sulphate 46
2.3.4.3 IR analysis of 7-hydroxycoumarin sulphate 46
2.3.4.4 Liver slice preparation and incubation 47

2.3.4.5 Preparation of Krebs-Hanseleit buffer 47
2.3.4.6 Preparation of standards 48
2.3.4.7 CE separation 48
2.3.5 Microchip capillary electrophoresis – Immunoassays for warfarin and parathion .. 49
2.3.5.1 Confirmation of antibody reactivity 49
2.3.5.2 Fluorescein isothiocyanate (FITC) labelling of anti-warfarin and anti-parathion antibodies 49
2.3.5.3 Affinity purification of FITC-labelled antibodies 50
2.3.5.4 Capillary electrophoresis analysis of FITC-labelled antibodies 50
2.3.5.5 Labelling of BSA conjugates 50
2.3.5.6 Microchip immunoassay 51
2.3.6 Single liposome analysis using CE with post column LIF 52
2.3.6.1 Preparation of liposomes 52
2.3.6.2 Grignard coating of capillaries for CE analysis 52
2.3.6.3 CE-LIF analysis of liposomes 54
2.3.7 Mitochondrial analysis using CE-LIF 55
2.3.7.1 Labelling of mitochondria in whole cells 55
2.3.7.2 Fluorescent microscopy analysis of stained cells 55
2.3.7.3 Isolation of mitochondria from Chinese hamster ovary cells 55
2.3.7.4 Differential gradient ultracentrifugation 56
2.3.7.5 Analysis of mitochondria by CE 56
2.3.8 Mitochondrial protein analysis 56
2.3.8.1 3,(2-furoyl) quinoline-2-carboxaldehyde FQ-labelling of molecular weight markers and protein samples 56
2.3.8.2 Isolation of mitochondria from Chinese Hamster Ovary Cells 57
2.3.8.3 Purification of protein from mitochondria 57
2.3.8.4 Capillary gel electrophoresis of mitochondrial protein 57

3. High Performance Liquid Chromatography Applied to the Analysis of Coumarin Metabolism

3.1 Introduction 59
3.1.1 Instrumentation 59
3.1.1.1 Mobile phase delivery system 60
3.1.1.2 Sample injection 61
3.1.1.3 Separation column 61
3.1.1.4 Detection 61
3.1.2 Optimisation of column performance 62
3.1.2.1 Temperature effects 62

3.1.2.2 Viscosity 62
3.1.2.3 Extra column band broadening 63
3.1.3 Solvent programming 63
3.1.4 Reverse phase chromatography 63
3.1.4.1 Mechanism of reverse phase chromatography 65
3.2 Determination by reverse-phase HPLC of the UDP-glucuronyl transferase activity for 7-hydroxycoumarin in rabbit tissue samples 66
3.2.1 Coumarin metabolism 66
3.2.2 Sample preparation 66
3.2.3 Development of HPLC separation 67
3.2.3.1 Separation column 67
3.2.3.2 Mobile phase and gradient profile 67
3.2.3.3 Detection 68
3.2.4 Glucuronidation of 7-Hydroxycoumarin 69
3.2.5 Analysis of results 70
3.2.5.1 Rate of reaction for each organ 70
3.3 Discussion 73

4. Capillary Electrophoresis applied to the Analysis of Coumarins

4.1 Introduction 75
4.1.1 Instrumentation 76
4.1.1.1 Capillaries 77
4.1.1.2 Injection 77
4.1.1.3 Detection 77
4.1.2 Electroosmotic flow in capillary electrophoresis 78
4.1.3 Control of electroosmotic flow 80
4.1.3.1 Buffer changes and additives 80
4.1.3.2 Adsorbed coatings 81
4.1.3.3 Chemically bonded phases 81
4.1.4 Other modes of capillary electrophoresis 82
4.1.4.1 Micellar electrokinetic chromatography 82
4.1.4.2 Capillary gel electrophoresis 82
4.1.4.3 Capillary isoelectric focusing 83
4.1.4.4 Capillary isotachophoresis 84
4.2 In vitro glucuronidation of 7-hydroxycoumarin and determination of 7-hydroxycoumarin and 7-hydroxycoumarin-glucuronide by capillary electrophoresis 85
4.2.1 Coumarin metabolism 85
4.2.2 Sample preparation 85

4.2.3 Method development 85
4.2.3.1 Capillaries 85
4.2.3.2 Buffers 86
4.2.3.3 Detection 86
4.2.4 UDPGT assay results 87
4.2.5 β-Glucuronidase assay results 90
4.2.5.1 β-Glucuronidase activity calculations 91
4.3 Determination of 7-hydroxycoumarin and its glucuronide and sulphate conjugates for liver slice incubates by capillary zone electrophoresis 94
4.3.1 Synthesis of 7-hydroxycoumarin 94
4.3.1.1 NMR analysis 94
4.3.1.2 IR analysis 94
4.3.2 Sample preparation 95
4.3.2.1 Tissue slicer fabrication 95
4.3.2.2 Krebs Hanseleit buffer 99
4.3.3 CE separation 99
4.3.4 Results 99
4.3.5 Inter- and Intra-assay studies 102
4.3.5.1 Intra-assay performance 102
4.3.5.2 Inter-assay performance 103
4.4 Discussion 105

5. Microchip Capillary Electrophoresis – Development of Immunoassays for Warfarin and Parathion

5.1 Introduction 107
5.1.1 Microchip-based capillary electrophoresis 107
5.1.1.1 Sample injection on planar chips 107
5.1.1.2 Electrophoretic separations 109
5.1.2 Materials for microsystems 109
5.1.3 Microfabrication techniques 110
5.1.3.1 Photolithography 110
5.1.3.2 Alternative microfabrication techniques 111
5.1.4 Micro-chip CE and Immunoassays 111
5.1.4.1 Immunoassays – a brief introduction 111
5.1.4.2 Immunoassays using CE 113
5.1.4.3 Special issues for immunoassays by CE 114
5.2 Development of an immunoassay for Warfarin and Parathion 117
5.2.1 Materials for microchip manufacture 117

5.2.2 Device fabrication 117
5.2.3 Microchip station control and layout 119
5.2.4 Layout of chip station 120
5.2.5 Development of separation conditions 121
5.2.5.1 Conventional CE-LIF analysis 121
5.2.5.2 Microchip CE 121
5.2.6 Checking antibody activity 122
5.2.7 CE analysis with UV detection 125
5.2.8 Labelling and analysis of antibody 128
5.2.8.1 Conventional CE-LIF analysis 128
5.2.8.2 Micro-chip analysis of labelled antibodies 129
5.2.9 Development of immunoassay 130
5.2.9.1 Unlabelled BSA-conjugate as antigen 132
5.2.10 Labelling of BSA-conjugates with FITC 133
5.2.11 Micro-chip analysis 133
5.2.11.1 FITC BSA-Warfarin conjugate 133
5.2.11.2 FITC BSA-Parathion conjugate 134
5.3 Discussion 136

6. Analysis of Liposomes using CE with Post Column LIF Detection

6.1 Introduction 139
6.1.1 Liposomes as models for organelle analysis 141
6.1.1.1 Liposome preparation 141
6.1.2 Capillary electrophoresis instrument 144
6.1.2.1 Laser 147
6.1.2.2 Laser focusing 147
6.1.2.3 Spectral filters 147
6.1.2.4 Instrument construction and alignment 148
6.1.2.5 Collection optics 149
6.1.2.6 Instrument alignment 149
6.2 Single liposome analysis by capillary electrophoresis with laser-induced fluorescence detection 151
6.2.1 Detector characterisation and optimisation 151
6.2.1.1 Bead experiments to determine detector variation 152
6.2.2 Analysis of liposomes 154
6.2.3 Analysis of results 156
6.3 Discussion 161

7. Analysis of Mitochondria using CE with Post Column LIF Detection

7.1 Introduction 164
7.1.1 The mitochondrion 164
7.1.2 Origin of mitochondria 164
7.1.3 Function of mitochondria 165
7.1.4 Mitochondrial genetics 165
7.1.5 Intracellular distribution 166
7.1.6 Mitochondrial life cycle 166
7.1.7 Mitochondria and disease 167
7.2 Analysis of mitochondria by capillary electrophoresis with post column laser-induced detection 168
7.2.1 Analysis of whole cells by fluorescent microscopy 168
7.2.1.1 Nonyl acridine orange staining of Chinese hamster ovary cells 168
7.2.1.2 Rhodamine 123 and 5,5',6,6'-tetrachloro-1,1',3,3'-tetraethylbenzimidazolylcarbocyanine iodide (JC-1) staining of Chinese hamster ovary cells 169
7.2.2 Analysis of whole cells by capillary electrophoresis 173
7.2.3 Analysis of isolated mitochondria by capillary electrophoresis 174
7.2.3.1 Development of procedure for isolation of mitochondria 175
7.2.3.2 Mass measurements using Nonyl Acridine Orange 176
7.2.3.3 Analysis of results from uncoated capillaries 178
7.2.3.4 Analysis of mitochondrial activity using Rhodamine 123 180
7.2.4 Comparison of different separation voltages for analysis of mitochondria 180
7.2.5 Analysis of sample injection reproducibility 183
7.2.6 Analysis of mitochondria from different fractions following ultracentrifugation 189
7.2.7 Analysis of stability of prepared fractions 191
7.3 Mitochondrial proteome analysis using capillary electrophoresis 194
7.3.1 Use of coated capillaries for protein analysis 194
7.3.1.1 Analysis of molecular weight markers 194
7.3.1.2 CE analysis of mitochondrial protein extract using coated capillaries 196
7.3.2 Capillary gel electrophoresis 198
7.3.2.1 Analysis of molecular weight markers 198
7.3.2.2 Capillary gel electrophoresis of mitochondrial protein extract 202
7.4 Discussion 204

8. Conclusions 206

9. References 210

10. **Appendix** **235**

1 INTRODUCTION

1.1 Chromatographic analysis in biotechnology

The last half of this century has seen an exponential growth in the development of technology, from landing on the moon and putting robots on mars to cloning the human genome and nano-technology. In the area of biotechnology, a wide diversity of techniques is being developed to help researchers probe into ever smaller and intricate areas.

In order to make these new discoveries the instrumentation used must also advance. At present there exists a huge arsenal of equipment for scientists to investigate new ideas. Instruments are applied to many applications as researchers look for better ways to investigate and understand the life sciences. An example is chromatography. Since its beginnings it has branched into many areas, including thin layer chromatography (TLC), high performance chromatography (HPLC), gas chromatography (GC), and capillary electrophoresis (CE). With attention now focusing on "Total Chemical Analysis Systems" – devices capable of performing all handling and analysis steps all in one go (van den Berg and Lammerick, 1998) the drive to a universal instrument capable of analysis seems set to unfold as analytical scientists search to reduce the size and complexity of current methods of analysis. Perhaps a single instrument with interchangeable chips/compartments for different applications will be the way in the future.

The work presented in this thesis examines chromatographic analysis in biotechnology – high performance chromatography (HPLC) (chapter 3), and capillary electrophoresis (CE) (chapters 4, 5, 6 and 7). The technique of CE has proven to be more adaptable and is examined in different formats. These include microchip with laser-induced fluorescence (LIF) detection (chapter 5) and different conventional narrow bore capillary formats, i.e. zone electrophoresis with on-column UV-Vis/LIF detection and zone and gel electrophoresis with post column LIF detection. While HPLC is one of the most common chromatographic method of analysis in use today, it has proven not to be as flexible as CE. Micro LC in both open tubular and packed formats (Ishii, 1978; Hirata, 1979) showed promise, but technical difficulties in the design of high pressure-low volume solvent delivery systems and in the operational challenges in handling the severe pressure drop in packed column chromatography deterred commercial development. To examine if CE could be applied across a broad spectrum, two models were chosen, the first, analysis of the metabolites of the drug coumarin, providing a look at CE in the analysis of small molecules, and the second, analysis of cellular organelles, which would present CE with the challenge of large biological

particles. For micro CE studies it was necessary to devise a format that could be applied on-chip. For this reason and also due to the limitations in detection schemes available, an immunoassay for a member of the coumarin family, warfarin, and the insecticide, parathion was investigated. As the analysis of cellular organelles was a new area for CE, it was necessary to examine the validity of the method with the use of liposomes, membrane-bound vesicles, as models for organelles, and in particular for the analysis of mitochondria.

Section 1.2 investigates the coumarins and gives a brief background on the compound including its occurrence, clinical applications and toxicology, before examining some of the different methods used for its identification and analysis. While there are no reported applications of analysis of coumarins using microchip technology, section 1.3 gives an introduction to microchip technology and introduces some of the work already carried out. Section 1.4 examines cellular organelles, giving an outline of each and the various methods of analysis applied including gradients, flow cytometry, and free flow electrophoresis. For organelle analysis by CE the mitochondrion was chosen, as it has attracted a lot of attention for its role in a number of diseases (section 7.1.6) and there are no reported methods for its analysis using CE to date. For this reason it would also be an excellent candidate for analysis. In order to give a more complete analysis, a brief look at a new area of biotechnology and the use of CE was investigated – proteomics - with the analysis of the mitochondrial proteome by CE, introduced in section 1.4.3.

1.2 Coumarins and analysis

1.2.1 Coumarin

Coumarin, a white crystalline solid, mol. wt. 146.15, mp 68-70^{0}C, bp 297-299^{0}C, belongs to a group of compounds known as the benzopyrones, all of which contain the same backbone structure, consisting of a benzene ring joined to a pyrone – a six membered heterocyclic ring containing one oxygen atom and five sp^2-hybridised carbons. Coumarin is freely soluble in ethanol, chloroform, diethyl ether and oils and is slightly soluble in water.

The coumarin family is large with two main branches, the benzopyrones, containing the α-pyrone group, and the flavanoids, containing the γ-pyrone group. Figure 1.1 shows the structure of coumarin, one of its primary metabolites, 7-hydroxycoumarin, and secondary metabolites 7-hydroxycoumarin glucuronide and 7-hydroxycoumarin sulphate along with the names of the catalysing enzymes for the sequence of metabolic reactions examined in chapters 3 and 4.

1.2.2 Occurrence

Coumarins are found in many dicotyledonous plant families. Many monocotyledonous plants are also known to contain large amounts of coumarins (Weinmann, 1997). The compounds are found in various parts of plants including the trunk, stem, foliage, flowers, fruits and seeds and can be isolated by extraction with suitable solvents. Coumarin is also found in various fruits, bilberry, cloudberry, and in green tea (Lake, 1999). The first isolation of coumarins was from Tonka beans in 1822, and the first published record of its synthesis was in 1868. The presence of coumarin in various plants seems to be linked with the ability to inhibit the growth and sporulation of fungal pathogens and other ailments (Weinmann, 1997).

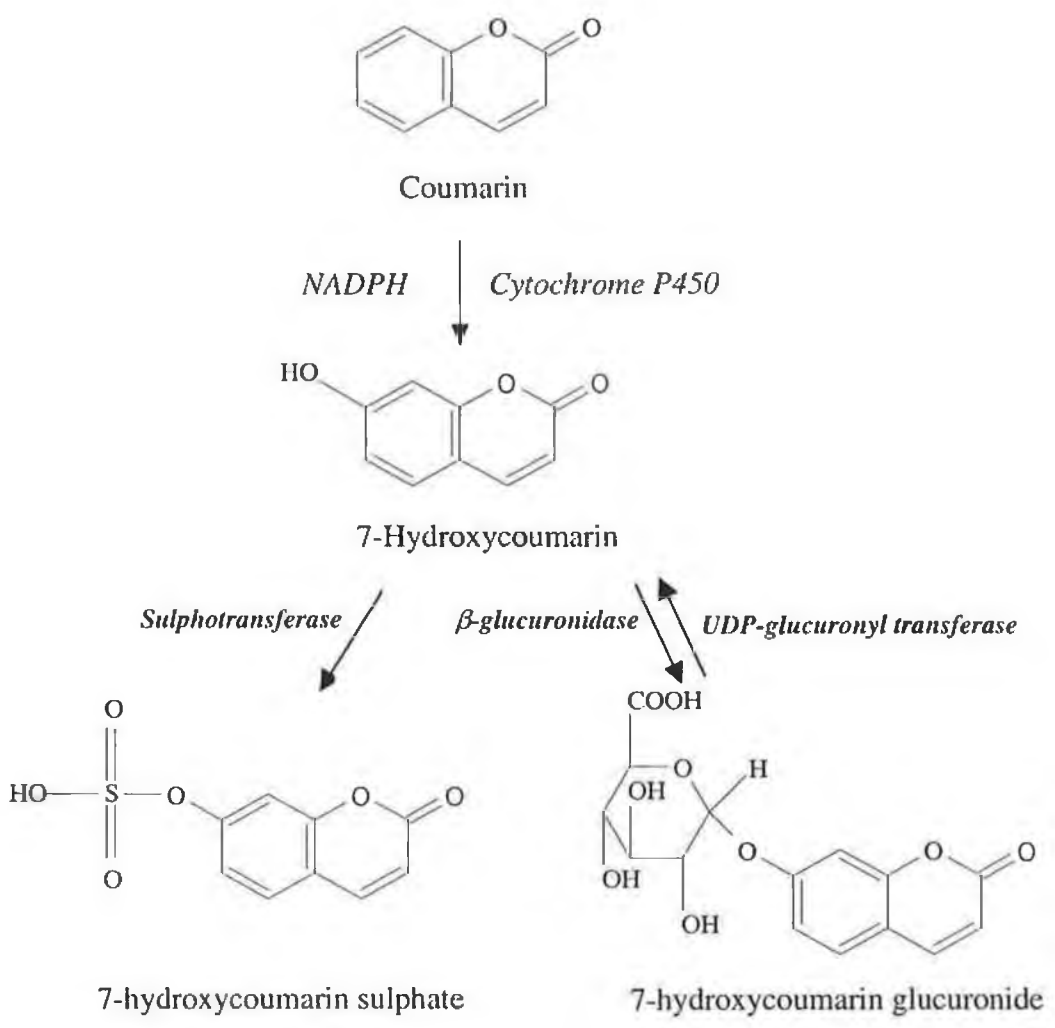

Figure 1.1 *Reaction scheme showing the structures of the parent drug coumarin, 7-hydroxycoumarin, 7-hydroxycoumarin glucuronide, 7-hydroxycoumarin sulphate and the production of 7-hydroxycoumarin glucuronide by uridine diphosphate glucuronyl transferase enzymes and 7-hydroxycoumarin sulphate by sulphotransferase enzymes.*

1.2.3 Human exposure

Coumarin is listed as an "active principle" by the Council of Europe and there are maximum allowed concentrations for in foodstuffs, 2 mg/kg for food and non alcoholic beverages and 10 mg/kg for alcoholic beverages (Annex II of European Directive, 88/388/EEC). Lake (1999) in a review, details areas where human exposure to coumarin is increased. Examples include exposure to coumarin from various foods and beverages, where it can be assumed that over a long period of time, less than 5% of solid food would be flavoured with cinnamon or other ingredients capable of imparting the 2 mg/kg maximum concentration of coumarin. This would take the daily dose of coumarin to around 1.235 mg/day. Lake also lists areas of coumarin exposure from fragrant cosmetic products containing coumarins (shampoos, shower gels, antiperspirant and bath products) where the dermal absorption of coumarin in human subjects has been shown to be 60%. This value was obtained in a simulated study where 2 mg of coumarin, in 70% aqueous solution, was applied to a 100 cm^2 skin area for 6 hours (Huntingdon Life Sciences, 1996).

1.2.4 Metabolism of coumarin

The work presented in this thesis is not intended to be an investigation into the metabolism of coumarin and while chapters 3 and 4 examine the metabolism of 7-hydroxycoumarin in the various tissues of New Zealand White rabbit, the focus is on the chromatographic methods of analysis used. For a more detailed review on coumarin metabolism the reader is referred to Pelkonen *et al.* (1997) and Egan *et al.* (1990). Coumarin and its derivatives are metabolised in a number of ways, all of which are influenced by the substrate, species, and the presence of other drugs (Casley-Smith and Casley-Smith, 1986). In humans the major metabolic pathway is via 7-hydroxylation, catalysed by the P450 enzyme CYP2A6. Bogan *et al.* (1996b) looked at the interspecies differences in coumarin metabolism, showing that human liver microsomes have the highest level of 7-hydroxylation, with rat, pig and dog having undetectable levels. The second major metabolic pathway in man is via 3-hydroxylation. Only between 1 and 6% of an oral dose is excreted in this form in man, compared to 80% via 7-hydroxylation (Casley-Smith and Casley-Smith, 1986). Figure 1.1 shows the sequence of reactions studied in chapters 3 and 4 following on from 7-hydroxylation, with the formation of the glucuronide

via the enzyme uridine diphosphate glucuronyl transferase (UDPGT) and the sulphate conjugate via sulphotransferase. While glucuronidation is known to be the major pathway for 7-hydroxycoumarin in humans (Egan *et al.,* 1990), sulphation is reported to occur in the perfused rat liver as a high affinity, low capacity pathway (Zimmerman *et al.,* 1991).

1.2.4.1 Glucuronidation of coumarins

Glucuronidation has its primary role as a major detoxification pathway for drugs in vertebrates and accounts for most of the detoxified material in bile and urine (Dutton, 1991). The process is carried out by a family of enzymes known as Uridine Diphoshate Glucuronyltransferases (UDPGTs) and involves the coupling of the sugar acid, D-glucuronic acid, to the compound in question. In the case of the studies carried out in chapters 3 and 4 this compound is 7-hydroxycoumarin (Fig 1.1). It is well established that the liver is the major site for glucuronidation, and also the major source of D-glucuronic acid (Dutton, 1991). Studies carried out on rabbit tissues in this thesis, by both high performance liquid chromatography and capillary electrophoresis, also confirm this to be the case. The next major site was found to be the kidney. Within the tissues, the UDTGP enzymes are located primarily in the endoplasmic reticulum of both hepatic and extra-hepatic tissues (Roy Chowdhury *et al.,* 1985).

1.2.4.2 Sulphation of coumarins

Sulphate conjugation is another important step in the biotransformation of many drugs and other compounds. Although the process of sulphation is not as clearly understood as glucuronidation, it is carried out by the sulphotransferase (ST) enzymes (Weinshilboum, 1994). Like glucuronidation, sulphation increases the water solubility of most compounds and, therefore, their excretion, as well as causing a general decrease in biological activity. However, for certain compounds sulphate conjugation is required for activation of enzymes (Weinshilboum, 1994). For coumarin, Figure 1.1 shows the metabolic pathway with the substrate 7-hydroxycoumarin being sulphated at the same position as for glucuronidation. A

CE method for analysis of the sulphation of 7-hydroxycoumarin using liver slice incubates is developed in chapter 4. The co-substrate for the reaction is 3'-phosphoadenosine-5'-phosphosulphate (PAPS) which is synthesised from inorganic sulphate and adenosine triphosphate (ATP). For generation of the sulphate conjugate of 7-hydroxycoumarin, magnesium sulphate was used as the source of inorganic sulphate. The process involves two enzymatic steps with sulphate adenylyltransferase catalysing the formation of adenosine-5-phospho sulphate (APS) from ATP and inorganic sulphate, and adenylylsulphate kinase catalysing the formation of PAPS from APS and a second molecule of ATP.

1.2.4.3 De-conjugation of glucuronide and sulphate conjugates

Conjugation of drugs in liver and extrahepatic tissues is a complicated process involving the availability of substrates (D-glucuronic acid and PAPS) (Reinke *et al.,* 1986), the uptake of substances across cellular membranes and the formation and release of conjugated products (DeVries *et al.,* 1986). Generated conjugates are involved in "futile cycling" via specific transferases and hydrolases located within the same or adjacent subcellular compartments. The process is termed "futile" as conjugates may undergo successive cycles of synthesis to the conjugate and hydrolysis back to the free metabolite. This cycling is potentially an important site of regulation since factors affecting the activity of a transferase or associated hydrolase will ultimately affect the net conjugate production and utilisation in cells (Kauffmann, 1994). Following conjugation by UDPGT enzymes, glucuronides are hydrolysed by an enzyme known as β-glucuronidase (EC 3.2.1.21, β-D-glucuronide glucuronohydrolase). The enzyme is a glycoprotein, consisting of several complexes, M_1 to M_4 (Dutton, 1991). Glucuronidase is an unusual enzyme in that 30 – 50% of total liver enzyme is actually located in the microsomal fraction (Brown *et al.,* 1987). Studies have reported the liver and kidney to have relatively high concentrations of ER glucuronidase (Lusis and Paigen, 1977), while no glucuronidase complex has been detected in spleen, brain, heart or fat (Swank *et al.,* 1994). Chapter 4 examines various rabbit tissues for β-glucuronidase activity towards 7-hydroxycoumarin-glucuronide.

1.2.5 Clinical applications of coumarins

The introduction of coumarin for clinical use required testing of its biopharmaceutical properties. Pharmacokinetic data in humans indicates a wide-spread distribution within the body (Ritschel, 1981). Intestinal and renal adsorption are not influenced by varying gastrointestinal or urinary pH because coumarin is non-charged and 7-hydroxycoumarin has a pK_a of 7.77. The extent of protein binding is well below the critical value of >80% (being 35% and 47% for coumarin and 7-hydroxycoumarin, respectively). In animal and human organisms, central effects, for example, sedative, hypnotic and antipyretic have been shown (Kitagawa, 1963). The various effects of coumarin and derivatives have been well documented over the past few years, and a detailed list of the range of physiological effects, both in plants and animals can be found in a number of areas (Saoine, 1964; Nakajima and Kawazu, 1980; Egan *et al.,* 1990).

The interest in coumarin as an investigator drug is still valid, though the parent drug has being submitted to a thorough derivatisation and screening of the derivatives between 1950 and 1970. Except for the group of anticoagulants derived from 4-hydroxycoumarin, other coumarin derivatives such as the antibiotic novobiocin (complex coumarin from two *Streptomyces* species) or hymecromen, a spasmolytic agent for bilious affections and complaints, did not attain clinical use or a true medical importance. The furanocoumarins are playing a role in the treatment or psoriasis and other dermatological diseases (PUVA – psoralen ultraviolet A range therapy).

Coumarin and 7-hydroxycoumarin have been patented in Australia (Casely-Smith and Casely-Smith, 1986). Patents cover applications related to the resolution of high-protein oedemas. Promising findings in more than 700 patients suffering from renal cell carcinoma have been available for at least eight years. Cancers of the prostate were treated after primary therapy by tumour resection and/or nephrectomy with varying doses of coumarin or 7-hydroxycoumarin (sustained release tablets) over different periods of time or until regression of the disease (Weinmann, 1997). Yamada *et al.* (1999) reported on the inhibition of matrix metalloproteinases (MMP) in cartilage explants by esculetin (6,7-dihydroxycoumarin). Studies were carried out on rabbit articular cartilage explants. Also investigated were the effects of oral administration of its prodrug, CPA-926, which was reported to reduce the effects of induced osteoarthritis (OA) at doses of 200 mg/kg and 400 mg/kg. The report

concluded that esculetin inhibits matrix degradation in rabbit joint cartilage explants through suppression of MMP systhesis, secretion or activity, and that prophylactic administration of its prodrug, CPA-926, appears to provide some protection against cartilage destruction in a short term rabbit experimental OA model.

1.2.6 Toxicology

Coumarin exhibits a very species-dependent metabolism (Ritschel, 1981) and, therefore, the procedure of extrapolation from animal studies to the human situation requires great care. A number of studies have examined the acute, chronic and carcinogenic effects of coumarin in the rat and mouse. These studies, carried out at the maximally tolerated doses, revealed that a threshold does exist for coumarin toxicity, and below these levels, such effects are not observed. In the case of various rat strains the acute oral LD_{50} was reported to range from 290mg to 680mg/kg (Egan *et al.,* 1990). Effects observed in the rat include increase in relative liver weight, and changes in various hepatic biochemical parameters, and reduction of microsomal glucose-6-phosphate activity, depending on the dose. Observations made on liver sections of coumarin-treated rats dependent on dose magnitude and duration of treatment, include necrosis, apoptosis, vaccuolation, and fatty acid and bile duct hyperplasia (Lake, 1999). In plant cells, coumarin can cause chromosome and DNA breakage (Grigg, 1977). It also exhibits antimutagenic effects against genotoxicity generated by 4-nitro-quinoline-1-oxide or UV radiation in *E. coli* (Ohta *et al.,* 1983).

Due to differences in metabolism between the species, some alternative methods have been tried to extrapolate from animal to human. These include the use of liver preparations (cryopreserved hepatocytes, liver microsomes of precision cut liver slices), liver, lung and kidney slices (De Kanter *et al.,* 1999) and have shown promising results. Specimens of human liver have been tested and compared with preparations from monkey, rat, mouse, hamster, guinea pig and other mammals. However, the great differences in the patterns of coumarin metabolites in humans and animals clearly indicate the polymorphism of the metabolising enzymes activity (Pearce *et al.,* 1992).

1.2.7 Coumarin analysis

Since its first isolation in 1822, coumarin and its many derivatives have been the subject of many rigorous tests and analysis. To date, many methods of analysis have been developed. High performance liquid chromatography has seen many applications in both identification and studies of metabolism and gas chromatography coupled to mass spectrometry has been used to identify coumarin structures following separation. More traditional methods like thin layer chromatography have also been used as quantitative methods in coumarin analysis. For a detailed review on the analysis of coumarins the reader is referred to Bogan *et al.* (1997). The following section reviews some of these methods, concentrating mostly on chromatographic methods, and the results, following analysis.

1.2.7.1 Thin layer chromatography

Separation and identification of coumarins: A thin layer chromatographic method was developed to determine the authenticity of natural vanilla extracts (Poole *et al.*, 1993). The method looked for the presence of compounds used in the production of counterfeit vanilla products. These compounds include coumarin, piperonal and ethyl vanillin. Separations were carried out on Whatman HP-K high performance silica gel plates. The solvents found to be most suitable for the separation were chloroform - ethyl acetate – propan-1-ol, 92 + 2 + 2 v/v). The presence of coumarin was confirmed by a second solvent system consisting of a $1 \times 10 + 1 \times 12$ minute development with hexane-methyl *t*-butyl ether (4 + 1 v/v) on the silica gel plates. Selective visualisation was achieved by postchromatographic application of 2,4-dinitrophenylhydrazine reagent. The plate was dipped into this solution for about 5 seconds and allowed to drain on a paper towel. The reaction was virtually instantaneous and the plate was scanned a few minutes after application of the reagent. Harmala *et al.* (1992) examined the retention behaviour of fourteen closely related coumarins in normal phase thin layer chromatography and high performance liquid chromatography. TLC separations were carried out on alufoil, silica gel 60 F_{254} TLC plates (average particle size - 10μm). Ethyl acetate ($S_{T\ (solvent\ strength)} = 4.4$), chloroform ($S_T = 4.1$), and tetrahydrofuran ($S_T = 4.0$) in hexane ($S_T = 0$) gave the best separation of the fourteen

coumarin compounds. The migration distances and solvent fronts were measured with a densitometer at 320 nm. The report concluded that a change in solvent strength caused a different response in TLC than in HPLC, although it is possible to evaluate the effect on HPLC of solvent change from TLC runs. Overall the selectivity in HPLC can be described by experiments in TLC, however, when transferring the mobile phase, the fact that the elution process is different in TLC and HPLC must be taken into account.

Metabolic studies: Cholerton *et al.* (1992) compared the use of a thin layer chromatographic fluorescence detection method to a spectrofluormetric method for the determination of 7-hydroxycoumarin in human urine. Precoated high performance glass backed silica TLC plates were used. Chromatography was carried out in a Camag horizontal developing chamber in the saturation configuration using the lower phase of chloroform – water - ethyl acetate - acetic acid as mobile phase. Detection and quantitation of 7-hydroxycoumarin was carried out using a Camag TLC scanner II connected to a Camag SP4290 TLC integrator. The lanes were scanned at a wavelength of 313 nm using the mercury lamp in the reflection mode. For analysis of conjugated 7-hydroxycoumarin, samples were treated with β-glucuronidase (4000 units) for 16 hours at 37^0C. The limit of quantitation was 1 ng/ml, with a linear calibration curve up to 4 μg/ml. Indahl and Scheline (1971) reported the use of TLC for analysis of the metabolism of umbelliferone and herniaren in rats and in the rat intestine microflora after oral and intraperitoneal administration. Separation was performed on thin layer cellulose plates, with observation under UV light at 254 nm and by spraying with fast blue B salt. The mobile phase used was benzene - glacial acetic acid – water (6:7:3 v/v) and potassium chloride – glacial acetic acid (100:1 v/v).

1.2.7.2 High performance liquid chromatography

Separation and identification of coumarins: High performance liquid chromatography was used to identify coumarin as an adulterant in vanilla-based liquid flavourings of Mexican origin (Thompson, 1988). In total 40 samples representing fourteen different brands were assayed for coumarin, vanillin, and ethyl vanillin. Separation was carried out on a 30 cm × 3.9 mm ID μBondapak C_{18} column with a 40:60 methanol water mobile phase (flow rate

1ml/min) with detection at 275 nm. Coumarin was reported to be present in 27 (67.5%) of the products examined, with a concentration range of 0.2 – 2.56 mg/ml, with a mean of 1.17 mg/ml. Vanillin was present in 38 (95%) and ethyl vanillin was present in 11 (27.5%) of the products. Gamache *et al.* (1993) reported on the analysis of phenolic and flavanoid compounds in juice beverages using HPLC with coulometric array detection. In total 27 components were separated in a 16 channel chromatogram including 4-hydroxycoumarin, 7-hydroxycoumarin, coumaric acid, and 7-methoxycoumarin (analysis time 45 minutes). The method was demonstrated to be applicable to the analysis of orange, apple and grapefruit juices.

Metabolic studies: An automated high performance liquid chromatographic assay using fluorescent detection for the determination of 7-ethoxycoumarin and umbelliferone from microsomal incubations was reported by Evans (1992). Following a 30 minute incubation, 7-ethoxycoumarin, 4-methylumbelliferone (internal standard) and the metabolite umbelliferone were extracted by chloroform and separated using an isocratic mobile phase (methanol : 0.05M acetate buffer, pH 4.7, 55:45 v/v). Separation was carried out on a μBondapak phenyl (300 mm × 3.9 mm ID) analytical column. The eluent was monitored with an excitation wavelength of 360 nm and an emission wavelength of 470 nm. A detection limit of 0.07μg/ml was reported, with the extraction recovery of umbelliferone ranging from 91% to 98% over the concentrations in the standard curve.

Egan (1992) demonstrated the use of HPLC for the determination of coumarin, 7-hydroxycoumarin and its glucuronide conjugate in urine and plasma. Samples were extracted using 3 ml of diethyl ether following mixing for 3 min. The mixture was centrifuged for 10 minutes at 600g before removal of the organic layer, evaporation to dryness and reconstitution in 200μl of methanol. Conjugated 7-hydroxycoumarin was determined after treatment of 1 ml of the sample with 1 ml of β-glucuronidase at a concentration of 5000 units/ml, incubation for 30 minutes and extracted as before. Lamiable *et al.* (1993) used HPLC for the determination of coumarin in plasma at low concentrations. The method involved a single step extraction of the alkalinised sample with hexane and subsequent evaporation of the organic phase in the presence of hydrochloric acid to collect and concentrate the coumarin. Analysis was performed on a C_8 column with detection by UV absorbance at 275 nm. The assay was used to study the evolutions of concentrations of

coumarins in one volunteer after oral administration of a single 10 mg dose. Results showed the maximum concentration to be found with 5 minutes after a single oral administration, reaching 5.81 mg/ml, falling beneath the limit of detection after 240 minutes.

Runkel *et al.* (1996) describe the combined use of HPLC and TLC for the examination of the metabolic and analytical interactions of grapefruit juice and coumarin in man. The study investigated the influence of the juice on the fate of coumarin metabolised by CYP2A6 in man. Analysis was carried out on samples collected up to 24 hours after dosing. After *in vitro* hydrolysis samples were analysed fluorimetrically for 7-hydroxycoumarin. HPLC and TLC identified the fluorescent metabolites from the juice. The study concluded if coumarin is administered in water its excretion is completed after 6 hours and 70% of the dose is recovered, while up to a litre of juice is required to enhance the delay of metabolism and bring coumarin recovery up to nearly 100%.

Genetic variation among mice in the metabolism of coumarin was reported recently by Lovell *et al.* (1999). In all strains the major metabolic pathway was the 3,4-epoxidation with *o*-hydroxyphenylacetaldehyde as the major metabolite. Major variations were discovered in female mice in relation to coumarin 7-hydroxylase activity ranging from high to very low levels metabolised. The difference between the strains in the male mice was much less pronounced. Analysis by HPLC also revealed evidence for strain variation in the metabolism of a number of other coumarin metabolites. A significant discovery was made regarding the DBA/2 mouse, which has been suggested as a model for coumarin metabolism for humans in that the profile of 7-hydroxylation differed considerably from humans as well as other species.

Killard *et al.* (1996) looked at the glucuronidation of 7-hydroxycoumarin in bovine liver homogenate using HPLC. The method separated coumarin, 7-hydroxycoumarin, 7-hydroxycoumarin-glucuronide and an internal standard, 4-hydroxycoumarin. Samples were separated by reverse-phase HPLC on a C_{18} column with detection at 320 nm. The limit of detection was 1.47μM for the glucuronide with a linear range from 0 – 295.7μM. Several researchers have investigated coumarin metabolism using liver slices. Hiller and Cole (1995) and Walsh *et al.* (1995) both examined 7-ethoxycoumarin metabolism in liver slice incubates. The method of Walsh *et al.* looked at the metabolism in both rat and human liver slices. Separation was carried out on a C_8 Hypersil BDS column using ion pairing conditions for separation of 7-ethoxycoumarin, 7-hydroxycoumarin and the glucuronide and sulphate conjugates. Hiller and Cole improved upon the analysis time for this method, using short

column gradient elution with a total assay run time of 10 minutes using liver slices from mice. A 33 mm × 4.6 mm ID, 3 μm particle size LC-8 column was used with a flow rate of 1.5ml/min. Solvent A was composed of 90% acetic acid (0.25%), 50% acetonitrile and 0.17% tetrabutyl ammonium phosphate (w/v), solvent B composed of 50% acetic acid (0.25%), 50% acetonitrile and 0.17% tetrabutyl ammonium phosphate (w/v), detection with a variable wavelength absorbance detector. A recent method for looking at coumarin 7-hydroxylation and 7-ethoxycoumarin o-deethylation by human liver cytochrome P450 enzymes claims 100-fold improvement in sensitivity over previous spectrofluormetric methods in detecting the metabolite, 7-hydroxycoumarin (Yamazaki *et al.,* 1999). Using 36 different concentrations of coumarin between 0.17 μM and 100 μM, 7-hydroxylation was monitored via the single enzyme CYP2A6 (K_m: 0.4μM, V_{max}: 0.56 nmol/min/mg/protein). 7-Ethoxycoumarin oxidation was monitored using 100 different substrate concentrations between 7.5 μM and 1 mM by several enzymes, CYP2E1, CYP3A4, CYP2B6 and CYP1A2. Of the enzymes monitored, CYP2E1 demonstrated the highest activity with a K_m value of 109 μM, and a V_{max} value of 1.8 nmol/min/nmol P450). Incubation mixtures consisted of human liver microsomes (0.025 mg protein/ml) or recombinant P450 (10 pmol/ml) with several concentrations of coumarin or 7-ethoxycoumarin in a final volume of 0.20 ml of 100 mM potassium phosphate buffer, pH 7.4, containing a NADPH generating system. Incubations were carried out at 37^0C for 10 min and terminated by adding 10 μl of 60% $HClO_4$. (w/v) for the HPLC method, or 10 μl of Cl_3CCO_2H (w/v) for the spectrofluorimetric method. Mobile phase for the HPLC separation consisted of 45% CH_3CN (v/v) containing 20 mM $NaClO_4$, pH 2.5, at a flow rate of 1.2 ml/min with separation carried out on a C_{18} 5 μm analytical column (Mightsil RP-18, 150 × 4.6 mm ID, Kanto, Tokyo, Japan). Fluorimetric detection for the HPLC method was done at an excitation wavelength of 338 nm and an emission wavelength of 458 nm. For the spectrofluorimetric assay, formation of 7-hydroxycoumarin was determined at similar ex/em wavelengths with a Shimadzu RF-5000 spectrofluorimeter (Shimadzu, Koyoto).

1.2.7.3 Gas chromatography

Separation and identification of coumarins: A method involving solvent extraction and gas chromatography coupled to mass spectrometry was reported by Weinberg *et al.* (1993) for the identification and quantification of coumarin, phthalide, and Sequiterpene Compliance markers in an umbelliferous vegetable mix. Analysis was carried out on a 25 m, 0.32 mm ID HP-5 gas chromatographic capillary column coated with a 0.52 μm bonded-phase film of methyl silicone with helium as the carrier gas. Column temperature was maintained at 45^0C for 3 min and then heated to 300^0C at 8^0C/min. The mass spectrometer transfer line was operated at 300^0C, the ion source at 260^0C and the electron voltage was 70eV. The magnet was scanned from mass 300 to 350 at 1 s/decade, with a rest time of 0.5 s. Nominal resolution was 1000. Large quantities of carrot and celery juice were extracted with methylene chloride. Among the many components identified were umbelliferone and psoralen, although at extremely low concentrations, so low that no further attempt was made to quantify them. Hawthorn *et al.* (1988) demonstrated the use of GC with flame ionisation detection and GC-MS for analysis of spices for the presence of flavour and fragrance compounds. Analysis was carried out on capillary fused silica DB-5 columns. For GC-FID, the carrier gas was hydrogen, and for GC-MS, helium gas with electron impact ionisation (70eV) detection was used. Supercritical fluid extractions were preformed by using an SFT Model 250-TMP supercritical fluid pumping system. Of the spices examined, cinnamon was the only one with coumarin shown to be present, although coumarin spiked into Rosemary at a concentration of 1.14 mg/g showed an average percentage recovery of 105% with a RSD of 12% for the method.

Metabolic studies: Determination of 2-hydroxyphenylacetic acid (2HPAA) in urine after oral and parenternal administration of coumarin by gas-liquid chromatography with flame ionisation detection was reported by Meineke *et al.* (1998). Prior to analysis the samples were extracted into ethyl ether and the analytes were derivatized with trimethylphenylammonium hydroxide. 3-Hydroxyphenyl acetic acid was used as an internal standard to establish a calibration range from 0.3 to 150 μg/ml. It was concluded from the study that, on average, less than 10% of the coumarin administered was excreted in the form of 2HPAA. Jirovetz *et al.* (1992) analysed blood samples of mice following inhalation of

coumarin (3.0 g) placed in the mice cage. The air concentration of the coumarin was measured to be in the range of 50 – 108 mg/m^3, (8.4 l cage). For GC-FID a 25 m HP-5 fused silica column, 0.32 mm ID, film thickness 0.17 μm with hydrogen carrier gas. For GC-MS and GC-FTIR helium carrier gas was used with the same conditions. For GC-MS the interface heating was 280^{0}C. Following identification of coumarin in the blood serum of mice, quantification was carried out using tiglinic acid benzyl ester as an internal standard. Coumarin concentration in the blood serum was measured at a concentration of 7.7 ng/ml.

1.2.7.4 Voltametric and polarographic methods

Separation and identification of coumarins: Carrazon *et al.* (1989) reported the use of voltammetric techniques for the determination of coumarins in micellar and emulsified media. The apparatus consisted of an electrochemical cell comprising a Metrohm 6.1204.000 glassy carbon rotating disc electrode, an Ingold 10-303-3000 saturated calomel reference electrode and a platinum wire counter electrode in a double wall Metrohm EA867-20 vessel. Differential pulse voltammetry at the stationary electrode gave a limit of determination for umbelliferone at 2.9×10^{-6} mol 1^{-1}, and a limit of detection of 8.7×10^{-7} mol 1^{-1} for the micellar solution with similar results for the emulsified media (%RSD = 3.5). Linear sweep voltammetry with the stationary electrode gave a limit of determination of 1.8×10^{-5} mol 1^{-1}, and a limit of detection of 4.9×10^{-6} mol 1^{-1} (%RSD = 3.0). Orlov (1988) demonstrated the use of polarography for the determination of coumarin percentage in yellow and white sweet clovers. Measurements were carried out on an LP-7 polarograph with dropping mercury electrode. Using this procedure, 0.54% of coumarin was found in the herbage of yellow sweet clover (five samples) and 0.34% in that of white sweet clover (five samples).

Metabolic studies: Dempsey *et al.* (1993) reported on the use of differential pulse voltammetry for the determination of 7-hydroxycoumarin in urine. A conventional three electrode system was used (platinum gauze as counter, glassy carbon as working and saturated calomel as reference. Analysis of urine samples from a human volunteer before and after drug administration (100 mg) was carried out. The concentration of free 7-HC excreted was determined at regular time intervals (0 – 24 hr). The free 7-HC excreted over the period

studied was found to be 5.07 mM. The amount of 7-HC conjugated was determined after treatment with β-glucuronidase (10,000 units/ml). Total 7-HC was calculated as 5.67 mM, 0.6 mM conjugated 7-HC.

1.2.7.5 Capillary electrophoresis

Several researchers (Bogan *et al.,* 1995a; Bogan *et al.,* 1996; Cole *et al.,* 1996) have applied this tool to the separation of coumarin metabolites in a variety of matrices for *in vitro* and *in vivo* studies. The number of applications has increased sharply, most notably in the last four years.

Metabolic studies: Bogan *et al.* (1995a) reported on the analysis of 7-hydroxycoumarin and coumarin in urine and serum. Samples were prepared by extraction of the analyte into diethyl ether, and reconstitution into electrolyte buffer, 25 mM phosphate, pH 7.5. Separation was performed on untreated fused silica capillaries with detection at 210 nm. The method had a linear range between 0 and 50 μg/ml with a limit of detection of 1 μg/ml. Separation and detection of 7-hydroxycoumarin and 7-hydroxycoumarin glucuronide in urine was demonstrated by Bogan *et al.* (1996a). The separation was carried out on an untreated silica capillary with a phosphate buffer / deoxycholic acid / acetonitrile electrolyte solution with detection was at 320 nm. While 214 is a more sensitive wavelength, absorbance from species present in the matrix prevents the use of this wavelength for detection. At 320 nm it was possible to analyse for 7-HC and 7-HCG without absorbance from interfering species. The linear range of the assay is 0-100 μg/ml, with a limit of detection of 2 μg/ml. (%RSD from 1 – 10%). Separation of 7-HC and 7-HCG is achieved in under 7.5 min. This method represented a major improvement over previous methods for analysis of free and conjugated 7-HC as the glucuronide can be measured directly with minimal sample clean up and hence no need for deconjugation, extraction, and evaporation steps. Bogan *et al.* (1996b) and Deasy *et al.* (1995) reported on the applications of capillary electrophoresis to the *in vitro* study of coumarin and 7-hydroxycoumarin metabolism. Liver microsomal preparations from a variety of sources (human, rabbit, bovine, porcine and murine) containing cytochrome P4502A6 were prepared. A reaction mixture consisting of coumarin, the microsomal preparation and an NADPH regeneration system in phosphate buffer was prepared and sampled periodically. The production of 7-hydroxycoumarin was monitored over time. The

methods reported on the cytochrome P4502A6 activity in the different species (Bogan *et al.*, 1996) and the method of Deasy *et al.* (1995) assessed interindividual differences within a species. The limit of detection was 1 μg/ml, with a linear detection range 0 - 50 μg/ml. The study demonstrated highest 7-hydroxycoumarin production in human liver microsomal preparations with no detectable levels of 7-hydroxycoumarin produced in rat, pig, or dog.

Bogan *et al.* (1995) reported on the use of CE to monitor the *in vitro* production of 7-hydroxycoumarin glucuronide from a crude preparation of bovine liver uridine diphosphate (UDP) glucuronyl transferase. Separation was carried out using a phosphate buffer:deoxycholic acid:acetonitrile electrolyte solution on an untreated fused silica capillary. The reaction was incubated at 37 °C and samples were removed periodically and analysed directly with no sample preparation. The rate of reaction reported for the bovine liver for the first 70 min was 3.1 ± 0.13 nmol of 7-hydroxycoumarin glucuronide produced per minute per mg of protein. Cole *et al.* (1996) while evaluating extended light paths in capillaries for use in CE with laser induced fluorescent detection, looked at the detection of 7-ethoxycoumarin (7-EC) and its metabolites in liver slice incubates. Samples were incubated 4-6 hr with 7-EC prior to reaction termination and analysis. Excitation was 325 nm and emission at 540 nm. While the use of extended light paths for the capillaries showed a marked improvement in detection limits over conventional capillaries (ca. five-fold), only the parent compound, 7-EC, and 7-hydroxycoumarin were detected. The glucuronide and sulphate conjugates, due to their significantly different ex/em wavelengths could not be detected.

Method/ Application	Detection	LOD	Reference
TLC – Vanilla extract analysis	UV Absorbance	500ng	Poole *et al.* (1993)
TLC – Analysis of urine	Fluorescence	1 ng/ml	Cholerton *et al.* (1992)
HPLC – Coumarin metabolism	UV Absorbance		Thompson *et al.* (1988)
HPLC – 7-HC detection	UV Absorbance	500 ng/ml	Egan *et al.* (1992)
GC – Coumarin identification	Mass spec.		Weinberg *et al.* (1993)
CE – Coumarin metabolism	UV Absorbance	1 μg/ml	Bogan *et al.* (1996a)

Table 1.1 *Limits of detection and detection modes for some methods of analysis for coumarins*

1.3 Chip-Based microcolumn separation systems

The use of modern micromechanical fabrication technology for analytical chemical applications has created a rapidly advancing interdisciplinary field of research (Effenhauser, 1998). For some time researchers have looked for ways to miniaturise analysis systems. This knowledge has lead to the development of small diameter packing materials and open-tubular microcolumn separation techniques such as microbore HPLC (Knox, 1980) and capillary electrophoresis (Jorgenson *et al.,* 1981). Regarding CE, column diameters ranging from 10 – 100 μm internal diameter provided a feature that was easily accessible by micromachining technology. In addition to just small bore separation channels, microfabrication technology offers features such as networks of channels, flow restrictors, reagent compartments, etc. of virtually any shape. Most importantly, this can be done without introducing significant dead volume into the system, which would be detrimental to the precise handling of pico- and nano-litre sample volumes. There are many incentives of chip-based integrated chemical separation of which the following are perhaps uppermost:

- Reduced consumption of sample reagents and mobile phase.
- Improved analytical performance in terms of resolution power per time unit.
- Multifunctional, interconnected channel networks with negligible dead volumes.
- Suitability for inexpensive mass fabrication.

While all of these are advantages, the benefit of a reduction in the consumption of sample, reagents, and mobile phase can present problems regarding detection, hence the use of extremely sensitive laser-induced fluorescence (LIF) as the choice mode of detection for most chip based systems to date. Although microfabrication has its basis in microelectronics and most research in microfabrication has being focused on microelectronic devices (Moreau, 1988), applications in other areas is rapidly appearing. These include systems for microanalysis (Jacobson, 1994; Bratten, 1997), micro volume reactors (Sond, 1994), combinatorial synthesis (Briceno, 1995), and now in the area of separation and analysis of chemical and biological substances (Jacobson, 1994a; Chiem and Harrison, 1997). The past few years have seen the development of miniaturised total chemical analysis systems (μ-

TAS) capable of performing all sampling steps in an integrated fashion (van der Bery, 1995). Systems for free flow electrophoresis (Raymond, 1994), gas chromatography (Terry, 1979), capillary electrochromatography (Jacobson, 1994b), and micellar electrokinetic capillary chromatography (MECC) (Heeren, 1996), have been developed. Rapid and efficient capillary zone electrophoresis electrophoretic separations in micromachined channels (open, gel filled or polyacrylamide coated) on quartz substrates have also being demonstrated (Effenhauser 1993; Jacobson, 1994; Effenhauser, 1994). Devices for performing not only analysis, but also chemical synthesis are also being developed. An array of chemical tools on a chip makes it possible to synthesise, analyse and characterise extremely small amounts of product. Examples include DNA chips for high speed DNA sequencing (Goffeau, 1997) and microchips for carrying out the polymerase chain reaction (PCR), (Fodor, 1991).

1.3.1 Immunoassays on-chip

Applications of microchip CE to immunoassays as investigated in chapter 5 for warfarin and parathion have also been reported. Koutny *et al.* (1996) performed the first microchip electrophoretic immunoassay in serum by adapting to chip format a cortisol assay performed earlier using conventional CE. A calibration curve for cortisol in serum over the range of clinical importance was established with the device, the peak area of free labelled cortisol was measured. Two different assays performed on-chip were reported by Chiem and Harrison (1997). The injection volume was 100 pl and the channels were uncoated. Injector to detector distance was 5 cm. The assays were for BSA, in direct format, and the drug theophylline, in competitive format. For theophylline the reported separation time was ~40 seconds, and a calibration curve covering the clinically relevant range of 10 – 20 μg/dl for serum samples was shown.

1.4 Organelles and Chromatographic analysis

There is very little reported on the analysis of cell organelles using chromatographic techniques, although a recent publication of the Journal of Chromatography (Vol. 722, February, 1999) devoted the entire journal to articles on the analysis of cells, functional

aggregates and their components. This is an indication that the use of chromatographic methods for analysis of small particles is becoming more popular in an effort to understand more about cells and their organelles. While none of the articles reported on the analysis of the organelle analysed in chapter 7 (mitochondria), a review on the analysis of subcellular particles reported on the current developments on liposome analysis. The results, however, showed exactly the same format as the few earlier publications (see chapter 6) for liposome analysis by CE and are very far from the quality and precision discovered for the first time in this thesis and reported in chapter 6. As the work in chapters 6 and 7 is intended to lead to methods capable of analysing all organelles by CE, a general review of organelles is given in this section, before examining the various methods currently used for their analysis.

1.4.1 Analysis of cell organelles

The majority of work on the analysis of cellular organelles, has focused on populations of organelles, either inside cells or isolated, with few cases looking at the single organelle level (Cossarizza, 1996). Classical methods of analysis have revolved around subcellular fractionation using gradients for separation following homogenisation. Perhaps the biggest stumbling block in the analysis of subcellular particles has been the homogenisation step. The production of an "ideal homogenate" (release of functional, intact organelles as a free suspension) is difficult to obtain. Problems involve the formation of cytoplasmic aggregates which can clump organelles together and precipitate, and damage to organelles during homogenisation. As the cytoplasmic and cytoskeletal organisation of different tissue culture cells differ enormously, a homogenisation procedure for every case must be developed separately, with monitoring by morphological means (phase contrast microscopy). The following five sections (1.4.2.1 –1.4.2.5) examine methods used for analysis of subcellular components, giving examples of the various applications.

1.4.1.1 Gradients

To date, centrifugation has proven to be the most effective method of organelle isolation and purification. Isolation of subcellular particles by density gradient methods is achieved by the

different positions taken up by particles following centrifugation. The position of the particle is determined mainly by their lipid to protein ratios. The higher the protein content of the membrane, the higher the density. The content of the vesicles will also influence the density, as will the presence of attached components, for example ribosome's on the surface of rough endoplasmic membranes. One of the other factors responsible for separation is the choice of separation medium. Sucrose is most commonly used along with Metrizamide, Percoll, Ficoll or Nycodenz (Pasquali *et al.,* 1999). The use of discontinuous gradients has also been applied successfully for separation of various organelles. Madden and Storrie (1987) used discontinuous gradient ultracentrifugation for isolation of mitochondria from Chinese hamster cells. The gradient used 6% (v/v) Percoll overlaid on 17% (w/v) Metrizamide in turn overlaid on 35% (w/v) Metrizamide (all in 250mM sucrose), and centrifuged for 15 minutes at 50,000g. Mitochondria were localised at the Percoll/Metrizamide interface and at the 17/35% (w/v) Metrizamide interface, with the 17/35% (w/v) providing the most pure fraction. Separation by gradients can be achieved by two different centrifugation methods. The first method uses velocity, in which particles move in the direction of the centrifugal force, and separate based on size and density, this method is time-dependant, as eventually everything will pellet, or by equilibrium, in which particles move to a position in the gradient which matches their density. Walmsley *et al.* (1999) used a combination of cross linking and sucrose gradient analysis to examine intracellular retention of proteins within the endoplasmic reticulum (ER). The ability of the ER to retain unassembled or malfolded proteins was investigated using procollagen as a model. The accumulation of these partially folded intermediates occurs during vitamin C deficiency due to incomplete proline hydroxylation, as vitamin C is an essential co-factor of the enzyme prolyl 4-hydroxylase. It was demonstrated that the retention is tightly regulated with little or no secretion from the ER under conditions preventing proline hydroxylation.

1.4.1.2 Immunoisolation

Immunoisolation techniques differ from those of gradients in that they exploit biological properties of organelles rather than physical aspects. The high specificity of antibodies is utilised to locate organelles containing the antigen of interest. This method is more complicated and requires more time and skill than gradient analysis. A prerequisite for

immunoisolation is the identification of a suitable antigen on the organelle and the generation of a high affinity antibody to this antigen. Often this technique will be preceded by a gradient step to provide a more pure homogenate. Solid supports such as cellulose fibres, monodisperse magnetic beads and Eupergit particles have been used to immobilise the antibody (Pasquali *et al.*, 1999). Salamero *et al.* (1990) used magnetic beads with an immobilised antibody against the cytoplasmic domain of the polymeric IgA receptor to isolate golgi fractions. The method was used to generate a cell-free assay that reproduced vesicular budding during exit from the golgi complex by incubation of the stacked golgi fraction under conditions to sustain vesicular transport. From the total population of budded vesicles those destined to the basolateral plasma membrane were immunoisolated and characterised.

1.4.1.3 Free flow electrophoresis

The technique of free flow electrophoresis (FFE) separates subcellular particles based on their unique charge properties. Again the method relies on the production of a homogenate of organelles, which are loaded onto a liquid buffer that flows between two electrodes. The electrophoretic mobility is independent on the size and shape of the particles. In fact, the particles with the greatest mobility were found to be those with the ability to acidify their interiors, (Pasquali *et al.*, 1999), such as lysosomes and trans-golgi network vesicles, thus generating a membrane potential with negative charge outside. While the normal conditions of FFE works best for these organelles with the main peak of a free flow electropherogram composed mostly of lysosomes and endocytotic vesicles, there is also cross contamination from smooth and rough endoplasmic reticulum, and light mitochondria. Among the advantages of FFE are the speed of purification and the amount of sample that can be processed. However, it is unlikely that FFE will ever be a one step separation procedure, but used in conjunction with other steps can yield good results.

1.4.1.4 Flow cytometry and organelle analysis

Perhaps by far the majority of work on organelle analysis was performed by flow cytometry. Flow cytometry can be used as an analytical tool as well as for sorting cells and other smaller particles. One example is a fluorescence activated cell sorter (FACS), consisting of two main parts, the sample flow and data analysis system, which are connected by optical devices. A continuously flowing buffer stream carried the particles from a sample tube through a light beam at a measuring point. Light signals from an individual particle are obtained by an array of light detectors. Particle size is measured by forward scatter of light, and light deflected sideways (90^0) relative to the incident laser light (side scatter) is proportional to the quantity of granular structure in the particle. The particles can also generate light at different wavelengths as a result of fluorescence from specifically bound probes. In an ideal situation, the amount of fluorescence is proportional to the number of dye molecules. The most commonly used system for sorting of fluorescent particles is the 'stream in air' system, in which the particles, embedded in a stream of flow buffer, exit from a nozzle tip after which the stream is broken up into defined droplets containing single particles by mechanical vibration of the nozzle. Droplets containing particles to be purified (depending on their size and/or fluorescence intensity) are charged, separated from other droplets during passage through a strong electric field and collected in separate tubes.

The technique of flow cytometry has been used extensively for the analysis of many organelles. Cossarizza (1996) examined the heterogeneity among individual mitochondria membrane potentials isolated from rat liver with the fluorescent probe 5,5',6,6'-tetrachloro-1,1',3,3' tetraethylbenzimidazolylcarbocyanine iodide, JC-1. Highest heterogeneity was found in de-energised mitochondria, while the highest homogeneity was observed during the first phase of the phosphorylative process. The effect of cryopreservation of bovine sperm organelle function was examined by (Thomas *et al.*, 1998), in which the plasmalemma, acrosome and mitochondria were analysed. Results showed that these organelles in unfrozen spermatozoa varied as to their functional status, while the cryopreservation process resulted in a more uniform status. Macouillard-Poulletier de Gannes *et al.* (1998) demonstrated that mitochondrial volume changes can be followed by flow cytometry when examining changes in the mitochondrial matrix volume using multiparametric flow cytometric analysis. The use of specific effectors of mitochondrial activity (oligomycin and KCN) showed mitochondrial

swelling to produce a concomitant increase in forward scattering and decrease in side scattering of the cell population.

Mitochondrial membrane potential (MMP) in dissociated rat cerebellar neurons was measured using rhodamine 123 (Rh123) (Sureda *et al.,* 1995). Dye distribution was studied by confocal scanning microscopy, while Rh 123 fluorescence following exposure of cell populations to various agents was monitored by flow cytometry. Results showed that exposure of cell populations to the mitochondrial specific uncoupling agent and impairment of glucose bioavailability caused a decrease in fluorescence, while oxidative stress induced by H_2O_2 did not affect fluorescence. It was also demonstrated that application of L-glutamate and N-methyl-D-aspartate (NMDA), the excitatory amino acids, decreased Rh 123 uptake, suggesting that the measurement of MMP by flow cytometry in dissociated cerebellar neurons can be used to monitor the activity of drugs acting on glutamate receptors.

Mitochondria dysfunction is considered to be a major cause of the modifications that occur during cell ageing. To examine this further, cardiolipin, a suitable marker of the chondriome, as well as the mitochondrial transmembrane potential were examined in keratinocytes from 9- to 75 year old women (Maftah *et al.,* 1994). Using the dyes nonyl acridine orange (specific for cardiolipin) and rhodamine 123, results showed a 57% drop in cardiolipin levels in cells from the elderly donors compared to the children, although the membrane potential remained the same. The stability of the membrane potential was proposed to come about by either the same pool of organelles able to maintain membrane potential even when cardiolipin levels decrease, or mitochondria membrane potential does indeed decrease with age, but is compensated by energy production involving glycolysis.

Peroxisome induction and degradation was monitored by flow cytometric analysis of Hansenula polymorpha (yeast) cells grown in methanol and glucose media. Cell volume, refractive index and fluorescein isothiocyanate (FITC) retention were monitored (Smeraldi *et al.,* 1994). Peroxisomes are inducible organelles which may occupy a large fraction of the cell volume when yeast cells are growing in methanol media, and undergo a degradation process mediated by vacuoles (monitored by FITC retention) whenever they and their enzymes become metabolically redundant (when grown on glucose). Results showed the peroxisome development in the cells to be substrate-dependent and demonstrated the dynamics of peroxisome proliferation and degradation in response to environmental factors.

Another investigation used analysis of peroxisome proliferation and the effects of humic acid as a possible method for studying the molecular control of determination and differentiation of mesodermal cell lineages (Lee *et al.,* 1999). The use of fluorescent lectin binding in conjunction with flow cytometry for analysis of surface carbohydrates on the golgi apparatus was reported by Guasch *et al.* (1995). Several fluorescein isothiocyanate-conjugated lectins were used to detect and quantify specific surface sugars on isolated elements from purified *cis*- and *trans*-golgi fractions from rat liver. It was suggested that the method may be used to study golgi composition and function, since it was possible to reveal the intensity of specific binding of different lectins to each golgi fraction and the percentage of elements binding the lectins specifically. Reported were that *cis*-golgi elements appear homogenous in mannose and fructose, whereas galactose and N-acetyl-glucosamine residues are more abundant in *trans*-golgi elements.

Analysis of nuclei by flow cytometry has been reported in a number of cases. Sabe *et al.* (1999) demonstrated its use for the analysis of estrogen receptor expression in isolated nuclei and cells, while Gschwendtner *et al.* (1999) used high resolution image cytometry for quantitative assessment of bladder cancer by nuclear texture analysis.

1.4.1.5 Microscopy

SR31747A is a sigma ligand previously described as having immunosuppressive properties. Two of its receptors were recently identified and termed $sigma_1$ and human sterol isomerase (hSI). Dussossoy *et al.* (1999) reported on the co-localisation of sterol isomerase and $sigma_1$ receptor at endoplasmic reticulum and nuclear envelope level using confocal and electron microscopy. Western-blotting techniques with polyclonal antibodies raised against hSI (human sterol isomerase) were first used to demonstrate the presence of the protein in B- and T-cell lines. The use of both confocal microscopy and electron microscopy enabled the subcellular localisation within the ER and with the outer and inner membranes of the nuclear envelope. Electron microscopy was used to examine the mitochondrial pathology in human schizophrenic striatum, (Kung and Roberts, 1999), to investigate the possibility that abnormalities in schizophrenia brain might be due, in part, to pathology in mitochondria. Results showed significantly fewer (~26%) mitochondrial profiles throughout the neurophil of the schizophrenic samples than controls, although the structural integrity of the

mitochondria did not seem to differ significantly between either control or schizophrenic sample. Also reported were the numbers of mitochondrial profiles per axon terminal which appeared lower in the subset of schizophrenics off drugs as compared to either the schizophrenics on-drugs or the controls.

1.4.2 Limitations involved in analysis of whole cells and organelles

While the above methods have provided valuable information and yielded many ways to probe and analyse both cells and organelles, there exist limitations among them, furthering the need for methods of analysis for organelles to be performed on an individual basis for clear-cut unambiguous results.

Flow cytometry: In the case of mitochondrial analysis one of the most important limitations of flow cytometry is that it does not permit a direct discrimination between respective probe responses to plasma and mitochondrial membrane potentials. For this reason, it is limited in the choice of dyes that can be used. For example, if membrane potential studies on whole cells are required, then anionic oxanols and bis-oxanols are more suitable for cells abundant in mitochondria, as these negatively charged dyes are strongly repelled from mitochondria.

Conventional fluorescence microscopes: An important problem with the use of conventional fluorescence microscopes concerns the resolution obtained. As fluorescence comes from above and below the plane observed by the microscope, results will be marred due to this. This effect can be partially overcome by the use of correction factors (Ehrenberg *et al.,* 1988).

Laser scanning confocal fluorescence microscopy: The use of this technique overcomes, to some extent, the problem described above, with fluorescence from layers about 0.4-0.6μm thick capable of being measured. However, the use of a focused laser beam to obtain the unique vertical resolution of confocal microscopy brings with it the side effect of

fluorescence photobleaching. Some dyes are more resistant to this than others, for example, (tetramethylrhodamine methylester perchlorate, TMRM, and tetramethylrhodamine ethylester perchlorate, TMRE). However, caution is needed even for these cases to avoid errors in membrane potential (Ehrenberg *et al.,* 1988). For very small objects such as mitochondria, even confocal microscopy fails to provide enough space resolution to determine reliably the intensity of fluorescence from its interior. To overcome this, the use of a computer aided digital image restoration, which is based on a 3D deconvolution of a series of object images acquired with a conventional microscope at a vertical spacing of 0.3μm, can provide enough space resolution for a reliable determination of mitochondrial membrane potential in situ, (Loew, 1993).

The above methods describe the analysis of organelles on the basis of size, morphological parameters, activity and levels of particular constituents (lipid components etc). There is another avenue open to exploration, not only for organelles, but any tissue or organism, and it involves the analysis of the protein content (the proteome). This is a new area developing in biology and gathering momentum fast as biologists seek to understand more about the complex proceedings inside and between organelles, cells and whole organisms. The term associated with this new field is *proteomics.*

1.4.3 Proteomics

The term "proteome" is a relatively new concept in biology, first appearing in late 1994 at the Siena 2-D Electrophoresis meeting, and in 1997 was the subject of a number of conferences. Proteome indicates the PROTEins expressed by the genOME or tissue at any given time. Embarking on the analysis of the proteome will perhaps lead biology into a new era of completeness, similar to when the periodic table was defined for chemistry. The proteome, unlike the genome, is not a fixed feature of an organism, continuously changing as the state of development of the tissue and the environment changes. It was this understanding that put paid to one of the old dogmas of biology, the one-gene-one-enzyme theory, as there are far more proteins in a proteome of an organism than genes in the genome. This comes about from the many changes that can occur between the DNA translation stage to final protein

expression, from the many ways a gene can by spliced in forming mRNA, to the multitude of ways the same protein can by post-transitionally modified.

In the search to understand and find cures for the many diseases, the race to sequence DNA and use differential display of mRNA to search for key molecules involved in both normal physiological pathways and in disease is continuously driven by industry. For example, in the occurrence of cancer there appears to be several genetic alterations needed. The short cut to understanding these protein networks is to study them directly. This is proteomics. Currently the only separation technology that provides highly purified proteins separated in a simple parallel process is 2-D gel electrophoresis. Although electrophoresis was first used in 1909 by Michaelis, and again by Tiselius in 1937. In the early 1970's two dimensional electrophoresis was described by Dale and Latner (1969) and Macko and Stegemann (1969) through the combination of IEF followed by PAGE. Stegemann (1970) introduced IEF in polyacrylamide gels followed by SDS-PAGE. However, it was not until 1975 that the method most separations are based on today was developed (O'Farrell, 1975). Other methods such as serial liquid chromatography and capillary electrophoresis methods are currently being evaluated, however, to date, none are able to come near 2-D electrophoresis for resolution.

Proteome projects, which aim to identify and characterise all proteins expressed by an organism or tissue, provide information which is detailed in many ways. Identification gives a name or database accession code to a protein (or spot on a gel if 2-D electrophoresis is used to identify the protein), linking the amino acid sequences of proteins to DNA sequences of genes, thereby linking genomes to proteomes. This information also provides us with a first step towards analysing co- and post-translational modification of proteins, which will lead ultimately to a greater understanding of function. The ability to create reference maps for individual organisms is possible, and hence discover which proteins are "common", and which ones are unique to a particular tissue. As detection methods for proteins on gels improve, identification will also provide quantitative data on the amount of protein expressed which could ultimately be used in conjunction with data from mRNA microarray analysis (Schena, 1996). This will allow a better understanding not only of when and where a protein is expressed, but also information on the numbers per cell, pool size and half-life.

1.4.3.1 2-D gel electrophoresis

As an analytical technique, 2-D gel electrophoresis is the proven leader when it comes to the power to resolve hundreds of proteins on the one single gel. Separation is based by exploiting two physical properties of the proteins, molecular weight and isoelectric point. Data on relative abundance and electrophoretic pattern as well as those properties mentioned above is collected. The number of investigators that have reported on the use of 2-D gel electrophoresis for identification of various proteins is vast, and to try and review even a small amount would be a major task. However, in recent times, within the new world of proteomics, 2-D gel electrophoresis has been applied to the analysis and identification of the proteome. Sazuka *et al.* (1999) reported proteomic studies on the cyanobacterium Synechocystis (sp. strain PCC6803) and updating the 2D protein-gene linkage database with the further identification of 97 proteins and their genes, to total 277 the number of proteins identified and linked to their genes for this organism. Perrot *et al.*(1999) identified 92 novel protein spots on the yeast protein 2-D map, extending to 401 the number of proteins identified on their yeast 2-D reference map. These spots correspond to 279 different genes and were identified by three different methods – gene overexpression, amino acid composition and mass spectrometry.

2-D gel electrophoresis has been used in functional proteomic studies and applied to the investigation of signal transduction systems involving platelet-derived growth factor (PDGF), endothelin and bradykinin. Following the stimulation of mouse fibroblast cells, phosphorylation/dephosphorylation of several hundred proteins was followed as a function of time using 2-D gel electrophoresis (Godovac-Zimmermann *et al.,* 1999). Up to 100 proteins showed changes in phosphorylation within minutes of receptor stimulation. Using matrix-assisted laser desorption/ionisation – time of flight (MALDI-TOF) mass spectrometry, new proteins not previously know to be associated with signal transduction were identified. Hermann *et al.* (1998) used 2-D gel electrophoresis as the first step in proteome analysis of *Corybacterium glutamicum*. The map revealed over 1000 silver stained spots for cytoplasmic proteins and approximately 700 silver stained spots for the membrane fraction. 10 proteins were identified using N-terminal sequencing, the 35kDa antigen, antigen 84, ATP synthase subunits α, γ and δ, cysteine synthase, elongation factor G and Ts, enolase, and rotamase.

Although 2-D gel electrophoresis is used almost exclusively as the precursor step to proteome analysis of any organism, a study carried out by Wilkins demonstrates it is not without its short comings and limitations. The effects of protein hydrophobicity and cellular protein copy number on a proteins absence or presence on a 2-D gel was investigated. (Wilkins *et al.*, 1998) By calculating the average hydropathy of all known proteins from *Bacillus subtilis*, *Escherichia coli* and *Saccharomyces cerevisiae*, and defining the range of hydrophobicity and hydrophilicity in these organisms, the average hydropathy values were calculated for a total of 427 proteins from these species, which had being identified by 2-D gels on previous occasions. It was shown that there have been no highly hydrophobic proteins identified by 2-D gel separations to the date of the publication (1998). A clear hydrophodicity cut off point was seen, above which the authors concluded, that 2-D gel electrophoresis did not appear to be useful for protein separation. On investigating the effect of a proteins cellular copy number on its presence on the gel, use of a graphical model showed that variations in loading and copy number per cell interact to determine the quantity of protein that will be present on a gel. Considering the current loading capacity, the authors concluded that 2-D probably could not visualise or produce analytical quantities of proteins present at less than 1000 copies per cell. From these conclusions, it is clear that improvements are needed to 2-D gel technology to enable the visualisation and analysis of all proteins expressed by a cell or tissue. Chapter 7 takes a look at the use of CE for analysis of the mitochondrial proteome. The work presented marks the beginning investigations towards the use of capillary gel electrophoresis in analysing fluorescently labelled proteins extracted from isolated mitochondria.

2 MATERIALS AND METHODS

2.1 Materials

Unless otherwise stated, all standard laboratory reagents were purchased from Sigma Chemical Co., Poole, Dorset, England and St. Louis, MO, USA.

HPLC grade solvents were purchased from Labscan, Unit T26, Stillorgan Industrial Park, Co. Dublin.

Warfarin polyclonal antibodies and Warfarin-BSA conjugate were a gift of Brian Fitzpatrick, Dublin City University.

Parathion polyclonal antibodies and BSA-Parathion conjugate were a gift of Paul Dillon, Dublin City university

Enzyme-labelled antibodies for ELISA were purchased from Sigma Chemical Co.

Chinese Hamster Ovary and Hybridoma cells were kindly donated by Dr. Wei-Shu Hu, University of Minnesota.

Fluorescent stains (nonyl acridine orange, NAO, Rhodamine 123, Rh 123), labels (fluorescein isothiocyanate, FITC, fluorescein and 3,(2-furoyl) quinoline-2-carboxaldehyde, FQ, 5,5',6,6'-tetrachloro-1,1',3,3' tetraethylbenzimidazolylcarbocyanine iodide, JC-1) and fluorescein loaded 6 μm diameter polystyrene beads were purchased from Molecular Probes, Eugene, Oregon, USA.

Protein determinations were made using a Bicinchoninic acid (BCA) assay kit (Pierce, Illinois, USA) on microtitre plates.

Rabbits used for organ donation were kept at 16-18^{0}C at DCU animal house.

2.2 Equipment

Untreated fused silica columns used for capillary electrophoresis were supplied by Polymicro Technologies, Phoenix, Arizona, USA.

HPLC columns were supplied by Phenomenex, Melville House, Queens Avenue, Hurdsfield Industrial Estate, Macclesfield, Cheshire, England.

High performance liquid chromatographic (HPLC) analysis was performed using Beckman System Gold 507 Autosampler, 126 pump, 166 UV detector and 168 photo diode array detector, all controlled using Beckman System Gold software.

Capillary Electrophoresis was carried out on the following instruments: Beckman System 5500 P/ACE (UV and LIF detection) instruments, an 'in-house' constructed CE instrument with post-column LIF detector, University of Minnesota, parts supplied by Melles Griot, USA, University of Alberta machine shop, Edmonton, Canada, and University of Minnesota Electronics shop. Microchip capillary electrophoresis was carried out on an 'in-house' constructed instrument, University of Alberta, parts and equipment supplied by Melles Griot, and University of Alberta machine shop.

Microchip substrates were part made in the Alberta Microelectronic Corporation (AMC) and assembled in-house, Alberta Microelectronic Corporation, #318, 11315 - 87 Avenue Edmonton, Alberta, Canada, T6G 2T9

pH measurements were made using Jenway 3015 pH meter (Jenway Ltd., Gransmore Green, Felsted, Dunmow, Essex CM6 3LB, England.

Standard photometric measurements were made using a Shimadzu UV160A, Shimadzu Corp., 1 Nishinokyo-Kwabaracho, Nakagyo-Ku, Kyoto 604, Japan.

Bench centrifugation was performed using a Heraeus Sepatech (Heraeus Instruments Inc., 111-A Corporate Blvd, South Plainsfield, NJ 07080, USA). Ultracentrifugation was performed on a Beckman J2-21 using a JA-20 rotor, Beckman Industries Inc., Bioindustrial Business Unit, Fullerton, CA, 92634-3100, USA.

Incubations for coumarin metabolism studies were carried out in 10ml blood tubes (Medical Supply Co., Dublin, Ireland).

Nuclear magnetic resonance (NMR) analysis was carried out on a 400MHz AC NMR Spectrophotometer, Brucker, Banor Lane, Coventry, England.

Infra red (IR) analysis was carried out on a Nicollet Spectrophotometer, Nicollet Instrument Corporation, 5225-1, Verona Road, Madison, WI, USA.

Analysis of microtitre immunoplates was carried out using a Titretek Multiscan Twinreader, Flow Laboratories Ltd., Woodcock Hill, Harefield Road, Rickmansworth, Hertfordshire, England.

Enzyme immunoassay microtitre plates were purchased from Nunc, PO Box 280, Kamstrip, Roskilde, Denmark.

Fluorescent microscopy was carried out on a Nikon Eclipse TE300 fluorescent microscope. Samples were visualised with an FITC cube under magnifications of 20×, 40× and a 60×, N. A. 1.3, oil immersion lens.

Homogenisation of Chinese hamster ovary cells was carried out using a 1 ml Potter-Elvehjem glass tissue homogeniser (clearance 0.1mm).

2.3 Methods

2.3.1 General methods

Phosphate-buffered saline: All phosphate-buffered saline (pH 7.4) used was according to Dulbecco 'A' formulation (Oxoid), as shown in Table 2.1.

Sodium chloride	8.0g/l
Potassium chloride	0.2g/l
Disodium hydrogen phosphate	1.15g/l
Potassium dihydrogen phosphate	0.2g/l
pH	7.4

Table 2.1 *Composition of PBS used on all occasions.*

2.3.1.1 Bicinchoninic acid (BCA) assay

10 µl of protein (tissue) sample to be assayed were placed in wells of a 96 well microtitre plate (Nunc). 190µl of BCA reagent (Pierce) (50 parts reagent A to 1 part reagent B) were added and incubated at 37^0C for 1 hour. The absorbance was read on a Titretek Twin reader Plus at 562nm and compared to a set of protein standards from 0 to 2 mg/ml.

2.3.1.2 Preparation of buffers for capillary electrophoresis

Phosphate buffers: Phosphate buffers were made by making an appropriate amount of each acid (NaH_2PO_4) and base (Na_2HPO_4) component, and titrating against each other until the desired pH was obtained.

Borate buffers: Made by dissolving a measured amount of sodium tetraborate in ultra-pure water for the desired molarity, and adjusted to the correct pH using NaOH.

Sucrose/HEPES buffers: These were prepared from stock solutions of both 100mM HEPES and 250mM Sucrose using the formula **(1)** to determine the required volumes to obtain the final concentrations desired. pH adjustments were made using NaOH.

$$V_1C_1 = V_2C_2 \qquad \textbf{(1)}$$

Tris/Borate buffers: Made by dissolving the correct amount of Tris-HCl and sodium tetraborate in ultra-pure water to achieve the desired molarity. pH adjustments were made with NaOH.

Glycine buffer: For affinity purification of FITC-labelled antibodies, glycine buffer, pH 2.8, was prepared by addition of 1.6 ml of 12 molar HCl to 190 ml ultra-pure water. This was then adjusted to pH 2.8 by addition of solid glycine, and the final solution made up to 200 ml.

2.3.1.3 Preparation of mobile phases for HPLC

HPLC mobile phases: For analysis by HPLC, mobile phases were made by mixing the relevant solvents (HPLC grade methanol and acetic acid, and water) thoroughly in a 1l Duran bottle and degassing prior to use. All mobile phases were used within 6 hours of preparation.

2.3.2 Determination by HPLC of the UDP-Glucuronyl transferase activity for 7-hydroxycoumarin in rabbit tissue samples

2.3.2.1 Tissue preparation

Organs were obtained from a New Zealand White Rabbit and stored at -20°C until required. The tissues prepared were from the liver, kidney, bladder, large intestine, lung, spleen, heart and fat. Table 2.2 shows the reaction mixture used for the assay. A 1g sample of each organ was weighed and homogenised in 10 ml of 50mM Tris-HCl, pH 7.4. The protein concentration in each organ was determined by Bicinchoninic acid (BCA) assay. A reaction mixture was set up and incubated at 37°C. Samples were taken every 15 mins from time 0 to 120 minutes. The reaction was terminated by addition of 200 µl of reaction mixture to 40 µl of 20% (w/v) trichloroacetic acid. This mixture was centrifuged in a benchtop centrifuge at 8000g for 5 minutes prior to analysis to remove the protein.

Component	*Stock solution concentration*	*Volume (µl)*	*Final concentration*
7-hydroxycoumarin	6.17mM	500	0.771mM
Enzyme prep.	10mg/ml	1000	2.5mg/ml
D-Saccharic acid-1,4-lactone	50mM	500	6.25mM
UDPGA	50mM	25	1.25mM
Absolute ethanol	----	100	----
$MgCl_2$	1mM	125	$6.25x10^{-6}$M
Tris-HCl (pH 7.4)	1M	500	125mM
Ultrapure Water	----	1250	----

Table 2.2 *Reaction mixture used for the uridine diphosphate glucuronyl transferase (UDPGT) assay.*

2.3.2.2 Preparation of Standards for HPLC UDPGT assay

A 1 mg/ml stock solution of 7-hydroxycoumarin was prepared in 10% methanol / 90% water and the 1 mg/ml stock solution of 7-hydroxycoumarin-glucuronide was prepared in ultra pure water. The internal standard used was 4-hydroxycoumarin and was prepared in methanol. The standards used for determining concentration of analytes were 0, 1, 5, 10, 20, 50, 80, 100 and 200 μg/ml.

2.3.2.3 HPLC Separation

Gradient elution was used for analysis. The solvents employed were A, water-methanol-acetic acid (950:50:2, v/v) and B, 100% methanol. The eluent was monitored at 320 nm. Sample (20 μl) was injected onto the column using the autosampler. The 1 ml/min gradient was as follows: 0-5 min 100% A → 50% A : 50% B ; 5-14 min 50% A : 50% B ; 14-15 min 50% A : 50% B → 100% A.

2.3.3 *In vitro glucuronidation of 7-hydroxycoumarin and determination of 7-hydroxycoumarin and 7-hydroxycoumarin glucuronide by capillary electrophoresis.*

2.3.3.1 Uridine diphosphate glucuronyl transferase (UDPGT) assay

Seven organs (liver, kidney, large intestine, lung, spleen, heart and fat) were obtained from New Zealand White Rabbit and stored at -20^{0}C until required. A 1g sample of each organ was weighed and homogenised in 10 ml of 50 mM Tris-HCl, pH 7.4. The resulting homogenate was adjusted to 10mg/ml (mg wet weight of organ/ml of buffer). This constituted the protein solution to be used in the reaction solution. The protein concentration in each was determined by Bicinchonnic acid (BCA) assay, after dialysis of an aliquot of protein solution in 50 volumes of phosphate buffered saline solution (PBS) overnight at 4^{0}C. A standard curve was constructed from a range of standards, 0 – 2 mg/ml, bovine serum albumin (BSA), prepared in PBS.

Table 2.2 shows the eight components necessary for the reaction, along with the respective volumes. A 1 mg/ml solution of 7-hydroxycoumarin was prepared in 10% ethanol : 90% ultra-pure water. All other solutions were prepared in ultra-pure water. Reactions were carried out in 10 ml blood tubes. The reaction was initiated by addition of 1ml of the protein solution, to make a final reaction volume of 4 ml. The reaction was incubated in a dark oven at 37^{0}C, and terminated by adding 50 µl of acetonitrile (Analar grade) to 150 µl of reaction mixture. This was then centrifuged at 8000g to remove the protein and any other material that might interfere with analysis. The supernatant was then immediately analysed.

2.3.3.2 β-Glucuronidase assay

A 1g sample of each organ assayed for presence of β-glucuronidase activity was weighed out and homogenised in 10 ml of 100 mM acetate buffer, pH 4.3. This constituted the protein solution to be used in the reaction. Protein determinations were made as for the UDPGT

assays, using the BCA kit (section 2.3.2.1). Table 2.3 outlines the reaction components necessary for the β-glucuronidase assay.

Component	Stock solution concentration	Volume (µl)	Final concentration
7-hydroxycoumarin	6.17 mM	40	1.76 mM
Enzyme prep.	10 mg/ml	40	2.86 mg/ml
Acetate buffer, (pH 4.3)	100 mM	60	42.86 mM

Table 2.3 *Reaction components and concentrations for the β-glucuronidase assay.*

2.3.3.3 Reaction solution for β-glucuronidase assay.

Table 2.3 lists the components used. The reaction was prepared to a final volume of 140 µl and allowed to continue for 30 minutes at 37^0C in a dark oven until it was stopped by the addition of 50 µl of 50mM D-saccharic acid-1,4-lactone (β-glucuronidase inhibitor). 50 µl of acetonitrile was then added and the solution centrifuged at 8000g for 5 mins. The supernatant was immediately analysed.

2.3.3.4 Controls

For the β-glucuronidase assay control a reaction solution similar to each of the tissue preparations was made with the addition of 50µl of D-saccharic acid-1,4-lactone to the reaction *before* the addition of 7-HCG (to prevent 7-HCG breakdown) and the reaction monitored after 30 minutes. In the case of all controls monitored, there was no breakdown to 7-HC observed. A similar control was prepared for the UDPGT assay. A reaction solution

was prepared with the protein precipitated out of solution by acetonitrile before addition of the UDPGA with monitoring for glucuronide after 30 minutes. There was no detectable production of the glucuronide in each of the controls monitored.

2.3.3.5 Standard curve preparation.

UDPGT assay: A range of standards were prepared consisting of 0 - 200 µg/ml of 7-hydroxycoumarin, prepared in 10% ethanol : 90% ultra pure water (v/v), and 7-hydroxycoumarin glucuronide prepared in ultra-pure water. 20 µl of each were spiked into 40 µl of 1M Tris-HCl, pH 7.4, 50 µl of acetonitrile and 40 µl of each protein solution. The resulting mixture was vortexed and centrifuged to remove the protein. Previous CE studies have used denaturation of protein solution by boiling to remove any interference due to endogenous β-glucuronidase present. However, in this case it was decided to remove the protein as this avoids any further reaction of any type in the mixture prior to analysis which might otherwise affect the results. The amount of 7-HCG produced was calculated from a plot of 7-HCG concentration standards versus absorbance (peak height).

β-glucuronidase study: The standard curve for the β-glucuronidase study was prepared from solutions that consisted of 40 µl of 7-hydroxycoumarin and 7-hydroxycoumarin glucuronide standards, 60µl of 100mM acetate buffer, pH 4.3, 50 µl of D-saccharic acid-1,4-lactone and 100 µl of enzyme solution, (either β-glucuronidase or homogenate). Immediately, 50 µl of acetonitrile was added to precipitate out the protein which was then centrifuged and removed as before. Concentrations of 7-HC and 7-HCG were calculated from plots of concentration versus absorbance (peak height).

For calculation of β-Glucuronidase activity in units/g wet mass of whole organ, the activity for each organ was compared to that of β-glucuronidase obtained from Sigma and from this the activity in units/g wet weight of organ could be determined. A standard curve with 0 – 10,000 units of β-glucuronidase incubated for 30 minutes with 200 µg/ml 7-HCG was prepared and used to calculate activities.

2.3.3.6 CE separation

Separation was carried out on a P/ACE System 5500 CE instrument, with detection by a P/ACE UV absorbance detector using a 27 cm untreated fused silica capillary, 50 μm ID, 375 μm OD, (19.3 cm capillary inlet to detector distance). Prior to running samples, the capillary was conditioned with 0.1M HCl for 10 minutes, 0.1M NaOH for 10 minutes and finally 100mM phosphate buffer, pH 7.0, for 10 minutes. The capillary was conditioned between each run by a 3 minute rinse with 100 mM phosphate buffer. Samples were applied by 8-second pressurised injection at 0.5 psi. Separation was achieved at 17.5 kV, 25^0C, with detection at 320 nm. Typical running current was 150 μA.

2.3.4 Determination of 7-hydroxycoumarin and its glucuronide and sulphate conjugates in liver slice incubates by capillary zone electrophoresis

2.3.4.1 Synthesis of 7-hydroxycoumarin sulphate

7-hydroxycoumarin (200mg, 1.23 mmol), *tetra-n*-butylammonium hydrogen sulphate (627mg, 1.85 mmol), and dicyclohexylcarbodiimide (2.5g, 12.1 mmol) were combined in dry pyridine (15 ml), stirred to effect solubilisation, and the reaction left at 5^0C for 5 days. The reaction mixture was then diluted with an equal volume of methanol and filtered. The filtrate was evaporated to give an oil that was treated with methanol (20 ml). This was concentrated to ~10 ml and filtered again. The methanol filtrate was then applied to a lipophilic Sephadex LH-20 column (2.5 x 18 cm) equilibrated in methanol. The column was eluted with methanol, and after collecting 40 ml of eluant the sulphate was collected over the next 30 ml. This latter fraction was concentrated to 5-10 ml, and 1M potassium hydroxide in methanol (1.1 ml) was then added. After cooling in an ice bath, the crystals were filtered off, washed with cold methanol and dried under vacuum.

2.3.4.2 NMR analysis of 7-hydroxycoumarin sulphate

For NMR analysis 20 mg of 7-hydroxycoumarin sulphate was dissolved in D_2O and analysed using a 400MHz AC NMR Spectrophotometer.

2.3.4.3 IR analysis of 7-hydroxycoumarin sulphate

For IR analysis, 15 mg was mixed with potassium bromide (KBr), pressed between KBr plates and analysed using a Nicollet Infra Red Spectrophotometer.

2.3.4.4 *Liver slice preparation and incubation*

Liver was obtained from Balb\C mice and stored at -20^{0}C until required. Liver slices were prepared using an 'in-house' made razor-bladed instrument based on that described by Krumdieck *et al.* (1980) (section 4.3.2.1), ensuring that the slices were submerged in buffer at all times during preparation. Incubations were carried out in blood tubes at 37^{0}C. Tissue slices were pre-incubated for 90 minutes at 37^{0}C in a warm room using a blood tube mixer with the revolving face of the mixer horizontal to ensure gentle mixing of the buffer. The slices were then incubated with 100 μM 7-hydroxycoumarin for 6-10 hours prior to analysis.

2.3.4.5 *Preparation of Krebs-Henseleit buffer*

Krebs-Henseleit buffer (pH 7.4) was made by addition of the ingredients listed in Table 2.4 to 250 ml of ultra-pure water. 0.42 ml of gentamycin sulphate (from a stock solution of 50 mg/ml) was added to the final solution to complete the buffer composition prior to use.

Compound	Weight (g)
Sodium chloride	1.725
Potassium chloride	0.090
Magnesium sulphate anhydrous	0.064
Monosodium phosphate anhydrous	0.036
d-Glucose	1.125
HEPES*	1.486
Calcium chloride dihydrate	0.425

*(N-[2-Hydroxyethyl]piperazine-N-[ethanesulphonic acid])

Table 2.4 *Composition of Krebs-Henseleit buffer for liver slice incubations.*

2.3.4.6 Preparation of standards

7-HC standards were prepared from a 1mg/ml stock solution prepared in ethanol and ultra pure water (10 + 90%, v/v). Both 7-HCG and 7-HS standards were prepared from a 1 mg/ml stock prepared in ultra pure water. All standards were diluted with Krebs-Henseleit buffer.

2.3.4.7 Capillary Electrophoresis separation

Separation conditions were as outlined in section 2.3.4.6.

2.3.5 Microchip capillary electrophoresis - Immunoassays for Warfarin and Parathion

2.3.5.1 Confirmation of antibody activity by ELISA

Nunc maxisorp immunoplates were coated with 100 µl of 50 µg/ml conjugate (warfarin/parathion-BSA) in PBS and allowed to coat overnight at room temperature. The wells were then washed with 5 × 200 µl of wash buffer (PBS-Tween) and the wells blocked with the addition of 100 µl of 5% (v/v) foetal calf serum in PBS. This was incubated for 90 minutes at 37^0C and then washed (5 × 200 µl of wash buffer). Different concentrations of warfarin/parathion) (24 – 790 ng/ml) and primary antibody (FITC-labelled/unlabelled), constant concentration, were added to each well and incubated for 90 minutes at 37^0C. The plate was then washed (5 × 200 µl of wash buffer), secondary antibody added (anti-rabbit labelled with alkaline phosphatase), and allowed to incubate for 90 minutes at 37^0C. The plate was washed again (5 × 200 µl of wash buffer) and the substrate added (para-nitrophenyl phosphate). The substrate was provided in tablet form and diluted in the required volume of ultra pure water prior to use. The plate was allowed to develop for 60 minutes at room temperature before reading the absorbance at 405 nm using a titretek plate reader.

2.3.5.2 Fluorescein isothiocyanate (FITC) labelling of Anti-Warfarin and Anti-Parathion antibodies.

The concentration of antibody solution was adjusted by the addition of BSA to give a final protein concentration of 4 mg/ml in 0.1M sodium carbonate buffer, pH 9.0. BSA was added as the labelling conditions used were optimised for 4 mg/ml solutions of protein. Labelling was carried out by mixing of antibody (in 0.1M carbonate buffer, pH 9.0) in an eppendorf tube with FITC (25.7 mM in DMSO) in 5 µl aliquots with vigorous vortexing between additions (giving a final concentration of 50 µg FITC added per mg of protein). The solution was then left in the dark at room temperature for three hours, before being dialysed against 1000 volumes PBS, pH 7.4, with 0.02% (w/v) sodium azide to remove any unreacted FITC.

2.3.5.3 Affinity purification of FITC-labelled antibodies

The antibody was purified from solution, which also contained labelled BSA, by protein G affinity purification (protein G immobilised on Sepharose 4B). The column was equilibrated with 20 ml of PBS (pH 7.4). 1 ml of antibody solution was added to the column, let run through, and the eluate collected.1 ml of PBS was then added to the eluate and this was run through the column again until just above the level of the solid support. This was repeated with another 4 ml of PBS added to the elute, followed by 25 ml of PBS only. The column was washed with 0.1M Tris-HCl buffer, pH 8.7, and eluted with 0.1M glycine buffer, pH 2.8, followed by dialysis into PBS. The column was equilibrated with PBS containing 20% (v/v) ethanol and stored at 4^0C.

2.3.5.4 Capillary Electrophoresis analysis of FITC-labelled antibodies

On-column CE-LIF analysis: Separation was carried out in a fused untreated silica capillary (27 cm × 50 μm ID × 375 μm OD, 19.3 cm to detector window). The samples were analysed on a Beckman CE P/ACE 5500 instrument with detection by a P/ACE LIF detector. Borate buffer, pH 9.0, was used as electrolyte buffer. All components were controlled by System Gold™ software. Separations were carried out at 16kV, 25^0C, using an argon-ion laser for detection with excitation at 488nm, and emission at 520nm. Typical running current was 6.1 μA

Microchip analysis: Both antibodies were analysed on chip. Analysis conditions were 5mM borate buffer, pH 9.0, as electrolyte. Injections were made for 10 seconds at 1.5kV, with a separation voltage of 6kV.

2.3.5.5 Labelling of BSA Conjugates.

The labelling of the BSA-parathion and warfarin conjugates was carried out in the same manner as the labelling of the antibodies as outlined in section 2.3.5.2, with the only change

being the protein concentration for the warfarin conjugate was 3.03×10^{-6}M, and 1.9×10^{-5}M for parathion conjugate. The concentration of FITC used was a five-fold excess of the relevant conjugate concentration. Following labelling, the reaction was dialysed overnight in 1000 fold PBS to remove unreacted dye. The resulting solution was stored at 4^0C.

2.3.5.6 Microchip immunoassay

For both parathion and warfarin on-chip immunoassay trials, 50 mM Tris/borate buffer, pH 8.5, was used with an injection time of 2.7kV and a separation voltage of 7.3kV.

2.3.6 Single liposome analysis using CE with post column LIF

2.3.6.1 Preparation of liposomes

Liposomes with lipid membrane compositions similar to the outer mitochondrial membrane were prepared. Stock solutions of each phospholipid and cholesterol were prepared in chloroform: 1.23×10^{-2}M phosphotidyl serine (PS); 1.3×10^{-2}M phosphotidyl ethanolamine (PEA); 1.29×10^{-2}M phosphotidyl choline (PC) and 2.5×10^{-2}M Cholesterol. The phospholipids PC, PS, PEA and cholesterol were combined in a ratio of 39:2:35:3 respectively in a 5 ml round bottom flask (total volume 790 µl each) and mixed thoroughly. The chloroform was evaporated under a stream of argon at room temperature. When all solvent was evaporated, 1ml of 10^{-6}M fluorescein in 10mM borate, pH 9.3, (for flourescently labelled liposomes), and 1ml of 10mM borate for blank liposomes was added to each respective flask, vortexed until all lipid components were in solution and then placed at 4^0C for 2 hours to swell. The liposomes were then washed by centrifuging at 13,800g for 5 minutes in a benchtop centrifuge, followed by removal of the supernatant and addition of an equal volume of milli-Q water. This wash step was repeated four times. The resulting liposome preparation was stored at 4^0C in the dark until needed. Stability of preparations was monitored by microscopy on a daily basis.

2.3.6.2 Grignard coating of capillaries for CE analysis

Day 1: Approximately 5 m of capillary was cut, wrapped around a water bottle, leaving about 15 cm at either end, taped together (ensuring that the tape is folded onto itself so that it can be removed following baking). The oven was set to 120°C and one end of the capillary was placed into the adapter attached to the nitrogen (N_2), placing the other end in water. The capillary was then rinsed as outlined in Table 2.5. When the rinses were finished, the outlet end of the capillary was put into the oven, keeping the nitrogen flowing through at 5 psi overnight.

Solution	*Time (hours)*	*Pressure (psi)*
1M NaOH	3	20
ddH_20	1	20
MeOH	1	20

Table 2.5 *Sequence for rinsing of fused silica capillary prior to coating.*

Day 2: The oven temperature was reduced to 65°C with the capillary still inside it, the capillary was then removed from the oven, each end trimmed about 1 cm and the outlet end placed in water. The capillary was rinsed with $SOCl_2$ (in a glass vial) for 30 minutes at 20 psi. When completed, both ends of the capillary were capped with pieces of GC septum, placed into the oven and baked for 6-8 hours (or overnight). This step was repeated 6 hours after the initial run in order to ensure removal of all SiOH groups.

Day 3: To ensure all glassware was dry it was placed in a warm oven before use (2 glass vials, a 5 ml volumetric flask and stopper, and a glass syringe with needle). 1 ml of 1M vinylmagnesium bromide was placed in a 5 ml volumetric flask and the flask filled to 5 ml with *dry* tetrahydrofuran (THF). The syringe was rinsed with THF, and a glass vial of dry THF for the outlet end of the capillary was also filled. The capillary was removed from the oven, about 1 cm was snipped from each end of the capillary and the outlet end put back in the oven (to prevent it from becoming blocked in the rinse step). The capillary was rinsed with the THF/vinylmagnesium bromide solution (in a glass vial) for 30 minutes at 20 psi - keeping the outlet end in the oven until the solution was observed exiting the capillary. The outlet end was then removed from the oven and placed in a vial of THF. Both ends of the capillary were capped with a GC septum and placed in the oven overnight.

Day 4: All glassware required was dried again as on day three. The glass vial was filled with dry THF, the capillary removed from the oven, and about 1 cm snipped from each end, placing the outlet end back in the oven. The capillary was rinsed with dry THF (in a glass vial) for 30 minutes at 25 psi, and the outlet end removed from the oven when liquid was seen exiting the end of the capillary. The entire portion of the capillary spool that

remained outside the oven during the procedure was cut off and discarded. The capillary was cut into the sizes required and flushed with water for 10 minutes at 20 psi.

3% acryloyl amino propanol (AAP) was polymerized by adding1µl TEMED, 4 µl of 10% (w/v) APS (must be fresh) and stirring. This pAAP solution was flushed through the capillaries for 10 minutes at 25 psi, then the N_2 flow was stopped, the pAAP vial switched to water and the capillaries feft to sit in water for 30 minutes. The N_2 was then turned on for a few minutes, flushing the capillaries with water. The capillaries' ends were stored in water until required.

2.3.6.3 CE-LIF analysis of liposomes

The post column detection CE-LIF used was constructed 'in-house' as outlined in section 6.1.2. Separations were carried out in a coated fused silica capillary, 50µm ID, 150 µm OD at 200Vcm^{-1}. Injections were performed at 50Vcm^{-1} for 5 seconds. Excitation was at 488nm with detection at 535DF35nm.

2.3.7 Mitochondrial analysis using CE-LIF

2.3.7.1 Labelling of mitochondria in whole cells

The mitochondria used in this study were isolated from Chinese Hamster Ovary (CHO) cells. A stock solution of 1 mM nonyl acridine orange (NAO) fluorescent dye (used to measure mitochondrial mass), 10 mM Rhodamine 123 and 10mM 5,5',6,6'-tetrachloro-1,1',3,3' tetraethylbenzimidazolylcarbocyanine iodide, JC-1, (used to measure mitochondrial activity) prepared in 100% DMSO were used to label the mitochondria in whole cells. CHO's were labelled at a final concentration of 10 μM NAO and JC-1, and 1 μM for Rhodamine 123, for 5 minutes at room temperature in cell growth medium.

2.3.7.2 Fluorescence microscopy analysis of stained cells

Following staining of whole cells as outlined above, the uptake and fluorescence of dye was monitored by fluorescence microscopy. 5 μl of stained cells was taken, placed on a glass slide, covered with a cover slip and analysed by light and fluorescence microscopy (FITC cube) prior to homogenisation.

2.3.7.3 Isolation of mitochondria from Chinese hamster ovary cells

Following labelling the mitochondria, 2 ml of cells [1 x 10^6 cells/ml] were homogenised on ice using a Potter-Elvehjem tissue homogeniser. Homogenisation was closely monitored by light microscopy to ensure minimal strokes for membrane disruption. The homogenate was centrifuged at 1300g for 5 minutes to remove nuclear and membranous material. The pellet was resuspended in ice cold 250mM sucrose and recentrifuged. Both supernatant fractions were combined to give a total post-nuclear supernatant (PNS) which was then centrifuged using differential gradient ultracentrifugation.

2.3.7.4 Differential gradient ultracentrifugation

A hybrid percoll/metrizamide discontinuous gradient was prepared in 250mM sucrose, pH 7.5. 2 ml of 35% (w/v) metrizamide (ρ = 1.1907) was overlaid with 2 ml of 17% (w/v) metrizamide (ρ = 1.1079) which in turn was overlaid with 5 ml of 6% (v/v) percoll (ρ = 1.0406). Gradients were prepared in Labcor 16 ml ultracentrifugation tubes. The PNS was gently overlaid on top. Centrifugation was carried out at 50,000g for 15 minutes 4^0C with the brake setting at zero. Following centrifugation, the required fraction area/interface was carefully removed using a blunt ended needle and stored at 4^0C in the dark prior to analysis.

2.3.7.5 Analysis of mitochondria by CE

Analysis was carried out on an in-house built instrument with post column laser-induced fluorescence detection. Injections were performed electrokinetically and hydrodynamically. Hydrodynamic injections were performed by raising the sample vial to a height above the waste (outlet) reservoir until a background identical to that for an electrokinetic injection was obtained (i.e. the bulk flow from the capillary was identical for both injection modes). Both coated and uncoated capillaries were used for analysis.

2.3.8 Mitochondrial protein analysis

2.3.8.1 3,(2-furoyl)-quinoline-2-carboxaldehyde, FQ, labelling of molecular weight markers and protein samples

To label the molecular weight markers, 3,(2-furoyl) quinoline-2-carboxaldehyde, (FQ), was dissolved in methanol at a concentration of 10 mM and lyophilised in 10 µl aliquots in 500 µl vials. 9 µl of protein standard (10^{-3}M) was added to one of these vials and placed in a bath at 65^0C. The reaction was initiated by addition of 1 µl of 25 mM potassium cyanide (KCN) (in water). Protein samples isolated from mitochondria were labelled in the same manner.

2.3.8.2 Isolation of mitochondria from Chinese Hamster Ovary Cells

Mitochondria were prepared in the same manner as detailed in section 2.3.7.3 and 2.3.7.4, without the addition of fluorescent stain to the washed cells.

2.3.8.3 Purification of protein from mitochondria

Protein was purified from isolated mitochondria as follows: 0.1 ml of sample was treated with 0.4 ml of methanol and vortexed. This was then centrifuged for 10 min at 9000g. 0.1 ml of chloroform was added, vortexed and centrifuged at 9000g for 10 min. 0.3 ml of water was then added, the solution vortexed, centrifuged for 1 min at 9000g and the upper phase removed. 0.8 ml of methanol was added, vortexed, and centrifuged again for 2 min at 9000g, The supernatant was removed and the pellet dried under a stream of air. The final protein pellet was lyophilised and stored at -20^0C until required.

2.3.8.4 Capillary gel electrophoresis of mitochondrial protein

For analysis of mitochondrial protein the coated capillary was filled with 5% (w/v) dextran (Mol. Wt. 185,000), 6.7mM SDS and 5mM HEPES, pH 7.50. All samples were denatured at 95^0C for 5-mins prior to analysis. Injections were made for 20 seconds at $50Vcm^{-1}$ and separations were performed at $400Vcm^{-1}$.

3 HIGH PERFORMANCE LIQUID CHROMATOGRAPHY APPLIED TO THE ANALYSIS OF COUMARIN METABOLISM

3.1 Introduction

Liquid chromatography is the generic name used to describe any chromatographic procedure in which the mobile phase is a liquid. It includes thin layer chromatography (TLC), paper chromatography and the various types of column chromatography involving gravity fed columns. The beginnings of chromatography are attributed to Tswett, who in 1903 reported on the separation of chloroplast pigments into a series of coloured bands on a packed column (Bidlingmeyer, 1992). Bidlingmeyer (1992) gives a table outlining the important advances in chromatography from 1903 until the appearance of the first commercial instrument in 1969. It was in the late 1960s and early 1970s that high performance liquid chromatography (HPLC) became well established as developments and refinements to the instrumentation took place as well as an increase in applications (Brown, 1989). Today most biochemical and biomedical laboratories use HPLC routinely for analysis of a wide variety of analytes, with molecule sizes varying from the very small (MW 100) to hundreds of thousands. A major step in the development of HPLC came with its automation enabling the generation of a large amount of very reproducible data in a relatively short time.

3.1.1 Instrumentation

Although there are now a variety of manufactures producing HPLC systems, the basic layout is mostly the same. Most instruments produced incorporate the following components; one or more solvent reservoirs, a pumping mechanism to deliver the mobile phase, valves or loops for sample injection, a separation column, a guard column to prevent contamination of the separation column by small particles and finally a detector unit. A schematic of a basic HPLC unit is shown in Figure 3.1. A similar configuration was used for the work described later in the chapter

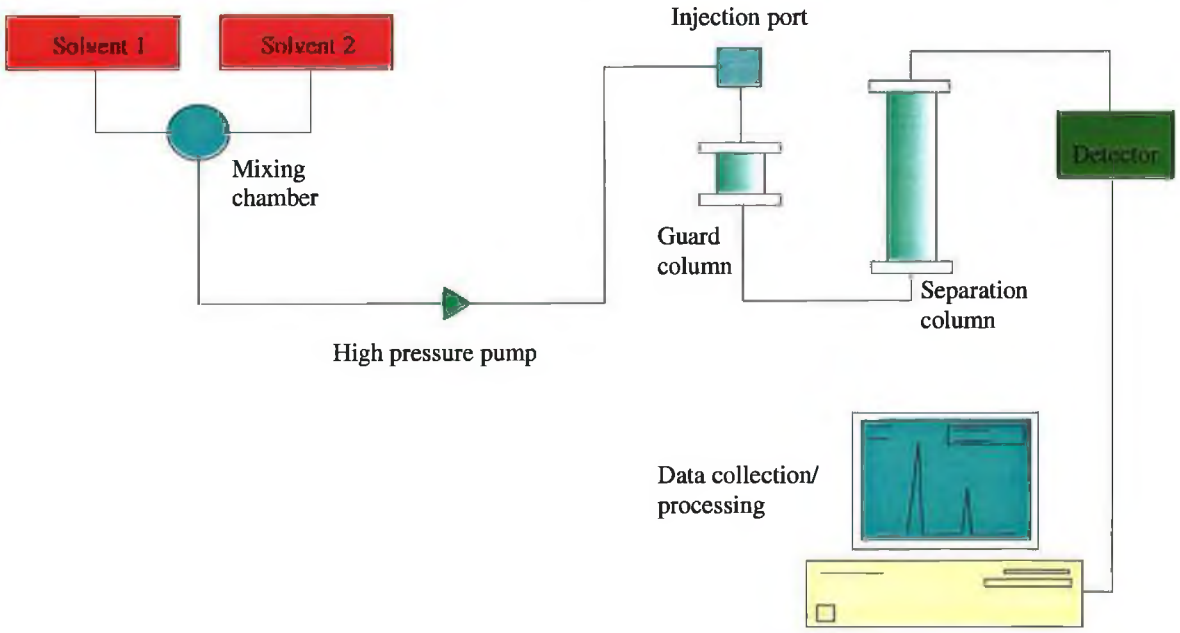

Figure 3.1 *Schematic of HPLC used for analysis of rabbit tissue samples*

3.1.1.1 Mobile phase delivery systems

The mobile phase must be delivered to the column over a wide range of flow rates and pressures. To permit the use of a wide range of inorganic and organic solvents, the pump, its seals and all connections must be made of materials chemically resistant to the mobile phase. Of the many types of pump design currently in use (syringe type, constant pressure), the reciprocating piston type is the most popular, involving a small motor driven piston which moves rapidly back and forth in a hydraulic chamber that may vary in capacity from 35 to 400µl in capacity (Knox, 1982). This type of pumping induces pulses, which are damped out using a flexible bellows or a compressible gas in the capped upright porting of a T-tube to take up some of the pulsation energy. When the pump refills, this energy is released to help smooth the pressure pulsations. Pressures in excess of 1000psi are required for effective operation. Pulse dampers that use a compressible fluid separated from the mobile phase by a flexible inert diaphragm offer several advantages including easy mobile phase changeover, effectiveness at low system pressure, wide dynamic range, and minimal dead volume. In this type of pulse damper, the compressible fluid expands when the pump system retracts, maintaining system pressure and constant solvent flow (Willard *et al.,* 1988).

3.1.1.2 Sample injection

Insertion of the sample onto the pressurised column must be as a narrow plug so that the peak broadening attributable to this step is negligible. The injection system itself should have no dead (void) volume. Most systems today are automated and sample injection onto the column is achieved without the use of syringes. Loop or valve injection is very rapid and can operate at pressures up to 470 atm with less than 0.2% error (Willard *et al.,* 1988). The system can be located within a temperature-controlled environment for systems that require handling at elevated temperatures. The method of injection for the work presented in this chapter used an autosampler with needle uptake into a 20 µl sample loop.

3.1.1.3 Separation column

Columns for HPLC are constructed of heavy wall, glass lined metal tubing, or stainless steel tubing to withstand high pressures (up to 680 atm) and the chemical action of the mobile phase. Column end fittings and connectors must be designed with zero void volume to avoid contributing to band broadening. Most column lengths range from 10 – 30 cm long, short, fast columns are 3 – 8 cm long. For the work described in this chapter column length was 30 cm constructed from stainless steel tubing. Many HPLC separations are done on columns with an internal diameter of 4 – 5 mm providing a good compromise between efficiency, sample capacity and the amount of packing and solvent required. Column packings feature particles that are uniformly sized and mechanically stable with diameters in the range of 3 –5 µm, occasionally up to 10 µm or larger for preparative chromatography (Snyder *et al.,* 1988).

3.1.1.4 Detection

Today there are a number of different detection formats available for HPLC including ultra violet-visible (UV-Vis) and fluorescence. Optical detectors based on UV-Vis adsorption are by far the most common format in use (Willard *et al.,* 1988). Basically three types of absorbance detectors are available: a fixed-wavelength detector, a variable–wavelength

detector, and a scanning ('real-time') detector. These systems have become so refined that fundamental noise limitations now originate from thermal instabilities in flow cells and in the optical and electrical components (Skoog *et al.,* 1998). Detector cell volumes on the order of 8 μl per centimetre of optical path length are acceptable for conventional-diameter separation columns. The detector used in the work presented in this chapter is the UV-Vis type with variable wavelength detection.

3.1.2 Optimisation of HPLC separations

Before analysis, in order for the best resolution to be achieved, the instrument must first be optimised for the separation being undertaken. While almost every separation reported in the literature lists conditions that require optimisation specific for the application, there are a number of precautions and steps that apply to all situations. These include temperature effects, viscosity and extra column band broadening, all of which were optimised for the system used in this chapter prior to analysis of samples.

3.1.2.1 Temperature effects

In many HPLC analysis, variations in temperature can cause significant changes in retention times, making qualitative analysis difficult and affecting the precision of quantitative measurements. Elevated temperatures are advantageous because of decreased mobile phase viscosity, increased mass transfer, and increased sample solubility result in either better resolution or faster analysis.

3.1.2.2 Viscosity

A solvent with low viscosity is always preferred in HPLC (Braithwaite and Smith, 1985). While maintaining constant pressure drop across the column, an increase in the viscosity of the solvent always decreases the flowrate of the mobile phase. To overcome this application of more pressure to maintain the flow rate is required, which can produce heat, and may have

a detrimental effect on the separation. There is also a practical limit to the pressure that can be applied to maintain flow rates determined by the packing material and column construction. The diffusion coefficients of solutes are also affected by the viscosity of the mobile phase. For the mobile phase used in this chapter the use of methanol ensured low viscosity, making the desired flow rate (1 ml/min) easily achievable without the need to lower the viscosity further.

3.1.2.3 Extra column band broadening

Extra column band broadening is caused by dilution factor the injector, column (dead) void spaces, the volume of connecting tubing before and after the separation column, and the detector volume. Any band spreading from these factors is added to the random dispersion within the separation column. For symmetrical solute elution bands, these factors are additive as variances:

$$\sigma^2_{tot} = (\sigma^2_{inj} + \sigma^2_{trans} + \sigma^2_{det}) + \sigma^2_{column}$$

Where σ_{tot} = total dispersion factor.

σ_{inj} = dispersion contribution from the injection.

σ_{trans} = dispersion contribution from the tubing.

σ_{det} = dispersion contribution from the detector.

σ_{column} = dispersion contribution from the column.

In order to neglect the variances from the terms within the parentheses, they must collectively amount to less than half the column variance at the flow velocities needed for HPLC (1 ml/min in this application). With the use of narrow bore columns, the detector volume must be 2 - 3µl to ensure the separations achieved within the separation are not lost through band spreading within the detector (Willard *et al.,* 1988). For the instrument used in this chapter all

tubing length before and after the separation column was minimised, the column set vertical and all connections carefully checked for correct fit and seal.

3.1.3 Solvent programming

A separation using a single solvent of constant composition is termed an isocratic elution (Skoog *et al.,* 1998). However, for the work carried out in this chapter a gradient profile was used. This technique involves the use of two solvents differing significantly in polarity and in the course of the separation the ratio of the two solvents combining to make up the mobile phase is varied according to a profile entered by the operator. This can be carried out by introducing both solvents into a mixing chamber at varying rates (Fig 3.1). Section 2.3.2.3 details the gradient profile used for analysis of coumarin metabolism in section 3.2. The optimum gradient for a particular separation is selected by trial and error, following selection of the solvents based on theory, as the case with the work presented later in this chapter. The use of gradient elution means it is possible to obtain both maximum resolution and sensitivity for every solute in the sample (Willard *et al.,* 1988).

3.1.4 Reverse phase chromatography

Reverse phase is one type of the many formats of chromatography available to HPLC. Reverse phase chromatography, as used for this work, uses a hydrophobic bonded packing, usually with an octadecyl (C-18) or octyl (C-8) functional group and a polar mobile phase, often a partially or fully aqueous mobile phase. Polar substances prefer the mobile phase and elute first. As the hydrophobic character of the solute increases, retention increases. Generally the lower the polarity of the mobile phase, the higher is its elution strength (Synder *et al.,* 1988). Hydrocarbons are retained more strongly than alcohols, thus water is the weakest eluent. Methanol and acetonitrile are popular solvents because they have low viscosity and are readily available with excellent purity (Biblingmeyer, 1992). Eluents intermediate in strength in between these solvents and water are obtained by preparing mixtures. Since the optimum composition of the mobile phase must generally be found by trial and error, it is sometimes convenient to start with a 1:1 water methanol mixture. If the

sample components elutes at or near the transit time of a non-retained solute, t_M, a lower concentration of methanol is indicated. Changing to acetonitrile, dioxane, or mixtures of 1,4-dioxane/methanol or acetonitrile/2-propanol can also improve selectivity (Skoog *et al.,* 1998). In reverse phase chromatography, solvent gradients are generated by a continuous decrease in the polarity of the eluent during the separation – for example by gradually increasing the organic solvent content in water/methanol or water/acetonitrile mixtures.

3.1.4.1 Mechanism of reverse-phase chromatography

When a solute dissolves in water, the strong attractive forces between water molecules get distorted or disrupted. These attractive forces arise from the three dimensional network of intermolecular hydrogen bonds. Only highly polar or ionic solutes can interact with the water network (Biblingmeyer, 1992). Nonpolar solutes are "squeezed out" of the mobile phase but bind with the hydrocarbon moieties of the stationary phase. In reverse-phase chromatography the driving force for retention is not the favourable interaction of the solute with the stationary phase, but rather the effect of the mobile-phase solvent in forcing the solute onto the hydrocarbonaceous bonded layer (Skoog *et al.,* 1998). In opposition is the interaction of the solutes polar groups with the mobile phase. As a result, hydrophobic retention involves mainly nonpolar substances or the nonpolar portion of molecules. Hydrophobic retention can be lessened by adding to water any organic solvent that is miscible with water. The less polar the added solvent the greater the effect.

3.2 Determination by reverse-phase HPLC of the UDP-glucuronyl transferase activity for 7-hydroxycoumarin in rabbit tissue samples

3.2.1 Coumarin metabolism

Section 1.2.4 outlined the metabolism of coumarin and the major phase I pathway in humans. In this chapter HPLC is used to examine the metabolic fate of the phase I metabolite, 7-hydroxycoumarin (7-HC) in various rabbit tissue samples, and to examine the rate of its metabolism. Analysis of these samples would provide information on inter-organ differences in the metabolism of 7-HC. The results would also provide a comparison for the CE method applied to a similar study (except for the bladder) in chapter 4.

3.2.2 Sample preparation

Eight different rabbit organs were chosen including liver, kidney, heart, lung, spleen bladder, large intestine, and fat. Samples were prepared from each organ as outlined in section 2.3.2.1 and incubations set up for metabolism of 7-HC. The protein concentration for each organ sample was calculated as outlined in section 2.3.1.1. The values obtained are shown in Table 3.1.

Organ	*Protein concentration (mg/ml) used in incubations*
Liver	0.77
Kidney	1.10
Heart	1.04
Lung	1.76
Spleen	1.66
Large intestine	1.35
Fat	0.00
Bladder	0.35

Table 3.1 *Protein concentrations for each of the organs analysed for uridine diphosphate glucuronyl transferase UDPGT activity*

3.2.3 Development of HPLC Separation

3.2.3.1 Separation column

For the separation of polar molecules, reverse phase chromatography (section 3.1.4) with the use of a non-polar stationary phase is the method of choice. For the application here a C_{18} column was used as it had been reported with success in the method of Killard *et al.* (1996) for separation of the same compounds.

3.2.3.2 Mobile phase and gradient profile

Section 3.1.2 outlines the preliminary checks made to the instrument prior to development of the method. A reverse-phase gradient HPLC method was adapted from that of Killard *et al.*, (1996). Development of the gradient elution profile was carried out by analysing a series of standards under different conditions until the optimum separation of analytes was achieved. Using a gradient profile has the effect of increasing the retention time of the glucuronide, moving it away from the void volume. Figure 3.2 shows the resolution obtained with the glucuronide (7-HCG) eluting at 8.3, 7-hydroxycoumarin (7-HC) at 10.4, and internal standard (4-hydroxycoumarin, 4-HC) at 12.2 minutes, respectively.

The choice of solvents used for the separation was selected because they had been successfully used previously by Egan and O'Kennedy (1992) and Sharifi *et al.* (1993). The composition of the mobile phase was Methanol: Water: Acetic Acid (950: 50: 2 v/v). The gradient profile was as follows: 0.5 min 100% A $\rightarrow$ 50% A: 50% B, 5 – 14 min 50% A: 50% B, 14 – 15 min 50% A: 50% B $\rightarrow$ 100% A. This profile represents a decrease in retention time by more than 8 minutes for the internal standard, 4-HC, and a 4 and 6 minute decrease for 7-HCG and 7-HC, respectively, over the method of Killard *et al.* (1996). Baseline resolution is still maintained between each peak (Fig 3.2)

3.2.3.3 Detection

Previous HPLC methods for analysis of coumarins used 320 nm as the detection wavelength of choice (Killard *et al.*, 1996). While the coumarins will absorb more strongly at lower wavelengths in the spectrum, detection at these wavelengths (214 nm) is hampered by absorbance from other species present in the matrix, making the lower wavelengths only suitable for analysis of pure samples of coumarins. Hence 320 nm was used here as the detection wavelength.

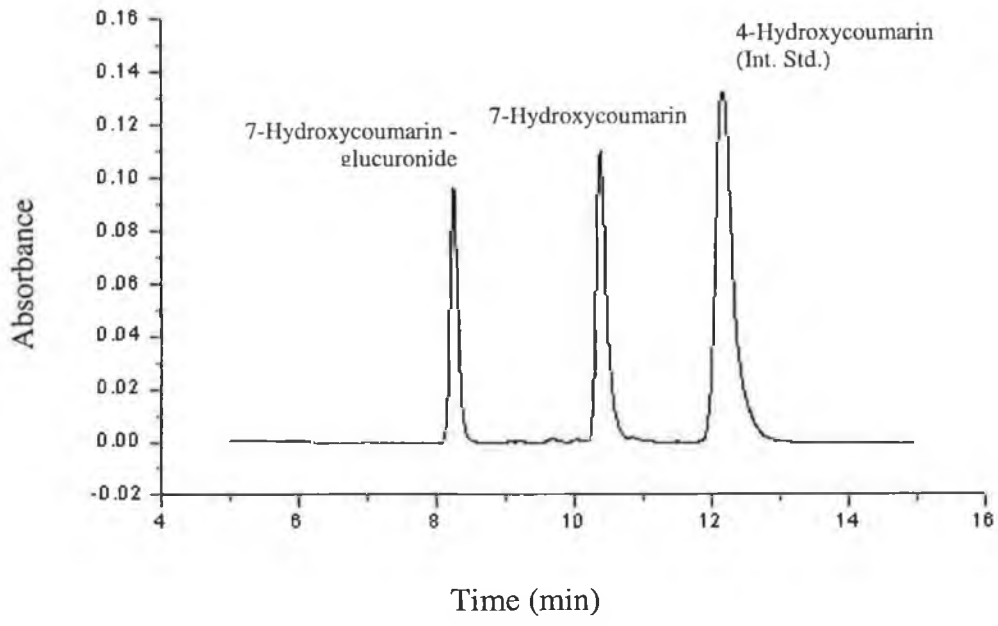

Figure 3.2 *Chromatogram showing separation of standards, 7-hydroxycoumarin, 7-hydroxycoumarin glucuronide and the internal standard, 4-hydroxycoumarin, in incubation medium, using reverse phase gradient elution chromatography (1 ml/min flow rate) with detection at 320 nm.*

3.2.4 Glucuronidation of 7-hydroxycoumarin by UDPGT

Section 1.2.4.1 outlined the metabolism involved in glucuronidation of 7-hydroxycoumarin (7-HC) with the enzyme UDPGT. There are few methods that allow the direct determination of 7-hydroxycoumarin-glucuronide (7-HCG) without deconjugation (Sharifi *et al.*, 1993; Killard *et al.*, 1996). However, with the method applied here the metabolite of 7-hydroxycoumarin, 7-hydroxycoumarin glucuronide, was monitored over time and its increase could be seen clearly (Fig. 3.3). The determination of 7-hydroxycoumarin (7-HC) or its metabolite allows a calculation of the metabolic rate of the reaction for the tissue in question. The pathway by which 7-HC is metabolised to 7-HCG is shown in Figure 1.1.

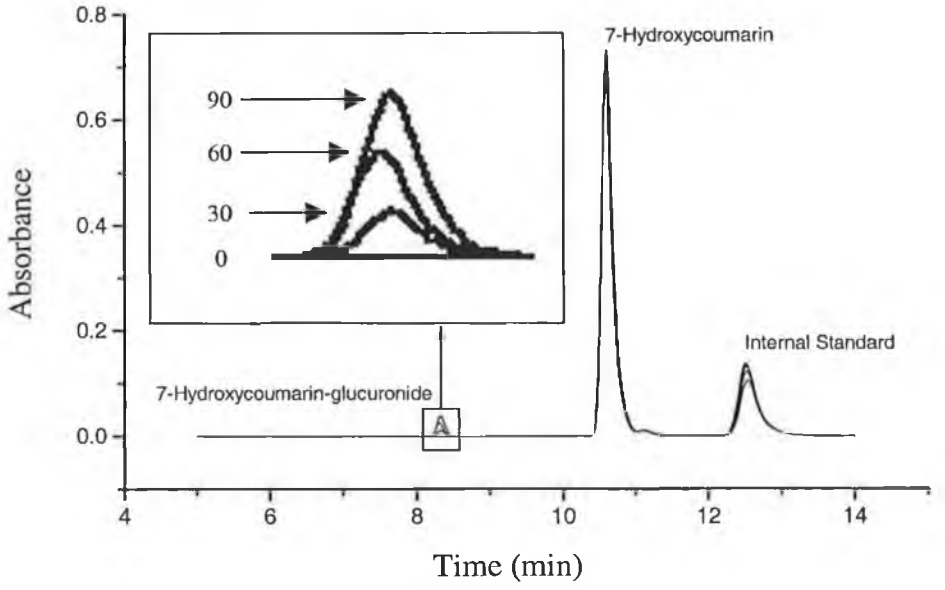

Figure 3.3 *Overlay of four chromatograms of kidney reaction mixture showing analysis for 7-hydroxycoumarin-glucuronide at time 0, 30, 60, and 90-min. HPLC conditions were as for Figure 3.1.*

Eight organs; liver, kidney, large intestine, bladder, lung, spleen, heart and fat were selected for the study. UDPGT activity was not observed in all tissues. The highest activity was observed in the liver, followed by the kidney and bladder. A very low level of 7-HCG production was observed in the large intestine with trace amounts of 7-hydroxycoumarin-

glucuronide observed for the spleen and lung after 90 minutes. The fat and heart tissue showed no detectable activity.

3.2.5 Analysis of results

The amount of 7-HCG produced was calculated using peak height ratios (7-HCG over internal standard) from a standard curve prepared as outlined in section 2.3.2.2. Tables 3.2 and 3.3 show the amount of 7-HCG produced at each time interval of sampling with the standard deviation and coefficient of variation (C.V.). C.V. was calculated using the formula:

$$C.V = \frac{S.D.}{mean} \times \frac{100}{1}$$

3.2.5.1 Rate of reaction for each organ

A plot of the mean 7-hydroxycoumarin-glucuronide concentration produced (n=3) versus time was used to calculate the activity of UDPGT in the tissue (Table 3.4). The rate of reaction was calculated from the linear part of the curve (Fig. 3.4) using the formula shown below.

$$Rate\ of\ reaction = slope \div [protein] \div molecular\ weight$$

Where: *slope* = slope of the linear portion of the graph

[*protein*] = protein concentration of the organ (Table 3.1)

Molecular weight = molecular weight of 7-HCG (338.14)

The liver and kidney produced appreciable quantities of 7-hydroxycoumarin-glucuronide with relative activities of 2300 and 220 pmol of 7-hydroxycoumarin-glucuronide produced per minute per milligram of protein, respectively. The bladder showed an activity of 140 pmol of 7-HCG produced per minute per milligram of protein, with a very low level of

activity in the large intestine of 7.8 pmol of 7-HCG produced per minute per milligram of protein.

Time (min)	Mean (n=3) 7-HCG concentration (μM) ± S.D.		C.V.	
	Kidney	*Liver*	*Kidney*	*Liver*
0	00.00 ± 0.00	00.00 ± 0.00	0.0	0.0
15	02.40 ± 0.09	02.50 ± 0.40	3.7	1.5
30	05.30 ± 0.20	49.60 ± 3.30	4.0	6.6
45	10.30 ± 0.04	81.50 ± 2.80	4.3	3.4
60	12.60 ± 0.60	102.0 ± 3.46	4.9	3.4
75	17.30 ± 0.48	129.0 ± 3.87	2.7	3.0
90	20.70 ± 1.53	133.0 ± 7.18	7.4	5.4

Table 3.2 *Mean concentrations of 7-hydroxycoumarin-glucuronide (± the standard deviation, S.D.) produced by rabbit kidney and liver UDPGT and the % relative standard deviation over time (n=3).*

Time (min)	Mean (n=3) 7-HCG concentration (μM) ± S.D.		C.V.	
	Lrg. Int.	*Bladder*	*Lrg. Int.*	*Bladder*
0	0.000 ± 0.00	0.000 ± 0.00	0.0	0.0
15	0.100 ± 1.78	0.940 ± 3.55	2.7	0.9
30	0.213 ± 0.80	1.756 ± 0.88	3.0	4.4
45	0.337 ± 1.37	2.980 ± 0.58	4.8	6.1
60	0.480 ± 0.95	3.250 ± 0.98	5.1	2.2
75	0.665 ± 0.41	3.685 ± 2.54	3.0	3.5
90	0.751 ± 0.22	4.666 ± 1.74	6.6	4.8

Table 3.3 *Mean concentrations of 7-hydroxycoumarin-glucuronide (± the standard deviation, S.D.) produced by rabbit large intestine and bladder UDPGT and the % relative standard deviation over time (n=3).*

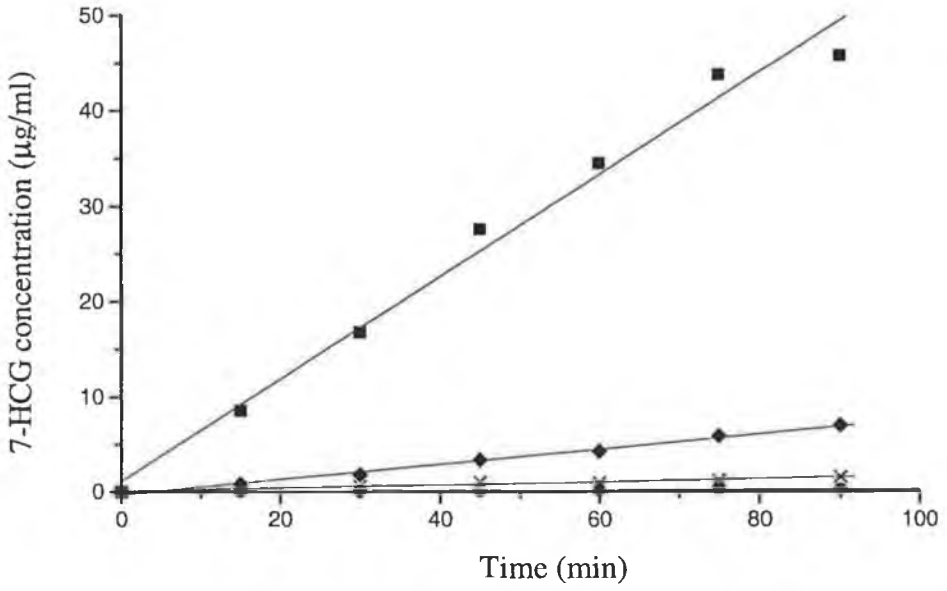

Figure 3.4 *Graph showing rate of production of 7-hydroxycoumarin glucuronide in four of the tissue samples; liver (A), kidney (B), bladder (C), and large intestine (D).*

Tissue	Concentration of 7-HCG produced per min per milligram of protein (pmol)
Liver	2300
Kidney	220
Bladder	140
Large intestine	7.8
Lung	0.0
Spleen	0.0
Heart	0.0
Fat	0.0

Table 3.4 *Table showing the activities of the different organs in the production of 7-HCG.*

3.3 Discussion

As discussed in section 1.2.4 glucuronidation of compounds is carried out by the UDPGT family of membrane-bound enzymes (Dutton, 1991). Analysis of glucuronidation is of vital importance for a number of reasons, primarily because of its role as the major detoxification pathway, accounting for most of the detoxified material in the bile and urine. Since the same family of enzymes carries out the glucuronidation of many different drugs, use of a model drug, while providing important information on that drug also provides the researcher with information on glucuronidation sites within an organism. This information helps elucidate the drug distribution within the species and, as drugs from almost all therapeutic classes are glucuronidated (Clarke and Burchell, 1994), understanding the location and rate at which it occurs provides valuable information required for generation of relevant dosage.

Another important feature of understanding glucuronidation is that for most drugs the glucuronide conjugate is formed mostly for the purpose of detoxification and excretion, as in the case of bilirubin (Dutton, 1991), and has no pharmacological properties. However, in the case of the drug morphine, it was discovered that morphine-6-glucuronide was 650 times more potent than the parent drug as an analgesic (Wahlstrom *et al.*, 1989). For this reason the development of methods to determine the major sites of glucuronidation and for its detection is important. UDTGT activity for 7-hydroxycoumarin is present in many organs of the one species, here in the rabbit it has been demonstrated to be present in the liver, kidney and to a lesser extent bladder and large intestine. Trace amounts of the glucuronide were found in the spleen and lung, with no detectable activity in the heart and fat tissue. The HPLC method used here was adapted from that of Killard *et al.* (1996) with a significant decrease in total analysis time. This was achieved by altering the gradient profile to decrease the retention time of all three analytes and internal standard, 4-HC (by up to 8 minutes in the case of the internal standard). This is the first time a study on the metabolism of 7-HC with different rabbit tissue has been undertaken, with analysis by HPLC. The results will provide researchers with information on the presence of the UDPGT enzyme system within the different organs of the rabbit as well as respective rates of metabolism of 7-hydroxycoumarin to the glucuronide. This information is very useful, not only for the understanding of coumarin metabolism, but also in understanding glucuronidation of drugs and for possible differences between the pathways used.

4 CAPILLARY ELECTROPHORESIS APPLIED TO THE ANALYSIS OF COUMARINS

4.1 Introduction

The term electrophoresis first appeared in 1909 when Michaelis discovered the separation of proteins based on their isoelectric points. The work of Tiselius (1937) gave the first indication of the potential of electrophoresis for analysis, demonstrating the separation of serum proteins, albumin, and the α-, β-, and γ-globulins by "moving boundary electrophoresis". However, this approach to electrophoresis was limited by incomplete separation of the proteins, the relatively large sample volume needed, and the necessity of relatively low electric fields due to the convection currents generated by Joule heating, despite the use of dense sucrose solutions. Consden *et al.,* (1944) and Wieland and Fisher, (1948) demonstrated paper electrophoresis to be applicable to a wide variety of molecules, while Kolin (1954) tried isoelectric focusing (IEF) but with little success as his pH gradients were short and unstable over time. The 1960's saw major improvements as polyacrylamide gels were optimised with stacking and resolving buffer systems for high resolution separations of native and sodium dodecyl sulphate (SDS)-complexed proteins (Brishammar *et al.;* 1961, Davis, 1964). The synthesis by Vesterburg (1969) of ampholine mixtures, facilitating stable pH gradients in isoelectric focusing gave rise to the use of this method as a routine biochemical method for analysis.

It was against a background of increasing demands for high resolution, quantitative precision of bio-pharmaceuticals and control of waste management costs (from HPLC), that capillary electrophoresis (CE) was developed. The pioneering work of Hjerten (1967) laid the groundwork for the CE analysis of diverse analytes, ranging from small molecules (inorganic ions, nucleotides) to macromolecular structures, such as proteins and viruses. Much of this work was conducted with a functional CE unit, albeit with 3 mm tubes, that was constructed in 1959.Virtanen (1974) followed this work with the use of smaller internal diameter tubes (0.2mm), which eliminated convection problems and simplified instrument design. In the late 1970's and early 1980's, CE was shown to be a viable analytical technique by Mikkers *et al.,* (1979), and Jorgenson and Lukacs, (1981). It was shown that CE had potential for producing high-resolution separations of biopolymers, as well as smaller pharmaceutical agents, and used minuscule amounts of both sample and reagents. Improvements in sensitivity of detectors, advances in automation technology and, most particularly, the widespread

availability of high quality narrow bore capillary silica tubing has allowed CE to be applied to many areas of analysis, several of which are examined in this thesis.

4.1.1 Instrumentation

A diagrammatic representation of a CE instrument is shown in Figure 4.1. The basic components include a high voltage power supply (0 – 60kV), a polyimide-coated capillary with an internal diameter of ≤200 μm, two buffer reservoirs that can accommodate both the capillary and the electrodes connected to the power supply, and a detector.

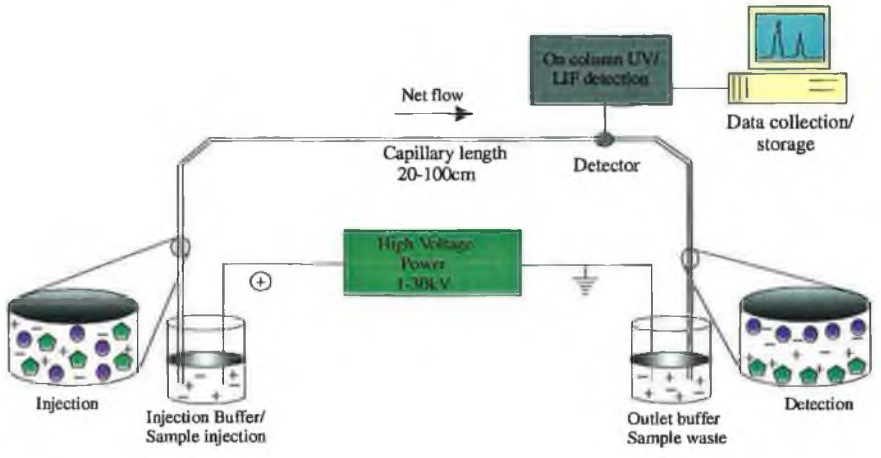

Figure 4.1 *General schematic of a CE instrument.*

To perform a separation the capillary is filled with an appropriate separation buffer at the desired pH and sample is introduced into the inlet. Both ends of the capillary and the electrodes from the high voltage power supply are placed into buffer reservoirs and up to 30kV applied to the system. The ionic species in the sample plug migrate with an electrophoretic mobility (direction and velocity) determined by their charge and mass, and eventually pass a detector where information is collected and stored by a data acquisition/analysis system.

4.1.1.1 Capillaries

Separation capillaries are mostly made of fused silica with an internal diameter between 10 and 100 μm and a variable length that can be up to 100 cm. Open tubes are used for free zone electrophoresis. Surface modification is necessary if electroosmotic flow is to be reversed or eliminated (section 4.1.2). Since this flow is generated by the silica wall, it is evident that the quality of the fused silica may play an important role in the separation process (Carchon and Eggermont, 1992)

4.1.1.2 Injection

In order to reduce the dispersion of the separated zones, the sample itself must be loaded onto the capillary in a narrow zone. The two most commonly used methods are hydrodynamic pressure injections and electrokinetic injections (Skoog *et al.,* 1998). Of the two, the former is the only unbiased method of injection, as electrokinetic injections have the disadvantage that the loading of sample ions onto the capillary depends on their charge and mobility, the faster migrating ions entering the capillary in larger numbers. Hydrodynamic injection allows the sample to be pressed into the capillary, hence it cannot be used for gel filled capillaries. Care must be taken before separation to ensure the capillary is in equilibrium. For both types of injection it is necessary to ensure buffer reservoir levels are the same to prevent siphoning in either direction which could reduce or increase sample loading. Gravity can also be used to introduce sample ions into the capillary. It is a very elegant and highly reproducible technique in which one end of the capillary is dipped into the sample and both are lifted for a preset time. Both height and time in combination with the viscosity of the sample determine the amount of sample loaded onto the capillary (Carchon and Eggermont, 1992).

4.1.1.3 Detection

The instruments most frequently used and commercially available are optical detectors using UV or fluorescence with reported representative limits of detection (LODs) of 10^{-15} to 10^{-13} for absorbance and down to 10^{-20} moles for fluorescence. For detection, the most common

format involves removal of a small section of the capillary polymer coating so that the capillary wall becomes transparent for UV/fluorescence detection. This type of arrangement (on-column) is available on most commercial CE instruments, but as seen later in chapter 6, even lower LOD's are obtainable using a post column detection format. Other forms of detectors have also been employed. These include Raman spectroscopic detection systems and electrical conductivity electrical systems as well as the coupling of CE to mass spectrometers. Representative detection limits for mass spectrometry is in the order of 1×10^{-17} moles with conductivity at 1×10^{-16} moles (Skoog *et al.,* 1998).

4.1.2 Electroosmosis in Capillary Electrophoresis

Electrophoretic mobility (μ) of a charged molecular species can be approximated from the Debye-Huckel-Henry theory

$$\mu = q/6\pi\eta r \qquad (1)$$

where q is the charge on the particle, η is the viscosity of the buffer and r is the stokes radius of the particle. The mass of the particle may be related to the Stoke's radius by M = (4/3) $\pi r^3 V$ where V is the partial specific volume of the solute. However, due to the non-spherical shape, counter-ion effects, and non-ideal behaviour of proteins and biological molecules inside the capillary these conditions are not met (Rickard, 1991). As electrophoresis ensues in normal polarity mode from positive to negative, the analytes separate according to their individual electrophoretic mobilities and pass the detector as "analyte zones". Since under the appropriate conditions, all species (net positive, negative and neutral) pass the detector indicate that a force other than electrophoretic mobility is involved. If the applied electric field were the only force acting on the ions, net positively (cationic) substances would pass the detector, while neutral components would remain static and net negatively (anionic) species would be driven away from the detector. The other force involved is "electroosmosis" (Chiari *et al.,* 1996).

Electroosmotic flow was first identified in the late 1800's when Helmholtz (1879) conducted experiments involving the application of an electrical field to a horizontal glass tube

containing an aqueous salt solution. Helmholtz discovered that the silica imparted a layer of negative charge to the inner surface of the tube, which, under an applied electric field, led to the net movement of fluid to the cathode. What happens is shown in Figure 4.2, the ionised silanol groups (SiO^-) of the capillary wall attract cationic species from the buffer. Obviously the buffer pH will determine the fraction of the silanol groups that will be ionised. The ionic layer that is formed has a positive charge density that decreased exponentially as the distance from the wall increases. The double layer formed closest to the surface is termed the "Inner Helmholtz or Stern Layer" and is essentially static. A more diffuse layer formed distal to the Stern Layer is termed the "Outer Helmholtz Plane" (OHP). Under an applied field cations in the OHP migrate in the direction of the cathode carrying the waters of hydration with them. Because of the cohesive nature of the hydrogen bonding of the waters of hydration to the water molecules of the bulk solution, the entire buffer solution is pulled towards the cathode. This EOF or "bulk flow" acts as a pumping mechanism to propel all molecules (cationic, neutral and anionic) towards the detector. It is this phenomenon that allows CZE to be a widely versatile tool today for analysis. This is the driving force behind all separations reported in this chapter.

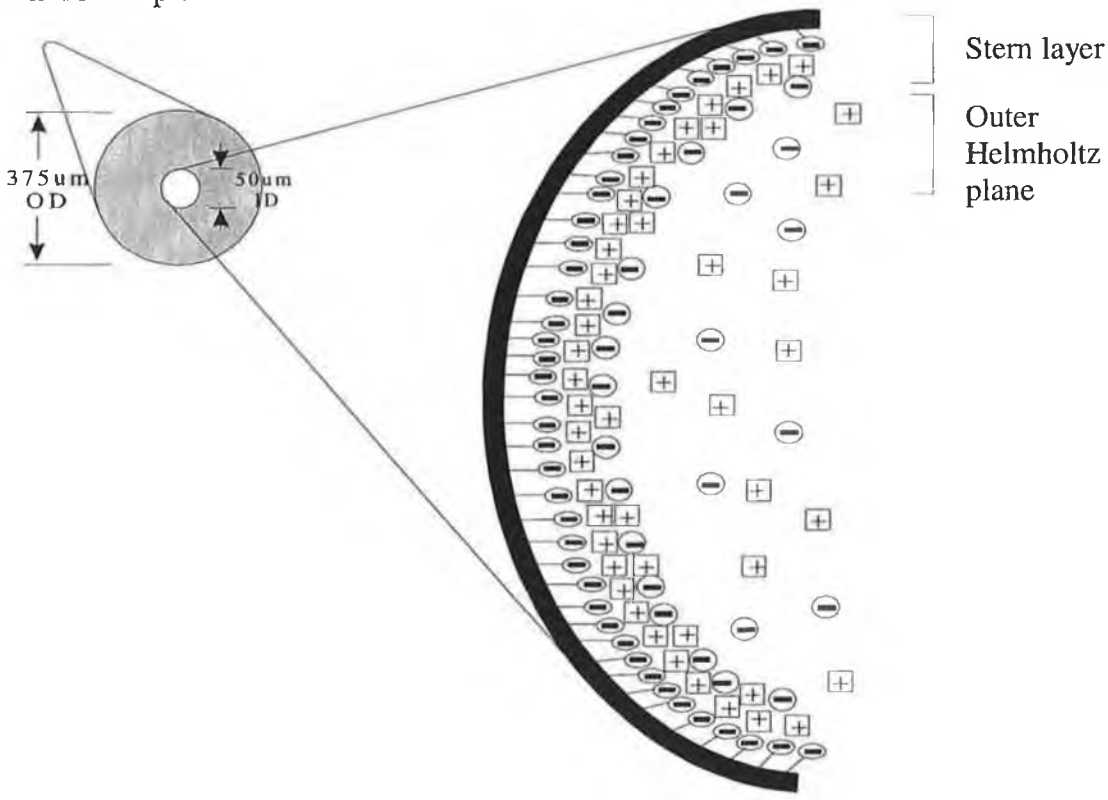

Figure 4.2 *Diagram of the capillary and the ionic layers critical in generating electroosmotic flow*

4.1.3 Control of electroosmotic flow

There are several ways to partially or fully control EOF (and adsorption). These include the use of additives and buffer changes (Bushey and Jorgenson, 1989), organic solvents (Campos and Simpson, 1992), adsorption of neutral and/or charged macromolecules (including surfactants) to the wall (Chiara *et al.,* 1996) and chemically bonded phases (Nashabeh, 1991). A brief outline of some of these measures will be given here.

4.1.3.1 Buffer changes and additives

Buffers cations: To evaluate the effect of the buffers cation on electroosmotic flow (μ_{eo}), Atamna, (1991), and Issaq, (1991), conducted a series of experiments in 0.1M each of Li, Na, K, Rb and Cs acetates. The results showed that the larger the crystal radius, the higher the effect of the cation in quenching μ_{eo}. It was hypothesised that the larger cations are more strongly adsorbed onto the silica wall, thereby altering its charge and effectively reducing EOF.

Zwitterions: Another way to control EOF (without altering the buffer conductivity) is to add zwitterions to the running buffer. Ideally these zwitterions should have a large ΔpK, so as to be isoelectric over the pH 3 – 10 range. Examples are trimethylammonium propyl sulphonate, triethylammonium propyl sulphonate, and tripropylammonium propyl sulphonate (Bushey and Jorgenson, 1989)

Solvents: Binary mixtures of water and a protic (methanol, ethanol, 2-propanol) or an aprotic dipolar solvent (acetonitrile, acetone, dimethyl sulphoxide) all in a 1:1 ratio, dramatically lower EOF and zeta potential by shifting the pK values of silanols to higher pH ranges (Schwer, 1991).

4.1.3.2 Adsorbed coatings

A number of substances adsorb to the silica wall through electrostatic interactions or hydrogen bonding following hydrophobic derivatisation of the capillary. These can be neutral molecules, e.g. polyvinal alcohol, or cationic surfactants, e.g. Fluorad FC134 (Chiari *et al.*, 1996). If the wall adsorbs a neutral polymer, electroosmosis is eliminated and the solutes may be sterically prevented from coming into contact with the wall and from being adsorbed. When cationic surfactants are added to the separation buffer, the charge on the surface will be changed from negative to positive and the EOF direction will be reversed.

4.1.3.3 Chemically bonded phases

The development of coatings covalently bonded to the capillary wall in recent years has led to significant improvements in the elution profile and separation efficiencies of biopolymers. The chemistry usually involves organosilanisation, a surface modification procedure derived from "silane-coupling" methodology, which has being successfully transferred to capillary electrophoresis. Fused silica capillaries are typically reacted with organosilanes to yield an Si-O-Si (siloxane) linkage.

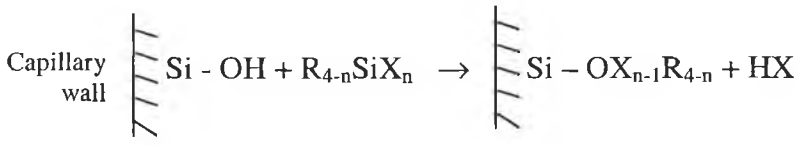

where n = 1 – 3, R is an alkyl or substituted alkyl group and X is an easily hydrolysed group such as halide, amine, alkoxy or acyloxy. In an ideal modification procedure the bonded phases should completely cover the original silica and the functions introduced should not interact with biopolymer solutes over a wide range of conditions. The coating should exhibit a defined or reproducible composition and the bonded phases should have high chemical stability and resistance in the presence of alkaline and acidic solvents used routinely in CE (Chiari *et al.*, 1996)

4.1.4 Other modes of capillary electrophoresis

While capillary zone electrophoresis is perhaps the most common form of CE used today, other forms of electrophoresis have been incorporated to the capillary format, including micellar electrokinetic capillary chromatography, capillary gel electrophoresis, capillary isoelectric focusing, and capillary isotachophoresis. These methods can be carried out with the same basic equipment and allow highly efficient separations of neutral species and/or ions.

4.1.4.1 Micellar electrokinetic capillary chromatography

Micellar electrokinetic capillary chromatography (MECC) which was first described by Terebe (1985), is based on micellar solubilisation and electrokinetic migration. The technique involves the addition of a surfactant to the buffer, e.g. deoxycholic acid, at a concentration just above its critical micelle concentration (CMC). This allows the formation of micelles inside the capillary, a pseudo stationary phase that enhances the separation of sample ions but also permits the neutral sample compounds to partition within the interior of the micelle. Separation of all sample analytes depends now on the differential partition between the hydrophobic interior of the charged micelle and the aqueous phase. Since electroosmotic flow still dominates the direction of the flow, all analytes are eluted at the end of the capillary. The retention order in MECC is determined by the solubility of the solutes in the aqueous mobile phase. The use of surfactants not only improves the separation of ionic compounds, but also extends the methods applicability to water-insoluble solutes, whereas the choices of anionic or cationic surfactants further increases the diversity of MECC (Matsubara and Terabe, 1996).

4.1.4.2 Capillary gel electrophoresis

The technique of capillary gel electrophoresis (CGE) is almost a direct transfer of conventional gel electrophoresis into a capillary. The traditional method, while relatively simple, is labour intensive involving the preparation of gels, long run times due to low

voltage applications, because of heat dissipation problems, and slow staining/destaining techniques for visualisation. The end result is only qualitative. In CGE the technique is more rapid, with tiny (by comparison) volumes of gel required, the ability to apply high voltages and hence short analysis times (due to the large surface area and thin walls of the capillary resulting in rapid heat dissipation). Since protein zones are registered by either UV adsorption or fluorescence (for labelled samples), CGE offer qualitative information. When polyacrylamide gels are used, the pore size can be manipulated by altering the ratio of monomer to cross linking agent in the polymerisation mixture, and thus the pores of the gel can be made comparable to the size of the molecules to be separated as demonstrated in chapter 7. Also the use of different molecular weight dextrans allows the separation to be tailored to the desired molecular weight range. In CGE, factors, including eddy diffusion and solute sorption, can influence zone broadening. The efficiency is lower than that obtained in open tubular CZE, but the selectivity in increased so that separation is still obtained (Campos and Simpson, 1992).

4.1.4.3 Capillary isoelectric focusing

In capillary isoelectric focusing (cIEF), amphoteric analytes such as peptides and proteins are separated on the basis of their isoelectric point (Rodriguez-Diaz *et al.,* 1997). Sample ions are mixed with the carrier ampholytes that span the desired pH range, and the mixture is loaded onto the capillary. When an electric field is applied, the ampholytes build up a pH gradient and the sample ions focus concurrently. This process can be followed by a current decrease. In cIEF resolution strongly depends on the slope of the pH gradient. After focusing, sample ions are eluted from the capillary by 1) a pressurised flow, 2) lifting one end of the capillary; and 3) adding salt (e.g. sodium chloride) to the electrode buffer. As the sodium ions replace protons in the capillary, a pH balance gradient is generated and is followed by elution of the components. In capillary isoelectric focusing (CIEF), the coating of the capillary is important because the electroosmotic flow must be eliminated completely (Hjerten, 1987). Since the entire capillary is filled with sample ions, larger sample amounts are used for isoelectric focusing, i.e., when proteins are focused, care must be taken that precipitation must not occur, because of protein concentration that is excessive. At the same time, the resistance in the

capillary increases at those sites where proteins are focused, so that heat development at these sites may cause protein precipitation.

4.1.4.4 Capillary isotachophoresis

Capillary isotachophoresis is performed in a discontinuous buffer system, as opposed to CZE which uses a uniform buffer carrier throughout. The sample is introduced in solution as a zone between a leading electrolyte and a terminating electrolyte, each containing only one ion species with the same sign as the sample ions to be separated. For the system to work, on application of the electric field, the leading electrolyte must have an effective mobility higher and the termination electrolyte must have an effective mobility lower than that of the sample ions.

When the system has reached equilibrium, all of the ions migrate with the same speed, but are separated into a discrete number of zones in immediate contact with each other and arranged in order of decreasing mobility. Because of these identical migration velocities, a voltage gradient in the consecutive zones occurs so that, by using a potential gradient detector, a stepwise pattern is recorded. The electropherogram has always been difficult to interpret as sample compounds are separated but the zones are close to each other. Quantitative information is got from the length of a zone as it reflects the amount of the component present. This means that the electropherogram may show very different patterns that are difficult to recognise. However the problems can be overcome by transforming the conductivity signal into a chromatogram like pattern. The electropherogram would then show peaks that are located at specific conductivities, and the area under the peak reflecting the amount (Carchon and Eggermont, 1989). UV detection can be used only if UV-absorbing ions are preceded and followed by non UV absorbing compounds or vice versa.

4.2 In vitro glucuronidation of 7-hydroxycoumarin and determination of 7-hydroxycoumarin and 7-hydroxycoumarin-glucuronide by capillary electrophoresis

4.2.1 Coumarin metabolism

Section 1.2.4 gave a brief description of coumarin metabolism. The majority of coumarin administered in humans is excreted as 7-hydroxycoumarin glucuronide (7-HCG). It is the principal phase II metabolite and is produced from the main phase I metabolite, 7-hydroxycoumarin (7-HC). Here using CE, various rabbit tissues are analysed for both their ability to glucuronidate 7-HC, involving uridine diphosphate glucuronyl transferase (UDPGT), and to carry out the reverse reaction, breakdown of 7-HCG to 7-HC, using β-glucuronidase. Figure 1.1 shows the reaction scheme for both UDPGT and β-glucuronidase.

4.2.2 Sample preparation

Seven rabbit tissue types were selected, consisting of liver, kidney, large intestine, lung, spleen, heart and fat. Samples were prepared from each organ and incubations set up as outlined in section 2.3.2.1. In order to calculate the rate of reaction for 7-HCG production the protein concentration for each organ sample was calculated as outlined in section 2.3.1.1. The values obtained are shown in Table 4.1.

4.2.3 Method development

4.2.3.1 Capillaries

Section 4.1.1.1 describes the capillaries used without surface modification, allowing EOF to be the overall driving force for all separations. The shortest capillary length allowed by the design of the instrument, 27 cm, was chosen to reduce analysis time (19.3 cm to detector).

4.2.3.2 Buffers

Phosphate buffer was chosen as electrolyte due to its buffering capacity within the desired pH region for the separations, pH 7.0-7.5. In order to determine maximum voltages that could be used for the separation an Ohm's Law plot was constructed for 100mM phosphate buffer (Fig 4.3). This would give an indication at what voltage joule heating inside the capillary might begin to affect the separation (from use of too high voltages). The plot shows a linear range up to ~10kV, but application of up to 17kV may be possible without affecting the separation. For separations it was found that 17.5kV gave good results in terms of total run time with reasonable current and no detrimental effects on the separation over the course of the study.

4.2.3.3 Detection

All analytes absorb at 214 as well as 320 nm. However, due to interferents in the media also absorbing at 214 nm, it was not possible to analyse at this wavelength. Hence 320nm was chosen as the wavelength of detection, despite a slight loss in sensitivity.

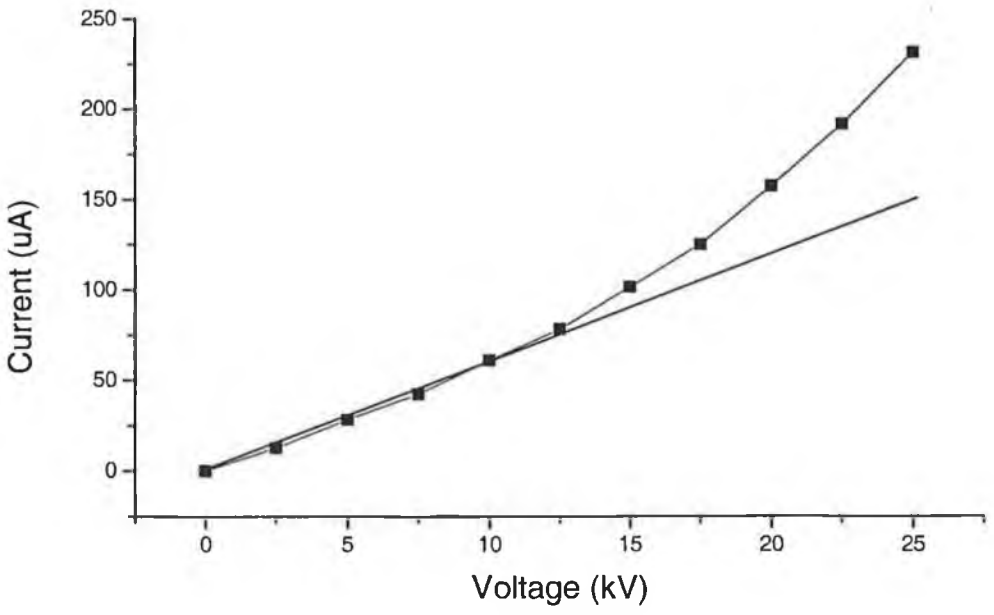

Figure 4.3 *Ohm's Law plot for 100 mM phosphate buffer*

4.2.4 UDPGT assay results

Separation of 7-HCG from endogenous species present in the metabolic mixture and from 7-HC is achieved in under 4 minutes. Figure 4.4 shows an electropherogram of the reaction mixture for the kidney. It also shows an overlay of electropherograms of samples taken at time 0, 40, and 80 mins. The increase in production of 7-HCG with time can be seen.

Organ	*Protein concentration (mg/ml) used in incubations*
Liver	0.76
Kidney	1.35
Heart	1.09
Lung	1.65
Spleen	1.68
Large intestine	1.29
Fat	0.00

Table 4.1 *Protein concentrations for each of the organs analysed for UDPGT activity. Protein concentration calculated as outlined in section 2.3.1.1*

A graph of mean (n=3) concentration of 7-HCG produced against time (Tables 4.2 and 4.3) was plotted for each organ and the slope of the graph used to calculate the reaction rates for each organ (Table 4.5). Rate of reaction was given by:

$$slope \div [protein] \div molecular\ weight$$

Where: *slope* = slope of the linear portion of the graph

[*protein*] = protein concentration from Table 4.1

Molecular weight in the case of 7-HCG = 338.14

The rates of reaction calculated for each organ shown in Table 4.4 are expressed as pico moles (pmol) of 7-HCG produced per minute per milligram of protein.

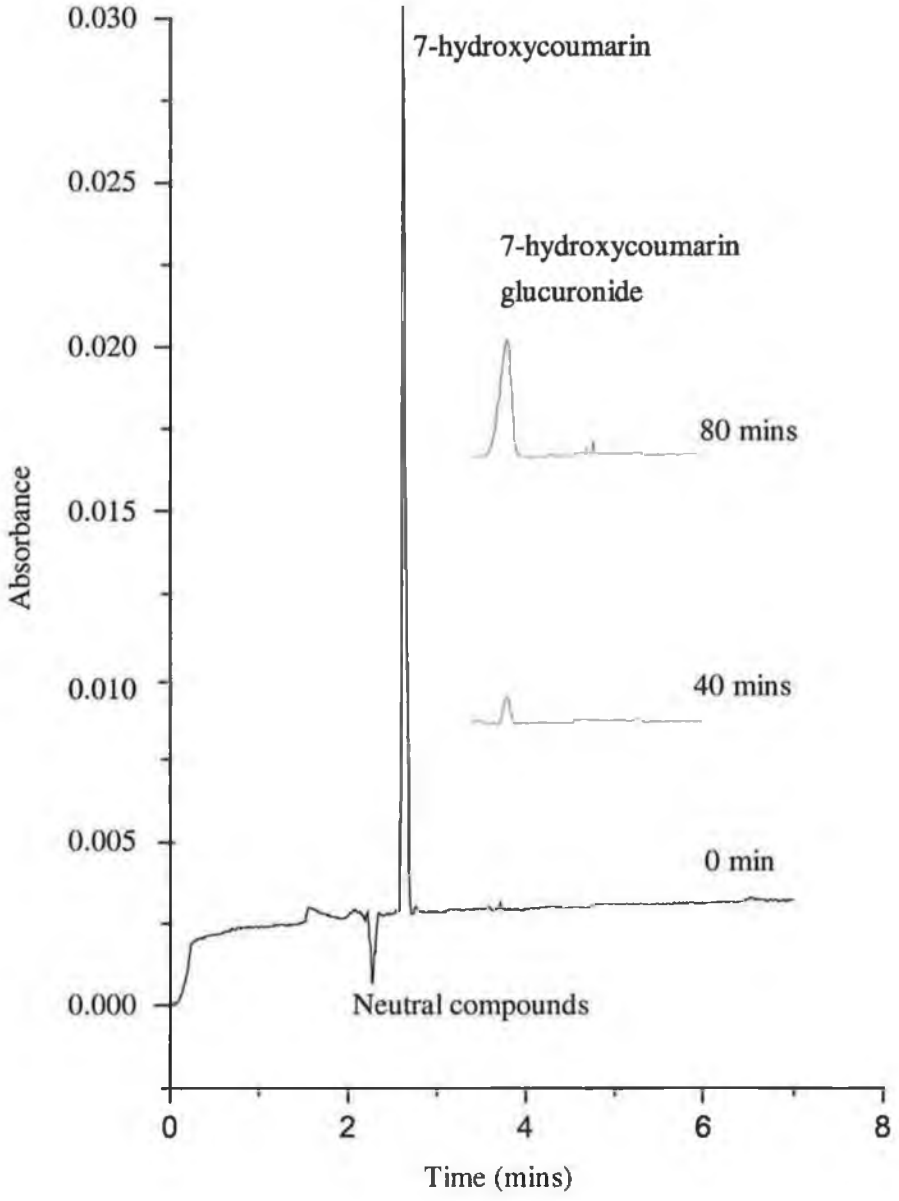

Figure 4.4 *CE electropherogram of the kidney metabolic solution. It shows an overlay of electropherograms of samples taken at 0, 40 and 80 min, respectively. Overlays shown between 3.4 and 5.9 min. Conditions: 27 cm fused silica capillary; 100mM phosphate buffer, pH 7.0; 8 s pressure injection; separation at 17.5kV, with detection at 320 nm.*

The mean amount (n=3) of glucuronide produced was calculated for each organ from a standard curve (0-200μg/ml) prepared as outlined in section 2.3.3.5. The results obtained demonstrate the liver to be the major site of glucuronidation for 7-HC, followed by the kidney, and with a small amount produced by the large intestine (Table 4.4).

Percentage relative standard deviation for each peak were all ≤ 9.8%. The concentration of 7-HCG produced with time was calculated for the liver, kidney and large intestine along with the CV for each time interval using the formula:

$$CV = \frac{Standard\ Deviation}{Mean} \times 100$$

Table 4.2 shows the % RSD for 7-HCG concentrations with time for the large intestine and kidney, with the results for the liver shown in table 4.3.

Time (min)	Mean (n=3) [7-HCG] (μM) ± SD		CV	
	Lrg. Int.	*Kidney*	*Lrg. Int.*	*Kidney*
0	00.00 ± 0.00	00.00 ± 0.00	0.0	0.0
20	00.00 ± 0.00	20.86 ± 0.80	0.0	3.8
40	00.00 ± 0.00	32.66 ± 3.21	0.0	9.8
60	00.00 ± 0.00	70.00 ± 3.60	0.0	5.1
80	00.00 ± 0.00	80.09 ± 3.11	0.0	3.8
100	00.00 ± 0.00	95.89 ± 1.34	0.0	1.4
120	00.00 ± 0.00	118.66 ± 2.72	0.0	2.3
140	0.497 ± 0.04	131.85 ± 2.07	8.0	1.6
160	0.563 ± 0.05	148.77 ± 2.79	8.0	1.8

Table 4.2 *Mean (n=3), standard deviation and % RSD for 7-HCG produced with time for the kidney and large intestine (Lrg. Int.). Results calculated as outlined in section 4.2.4.*

Time (min)	Mean (n=3) [7-HCG] (μM) ± SD	CV
0	00.00 ± 0.00	0.0
20	09.80 ± 0.50	5.0
40	23.66 ± 0.88	3.7
60	37.56 ± 0.83	2.0
80	48.55 ± 0.69	1.4
100	58.11 ± 1.01	1.7
120	63.11 ± 0.76	1.2
140	76.44 ± 1.17	1.5
160	87.11 ± 1.16	1.3

Table 4.3 *Mean (n=3), standard deviation and % RSD for 7-HCG produced with time for the liver. Results calculated as outlined in section 4.2.4.*

Tissue	Mean (n=3) [7-HCG] produced per min per milligram of protein (pmol)
Liver	2100
Kidney	200
Large intestine	7.8
Lung	0.0
Spleen	0.0
Heart	0.0
Fat	0.0

Table 4.4 *Table showing the activities of the different organs in amount of 7-HCG produced in pmol per minute per milligram of protein.*

4.2.5 β-Glucuronidase assay results

The method of Bogan *et al.* (1995) when applied as a new procedure for the assay of β-glucuronidase activity proved effective for detection of both 7-HC and 7-HCG. Separation of

both compounds was achieved in less than 4 minutes and the increase in 7-HC concentration with time can be seen as shown in Figure 4.5. The same seven organs chosen for the UDPGT assay were chosen for this study.

4.2.5.1 β-Glucuronidase activity calculations

Activity was expressed in the form of β-Glucuronidase activity units/g wet mass of whole organ. The activity for each organ was compared to that of β-glucuronidase obtained from Sigma and from this the activity in units/g wet weight of organ could be determined. A standard curve with 0 – 10,000 units of β-glucuronidase incubated for 30 minutes with 200 µg/ml 7-HCG prepared as outlined in section 2.3.3.5 was used to calculate activities. Figure 4.5 shows the increase in 7-HC concentration with increase in units of β-Glucuronidase for a 30 min incubation. Results show that in excess of 500 units is enough to completely liberate 102µg of 7-HC from 200µg of 7-HCG in 30 min.

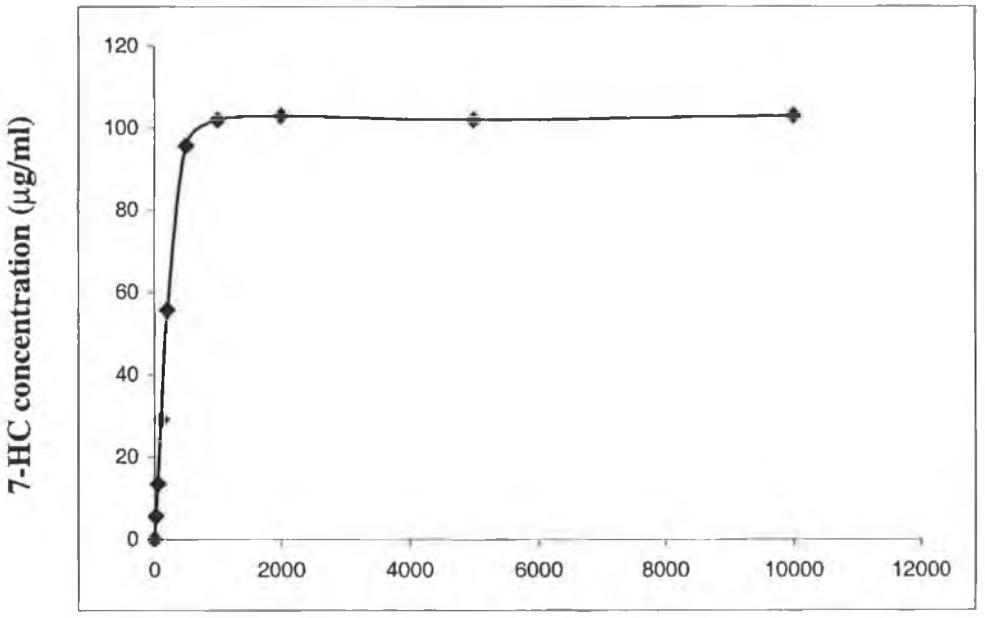

Figure 4.5 *Table showing amount of 7-HC produced from 7-HCG with increasing β-Glucuronidase enzyme units (obtained from Sigma) for 30 min incubation. Incubation conditions were as outlined in section 2.3.3.2.*

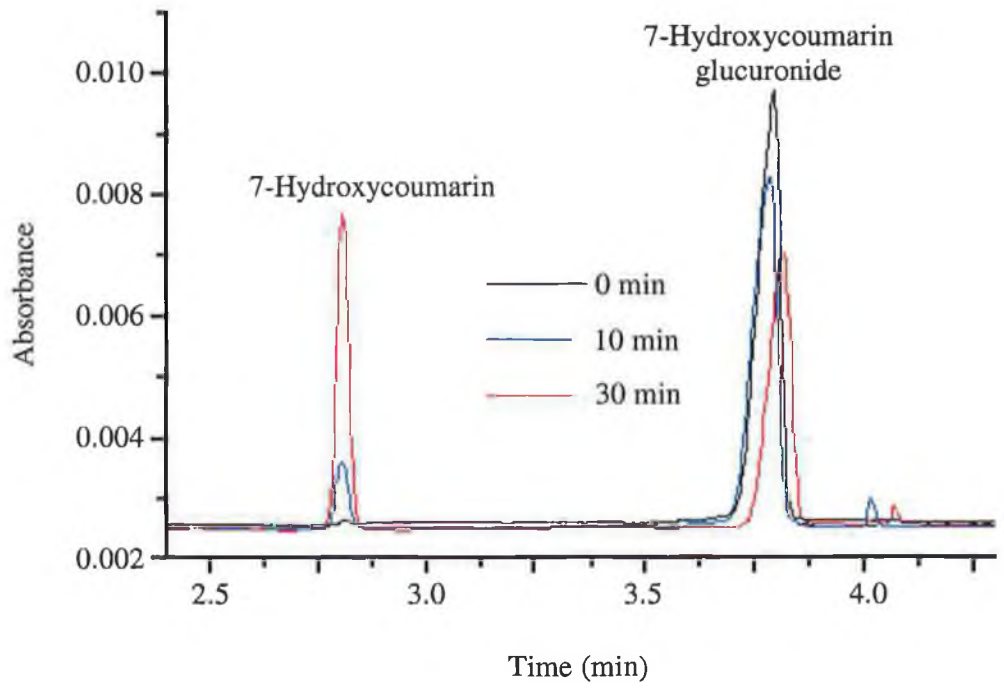

Figure 4.6 *Portion of electropherogram from liver incubation showing increase in breakdown of 7-HCG to 7-HC with time. Conditions: 27 cm fused silica capillary; 100mM phosphate buffer, pH 7.0; 8 s pressure injection; separation at 17.5kV, with detection at 320 nm.*

As in the case of the UDPGT assay the liver proved to be the most active site for deconjugation of 7-HCG (Table 4.5), followed by the spleen with about half the activity of the liver. The kidney and lung displayed low activity relative to the liver, with the heart and intestine showing the lowest activity. The fat, as expected, showed no detectable trace of 7-HCG breakdown. Figure 4.7 shows the comparison of endogenous β-glucuronidase activity in each organ versus 7-hydroxycoumarin produced. The activity is expressed in units, where 1 unit is that which will liberate 1.0 μg of phenolphthalein from phenolphthalein glucuronide per hour at 37^0C at pH 5.0 (30 min assay). The limit of detection for the 7-HC was 1μg/ml.

Organ homogenate	Average β-Glucuronidase activity units/g wet mass of whole organ (n=3)
Liver	12,660
Lung	1710
Intestine	1003
Fat	0
Spleen	6200
Heart	800
Kidney	1780

Table: 4.5 *β-glucuronidase activity (units/g wet weight of organ) in whole organ homogenates as determined after analysis by capillary electrophoresis.*

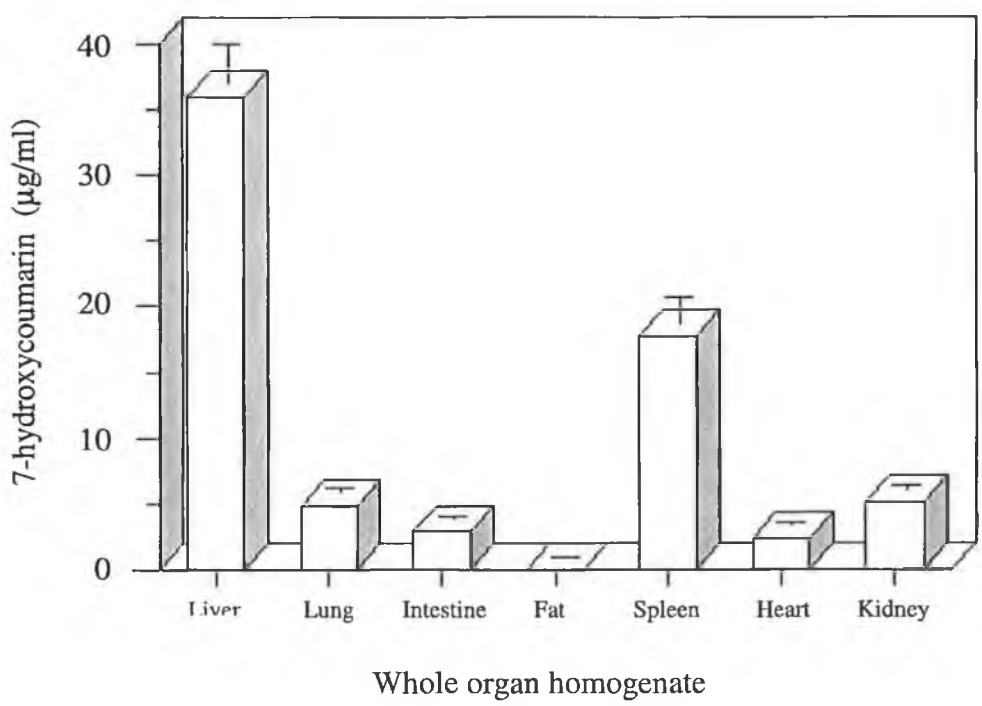

Figure 4.7 *Plot showing the comparison of endogenous β-glucuronidase activity in each organ (± SD) versus 7-hydroxycoumarin produced (µg/ml) for the study of the deconjugation of 7-hydroxycoumarin-glucuronide to 7-hydroxycoumarin.*

4.3 Determination of 7-hydroxycoumarin and its glucuronide and sulphate conjugates in liver slice incubates by capillary zone electrophoresis

Fig. 1.1 shows the reaction scheme for both the glucuronide and sulphate conjugates and outlines the preferential pathways for each phase II metabolite. While glucuronidation (examined in section 3.2 and 4.2) is preferential, this investigation establishes the use of CE for the measurement of the sulphate conjugate produced by mouse liver.

4.3.1 Synthesis of 7-hydroxycoumarin sulphate

7-hydroxycoumarin-sulphate was synthesised according to the method outlined in section 2.3.4.1. In total 216mg was synthesised. Due to its susceptibility to hydrolyse rapidly it was stored at -80^0C in a sealed glass vial until required for use. The compound was used within one week, and was analysed by CE each day prior to use. No evidence of breakdown to 7-hydroxycoumarin was detected.

4.3.1.1 NMR analysis

To check the structure for correct synthesis a sample of the compound was taken and analysed by nuclear magnetic resonance (section 2.3.4.2) (Figures 4.9 – 4.10). The scan shows the H doublet at 6.24 corresponding to position 2 on the structure (Fig 1.1), a doublet and a singlet at positions 4 and 8 at 7.09 and 7.11, respectively. The doublet linked with the carbon double bond is shown at 7.46, and the doublet associated with the oxygen (position 7) at 7.79.

4.3.1.2 IR analysis

A further structural study used IR for analysis of the compound (section 2.3.4.3). The scan is displayed in Figure 4.11. The fingerprint region shows a lot of peaks. However, stretches at

1725.86 indicate the carbonyl group and a stretch at 1622.41 shows presence of the carbon double bond. It is also possible that the –OH stretch at 3464 (from water) has contributions from the sulphate group.

4.3.2 Sample preparation

4.3.2.1 Tissue slicer fabrication

In order to obtain precision cut liver slices a small instrument based on that described by Krumdieck *et al.* (1980) was made. Figure 4.8 shows the two main units, the coring tube and piston. Freshly obtained liver from mice was cored with the coring tube several times to fill a portion of the tube.

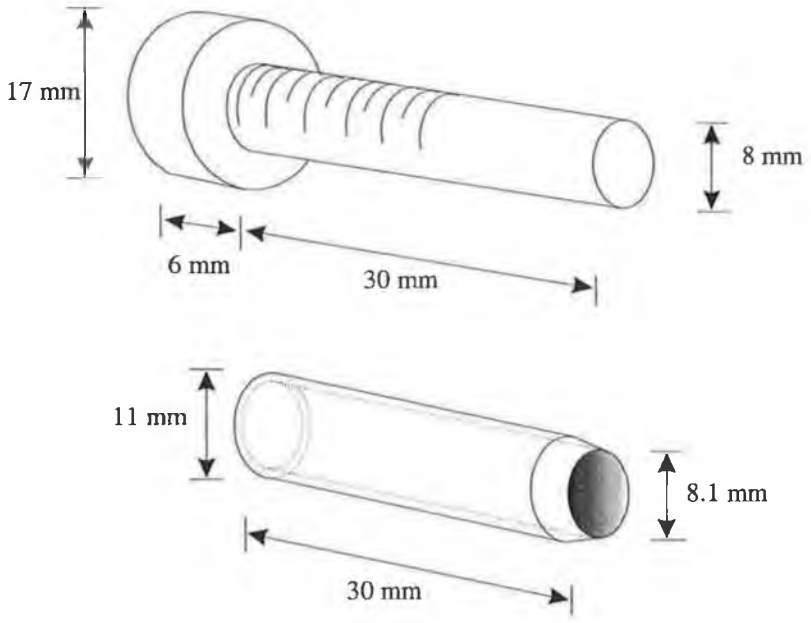

Figure 4.8 *Diagram showing main components of tissue slicer. The piston is shown with markings to ensure exact slice thickness, and below, the coring tube which contained the liver sample. Dimensions are in millimetres.*

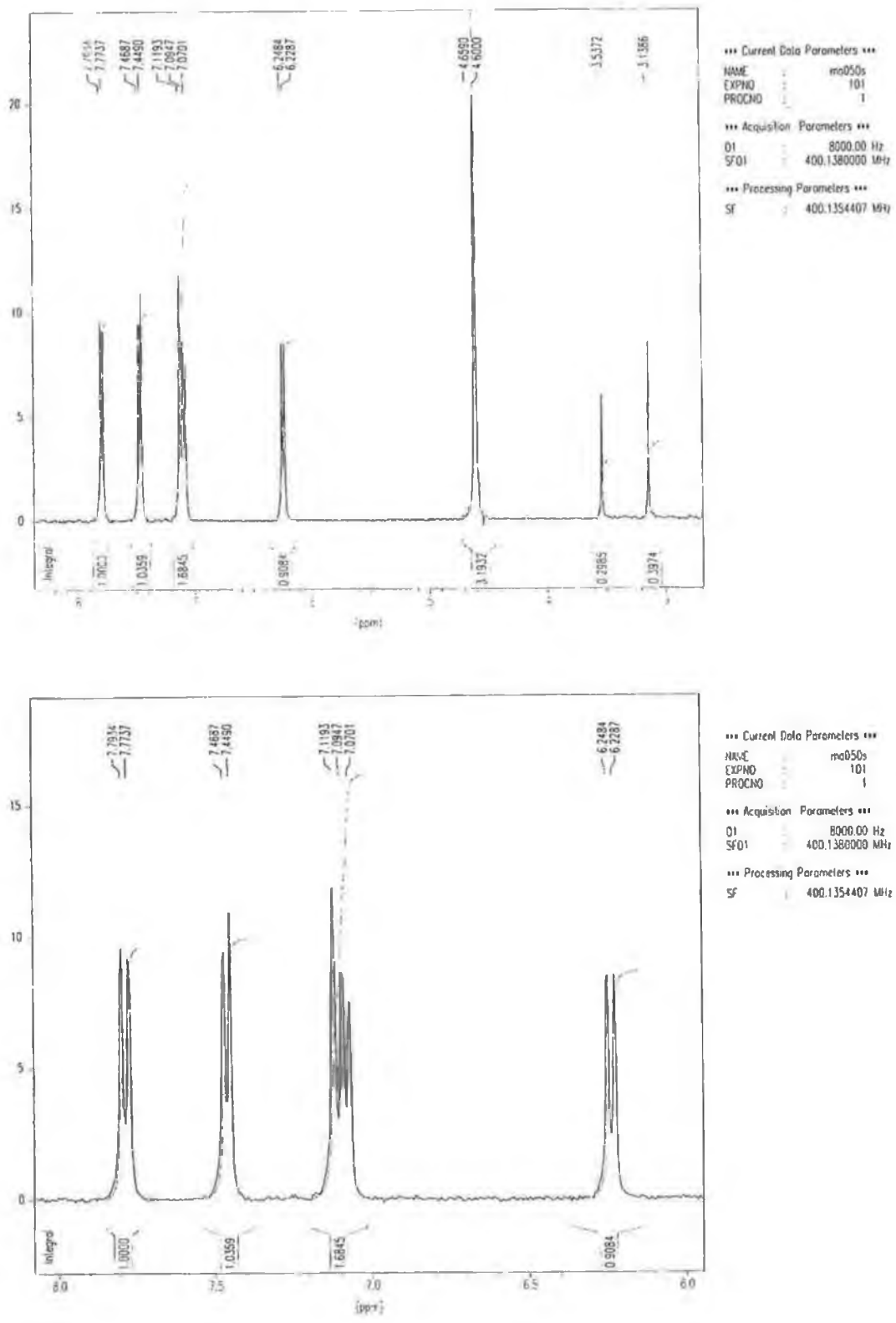

Figure 4.9 *Nuclear magnetic resonance scan of 7-hydroxycoumarin sulphate, complete scan (top), expanded reigon 6 – 8 ppm (bottom).*

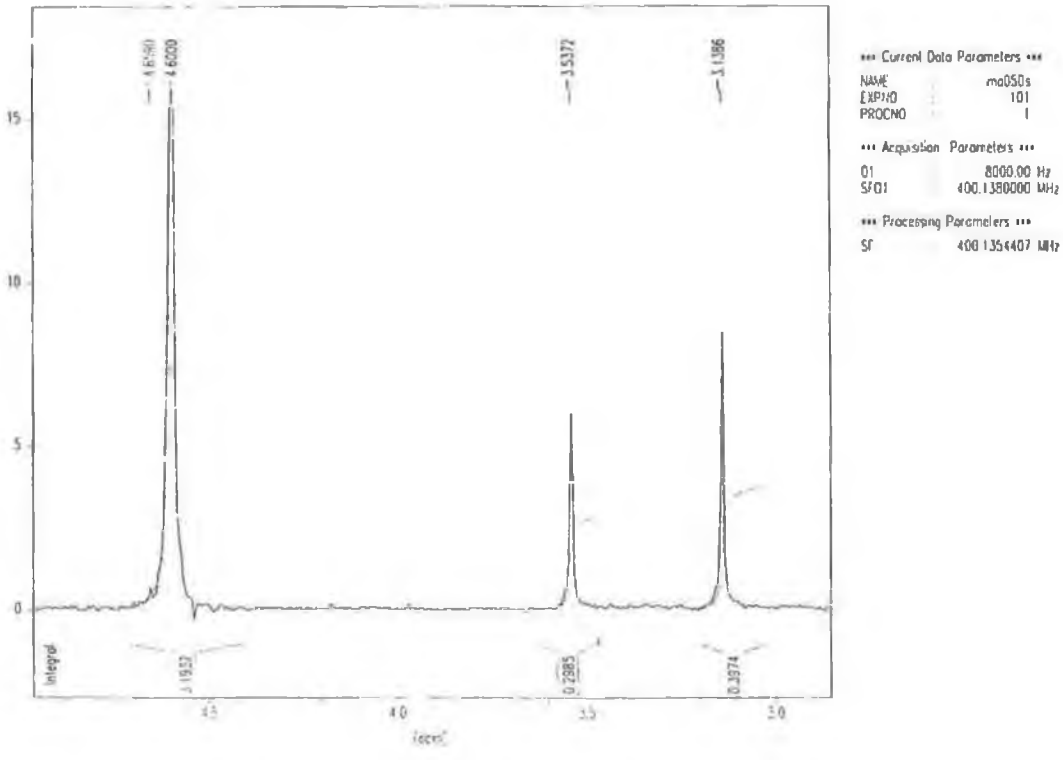

Peak constant PC = 1.00
Noise = 1496
Sens. level = 5985

Peak Picking region

Start(ppm/Hz)	End(ppm/Hz)	MI(%)	MAXI(%)
26.55/10623.8	-13.76/-5505.3	0.00	100.00

Peak Picking results

Peak Nr.	Data Point	Frequency	PPM	Intensity	%Int.
1	3812	3118.42	7.7934	262930	9.6
2	3816	3110.55	7.7737	252136	9.2
3	3878	2988.48	7.4687	258712	9.4
4	3882	2980.60	7.4490	300318	11.0
5	3949	2848.69	7.1193	324894	11.8
6	3954	2838.84	7.0947	236872	8.6
7	3959	2829.00	7.0701	205790	7.5
8	4126	2500.20	6.2484	233190	8.5
9	4130	2492.32	6.2287	233552	8.5
10	4449	1864.25	4.6590	18902	0.7
11	4461	1840.62	4.6000	2742434	100.0
12	4677	1415.35	3.5372	164248	6.0
13	4758	1255.87	3.1386	233396	8.5

Figure 10 *Nuclear magnetic resonance scan of 7-hydroxycoumarin sulphate, expanded region (3.0 – 5.0 ppm) of scan (top) and peak information (below).*

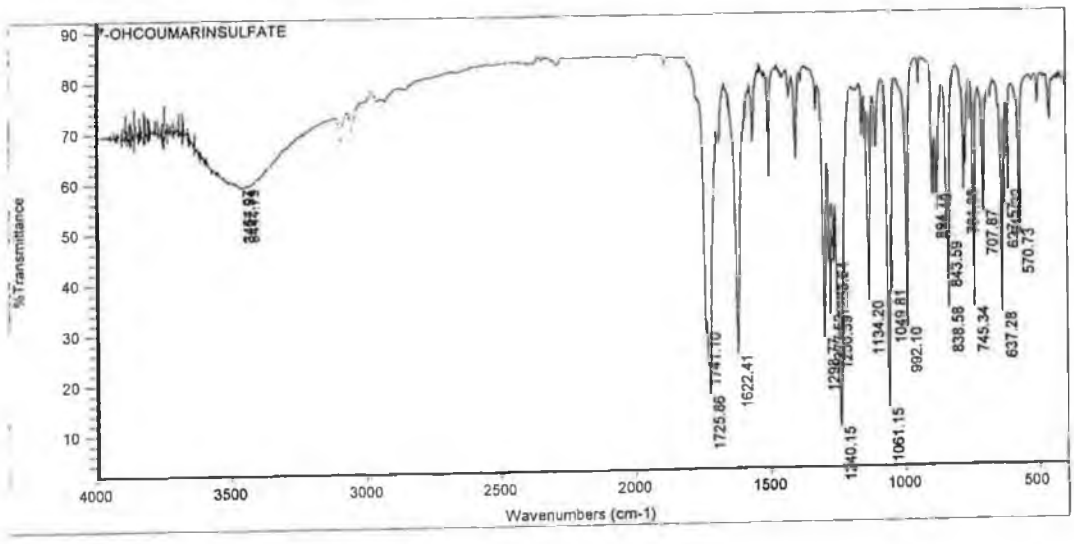

Thu Jul 24 15:51:40 1997
FIND PEAKS:

Spectrum:	7-OHCOUMARINSULFATE	
Region:	4000.00	400.00
Absolute threshold:	59.177	
Sensitivity:	50	
Peak list:		

Position:	1240.15	Intensity:	9.788
Position:	1061.15	Intensity:	13.340
Position:	1725.86	Intensity:	16.444
Position:	1622.41	Intensity:	24.644
Position:	1298.77	Intensity:	27.589
Position:	1741.10	Intensity:	29.103
Position:	992.10	Intensity:	29.377

Peak information:

Position: 1250.59	Intensity: 31.953
Position: 637.28	Intensity:32.111
Position: 1277.52	Intensity:32.217
Position: 745.34	Intensity:33.313
Position: 838.58	Intensity:33.276
Position: 1134.20	Intensity:34.780
Position: 1049.81	Intensity:36.976
Position: 1263.64	Intensity:42.536
Position: 843.59	Intensity:46.196
Position: 570.73	Intensity:48.613
Position: 707.87	Intensity:52.442
Position: 627.57	Intensity:53.729
Position: 849.73	Intensity:55.855
Position: 879.19	Intensity:55.914
Position: 613.32	Intensity:56.626
Position: 781.03	Intensity:56.672
Position: 3457.94	Intensity:59.013
Position: 3462.27	Intensity:59.072
Position: 3444.79	Intensity:59.083

Figure 4.11 *Infra-red spectrum of 7-hydroxycoumarin sulphate. Scan shows –OH peak at 3454 cm^{-1}, carbon oxygen double bond at 1725 cm^{-1} and carbon double bond at 1622 cm^{-1}.*

The piston was used to push the liver out where it was then sliced evenly with a razor blade pressed against the face of the coring tube. Regular spaced markings on the piston ensured slices of identical thinness while the diameter of the slice was determined by the diameter of the coring tube. The slicing procedure was carried out with the apparatus submerged in Krebs-Hanseleit buffer at all times. In order to avoid any possible reaction between the materials used for construction of the slicer and the liver or buffer, brass was used to manufacture the piston with high speed stainless steel used for the coring tube. Following slicing of liver and immobilisation on a flat surface, incubations were set up and as detailed in section 2.3.4.4.

4.3.2.2 Krebs-Henseleit buffer

Krebs-Henseleit buffer was prepared as outlined in section 2.3.4.5 and samples were prepared as outlined in section 2.3.4.4 using the tissue slicer detailed in section 4.3.2.1.

4.3.3 CE Separation

The CE method applied to the analysis of *in vitro* glucuronidation of 7-hydroxycoumarin in section 4.2 was used here. Capillary type, length and electrolyte buffers selection were made according to the same criteria outlined in section 4.2.3.

4.3.4 Results

The method proved very satisfactory for the resolution of all three analytes. Fig 4.12 shows an electropherogram of a standard mixture in Krebs-Hanseleit buffer. All three analytes were seen to resolve within 6 minutes. The Krebs-Hanseleit buffer was also run without any of the analytes added and no peaks which might interfere with results were noted. Figure 4.13 illustrates an electropherogram following an 8 hour incubation with 100μM 7-HC in Krebs-Hanseleit buffer showing the production of both phase II metabolites of 7-HC, namely, 7-hydroxycoumarin glucuronide and sulphate.

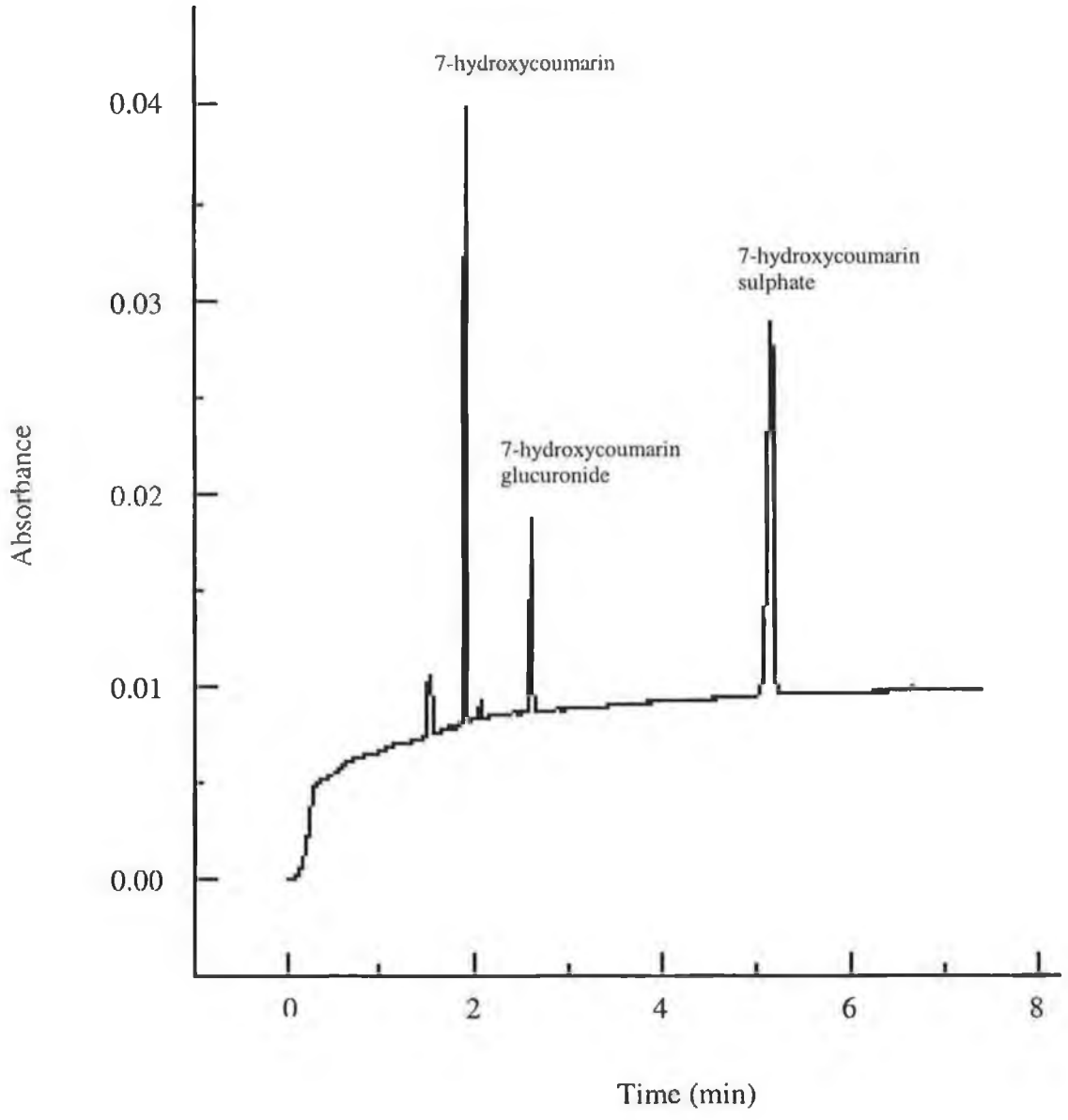

Figure 4.12 *Electropherogram of a standard solution of all three analytes in Krebs-Hanseleit buffer. Concentrations: 60μM 7-HC, 7-HS, 40μM 7-HCG. Conditions: 27 cm fused silica capillary; 100mM phosphate buffer, pH 7.0; 8 s pressure injection; separation at 17.5kV, with detection at 320 nm.*

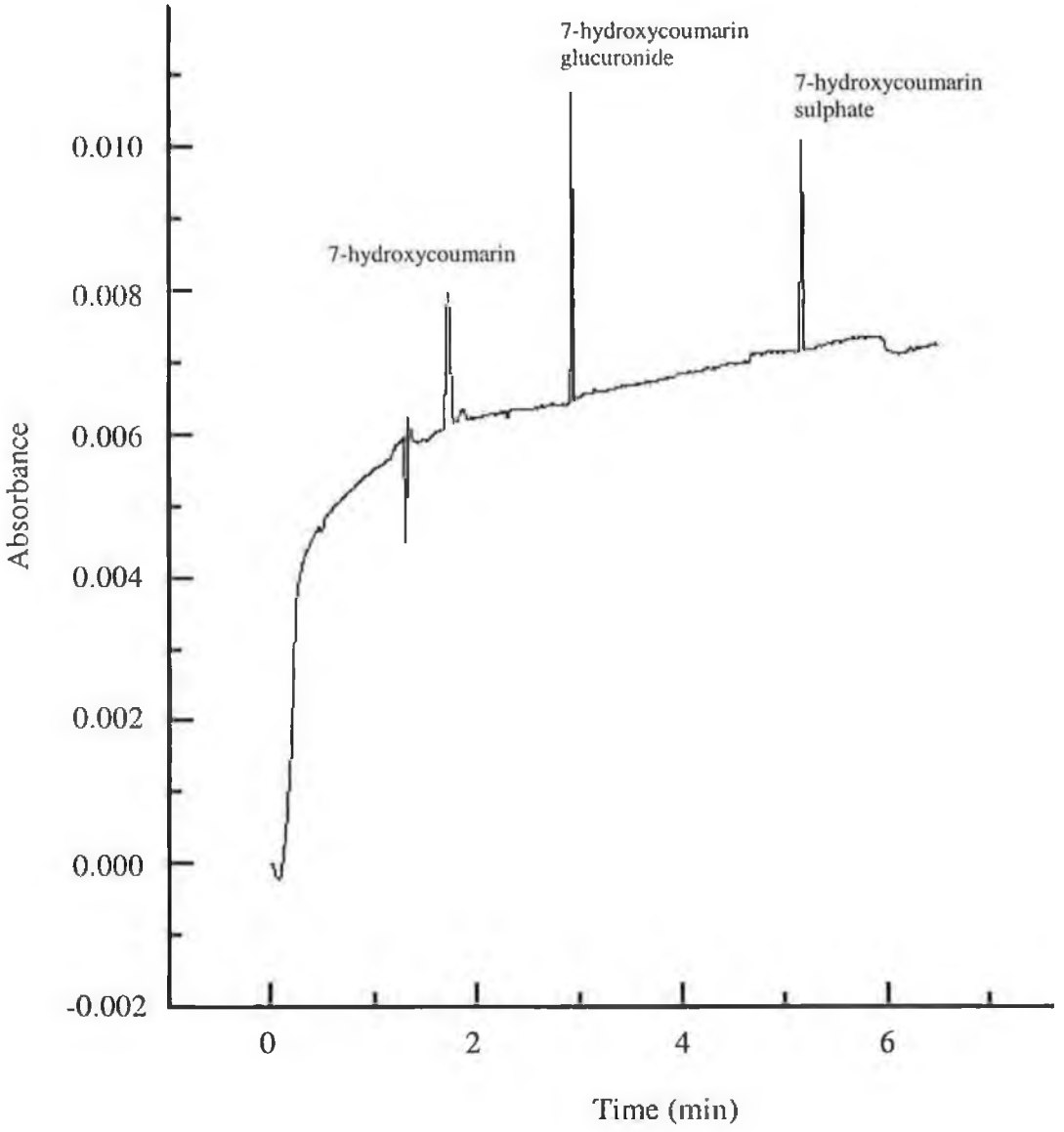

Figure 4.13 *Electropherogram showing the production of 7-HCG and 7-HS after an 8-hour incubation with 100-μM 7-HC in Krebs Hanseleit buffer. Samples filtered (0.22μm) prior to analysis. Conditions: 27 cm fused silica capillary; 100mM phosphate buffer, pH 7.0; 8 s pressure injection; separation at 17.5kV, with detection at 320 nm.*

4.3.5 Inter- and Intra-assay studies

To assess the method in terms of reproducibility and accuracy for analysis of the three analytes and as a method for analysis of liver slice incubations, both inter- and intra-assay studies were carried out using the following procedure.

Using peak heights mean (n=3) the concentrations of 7-HC, 7-HS and 7-HCG were calculated (calculated concentration, μM) along with the standard deviations. These were then compared to the actual known value of each analyte (nominal concentration). Values for coefficient of variation and percentage accuracy were calculated from peak heights using the following formulae:

$$\textbf{\textit{Coefficient of variation:}} \quad \frac{\textit{Standard deviation} \times 100}{\textit{mean}}$$

$$\textbf{\textit{Percentage accuracy:}} \quad \frac{\textit{calculated result} \times 100}{\textit{nominal result}}$$

4.3.5.1 Intra-assay performance

Intra-assay performance was assessed by analysing concentrations corresponding to the lower, middle and upper regions of the standard curve. The samples were analysed in replicates of five on the same day. Table 4.6 shows the results obtained. CV and percentage accuracy values are within ±14 and ±11%, respectively, with 80% of the values for both CV and percentage accuracy deviating within ±7%. As expected, precision and accuracy showed the largest deviation at the limit of detection of the method, most noticeable with 7-HC and 7-HS.

Intra-assay performance					
	Concentration (μM)				
	Nominal	Calculated	S.D.	% Accuracy	CV (%)
7-HC	6.17	5.55	0.52	89.95	9.37
	12.3	11.5	1.60	93.35	13.89
	30.9	31.6	1.28	102.4	4.05
	61.7	63.1	2.25	102.2	3.57
	123	121	5.76	98.26	4.75
7-HCG	2.76	3.07	0.22	111.2	7.17
	5.52	5.76	0.25	104.4	4.34
	13.8	14.1	0.76	102.5	5.37
	27.6	28.6	1.75	103.4	6.13
	55.2	57.0	0.32	103.2	0.56
7-HS	4.42	5.08	0.67	101.0	13.2
	8.84	8.55	0.56	96.72	6.54
	22.1	21.6	0.47	97.69	2.18
	44.2	44.2	0.40	102.0	0.89
	88.4	89.1	2.52	100.8	2.83

Table 4.6 *Intra-assay precision and accuracy results for the determination of 7-HCG and 7-HS conjugates of 7-hydroxycoumarin for liver slice incubates. Values calculated as outlined in section 4.3.5.*

4.3.5.2 Inter-assay performance

Inter-assay performance was assessed by analysis of samples in a range of four different concentrations of each analyte in triplicate over three different days. Table 4.7 shows the results obtained. CV and percentage accuracy values were between ±13 and ±6%, respectively. As with the intra-assay performance, both precision and accuracy showed the

highest values at the limit of detection of the method. Assay specificity was assessed by analysis of incubates without any 7-HC added. No significant interferents were noted in any of the migration zones of the analytes.

Inter-assay performance								
	Nominal	**Day 1**	**Day 2**	**Day 3**	**Mean**	**S.D.**	**CV (%)**	**% Prec.**
7-HC	12.34	13.64	12.34	12.34	12.69	0.83	102.8	6.54
	30.86	30.97	31.10	30.42	30.83	0.36	99.90	1.17
	61.73	61.14	62.26	61.45	61.22	0.58	99.82	0.94
	123.5	122.6	123.3	123.7	123.2	0.57	99.93	0.46
7-HCG	5.52	6.35	5.02	6.04	5.80	0.70	105.1	12.1
	13.8	14.0	13.5	14.5	14.0	0.52	101.1	3.71
	27.6	27.4	27.8	27.5	27.6	0.24	99.93	0.87
	55.2	55.0	55.3	55.4	55.2	0.22	99.98	0.40
7-HS	8.84	7.91	8.08	9.11	8.37	0.67	94.68	8.00
	22.1	22.4	23.5	21.9	22.6	0.80	102.2	3.54
	44.2	44.1	43.3	45.6	44.3	1.19	100.3	2.68
	88.4	88.1	89.3	91.6	89.7	1.78	101.4	1.98

Table 4.7 *Inter-assay percentage CV and accuracy results for the determination of 7-HCG and 7-HS conjugates of 7-hydroxycoumarin for liver slice incubates. Values calculated as outlined in section 4.3.5.*

4.4 Discussion

The CE method applied to the analysis of the glucuronidation of 7-HC by rabbit tissues was found to be very fast and reliable for the direct determination of 7-HC and 7-HCG as *in vitro* metabolites of reactions involving UDP-glucuronyl transferase and β-glucuronidase with total analysis times less 7 minutes, with injector to detector times for all analytes under four minutes. Minimal sample clean up was necessary thus reducing errors that may otherwise be introduced due to complex sample preparation steps (extraction, precipitation etc.). The method would also facilitate studies of promoters and inhibitors of both UDPGT and β-glucuronidase enzymes.

When compared to the HPLC method used in the previous chapter, the results show good agreement. Differences in the measurements of 7-HCG produced per minute per milligram of protein for the various organs are less than 10%. The liver shows a difference of 8.69% (2300pmol for HPLC, 2100pmol for CE), the kidney showed a variation of 9.09% (220 pmol for HPLC, 200 pmol for CE), while the large intestine showed a similar amount of 7-HCG produced per minute per milligram of protein (7.8 pmol) following analysis by either method. This study shows the CE method to be as reliable as the HPLC method. The advantages of speed of analysis coupled with vastly reduced sample and reagent requirements for CE (and hence much less waste) being significant differences.

The method may be applied for analysis of both the glucuronide and sulphate phase two metabolites proved to be very simple and effective for the determination of all three analytes, with good resolution and easy sample preparation, while still keeping the run time to a minimum. The method offers the advantage of speed (3 minute decrease in analysis over the fastest reported HPLC method) and minimal use of solvents (10 ml total solvent volume required for CE analysis) over pervious HPLC methods (Hiller and Cole, 1995; Walsh *et al.*, 1995). Its main advantage over other CE methods using LIF detection is that all three metabolites can be detected simultaneously (Cole *et al.*, 1996). Although UV detection does not offer the level of sensitivity of laser-induced fluorescence detection (LIF) it still offers acceptable levels at a much lower cost. Coupled to the lower sensitivity of UV, the sensitivity of the method is further affected by having to detect the coumarin metabolites at 320 nm instead of the more sensitive 214 nm. This is due to the absorbance of endogenous species present in the matrix interfering with the results when the lower wavelength is used for detection.

5 MICROCHIP CAPILLARY ELECTROPHORESIS - DEVELOPMENT OF IMMUNOASSAYS FOR WARFARIN AND PARATHION

5.1 Introduction

5.1.1 Micro-chip based Capillary Electrophoresis

Microchip CE was first developed in the early 1990s by Harrison and Manz (Harrison *et al.*, 1992). This system, with electrokinetic fluid handling has received ever increasing interest over the past eight years (Effenhauser, 1998) and is now a rapidly advancing area where the most notable results have been accomplished (Harrison *et al.*, 1993). Glass has been employed as the substrate of choice for CE applications as the micromachining techniques are well established and the general optical, electrical and chemical properties are favourable. The ability to transfer a variety of surface modification methods from conventional CE to planar chips is also an advantage. Glass is preferred over silicon devices for CE applications as these, despite being covered with insulating layers of thermal oxide and CVD nitride, have suffered from breakdown problems which limit the application voltages (Harrison *et al.*, 1993). Hence, while silicon substrates have been very successful in other areas (free flow electrophoresis and liquid chromatography), in CE, where high voltages are common, they have very little reported use (Effenhauser, 1998).

5.1.1.1 Sample Injection on planar chips

A means for sample injection was the first functional accessory that was successfully integrated into a planar CE device. The geometrical design for sample injection was first proposed by Verheggen *et al.* (1988) and has demonstrated its performance with the injection of microlitre sample volumes and sample plug lengths of several centimetres (Harrison *et al.*, 1992; Effenhauser *et al.*, 1993). Figure 5.1 shows the valveless design with a double "T" injector. Application of potential between reservoirs 1 (sample) and 4 (injection waste) electrokinetically pumps sample, filling a 150 μm length which is equal to 90 pl of the separation channel. This method of injection ensures that there is no electrokinetic bias in the sample injected as long as the potential is applied for enough time to ensure that even the slowest sample component has completely filled the injection volume. This is in contrast to

electrokinetic sample injection in conventional capillaries, which is known to bias the sample according to the respective ionic mobilities.

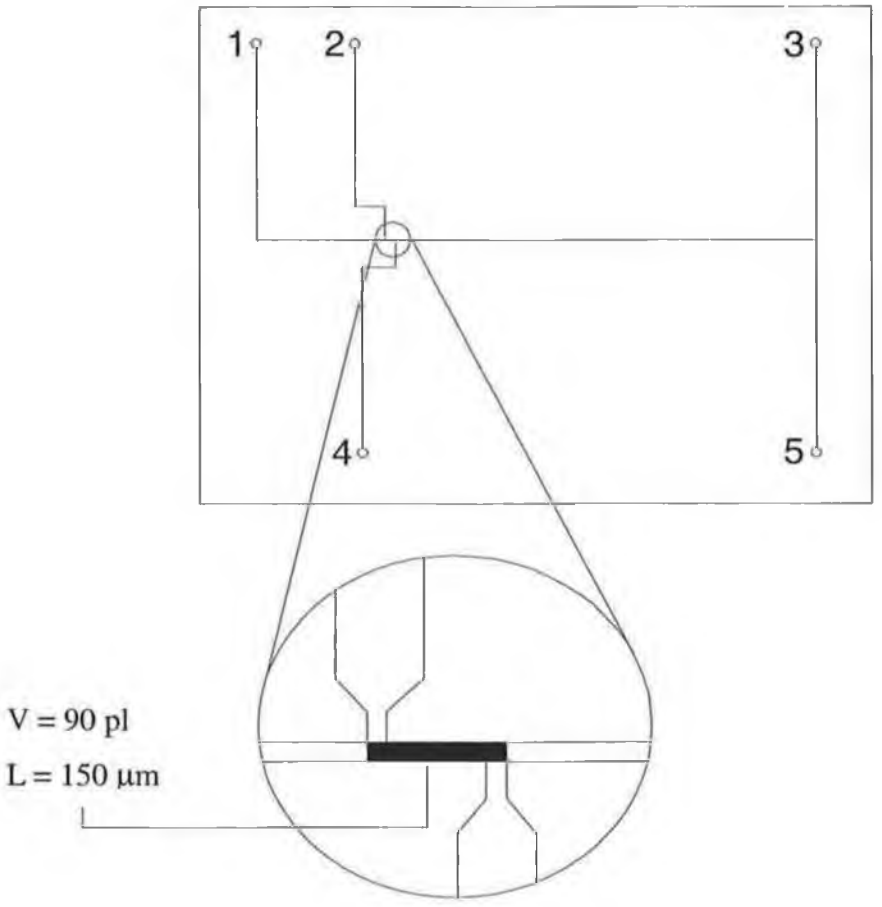

Figure 5.1 *Layout of a glass chip with integrated sample injection. The inset shows details of the geometry of the injection arrangement with a sample plug length of 150 µm and volume of 90 pl. 1,3 and 5 are buffer reservoirs, 2 is the sample reservoir, and 4 is the sample waste.*

Leakage from the injection channels into the separation channel is sometimes observed after application of the separation voltage. It can be avoided by more sophisticated voltage control protocols during sample injection and separation (Effenhauser *et al.*, 1994).

5.1.1.2 Electrophoretic Separations

To date a wide variety of separations have being performed on-chip, matching those of conventional CE in buffer solutions (Effenhauser, 1998; Chiem and Harrison, 1997). Mixtures of flourescently labelled (Fluorescein isothiocyanate, FITC) amino acids have been used as model case studies (Effenhauser *et al.,* 1993). Separations in polymer sieving matrices have also been reported (Effenhauser *et al.,* 1994). Separations are carried out in the same format on-chip as conventional CE. However, as the separation channel on a chip is much shorter than a capillary, lower voltages can be applied while still achieving the same electric fields.

5.1.2 Materials for microsystems

Miniaturised systems for performing chemical/biochemical reactions and analysis require cavities, channels, pumps, valves, storage containers, couplers, electrodes, windows and bridges (Qin *et al.,* 1998). The typical dimensions of these components are in the range of a few micrometers to several millimetres in length or width and between 100 nm and 100 μm in depth. The materials used are both rigid and elastomeric.

Rigid materials: There is a range of substrates on which microsystems can be built, including crystalline silicon, glass, quartz, metals and organic polymers. Rigid silicon-crystal structures have the advantage of a well established technology for manufacture, including the ability to form two and three-dimensional shapes and facilitate batch fabrication. However, disadvantages include the expense of the starting material, the fact that it is brittle and opaque in the uv/visible regions and its surface chemistry is complicated to manipulate (Qin *et al.,* 1998).

Elastomeric materials: A new route for fabricating optical elements and optical systems from elastomeric materials such as poly(dimethylsiloxane), PDMS, was developed (Qin *et al.,* 1998). These types of optical components and devices have characteristics that can be controlled by changing their shape by mechanical compression or extension. Among

the advantages to using PDMS are durability, ability to deform reversibly, optically transparent down to ~300 nm, and it is inexpensive. An example of its application is adaptive optics, which have previously been constructed from small individual rigid components that were moved independently to modify characteristics (Hubin, 1993).

5.1.3 Microfabrication techniques

The methods used for the manufacture of chips for CE applications include lithographic and other techniques as discussed in the following sections.

5.1.3.1 Photolithography

The most common lithographic technique in use today is photolithography (Moreau, 1988). The method involves a substrate which is spin coated with a thin layer of photoresist (photosensitive polymer), and exposed to a UV light source through a photomask. A quartz plate covered with patterned microstructures of an opaque material is used as the photomask and the pattern is transferred to the film of photoresist. Following this the substrate (glass chip) is then etched, a procedure carried out by placing the substrate in a dilute, stirred HF/NH_4F bath to form the channels. Only the surface area of the photoresist exposed to the UV light is removed allowing the desired pattern to be etched into the substrate (Fig 5.3). To form the closed network of channels, a cover plate is bonded to the substrate over the etched channels. For fused quartz substrates, gold/chromium films are necessary as an etch mask during HF/NH_4F etch. When examined in cross-section the channel profile is trapezoidal due to the isotropic etch of amorphous materials, with measurements of from 20 to 100 μm widths at half height and depths from 5 to 20 μm (Chiem and Harrison, 1997). Holes can be drilled in the cover plate to produce a communication link between an attached reservoir and channels and can be held in place by epoxy resin or interference fit.

5.1.3.2 Alternative microfabrication methods

Although photolithography is widely used to manufacture structures for microelectronic circuits, MEMS, microanalytical devices and micro-optics, it has a number of disadvantages. It is a relatively high cost technology, cannot be applied easily to curved surfaces, is applicable only to a small set of material and gives little control over the properties of the surfaces that are generated (Qin *et al.,* 1998). A set of non-photolithographic techniques for microfabrication have been developed. These techniques are discussed in detail by other authors, but include microcontact printing (Kumar *et al.,* 1995), micromolding in capillaries (Kim *et al.,* 1995) and replica molding (Xia *et al.,* 1996).

5.1.4 Microchip CE and Immunoassays

5.1.4.1 Immunoassays – a brief introduction

Immunoassays are among the most effective means for quantification of trace analytes in complex solutions (Schmalzing and Nashabeth, 1997). High selectivity results from specific antibody/antigen interactions while high sensitivity is achieved from a combination of strong binding, and fluorescent, chemiluminescent, radioactive or enzyme labels. The method of immunoassay was developed as far back as 1959 in New York by Solomon Berson and Rosalyn Yalow, when they developed the radioimmunoassay technique while working on the metabolism of ^{131}I-labelled insulin (Law *et al.,* 1996). Although there were some initial difficulties with the report, as the view that antibodies could be raised against small molecular weight material was considered controversial, the benefits of the method were soon recognised and the applications of the technique grew rapidly in the area of clinical biochemistry. Since 1984 enzyme immunoassays have become the most popular form of assay, with radiolabelled and fluorescent assays the other common formats in use.

The most important part of the immunoassay is the antibody. Figure 5.2 shows the structure of an IgG antibody and its fragments that can be used in assays (section 5.1.4.3). The basic structure consists of four polypeptide chains, two identical heavy chains, linked by one or more disulphide bridges, and two identical light chains, each paired with a heavy chain. Both heavy and light chains are comprised of two regions, a variable region (contributing to the

binding characteristics) and a constant region, which is constant for a given class of antibody. There are two classes, κ and λ, in the constant region for light chains and for the heavy chains there are five major variants: γ, α, ε, μ, and δ. These determine the five major classes of immunoglobulin, IgG, IgA, IgE, IgM and IgD and their biological properties (Law *et al.*, 1996).

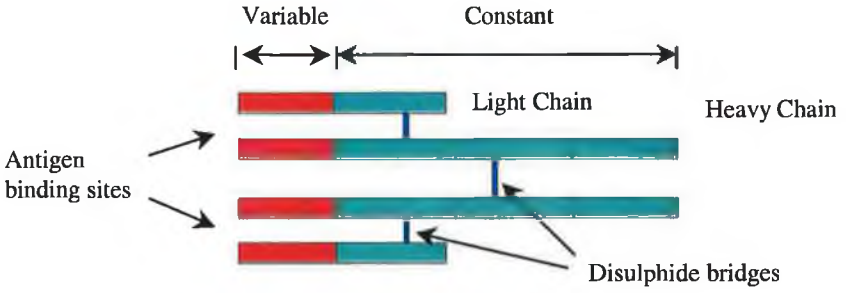

The basic antibody unit

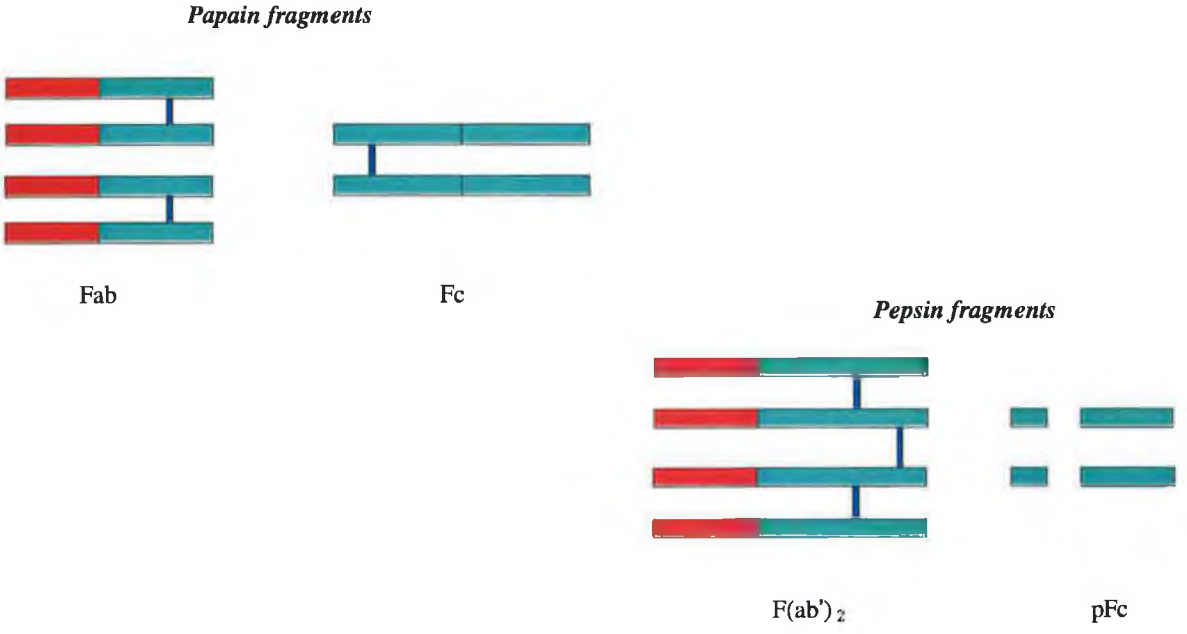

Enzyme derived antibody fragments

Figure 5.2 *The basic antibody unit used for the development of on-chip assays for warfarin and parathion (top). Also shown are the fragments (Fab, F(ab')$_2$ and pFc) enzymatically produced using papain and pepsin digests of whole antibody of which the Fab and F(ab')$_2$ can be used for immunoassays.*

A drawback of common immunoassays is that they tend to be slow and manually intensive and often require multiple incubation, washing and rinsing steps, which can take many hours to complete. In an attempt to develop more rapid and automated assay formats, microchip CE has being applied to this area.

5.1.4.2 Immunoassays using CE

The immunoassays that have being performed using CE can be classified as either competitive or non-competitive. In almost all cases reported to date, fluorescent labels have been used (Koutny *et al.*, 1996; Chiem and Harrison, 1997).

Non-competitive assays: In a non-competitive assay, an excess of labelled antibody (or antibody fragment) is added to a sample solution and is used to determine sample antigen. The labelled antibody, called the affinity probe, forms a complex specifically with antigen of interest.

The resulting equilibrium is:

$$Ab^* + Ag \rightleftharpoons Ab^*Ag$$

Where Ab* = labelled antibody
Ab = antigen
Ab*Ag = antibody-antigen complex

Therefore, a CE-LIF analysis of a non-competitive mixture should reveal two zones, one corresponding to the free Ab* and one corresponding to the Ab*Ag complex (provided there is excess antibody). Provided that the complex is stable on the time scale of separation, it should be possible to quantify Ag - based on the amount of complex formed, and/or decrease in the amount of free Ab* monitored by peak heights for each species

Competitive immunoassays: Competitive immunoassays utilise a competition between labelled antigen (Ag*), also called the tracer, and antigen (Ag) to bind antibody (Ab) in order to determine Ag in the sample. To perform the assay, a limiting amount of antibody is mixed with sample containing Ag and a fixed concentration of Ag*. The resulting equilibria are:

$$Ag^* + Ab \rightleftharpoons Ag^*Ab$$

$$Ag + Ab \rightleftharpoons Ag\,Ab$$

After incubation, Ag* and Ag*Ab are separated and quantified. As seen from the equilibria, a large [Ag] will result in lower [Ag*Ab] and higher [Ag*]. Therefore the amount of analyte can be indirectly determined by measuring the concentration of either bound Ag*, free Ag* or their ratio. This approach has the advantage over the non-competitive format as due to the large size of the antibody relative to the antigen, it may not be possible to achieve a separation between Ab* and Ab*Ag (binding of the antigen by the antibody may not produce a complex with significantly different migration time). In the competitive format, this problem is overcome by the use of the labelled antigen (Ag*) which will generally have a migration time significantly differing from that of the antibody/antibody complex, and should also provide a sharp peak for quantitation (Schmalzing and Nashabeh, 1997).

5.1.4.3 Special issues for immunoassays by CE

Labelling: The type of label and method of labelling of drug or antibody can be a key element in determining the success of the assay. Fluorescent labelling is an attractive choice due very low limits of detection.. However, it is important that the label does not interfere with the Ab/Ag complex formation, and that labelling results in a homogeneous product, critical for the formation of narrow well defined zones upon separation. The label may also be used to modify the electrophoretic mobility to improve resolution by changing the overall charge of the product.

Antibody: The correct choice of antibody is also of key importance. Monoclonal antibodies are better than polyclonal antibodies for producing well-defined zones for the antibody-antigen complex. Is has also being reported that the use of antibody fragments, such as Fab, or $F(ab)'_2$, (Fig. 5.2) produce better results than for whole antibody due to sharper Ab/Ag complex peaks produced (Shimura *et al.,* 1994). However, results have shown that whole antibody or even polyclonal antibody can be used effectively (Evangelista *et al.,* 1994; Schmalzing *et al.,* 1995). In each case the complex peak is not useful for quantification, as it does not migrate in a sharp well defined zone, however adequate quantification is possible based on the free tracer (which migrates in a sharp zone) provided it separates well from the antibody-antigen complex.

Separation conditions: Adsorption of analytes and assay reagents to the capillary surface degrades resolution and reproducibility, especially at the low concentrations associated with immunoassays. The migration buffer can be manipulated in order to decrease adsorption (section 5.2.5). However, with immunoassays this is limited since the buffer must be compatible with the formation of an immunoaffinity complex. Another issue that must be considered is speed and resolution of separation. Separation of Ab/Ag complex from free labelled reagent will disturb the binding equilibrium and result in dissociation of complex throughout the separation (Rief *et al.,* 1994). The magnitude of complex dissociation will depend on the dissociation rate of the complex and the rate of separation. It is for this reason that separations need to be performed as fast as possible with antibodies with slow dissociation rates. Figure 5.3 shows an ideal electropherogram that might be obtained from CE analysis following incubation of an antibody and antigen. Both UV and fluorescent formats were tried in the following sections.

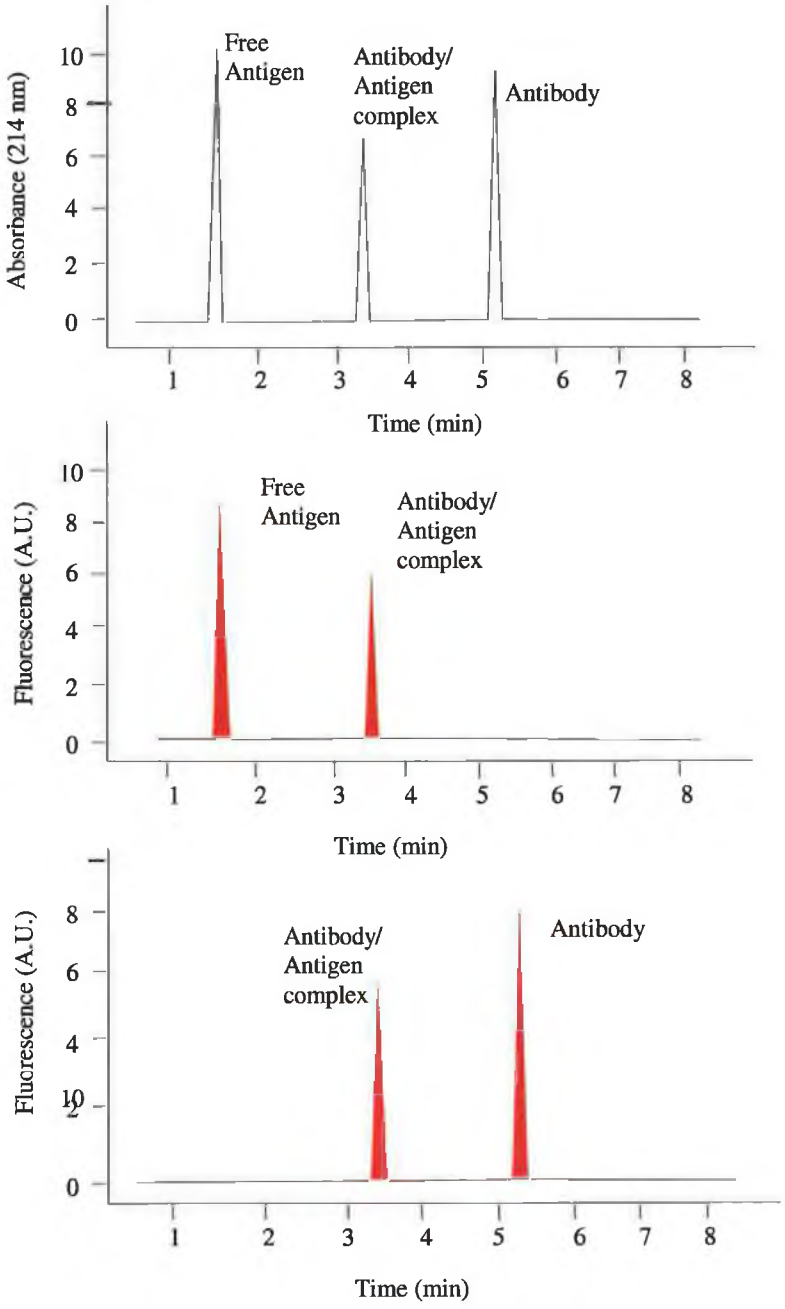

Figure 5.3 *Model electropherograms for CE immunoassays. (1) shows the expected result using UV detection, in which all three species absorb, and appear in the electropherogram. (2) shows the expected result using fluorescence detection with a labelled antigen, only the free labelled antigen and conjugate (made visible by binding the labelled antigen) appear in the electropherogram. (3) shows the electropherogram obtained when a labelled antibody is used, again the conjugate is visible by means of the label on the antibody, as is the antibody, but not the unlabelled antigen. These electropherograms represent the three strategies examined in the work presented in this chapter.*

5.2 Development of microchip based immunoassays for warfarin and parathion

5.2.1 Materials for microchip manufacture

Section 5.1.1 and 5.1.2 outline the criteria used in the selection of material for chip fabrication. Based on these considerations glass was chosen as the material of choice. For ease of handling it was important for the chip to be robust, and also as final assembly (drilling of cover plate and thermal bonding) was carried out "in-house", a more durable chip would reduce the possibility of breakage. Figure 5.4 shows the layout and dimensions of the chip used in the assays.

5.2.2 Device fabrication

Etching of the substrate was done in the Alberta Micromachining Centre according to the procedure outlined in section 5.1.3. Figure 5.4 shows the channel pattern etched into the glass. The injection design outlined in section 5.1.1.1 was incorporated to avoid sample bias during injections.

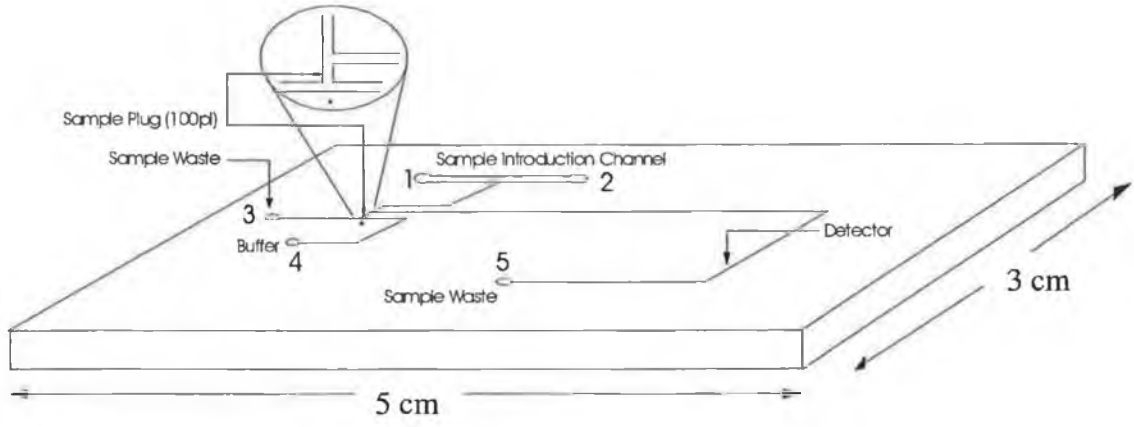

Figure 5.4 *Chip design. Dimensions are in centimetres*

A cover plate with 2mm diameter holes drilled under water using a diamond tipped drill, providing channel access points, was thermally bonded to a glass plate in which the channels were etched. This was done by hydrolysing both surfaces and contact bonding them followed by thermal processing at 500^0C for 6 hours.

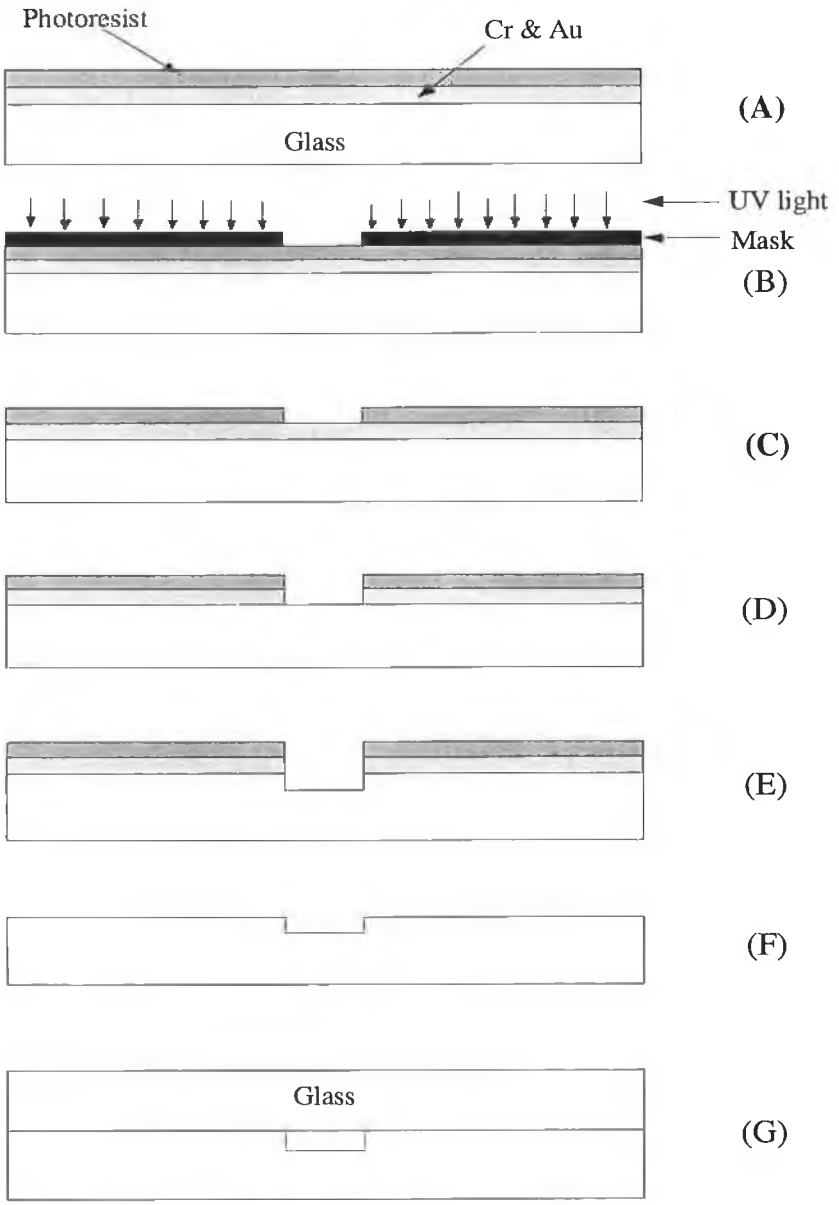

Figure 5.5 *Sequence of photolithographic fabrication: (A) Cr and Au masked glass plate coated with photoresist; (B) sample exposed to UV light through a master mask; (C) photoresist developed; (D) exposed metal mask etched; (E) exposed glass etched; (F) resist and metal stripped; (G) glass cover plate bonded to form capillary.*

The sample introduction channel (SIC) between reservoirs 1 and 2 was designed for previous experiments involving periodic sampling from a flow through system. For the purpose of these experiments both reservoirs were filled with sample with potential applied at reservoir 1. Reservoir 3 is the sample waste while the long channel between 4 and 5 is for separation. The length of the separation channel was 5 cm.

5.2.3 Microchip station control and layout

Figure 5.6 shows the computer-controlled relay system used to apply and switch the potentials on the four device reservoirs (1 and 4 positive; 3 and 5 grounded). A 488nm argon ion laser (Uniphase/Ionice Model 2011) was used to excite fluorescence after focusing to a ~40μm spot on the device channel. The fluorescence emission was collected with a 7:1 microscope objective and directed onto a photomultiplier tube using a pinhole at the image plane and an optical bandpass filter (508-533nm). The emission signal was electronically filtered with a Krohn-Hite Model 3342 six pole Butterworth filter with a 200Hz low-pass cut-off. Labview programs (National Instruments Corp., Austin, TX) written locally were used for calculations, data acquisition and instrument control.

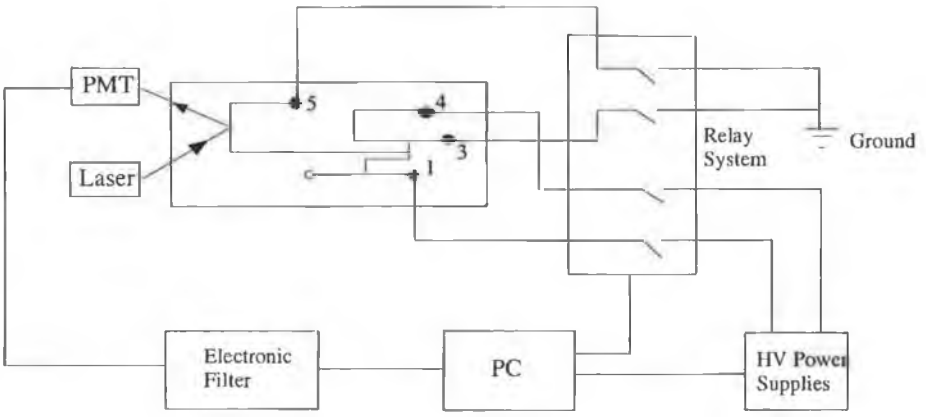

Figure 5.6 *Block diagram of the high voltage relay controlled system for the capillary electrophoresis power supplies, with computer control and digital data acquisition of laser excited (488 nm) fluorescence.*

5.2.4 Layout of chip station

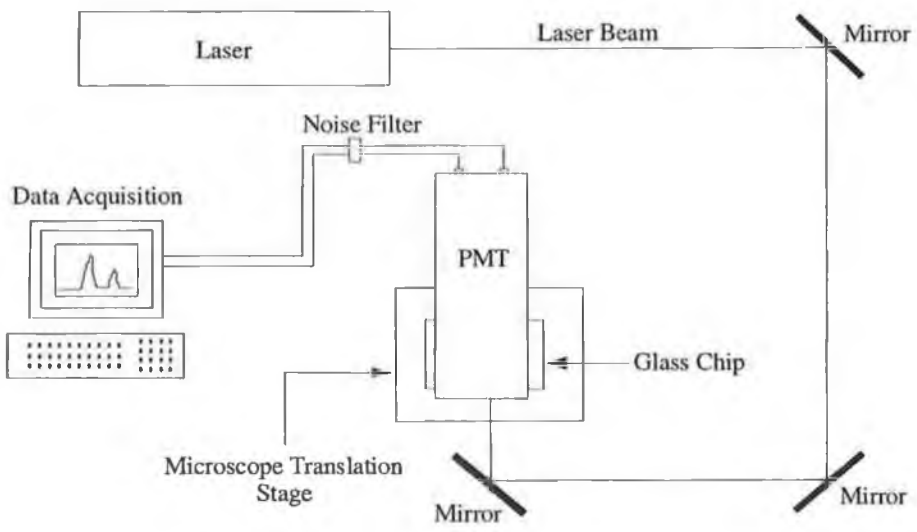

Figure 5.7 *Drawing showing overview of chip station and method for directing laser beam onto separation channel. Microscope translation stage allows movement in x and y planes.*

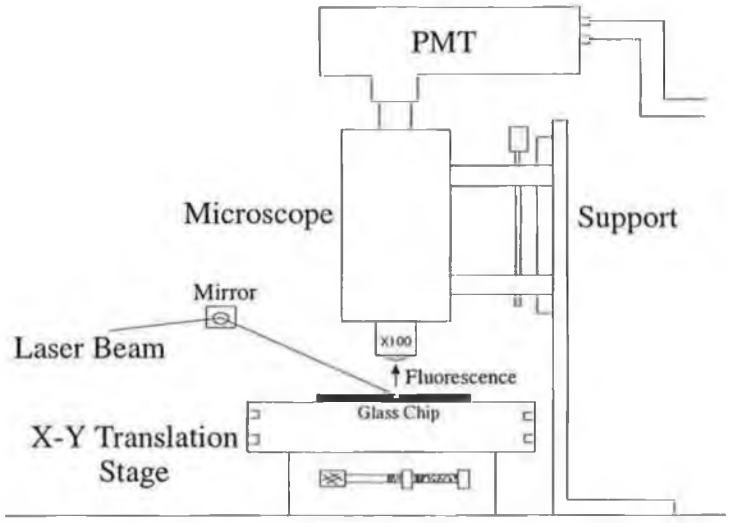

Figure 5.8 *Side view of chip on support with microscope and photomultiplier tube (PMT) mounted directly above spot where laser is focused onto the separation channel for collection of fluorescence.*

5.2.5 Development of separation conditions

Protein separation in untreated fused silica capillaries requires special considerations if interactions between the negatively charged silanol groups on the capillary wall and positively charges residues in the proteins were to be avoided. There are a number of ways these interactions can be stopped or reduced to such an extent that their effect on the separation is negligible. These involve surface modifications of the capillary wall (Nashabeh *et al.*, 1991), the use of buffer additives, (Bushy *et al.*, 1989) and high pH buffers (Lauer and McManigill, 1986). Based on the fact that surface modification is a complicated process and was not available to modify the chip surfaces, high pH buffers were chosen. Success with the use of buffer additives depends on the specific interaction of the additives with the sample, and in the case of immunoassays, might have a detrimental effect. With the use of high pH buffers electrostatic properties of the proteins can be exploited to favourable advantage. At a pH above its isoelectric point the protein will have a net negative charge and will be repelled from the wall of the capillary and chip.

5.2.5.1 Conventional CE

The use of borate buffers has been reported for separation of proteins and in immunoassays (including chip assays) with considerable success (Chiem and Harrison, 1997), and as the assay format was similar this was the buffer of choice. Concentrations varied slightly, with 10mM and 5mM used, pH 9.0.

5.2.5.2 Microchip CE

Borate buffers identical to those described in section 5.2.5.1 were used for microchip analysis of antibodies and unlabelled drug-protein conjugates. For analysis of FITC-labelled drug-protein conjugates, the use of buffer additives to improve the peak shape were assessed. SDS-borate buffers were tried, however, SDS gave rise to a high background, so Tris-borate

buffers (pH 8.5) were used with no increase in background. All buffers were filtered (0.22 μm) prior to use.

5.2.6 Checking antibody reactivity

Warfarin and parathion antibodies for use in the assays were checked for reactivity using competitive ELISA as outlined in section 2.3.5.1. A schematic showing the different steps involved in the ELISA is shown in Figure 5.9. Absorbance readings obtained for the series of decreasing concentrations of free drug in solution, A, over A_0 (absorbance obtained with no free drug in solution) were plotted against the log of free drug concentration in solution for each antibody (Fig 5.10).

Following confirmation of reactivity for both antibodies an analysis using conventional CE with UV detection was carried out for warfarin antibody. This was to examine binding of warfarin by antibody to confirm ELISA results. This examination also provided information on the stability of the complex under conditions applied during CE separations i.e. if any dissociation occurred during separation conditions (high pH buffers, pH 9.0, and high separation voltages, 16kV) (section 5.2.7). The results are shown in Figures 5.11 – 5.13.

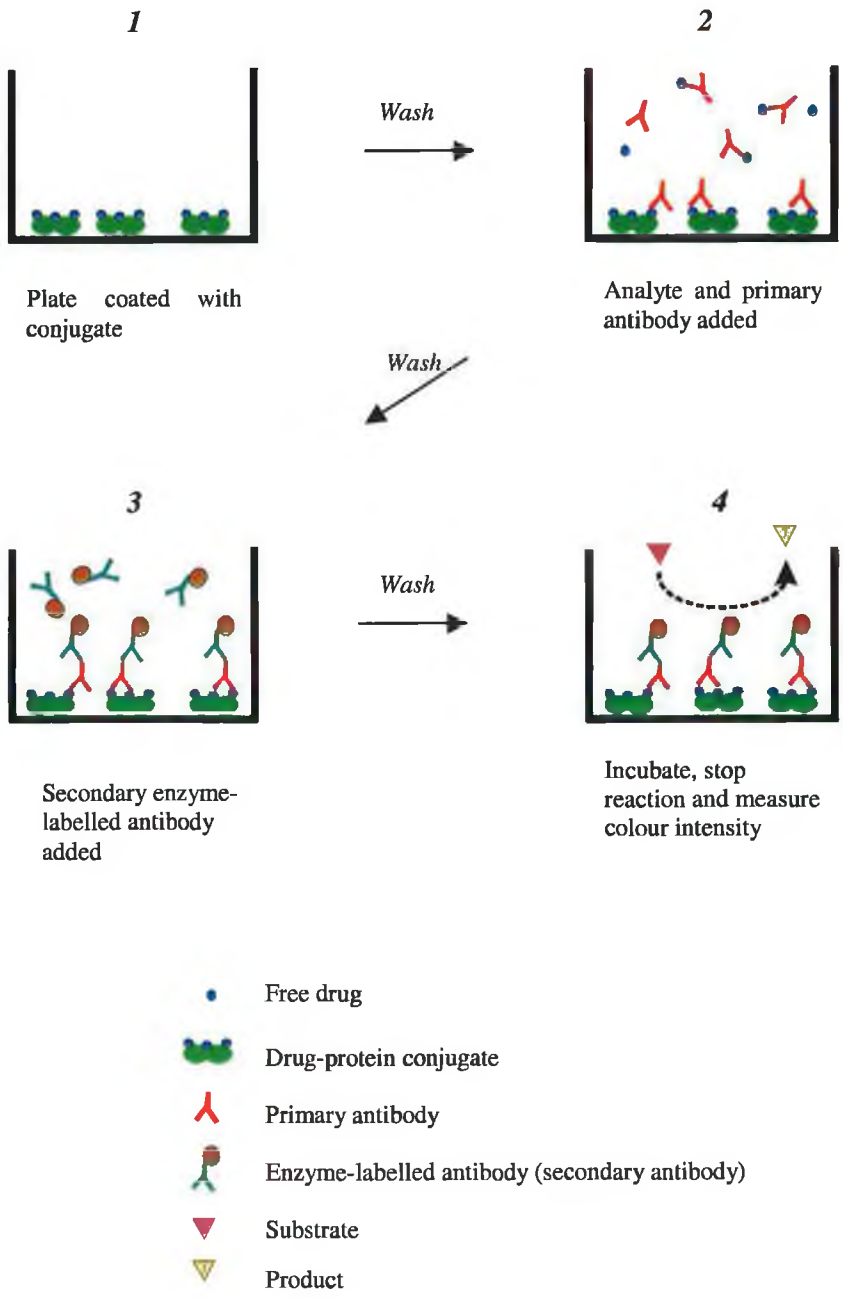

Figure 5.9 *Schematic diagram for competitive ELISA used to determine antibody reactivity. The procedure was carried out as outlined in chapter 2, section 2.3.5.1.*

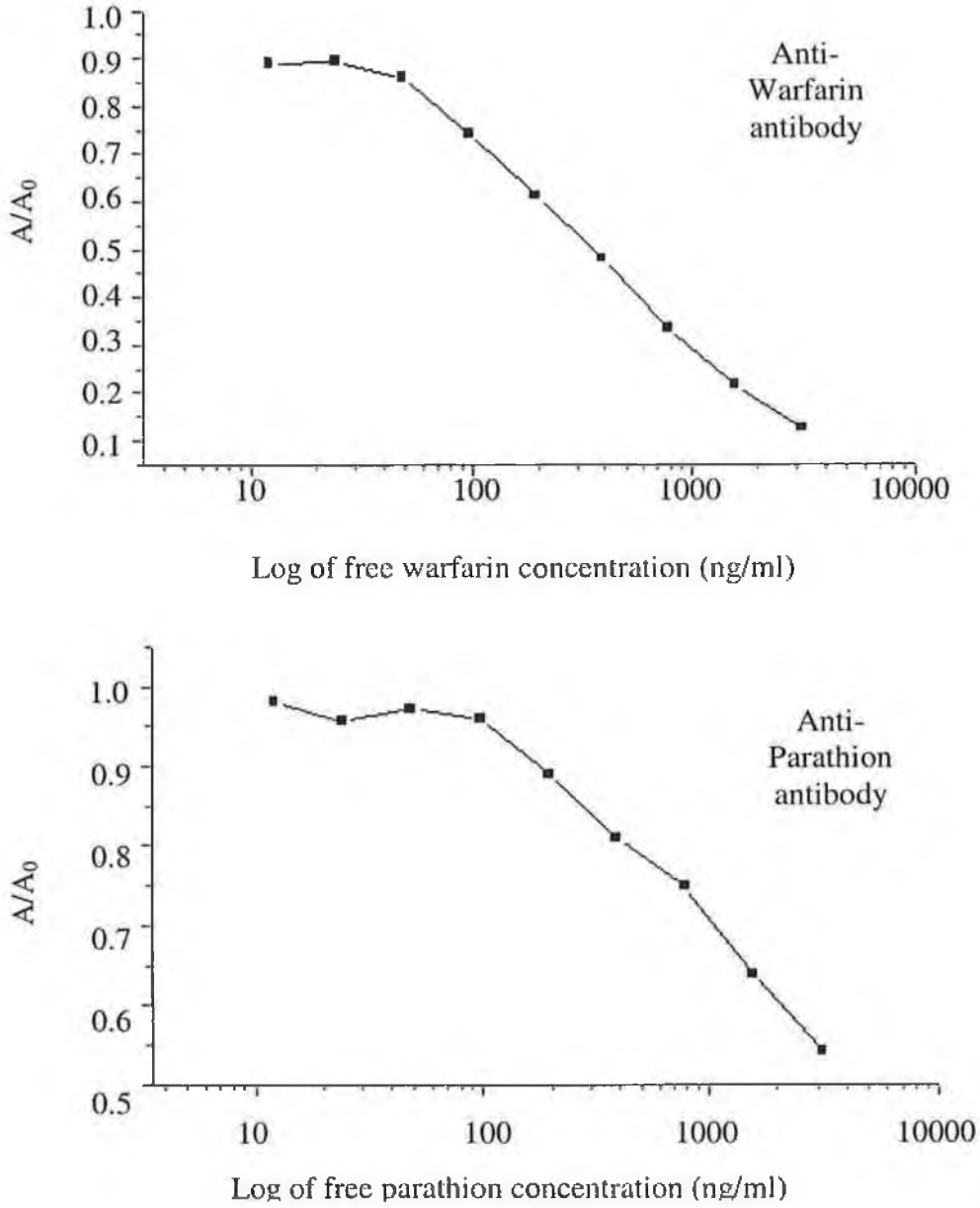

Figure 5.10 *Competitive ELISA test for antibody activity. A, absorbance obtained with decreasing concentration of free drug over A_0, absorbance with no free drug, is plotted against log of free drug concentration. Absorbance readings were recorded at 405 nm.*

5.2.7 CE analysis with UV detection

Figure 5.11 shows the electropherogram for free warfarin and Figures 5.12 and 5.13 show analysis of incubations of warfarin and increasing warfarin antibody concentrations (0.46, 0.92, 1.39, 1.84 × 10^{-6} M). Due to some initial delays in the preparation of the parathion antibody it was not assayed by conventional CE here but was assayed on the chip at a later date. The antibody displayed a migration time difference of about 30 seconds to that of free warfarin (Fig 5.11).

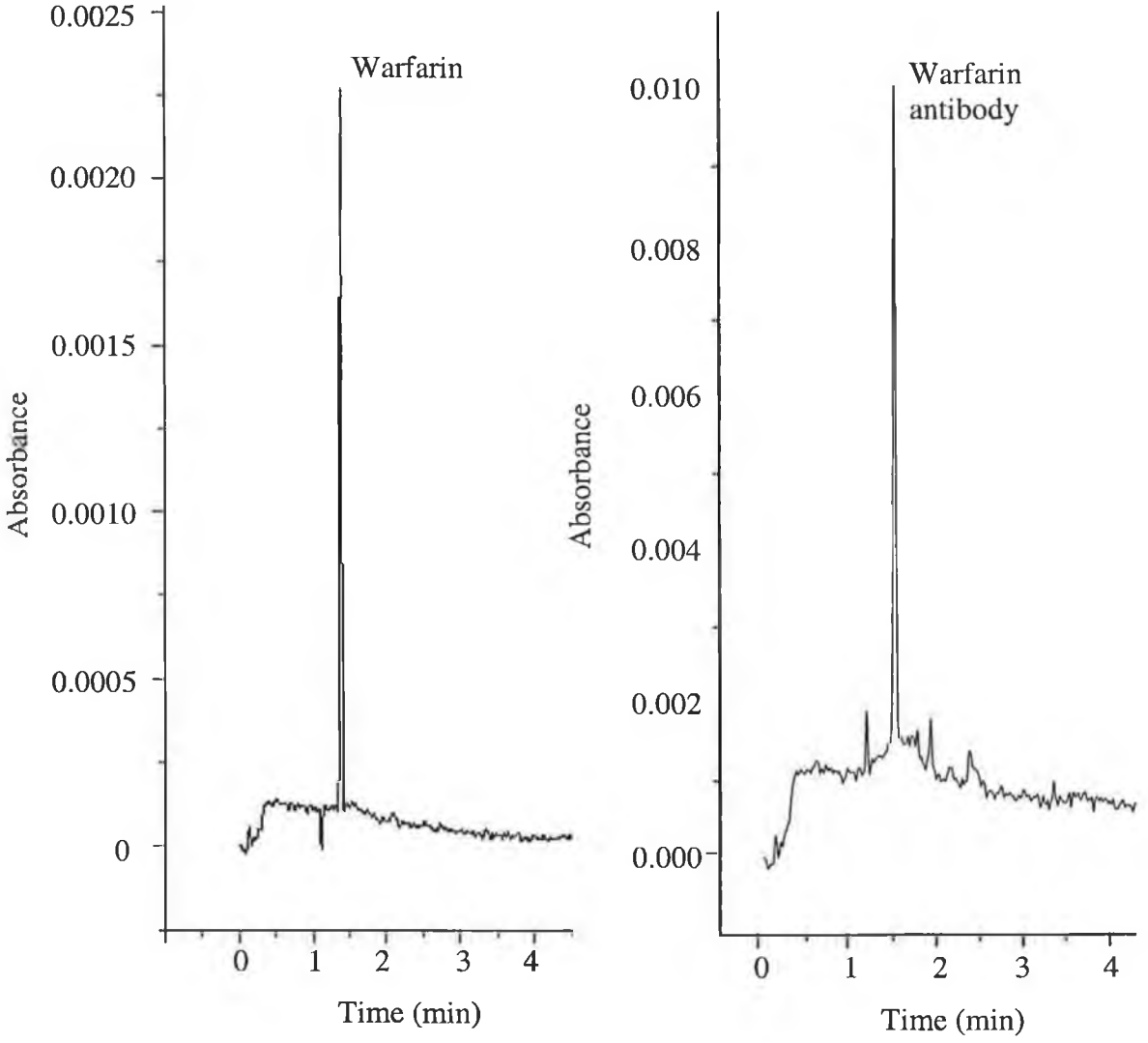

Figure 5.11 *Analysis by CE of warfarin (7.39 × 10^{-5}M) and anti-warfarin antibody (0.3 μM) with UV detection at 214 nm. Conditions; untreated fused silica capillary, 375μm OD, 50 μm ID; 19.3 cm to detector window, separation buffer; 5mM borate buffer, pH 9.0; 5 s pressure injection with separation at 16kV and detection at 214 nm.*

Addition of antibody results in a decrease in the peak for free warfarin (Fig 5.12). However, an increase in migration time for the antibody/warfarin complex is also seen, as well as a reduction in tailing for the complex. Tailing is caused by interactions between the antibody and the wall of the capillary, and the binding of warfarin seems to be having an effect on these interactions while also increasing the migration time. Repeated analysis showed identical results.

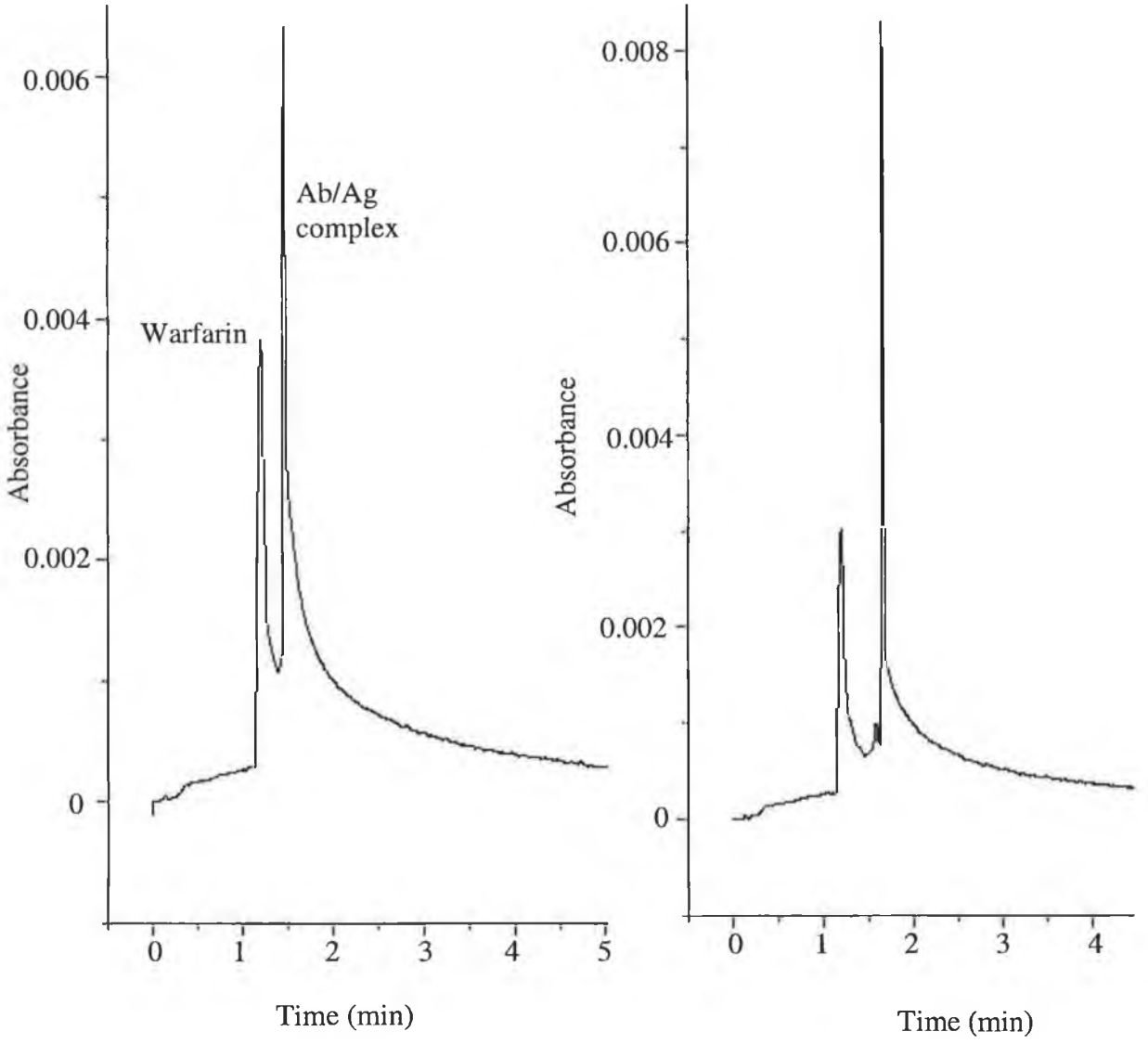

Figure 5.12 *Addition of anti-warfarin antibody (0.46μM, left, 0.92μM, right) to free warfarin (7.39×10^{-5}M). Conditions: untreated fused silica capillary, 375μm OD, 50 μm ID; 19.3 cm to detector window, separation buffer; 5mM borate buffer, pH 9.0; 5 s pressure injection with separation at 16kV and detection at 214 nm.*

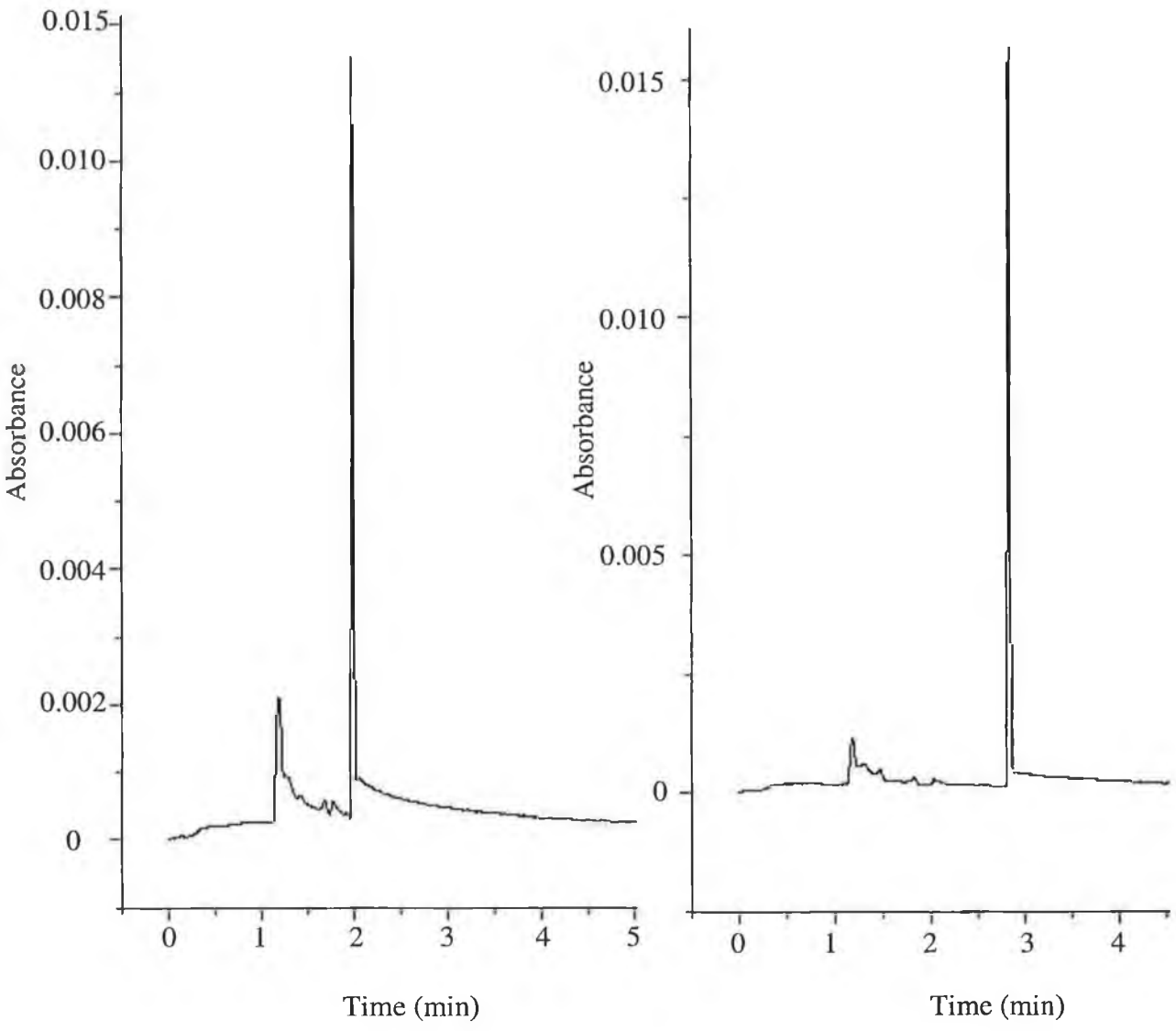

Figure 5.13 *Addition of anti-warfarin antibody (1.39μM, left, 1.84μM, right) to free warfarin (7.39×10^{-5}M). Conditions; untreated fused silica capillary, 375μm OD, 50 μm ID; 19.3 cm to detector window, separation buffer; 5mM borate buffer, pH 9.0; 5 s pressure injection with separation at 16kV and detection at 214 nm.*

In order to apply microchip technology to the above assay, it is necessary to flourescently label either the antigen or antibody, as LIF detection was the only format available. While the results above are not ideal for the assay, they do indicate that the antibody is capable of binding the warfarin under CE conditions. Addition of labels to either reagent could change their migration times somewhat and perhaps provide better resolution.

5.2.8 Labelling and analysis of antibody

5.2.8.1 Conventional CE-LIF analysis

Both anti-warfarin and anti-parathion antibodies were labelled with fluorescein isothiocyanate (FITC) as outlined in section 2.3.5.2 and affinity purified (2.3.5.3). Figure 5.14 shows an electropherogram obtained from analysis of anti-warfarin antibody with laser-induced fluorescence detection (LIF). Anti-parathion antibody was analysed directly on chip.

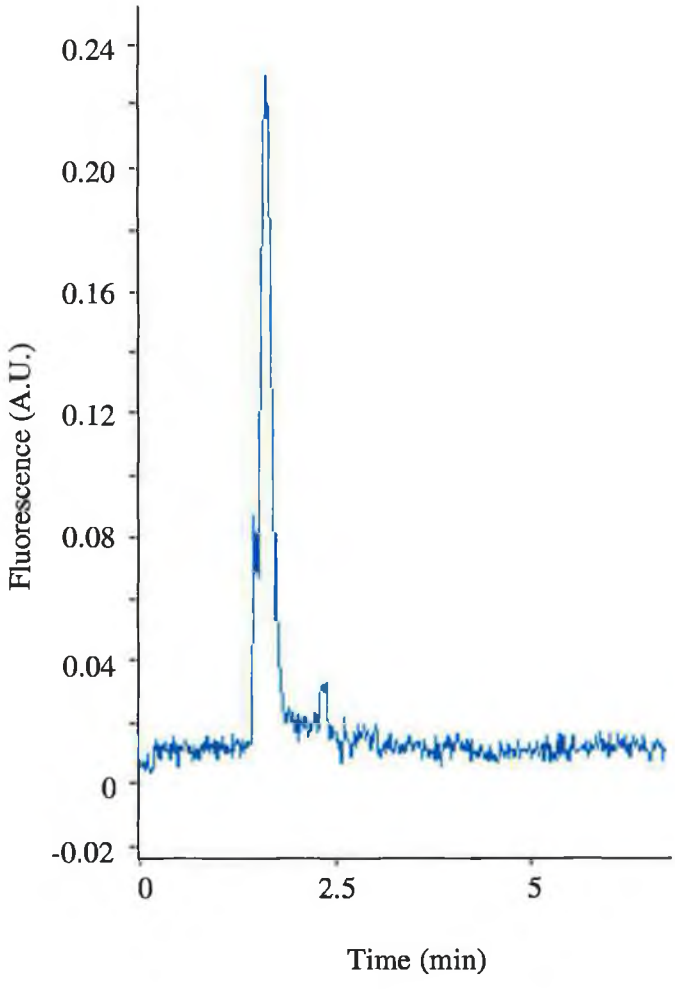

Figure 5.14 *CE-LIF analysis of anti-warfarin antibody (8.7×10^{-8}M). Conditions: 10mM borate buffer, pH 9.0; untreated fused silica capillary (50μm ID, 375μm OD, 19.3 cm to detector window), 3 s pressure injection; separation at 16kV, 25^{0}C, with excitation at 488 nm, and emission at 520 nm.*

5.2.8.2 Micro-chip analysis of labelled antibodies

The anti-warfarin and anti-parathion antibodies were analysed by microchip CE. Figures 5.15 and 5.16 show the electropherograms obtained. Both antibodies showed a constant migration time of 6 seconds (conditions as outlined in the legend). Following labelling both antibodies were assayed for activity by ELISA as outlined in section 2.3.5.1. Results obtained were similar to those shown earlier for unlabelled antibodies, confirming that labelling had not interfered with activity of either antibody.

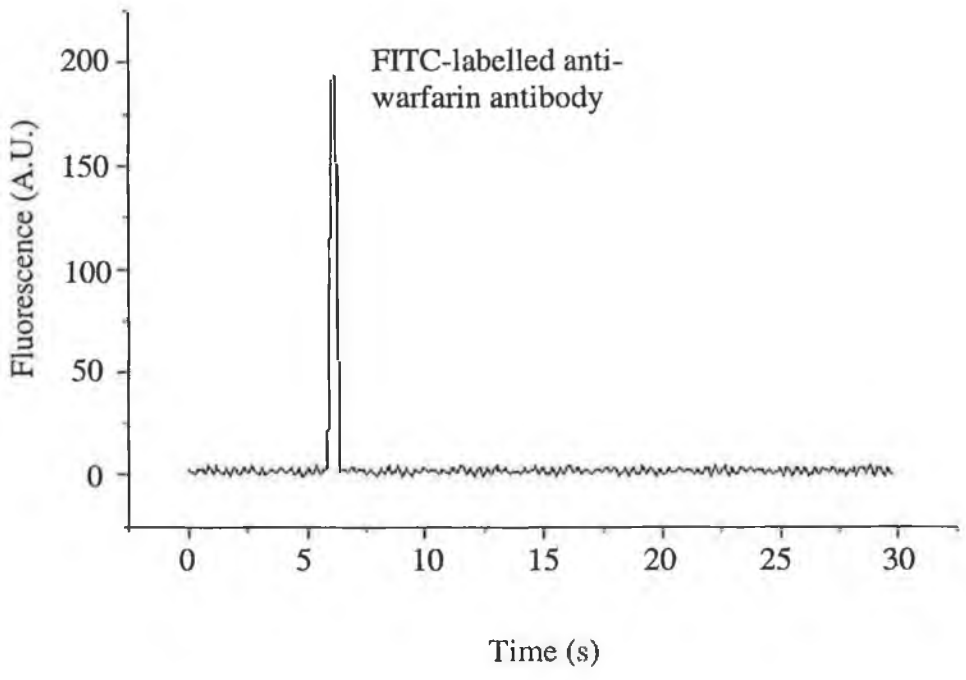

Figure 5.15 *Micro-chip analysis of FITC labelled anti-warfarin antibody, 8.7×10^{-8}M. Conditions: 5mM borate buffer, pH 9.0, 10-second injection at 1.5V, separation voltage 6kV, with excitation at 488 nm, and emission at 520 nm.*

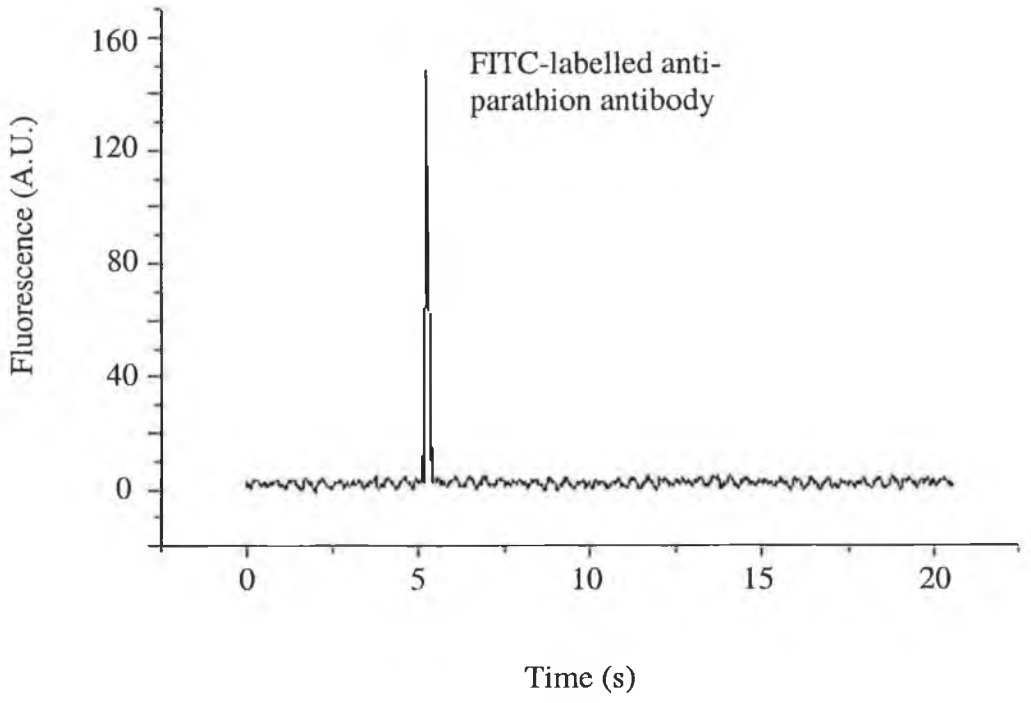

Figure 5.16 *Micro-chip CE analysis of FITC-labelled anti-parathion antibody (9×10^{-8}M). Conditions: 5mM borate buffer, pH 9.0, 10-second injection at 1.5V, separation voltage 6kV, with excitation at 488 nm, and emission at 520 nm.*

5.2.9 Development of immunoassay

A number of different approaches were tried for the development of the immunoassays. On reaction of labelled antibody (Ab*) with unlabelled antigen (Ag) (warfarin or parathion), it was not possible to see a separate peak corresponding to the antibody-antigen complex. If a complex was forming, it showed no change in migration time compared to that of the original antibody. Figure 5.17 illustrates this with repeated analysis (conventional CE) for a range of concentrations of added warfarin - 14, 42, 126 and 378μM - against a constant antibody concentration of 8.7×10^{-8}M. This is in agreement with results from UV studies shown earlier which also demonstrated no separation between antibody-antigen complex and free antibody.

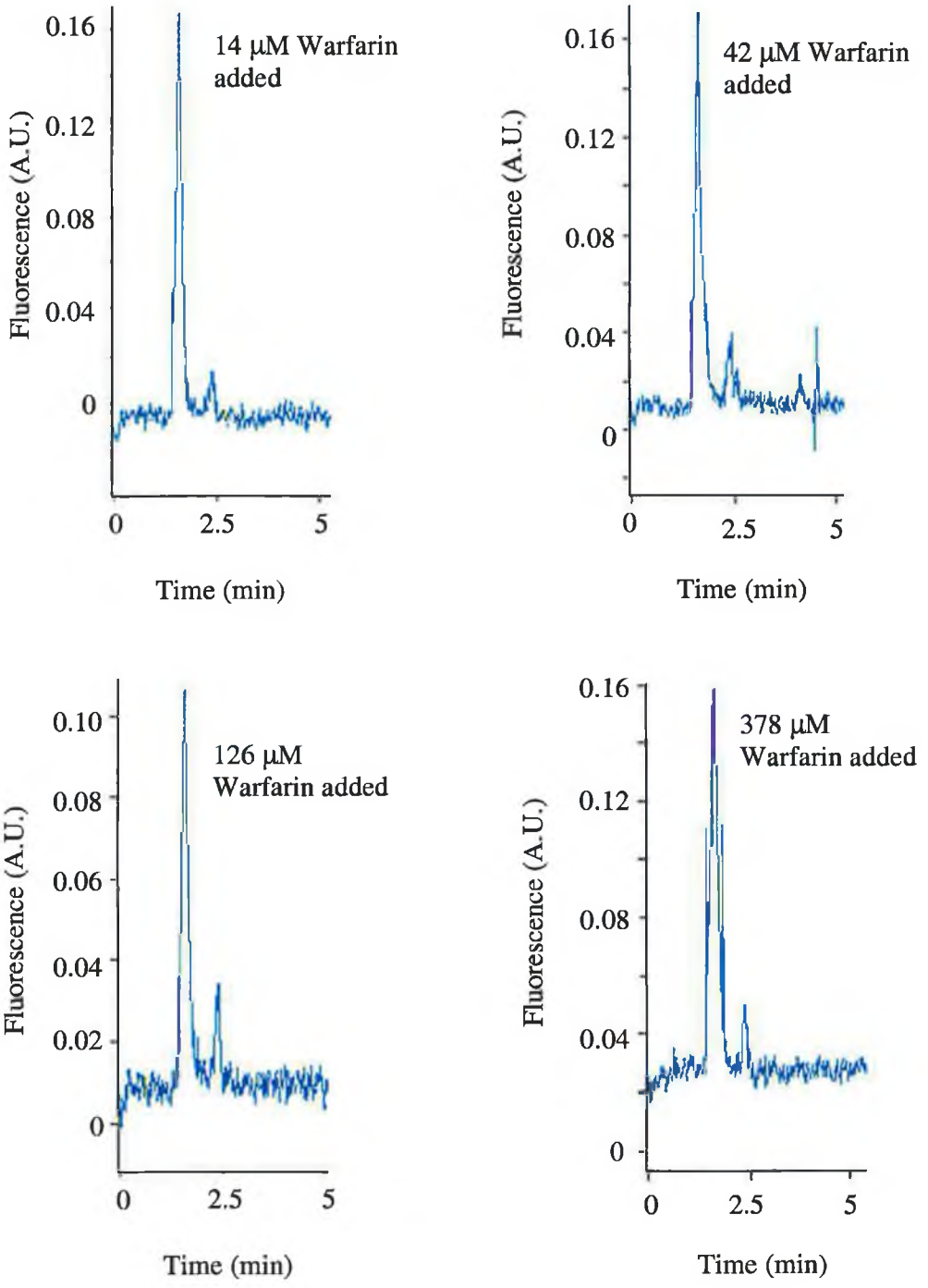

Figure 5.17 *CE analysis following addition of a range of concentrations (14, 42, 126 and 378µM) of warfarin to FITC-labelled warfarin antibody. No visible change seen for the formation of an Ab*Ag complex. Conditions: 10mM borate buffer, pH 9.0; untreated fused silica capillary (50µm ID, 375µm OD, 19.3 cm to detector window), 3 s pressure injection; separation at 16kV, 25^{0}C, with excitation at 488 nm, and emission at 520 nm.*

5.2.9.1 Unlabelled BSA-conjugate as antigen

The next approach was to use an unlabelled BSA conjugate of both drugs, parathion and warfarin, as antigen, and react this with the labelled antibody. The theory behind this step was that the larger molecular weight antigen (drug-protein conjugate) may produce a significant change in the migration time of the complex, and produce a separate peak in the electropherogram. This met with limited success for warfarin initially as can be seen by the appearance of a shoulder on the peak of the antibody corresponding to the Ab*Ag complex. (Figure 5.18). However, a similar strategy with the parathion conjugate yielded inconclusive results, and it was not possible to improve the resolution of the warfarin complex. Section 5.1.4.2 discussed how the use of a labelled antigen could possibly provide a solution to the problem. As it was not possible to label parathion or warfarin directly, the labelling of the parathion/warfarin-BSA conjugate was investigated.

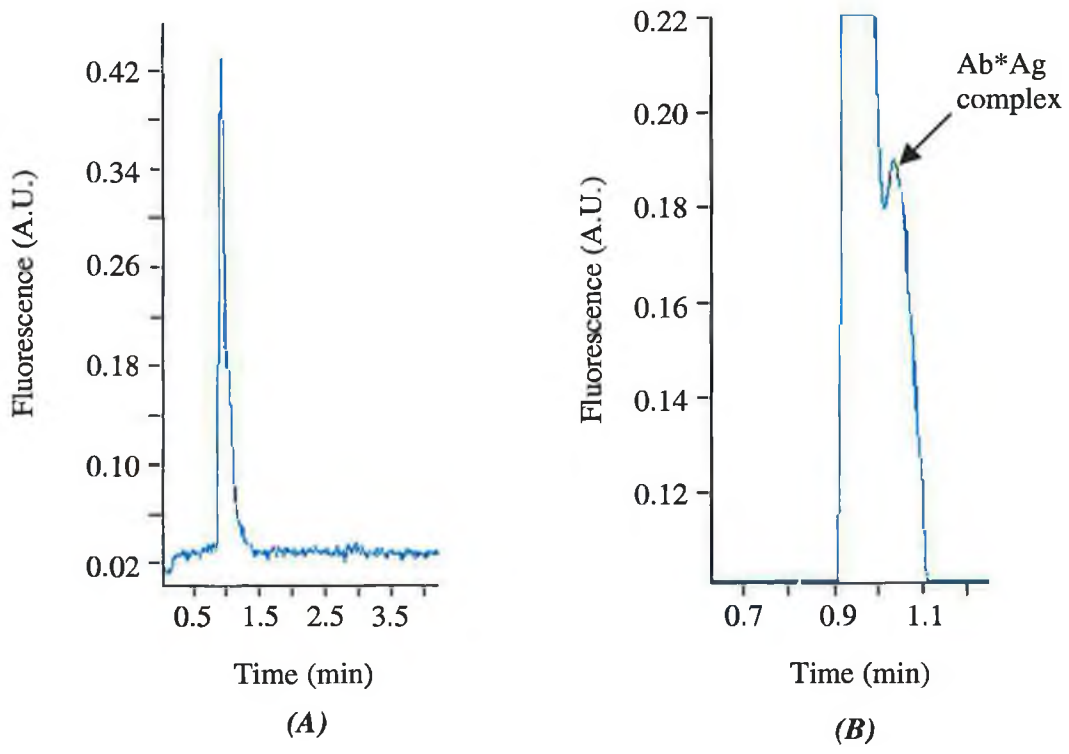

Figure 5.18 *CE analysis of labelled anti-warfarin antibody with unlabelled BSA-warfarin as Ag. (B) shows the expanded region of (A) where the complex can be seen as a shoulder on the antibody peak. Conditions: 10mM borate buffer, pH 9.0; untreated fused silica capillary (50μm ID, 375μm OD, 19.3 cm to detector window) 3 s pressure injection; separation at 16kV, 25^{0}C, with excitation at 488 nm, and emission at 520 nm.*

5.2.10 Labelling of BSA-conjugates with FITC

The labelling of the BSA conjugates was carried out in the same manner as the labelling of the antibodies (section 2.3.5.5), the only change being the protein concentration for the warfarin conjugate was 3.03×10^{-6}M, and 1.9×10^{-5}M for parathion conjugate. The concentration of FITC used in the labelling reaction was a five-fold molar excess of the relevant drug-BSA concentration.

5.2.11 Micro-chip analysis

5.2.11.1 FITC BSA-Warfarin Conjugate

Section 5.1.4.3 outlines the potential problems associated with the labelling of antibodies and antigens. Following labelling it was hoped that the product would exhibit a relatively narrow migration zone, allowing any complex formed to be completely resolved with no overlap. However, despite the addition of Tris to the separation buffer, on analysis it was clear that there was a large distribution of labels on the conjugate – evidenced by the width of the peak shown in Figure 5.19. On addition of unlabelled anti-warfarin it is possible to see the changes as the complex is formed (Fig 5.20) showing at ~35 seconds.

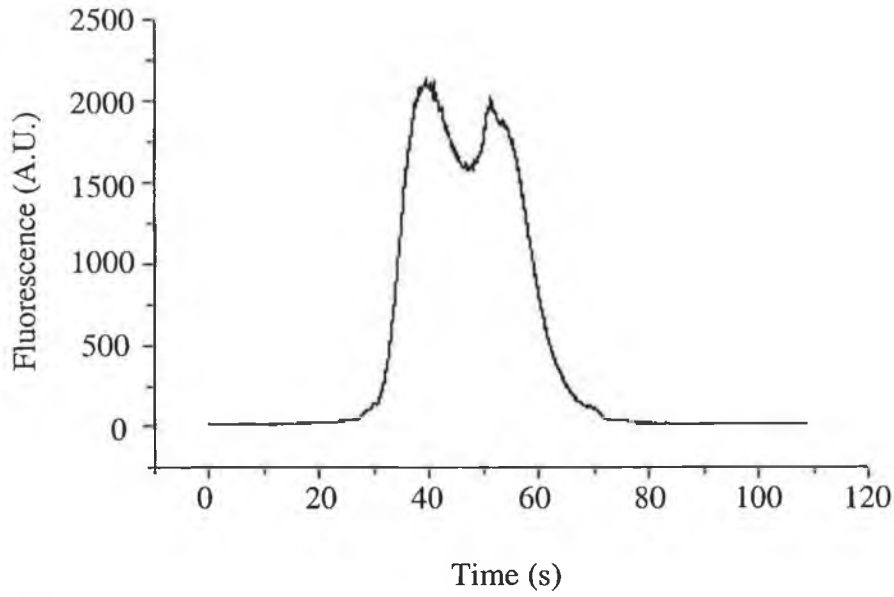

Figure 5.19 *Micro-chip analysis of FITC-labelled BSA-Warfarin Conjugate, 1.04×10^{-7}M. Conditions: 50 mM Tris/Borate buffer, pH 8.5, 10 s injection at 1.7kV, separation voltage 6kV, excitation at 488 nm, emission at 520 nm.*

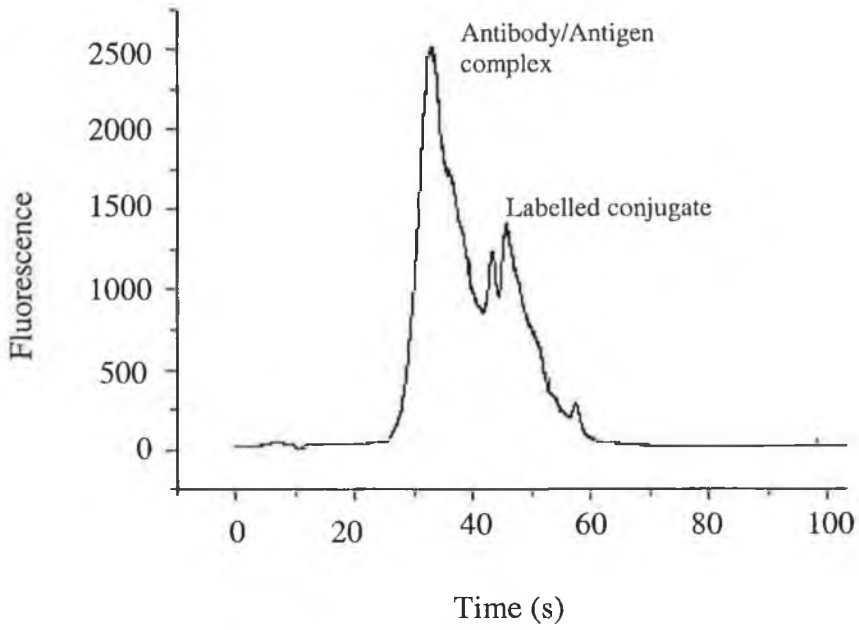

Figure 5.20 *Micro-chip analysis following addition of unlabelled anti-warfarin antibody to labelled BSA-warfarin conjugate, final concentrations; warfarin antibody 9.26×10^{-8}M, BSA-warfarin conjugate 1.04×10^{-7}M. Conditions: Tris/Borate buffer, pH 8.5, injection voltage 1.7kV for 10 seconds, separation voltage 6kV with excitation at 488 nm, and emission at 520 nm.*

5.2.11.2 FITC BSA-Parathion conjugate

On analysis it became clear that there was a wide distribution of large numbers of labels on the BSA-parathion conjugate as evidenced by the width of the peak shown in Figure. 5.21 (as obtained following analysis of the BSA-warfarin conjugate) However, on addition of unlabelled parathion antibody it is possible to see the conformational changes as the complex is formed (Fig 5.22). The antibody-antigen complex shows a migration time between that of the antigen and free antibody as expected (about 42 seconds). This effect was reproducible, like the warfarin assay, using the BSA-warfarin conjugate, but the separation did not provide complete resolution of both species It was not possible to obtain results that could be used to quantify either species due to this heterogeneity causing the overlap in peaks for both species.

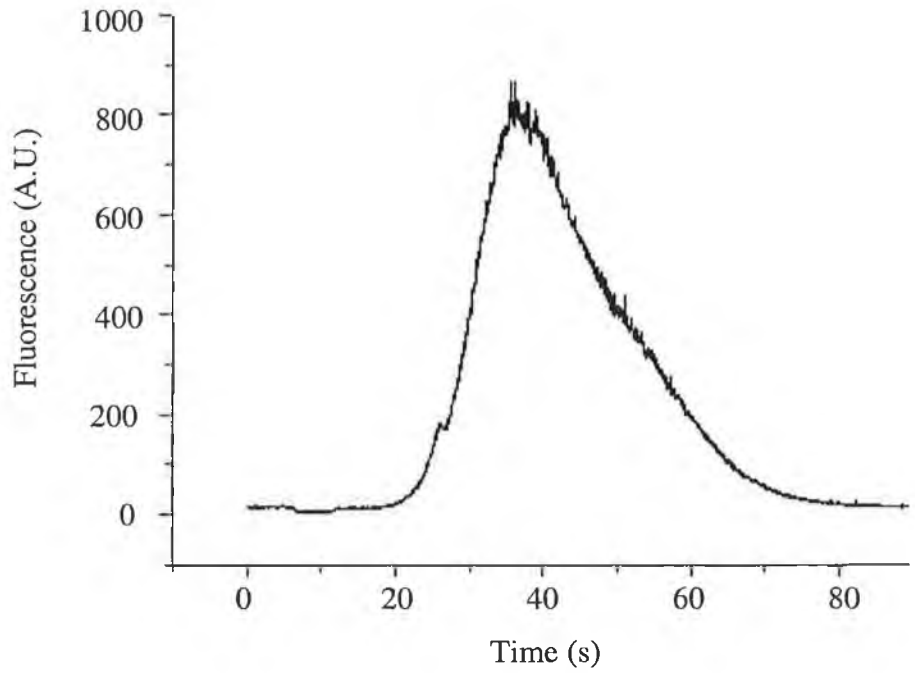

Figure 5.21 *Micro-chip analysis of FITC-BSA-Parathion, at a concentration of 3×10^{-7}M. Conditions: Tris/borate buffer, 50mM, pH 8.5, injection 2.7kV 5 seconds, separation voltage 7.3kV with excitation at 488 nm, and emission at 520 nm.*

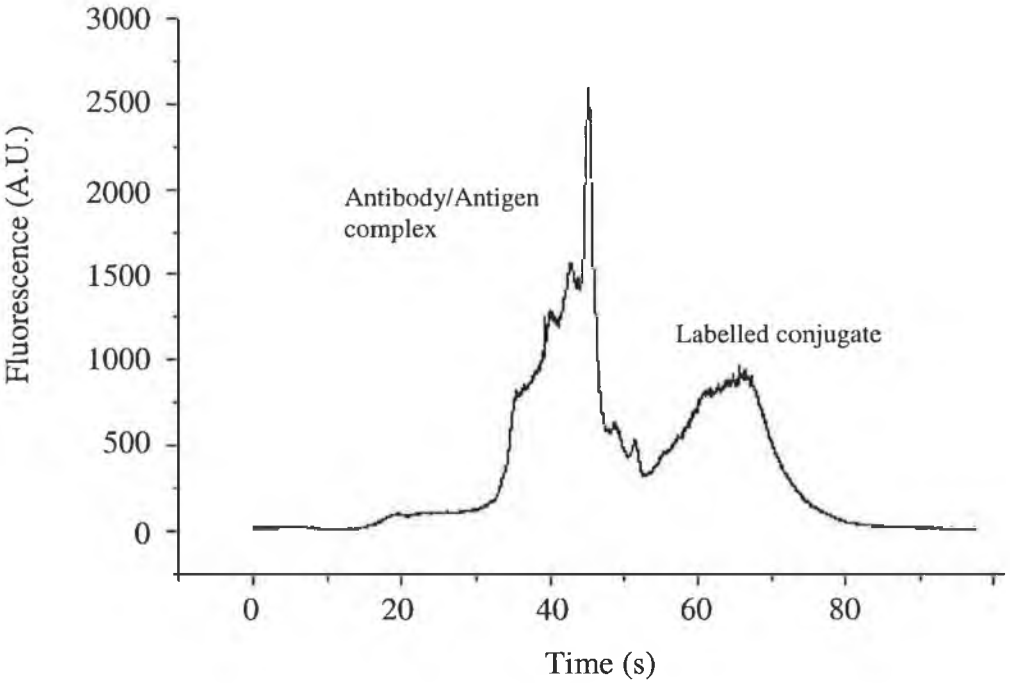

Figure 5.22 *Micro-chip analysis following addition of anti-parathion antibody to labelled – BSA-parathion conjugate (final concentrations, BSA-parathion conjugate: 1.04×10^{-7}M, antibody: 8.7×10^{-8}M) with the complex showing after ~40 seconds. Conditions: Tris/Borate buffer, 50mM, pH 8.5, injection 2.7kV 5 seconds, separation voltage 7.3kV with excitation at 488 nm, and emission at 520 nm.*

5.3 Discussion

The development of immunoassays using a labelled drug instead of a labelled antibody, or as in this case, a labelled drug conjugate, would be more effective than the use of a labelled drug-protein conjugate for obtaining complete resolution between all species involved (antigen, antibody and antigen-antibody complex). However, except for a few cases where it is deemed clinically worthwhile to manufacture such a labelled drug, the vast majority of drugs cannot be assayed in this manner. The research described investigated a number of different approaches in developing CE-based immunoassays for both parathion and warfarin using polyclonal antibodies without having to label the free drug. The reasoning for this was the difficulty in attaching a fluorescent label to the free form of the drug, as compared to the relative ease of labelling a drug-protein conjugate, and also the ease of producing polyclonal compared monoclonals antibodies. The first approach, using a labelled antibody with two different types of antigen (unlabelled free drug, and unlabelled drug-protein conjugates) was not successful as it was not possible to achieve a separation of antibody/antigen complex from free antibody. The second approach, using an unlabelled polyclonal antibody and a labelled drug conjugate was more successful, although it was still not possible to achieve complete resolution.

The results, while not satisfactory for the development of an immunoassay, are in agreement with those reported in the literature. Schmalzing *et al.* (1995) investigated the possibility of using polyclonal antibodies for a serum cortisol immunoassay. They discovered that the use of a polyclonal antibody gave a much broader complex signal, similar to that seen here for both the labelled drug-protein conjugates (antigen) and antibody-antigen complex and concluded it was not possible to obtain any quantitative data from this signal. However, for a later microchip assay, cortisol (free drug) was available labelled at a single location with a fluorescent tag, and this provided the investigators with a clear, sharp, and well resolved signal which could be used for quantitation as opposed to measuring the signal corresponding to the antibody-antigen complex. For this assay migration time for the labelled cortisol was under 20 seconds. In the cases presented here, the use of a heterogeneous polyclonal, in combination with a labelled protein conjugate (itself very heterogeneous in nature due to multiple labelling at numerous sites on the protein) did not allow the antibody-antigen complex to fully resolve from the free labelled drug-protein conjugate.

The research also shows that the conditions applied on-chip allowed a stable complex to form and not to dissociate during the separation. Separation of complex from free labelled antigen will disturb the binding equilibrium and result in dissociation of complex throughout the separation. This is a problem associated with CE immunoassays, as outlined in section 5.1.5.3. However, the extent to which any dissociation was occurring was not investigated, due to time restrictions. It is also difficult, to quantitate what contribution, if any, to the broadening of the signal for both free labelled drug-protein and complex came from adsorption (interactions between the glass surface of the channel of the chip). Use of high pH buffer (9.0) to help avoid adsorption and provide a sharp peak for the labelled antibody (Fig. 5.7) indicated that interactions were possibly minimal and that the broad nature of the signals was due almost entirely to the heterogeneity of both species.

Despite not achieving optimal results, the use of micro-chip CE demonstrated the speed at which it is possible to achieve separations with this system. The migration time for the antibody was 6 seconds, a large decrease in time over conventional CE, which takes over a minute. Other reports in the literature for immunoassays also report very fast analysis times. Chiem and Harrison (1997) reported total analysis times under 45 seconds for a theophylline micro-chip CE immunoassay, further demonstrating micro CE to be a major improvement in terms of total analysis time.

6 ANALYSIS OF LIPOSOMES USING CE WITH POST COLUMN LIF DETECTION

6.1 Introduction

The analysis of cellular components has become more of a focus in the scientific community in recent years, so much so that there are now individual companies being set up to deal specifically with organelle analysis and research. One such company is MitoKor, based in San Diego, California. MitoKor began in 1991, as Applied Genetics. The company is based around observed similarities in the pathology and history of diseases of the very young and very old. This was traced to energetic deficiencies and ultimately to mitochondria. This is perhaps the organelle with the highest profile at the moment, because of its proposed involvement in diseases like Parkinson's disease and Alzheimer's disease (section 7.1.6).

Classical methods have to date focused mostly on the analysis of whole cell populations and their organelles with the use of techniques like flow cytometry and fluorescent microscopy (section 1.4.2) with very little done on individual organelles. However, if we are to gain a more complete understanding of what is happening on a subcellular level, instrumentation and methods capable of analysing organelles on a more thorough *individual* level must be developed. Analysis based on a population of cells tells us nothing of what's happening on an individual cellular level. As this thesis looks at the development and application of chromatographic methods of analysis it was investigated if capillary electrophoresis could be applied successfully to the analysis of subcellular particles. In order to do this a model was needed, i.e. something that would mimic the properties (size, membrane composition) of an organelle.

An ideal solution was found in the choice of liposomes. These were chosen as a model for organelles, for several reasons. (i) They are easy to manufacture. (ii) Membrane bound vesicles can be produced with a membrane composition that mimics that of an organelle. (iii) The size of liposomes can be controlled depending on the method of production. Another important factor was that they could also be loaded with a fluorescent dye for their detection, which would be similar to the fluorescent probes available for the different organelles. A challenge also presented itself in that there are to date no reported methods capable of analysing individual liposomes. Several researchers have reported on the analysis of liposomes using capillary electrophoresis (Roberts *et al.,* 1996; Tsukagoshi *et al.,* 1998; Radko and Chrambach, 1999), however in every case the electropherogram was characterised by broad gaussian profiles for the liposome peaks, representative of the entire population of liposomes. The exciting discoveries detailed during research carried out in the University of

Minnesota represents a new departure from current thinking regarding liposome analysis using capillary electrophoresis.

The work presented here describes liposomes and their selection as models for organelle analysis using capillary electrophoresis (section 6.1.1). A description of an 'in-house' constructed capillary electrophoresis instrument is given (6.1.2). The procedure to set up this instrument and its use in the analysis of individual liposomes as a model for analysis of individual organelles (section 6.2.1) is given.

6.1.1 Liposomes as models for organelle analysis

Liposomes are colloidal particles formed when a lipid bilayer membrane, composed from self-assembled lipid molecules encapsulates part of an aqueous phase in which they are dispersed, or as A. D. Bangham (1981) so eloquently put it " 'smectic mesophases', layer lattices of alternating, closed bimolecular lipid sheets intercalated by aqueous spaces". The formation arises due to the properties of the phospholipid molecules, a polar head and double hydrophobic tail, and the energetically favourable association of the hydrophobic portion of the molecules to reduce interaction with the aqueous solvent. Liposomes are characterised by their lipid composition, particle size distribution, number of lamellae (number of 'layers') and inner outer aqueous phases. All of these properties dictate their stability and interaction characteristics (Chapman, 1984). Morphologically liposomes are distinguished between large (L), small (S), uni (U), oligo (O), and multilamellar (ML) vesicles (Lasic and Papahadjopoulos 1998). Figure 6.1 shows the structure of a single lamellar liposome. Other combinations of liposomes exist including multivesicular liposomes in which smaller liposomes are entrapped within a larger liposome. In terms of interaction properties liposomes are distinguished between sterically stabilised types, in which they are relatively inert and do not interact with their environment, conventional liposomes which are characterised by a nonspecific reactivity towards the mileu and polymorphic liposomes which are reactive towards various agents (Lasic and Papahadjopoulos, 1998).

6.1.1.1 Liposome preparation

While the common perception of liposome appearance is that of a spherical shape composed of differing numbers of layers, in fact there are many shapes possible, ranging from elliptical shapes to long tubules, varying in dimensions from several hundred angstroms to several microns. The method of preparation determines the size of liposomes obtained.

Large Multimembrane Liposomes: These are the type of liposomes made for the work described in this chapter. The spacing between the membrane is determined by a balance between van der Waals' forces of attraction and electrostatic and hydration forces of

repulsion arising between adjacent membranes (Chapmann, 1984). Altering the lipid composition or adding other charged molecules allows these distances to be varied. Large multimembrane liposomes are usually made by the method or a variation on the method described by Bangham *et al.* in 1965. This involves dissolving the appropriate lipids in an organic solvent which is then evaporated leaving a dried film of lipid on the surface of the flask. Addition of an aqueous solution containing the water-soluble solute to be trapped inside the liposomes and swirling/vortexing gently to release the lipids from the flask surface. The solution is then allowed to equilibrate for several hours before use. Any remaining solute in the external aqueous phase is removed by repeated centrifugation and washing. A feature of large multimembrane liposomes is that they respond to osmotic gradients by shrinking or swelling.

Small single membrane liposomes: These liposomes range in diameter from 200 to 500 angstroms and are constructed of a single bilipid layer surrounding an aqueous compartment (Huang, 1969). These liposomes differ from the large multimembrane liposomes in that they are osmotically insensitive, a disproportionate amount of lipid is located in the outer leaflet of the membrane (about 70%), and the small radius of curvature imposes strains on the packing of the lipid molecule (Chapmann, 1984). There are a number of methods which can be used to prepare small single membrane liposomes. The most common method is ultrasonic dispersion, in which an ultrasonic probe can be placed directly into a suspension of large liposomes or by suspending the flask of lipid dispersion in an ultrasonic bath. Narrow-bore needles can also used to inject an ethanolic solution of lipids into a rapidly stirred aqueous solution, forming small unilamellar vesicles. This method eliminates aerosols, but is dependent on the lipids being soluble in ethanol. Another method involves dissolving the lipids in detergent followed by its removal by dialysis.

Large single membrane liposomes: Large liposomes ranging in size from 500 angstroms to several microns have been prepared by Reeves and Dowben, (1970). The method involved slowly hydrating a thin layer of phospholipid in distilled water or an aqueous solution of nonelectrolyte to form the vesicles. The use of "ether injection" to produce a large "unimembrane" liposome was described by Deamer and Bangham (1976). In

this method, an ether solution of lipid is injected into warm aqueous medium and the liposomes formed are osmotically active and mostly unimembrane.

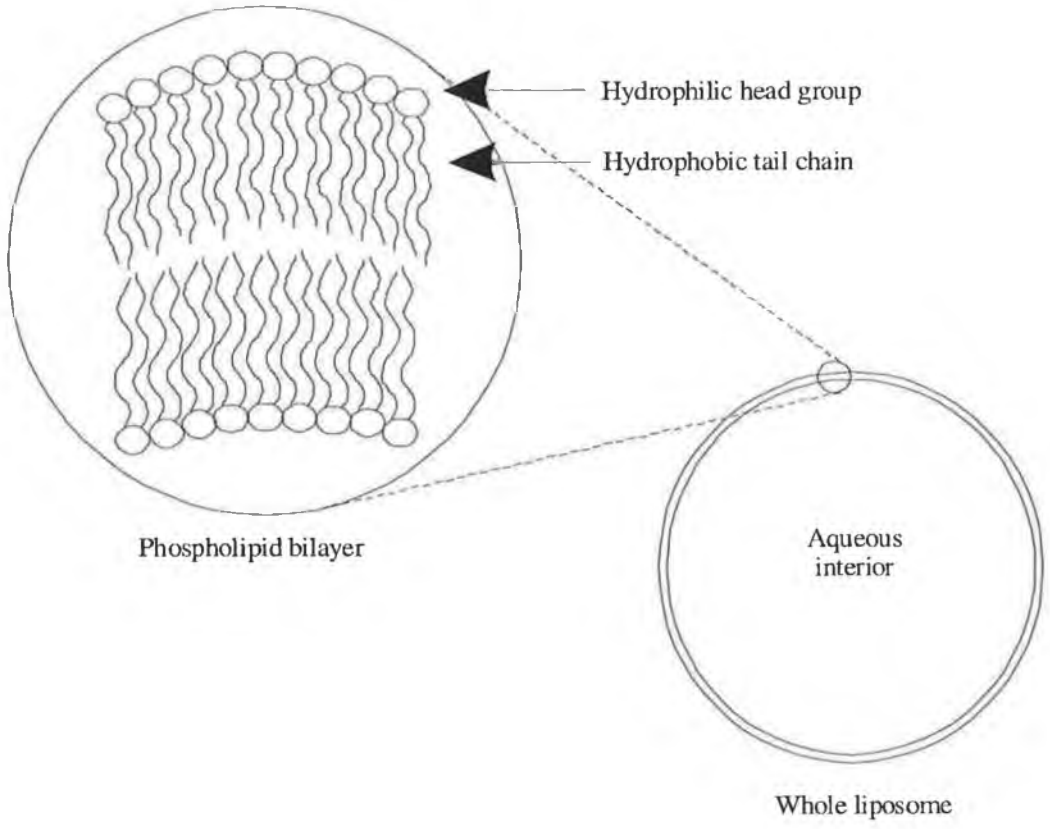

Figure 6.1 *Structure of a single lamellar liposome*

In the early 1960's there was a lot of emphasis on the study of the properties of lipid-water systems as model biomembrane structures (Chapman, 1984). The ability to alter the membrane composition of the liposome to mimic specific organelles (Table 6.1) makes the liposome an ideal model for organelle analysis. As separations in CE are influenced by electrostatic charge, which is conferred on the organelle due to the membrane composition, liposomes would also exhibit similar properties. Liposomes with a similar phospholipid composition would also be expected to interact with the walls of the capillary in a similar

manner to organelles. The capillary electrophoresis instrument used for analysis of liposomes is introduced in section 6.1.2.

6.1.2 Capillary electrophoresis instrument

The instrument used for analysis involves a different structure to commercially available CE instruments (Figures 6.2 and 6.3) and is constructed from the following parts:

- Argon-Ion Laser and power supply. (Figure 6.2 (A)).
- Spellman power supply for controlling the injections and separations. (Figure 6.2 (A)).
- Detector box with high numerical aperture lens for collection of fluorescence and photomultiplier tubes (×2) with power supply. (Figure 6.2 (B)).
- Microscope body for aligning capillary end tip with laser beam (instrument alignment. (Figure 6.2 (B)).
- Carousel for holding samples and separation buffers (Figure 6.3 (A)).
- Sheath flow cuvette (containing capillary end) (Figure 6.3 (B) and Figure 6.4).
- Sheath flow container (Figure 6.2 (A)) and waste reservoir to flush away sample exiting capillary. (Figure 6.3 (B)).

All components involved in the optics of the instrument (laser beam, cuvette and detector box) were on translation stages, which allowed movement in up to three planes for alignment.

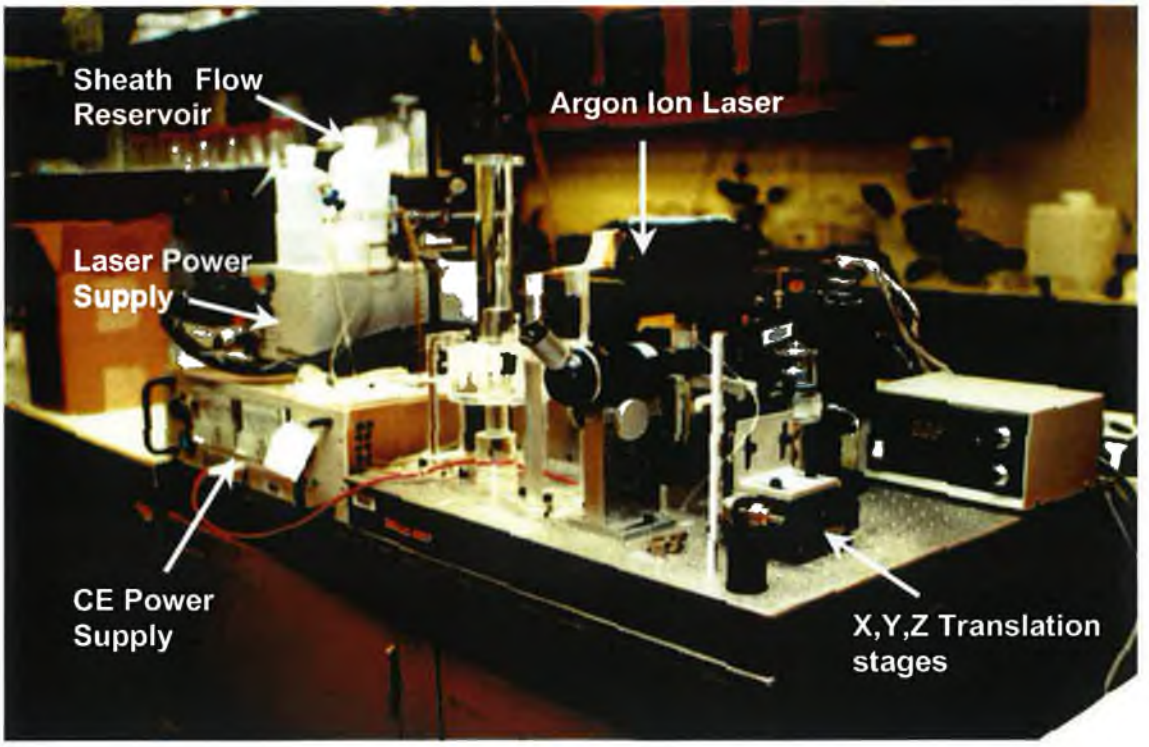

(A)

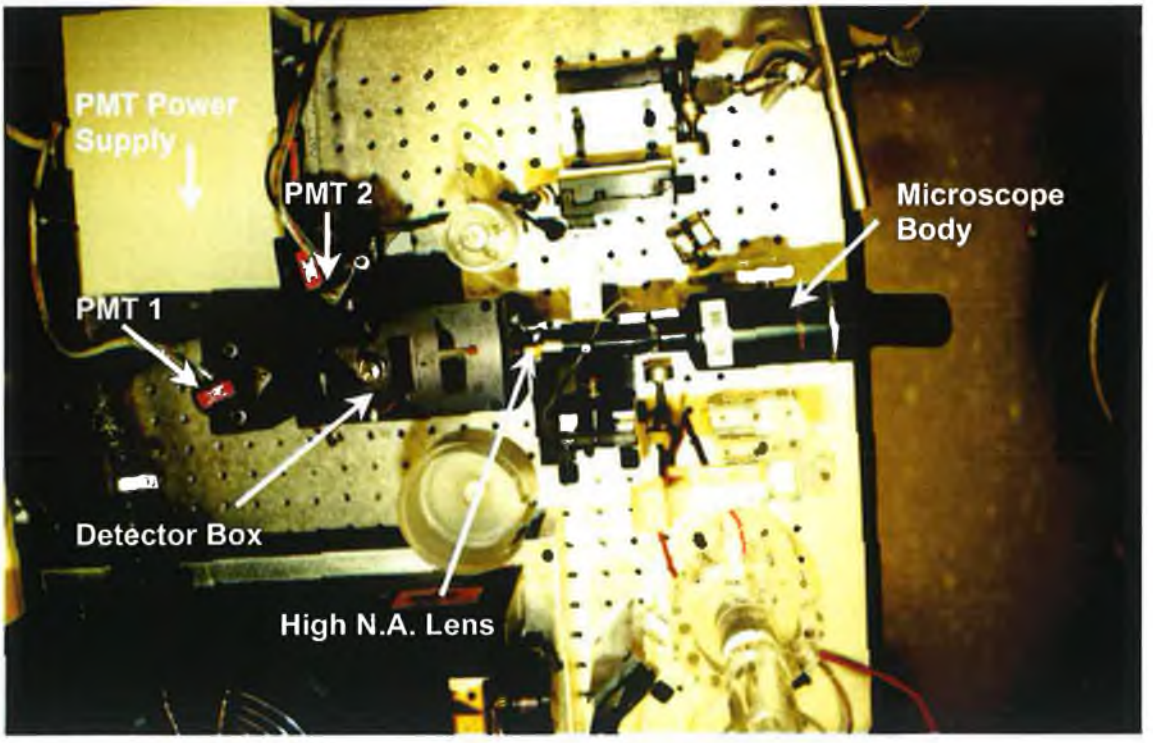

(B)

Figure 6.2 *Pictorial (A) and plan (B) of CE instrument used*

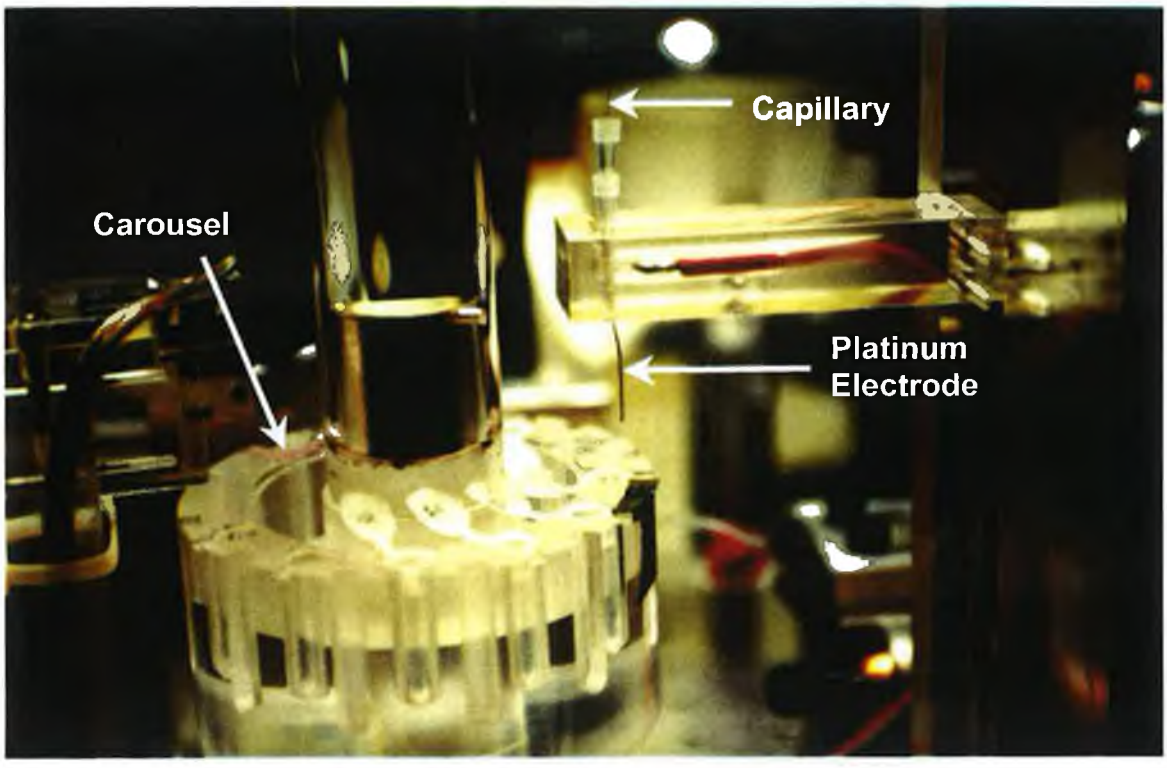

(A)

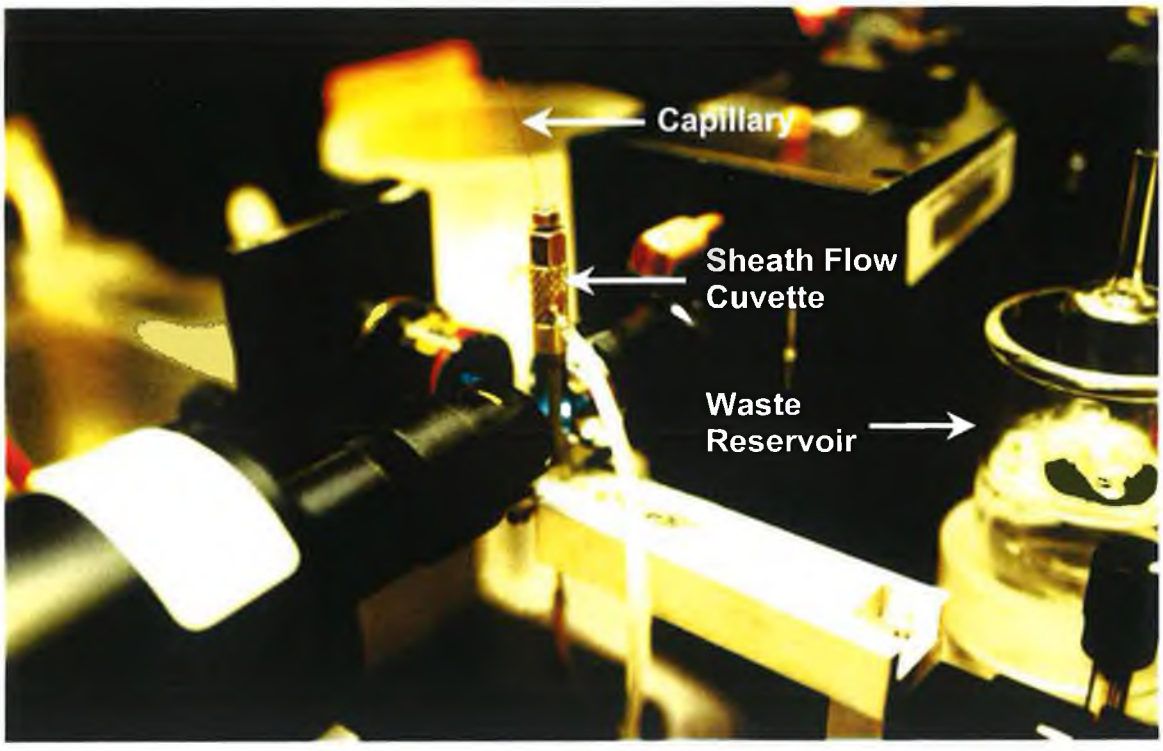

(B)

Figure 6.3 *View of injection (A) and detection (B) mechanism of instrument*

6.1.2.1 Laser

The laser used for liposome analysis was a continuous-wave argon ion. A major advantage of using continuous-wave as apposed to pulsed wave is the fact that they possess high spatial coherence, which enables the beam to be focused to a spot a few μm's in diameter, whereas pulsed lasers tend to have poor spatial coherence and are difficult to focus to a small spot (Wu, 1989). The argon ion laser used has a wavelength of 488 nm and was ideal for use with the fluorescent probes, most of which have their absorbance maxima at or near 490 nm. Detection at 520 nm or so also avoids overlap with the water Raman bands, of which there are two, one at 1650 cm^{-1} and another stretching from 3100 to 3700 cm^{-1} (Wu, 1989). Having a fluorescence emission at 520 nm ensures detection where the Raman signal is relatively weak. Laser power used for experiments was 12mW, as this was the optimum power for excitation given the time the sample was exposed to the beam with the flow rates used, and to avoid saturation and photodegradation.

6.1.2.2 Laser focusing

To focus the laser beam an inexpensive high quality microscope objective was used. This type of lens is well corrected for aberrations, and is easy to use. In the case of narrow bore capillaries used (20 μm's ID), it was necessary, on occasion, to focus the beam tightly, sometimes to less than 10 μm's, to match exactly the width of sample stream exiting the capillary and to minimise the detector volume.

6.1.2.3 Spectral filters

In order to selectively detect at a desired wavelength, two spectral filters were used. The first was used to block laser scatter from particles at 488 nm, (used for all applications), and the second interchangeable bandpass filter was applied for the different wavelengths of the dyes/labels. A 535 DF 35 nm filter was used for wavelengths corresponding to FITC/Fluorescein emissions and a 630 DF 35 nm filter was used for FQ-labelled samples (chapter 7).

6.1.2.4 *Instrument construction and alignment*

The plan of the instrument is shown in Figure 6.2 (B). The laser beam is deflected through an angle of 90^0 with a mirror and passed through a pinhole before being focused at the end of the capillary in the cuvette (Figure 6.4). For most applications it was necessary to align a focused laser beam spot that matches exactly the width the sample stream exiting the capillary. In some cases, it was necessary to slightly de-focus the beam for larger particles exiting the capillary to ensure all are exposed to the laser for excitation.

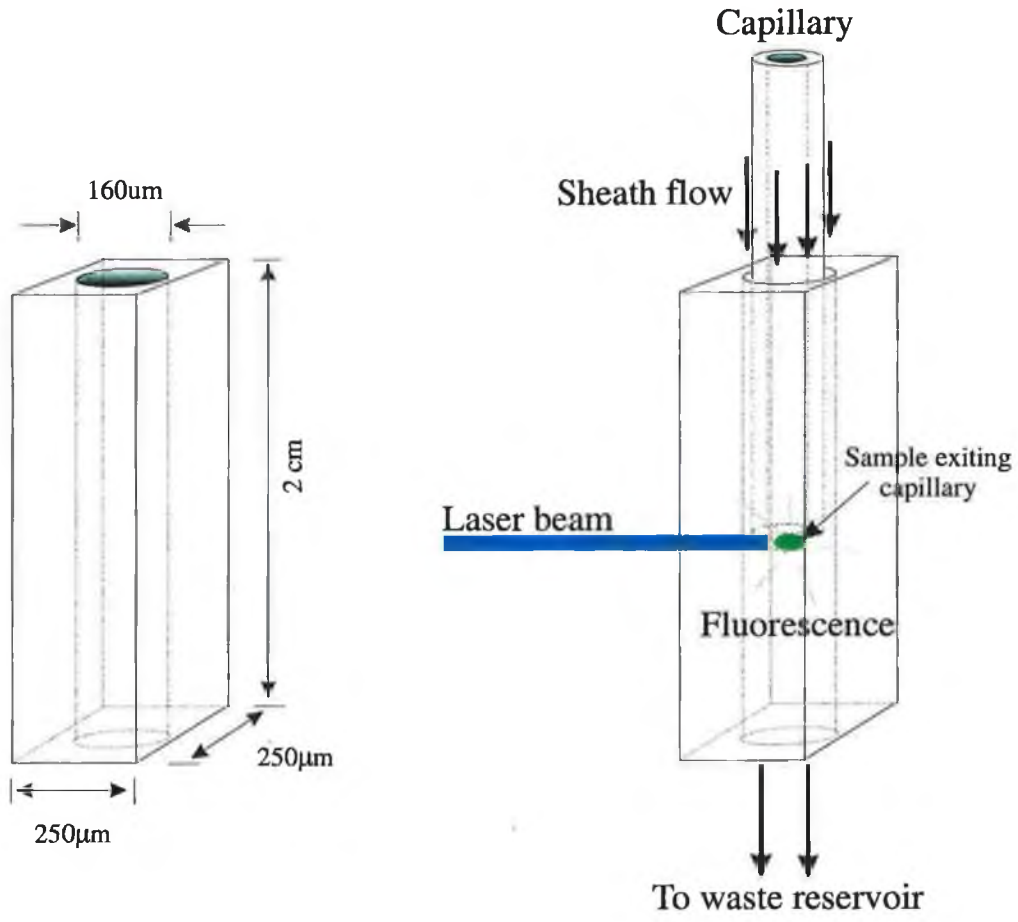

Figure 6.4 *Diagram of the sheath flow cuvette showing dimensions and working position of capillary and laser beam for post column LIF detection.*

The most common detection format detects fluorescence through the capillary wall, however there are large background signal contributions from this format (light scatter generated at the air-column and column-sample interfaces, signal degraded by capillary wall aberrations). For signal collection here, the capillary is placed into a 250 μm^2 square flow chamber (Fig 6.4) with the laser beam focused at the tip of the capillary. As the sample exits the capillary it is surrounded by the sheath buffer flow, of the same composition as the separation buffer, thus preventing any scatter at the interface. The size and shape of the sample area excited by the laser beam can be optimised by altering the flow rate of the sheath flow (accomplished by raising or lowering the reservoir).

6.1.2.5 Collection optics

The fluorescence emitted from the sample is collected using a high numerical aperture (N.A.) lens (0.65). A limiting factor in the choice of the lens is that a relatively high working distance is required as the fluorescence must be imaged from the centre of the cuvette, a distance of over 2mm and there are few lenses available with both high working distance and high N.A. A pinhole is placed in the image plane of the lens to eliminate light from scattering entering the detector as this would contribute to a high background signal.

6.1.2.6 Instrument alignment

Alignment is carried out in two steps. Rough alignment was achieved with the naked eye using a low concentration of fluorophore in the run buffer (10^{-10}M fluorescein) followed by precise optimising of signal output using the computer. Rough alignment is carried out by keeping the detector box fixed (photomultiplier tube and collection optic) and aligning all other components with respect to the light collection optic. The microscope body placed opposite the collection optic is used to align the cuvette. To prevent any potential hazard when the laser beam is on, the microscope eyepiece is fitted with a high efficiency coloured glass filter to block any scattered laser light. A pinhole is placed in the image plane of the of the collection optic to eliminate scattered light and isolate the illuminated region. Rough

alignment is then completed with the use of an LED placed after the pinhole but before the photomultiplier tube (multi-alkali), so that when it is switched on, light travels back in the reverse direction of fluorescence projecting the image of the pinhole through the collection optic. The microscope is then focused on the light to produce a sharp image of the pinhole. The position of the cuvette is adjusted (and hence the position of the fluorescent spot) in conjunction with the laser beam, until the fluorescent spot and pinhole image are exactly superimposed. The instrument is now roughly aligned. The shroud is placed around the cuvette and collection optic and the eyepiece of the microscope covered. Switching on the photomultiplier tubes allows the signal output from the flourophore in the run buffer to be detected and monitored on screen. Carefully moving the x, y and z translation stages of the cuvette and moving the detector box in the x/y plane until maximum signal output is achieved completes the alignment of the instrument. Alignment was carried out each day prior to instrument use.

6.2 Single liposome analysis by capillary electrophoresis with laser induced fluorescent detection

Liposomes with a lipid composition similar to that of the mitochondrial membrane (Table 6.1) were made as outlined in section 2.3.6.1. The preparations were monitored by fluorescence microscopy for uptake of fluorescein and size. For detection, liposomes were filled with 10^{-6}M fluorescein in 10mM borate (pH 9.3) and were visualised with a FITC cube and a 60×, N. A. 1.3 oil immersion lens. The fluorescence intensity was observed to decrease rapidly as fluorescein photobleaches and liposomes were not detectable after 30 seconds of illumination with the fluorescent source. Due to their susceptibility to photobleaching, liposomes were stored in the dark at 4°C prior to analysis by capillary electrophoresis.

Phospholipid	**Ratio total lipid by weight**
Cholesterol	3
Phosphatidylethanolamine	35
Phosphatidylserine	2
Phosphotidylcholine	39

Table 6.1 *Composition of liposomes similar to the outer mitochondrial membrane made for analysis by capillary electrophoresis*

6.2.1 Detector characterisation and optimisation

It was necessary to for the detector performance to be characterized before analysis of individual liposomes. There were a number of factors to be determined. It was of prime importance to establish if particles exiting the capillary were being exposed to the laser beam for identical lengths of time, and if so, was all of the emitted light being collected by the detector. Ideally for particles of identical diameter and containing the same amount of fluorescent dye, the signal output from the detector should be the same. In order to investigate this, a model was needed which would fulfil the requirements of constant size and

fluorescence intensity when equally excited. For this reason fluorescent beads were chosen as they had a constant size (6 μm's diameter) and the variation in fluorescein content was given by the manufacturer to be 5% CV as determined by flow cytometry.

6.2.1.1 Bead experiments to determine detector variation

The detector sensitivity and limit of detection for fluorescein (used as fluorescent marker) were determined. The values obtained were a LOD of 4.1516×10^{-21} moles with a sensitivity of 1.5605×10^{12} V/mole. Fluorescent beads with uniform fluorescent intensity and size were used to estimate the variation coefficient of the detector response to individual events. Due to the electrophoretic mobility of these beads (0.33 cm min^{-1}) it was feasible to use an electric field (200V/cm) to make them migrate. A continuous electrophoretic-propelled flow of the bead suspension (0.85 beads/nl) allowed for the detection of individual events (Figure 6.5) as beads reached the post-column laser-induced fluorescence detector. Peak height variation of individual peaks had contributions from the variation of fluorescein content in the beads and variations due to the detector design. Beads follow slightly different trajectories as they leave the capillary and enter the sheath flow regime (as monitored with a CCD camera attached to the observation microscope). Each trajectory exposed the eluting particle to different fluorescent excitation regimes. The bead trajectory could be controlled by increasing or decreasing the speed of the sheath flow, and using trial and error coupled with monitoring of events with a CCD camera, a setting was achieved for sheath flow speed at which the beads were uniformly exposed to the laser beam.

Neglecting variations attributed to their intensity measurement, the additional contribution due to the detector design was estimated to be 10.6%. This value was obtained by statistical analysis of electropherograms obtained from repeated continuous injections of beads (Fig. 6.5). Taller peaks were not taken into account to estimate the CV since they corresponded to beads sticking together or simultaneous elution of two or more beads (monitored by CCD camera). A low electric field (200 V/cm) was maintained to minimize taller peaks. At higher electric fields the number of events corresponding to agglomerated beads may have resulted from polarization of the surface charge of the beads and cohesion among them due to different polarities.

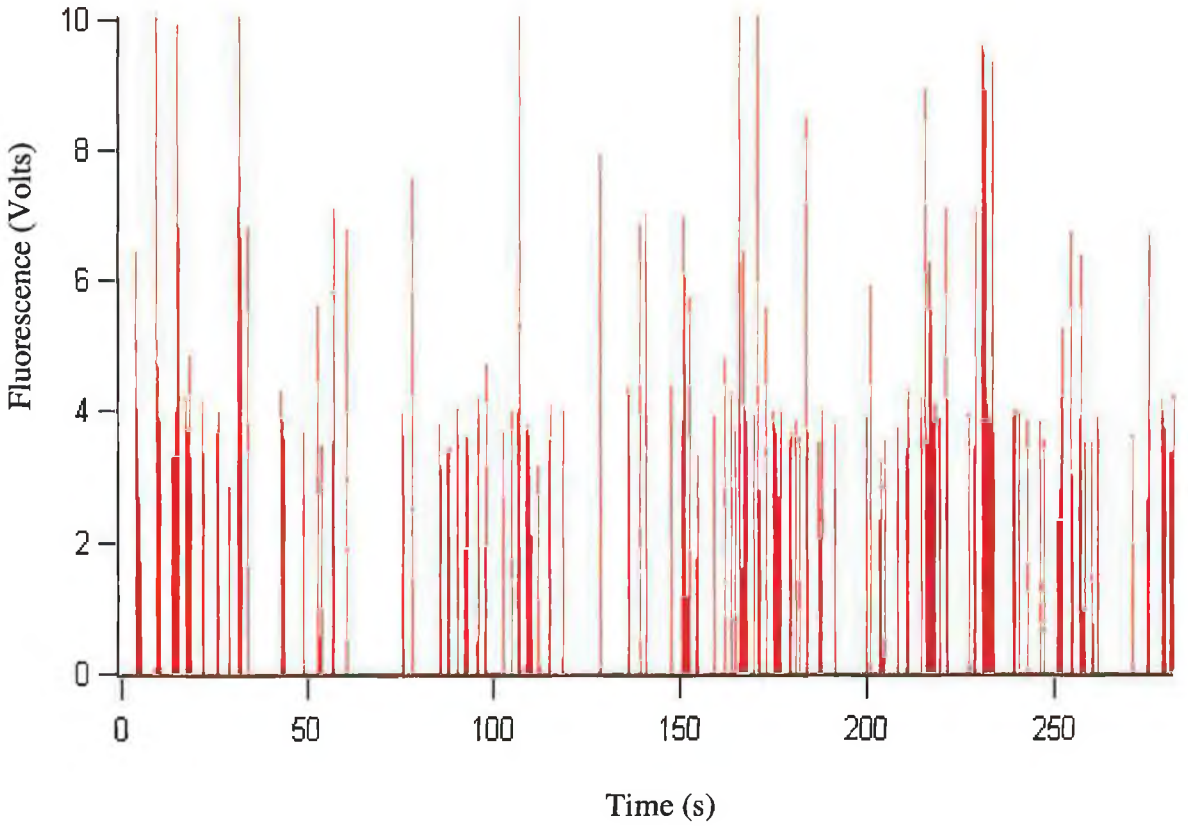

Figure 6.5 *Electropherogram showing peaks corresponding to fluorescent beads (8.5 × 10^5/ml). Conditions; continuous injection at 200Vcm^{-1}; separation buffer: 250mM sucrose, 10mM HEPES, pH 7.50. Average peak height (single event): 3.78 fluorescent units; standard deviation: 0.39; coefficient of variation: 10.8%. PMT at 800V with data acquisition at 50Hz. Excitation was at 488nm with detection at 535DF35nm.*

Having established a detector configuration that would accurately measure the fluorescence emitted from a particle based on its size and content of fluorescent agent, the liposomes prepared were analysed.

6.2.2 Analysis of liposomes

As shown for fluorescent beads, post-column laser-induced fluorescence is an appropriate system for detection of single events. Using capillaries coated as outlined in section 2.3.6.2 Figure 6.6 shows the electropherogram resulting from an electrokinetic injection of a liposome preparation (prepared as outlined in section 2.3.6.1). This electropherogram shows that Gaussian profiles used to describe the migration of a large sample of charged species (i.e. molecular ions) cannot describe the migration of a sample containing a small number of liposomes. Peaks of various heights corresponding to the migration of individual liposomes are localised in a migration zone. Figure 6.6 illustrates three electropherogram overlays, showing the expected dilution effect from high numbers of liposomes and a run of unlabelled liposomes.

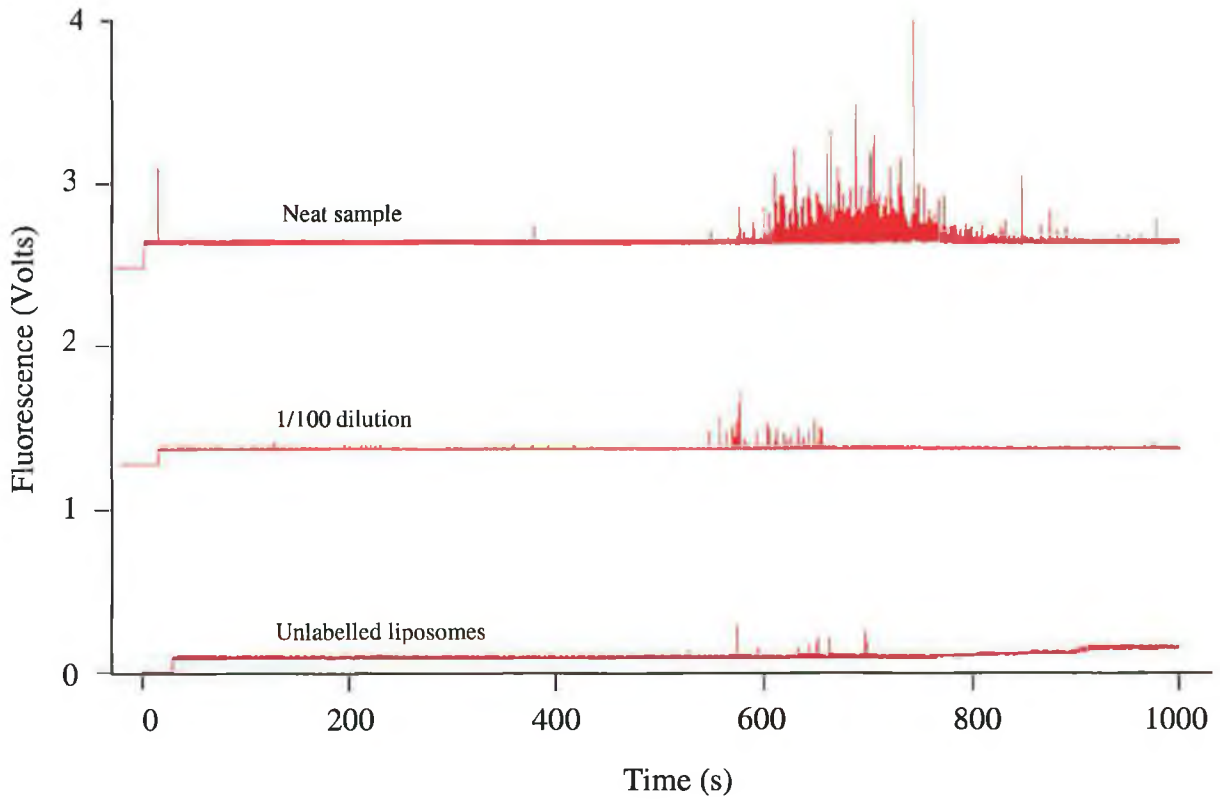

Figure 6.6 *Analysis of liposomes by capillary electrophoresis. Conditions: separation buffer; 250mM sucrose, 10mM HEPES, pH 7.50, coated fused silica capillary, 50μm ID, 150μm OD 5 s injection at 50Vcm^{-1}, separation at 200Vcm^{-1}. PMT at 800V with data acquisition at 50Hz. Excitation was at 488nm with detection at 535DF35nm.*

Liposome-liposome interaction also decreased as expected when the liposome density was varied (Figure 6.6). A dilution of liposome samples showed an increase in electrophoretic mobility and disappearance of intense events in the intensity distribution. This is probably due to polarisation of the surface charge (similar to the fluorescent beads) and cohesion between the liposomes due to the different polarities. Measurement of peak height and electrophoretic mobility for each event using a specially written software programme allowed for determination of statistical parameters.

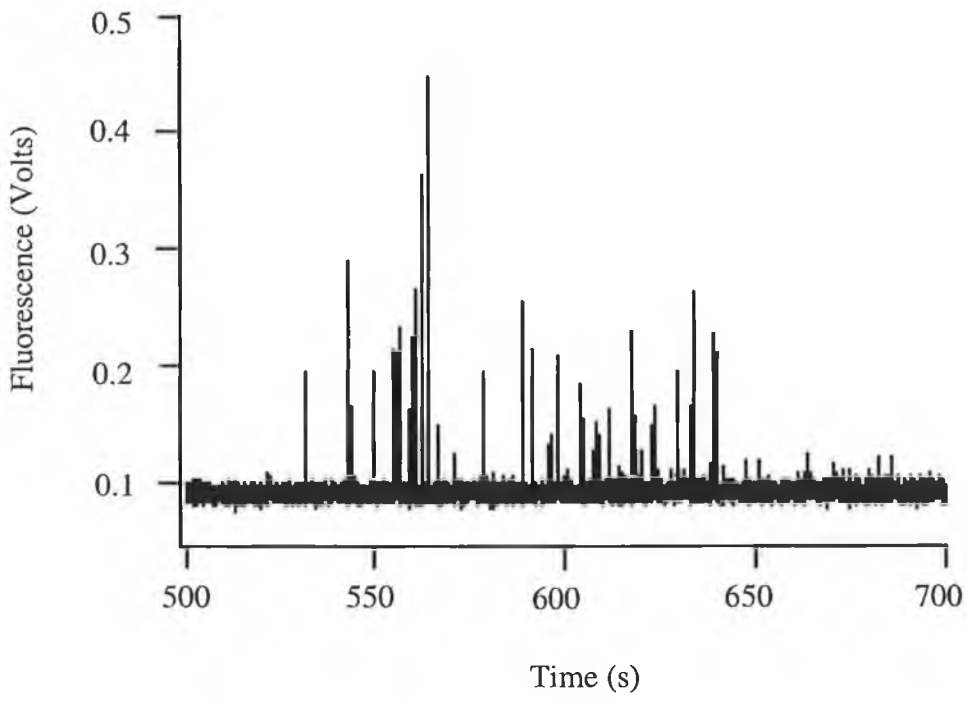

Figure 6.7 *Electropherogram of liposomes used for calculation of statistical parameters, peak height distribution, mobility distribution, size distribution and membrane charge distribution. Conditions; separation buffer; 250mM sucrose, 10mM HEPES, pH 7.50, coated fused silica capillary, 50μm ID, 150μm OD 5 s injection at 50Vcm^{-1}, separation at 200Vcm^{-1}. PMT at 800V with data acquisition at 50Hz. Excitation was at 488nm with detection at 535DF35nm.*

6.2.3 Analysis of results

A programme written for Igor Pro™ wavemetrics data analysis package was used to calculate the peak height (Figure 6.8) and mobility values for the liposomes. Appendix A gives the full programme used for the calculations. The programme, named PickPeaks, when used with Igor Pro allowed for the representation of the current and signal plots from the instrument and adjusted the waves to correct for the background. Mobility values for the liposomes in Figure 6.7 were calculated using the standard formula (1) and the distribution is shown in Figure 6.9.

$$\mu = \frac{L^2}{V \times t_m} \qquad (1)$$

Where: μ = *mobility*

L = *length to detector*

V = *separation voltage*

t_m = *migration time*

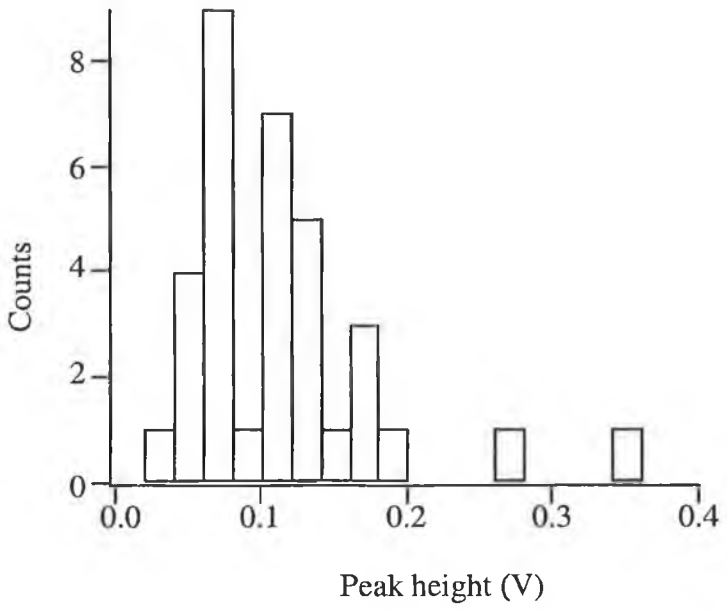

Figure 6.8 *Peak height distribution based on the liposome peaks detected in Figure 6.7, calculated using PickPeak analysis programme in IgorPro graphics package.*

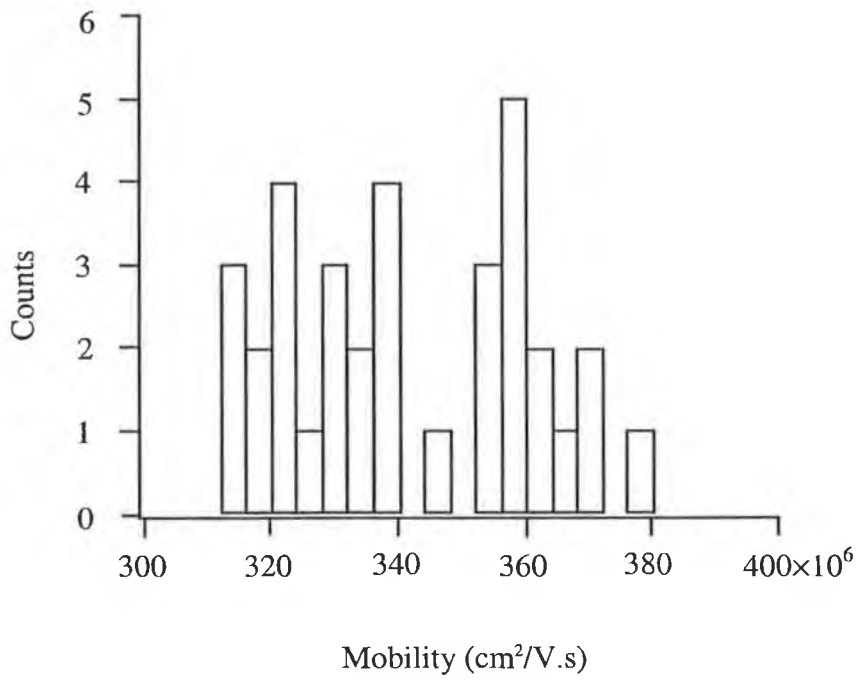

Figure 6.9 *Mobility distribution based on the standard formula of mobility and the migration time for each peak in Figure 6.7, calculated using PickPeak analysis programme in IgorPro graphics package.*

Calculation of liposome radius: For calculation of the liposome radius, it is assumed that they are spherical and that their volume can be estimated from the total amount of fluorescein entrapped in the liposome. In order to calculate the amount of fluorescein, the detector response, (transfer function) to a known injection of fluorescein solution must be calculated. Calculation of the ratio of signal area (Volts-sec) to the total amount of fluorescein (moles) is called the transfer function. The number of moles injected is calculated using the formula:

$$moles = V_{inj} \times c \qquad (2)$$

where

$$V_{inj} = V_{cap} \frac{t_{inj}}{t_m} \times \frac{v_{inj}}{v_{CE}} \qquad (3)$$

V_{inj} = *injection volume*
c = *concentration (molarity)*
V_{cap} = *volume of capillary*
t_{inj} = *injection time*
v_{inj} = *injection voltage*
v_{CE} = *separation voltage*

The value obtained for "t" was 3.4×10^{18} V/mole. Calculation of the amount of fluorescein inside a liposome requires measurement of the signal area for each liposome. Since each profile resembles a triangle with constant base (sec), and variable height (Volts), the base can be included in the transfer function, and its area is calculated by:

$$\frac{1}{2} Base \times height \qquad (4)$$

In order to calculate the radius of the liposomes the formula shown below was derived:

$$r = \sqrt[3]{3/4 \frac{k_1(signal)}{1000\pi}} \qquad (5)$$

Where:

r = *radius of liposome*

$k_1 = \frac{1}{t \times c}$

Signal = *signal from detector*

π = *3.14*

c = *concentration (moles/l) of fluorecsein used to label liposomes.*

t = *transfer function of detector*

The value of the factor inside the radical is expressed in "litres", however, changing to cubic metres (1000 litres in one cubic meter) gives a factor value of 4.68×10^{-18}, and gives the desired output value in m^3. Figure 6.10 shows the size distribution for the liposomes in Figure 6.7. This value is calculated by assuming the liposomes are spheres of radius r, that they are filled with 10^{-6} M fluorescein, concentration c, and that the transfer function (t) of the detector is 3.4×10^{18} V/mole. The output of the calculation is in meters.

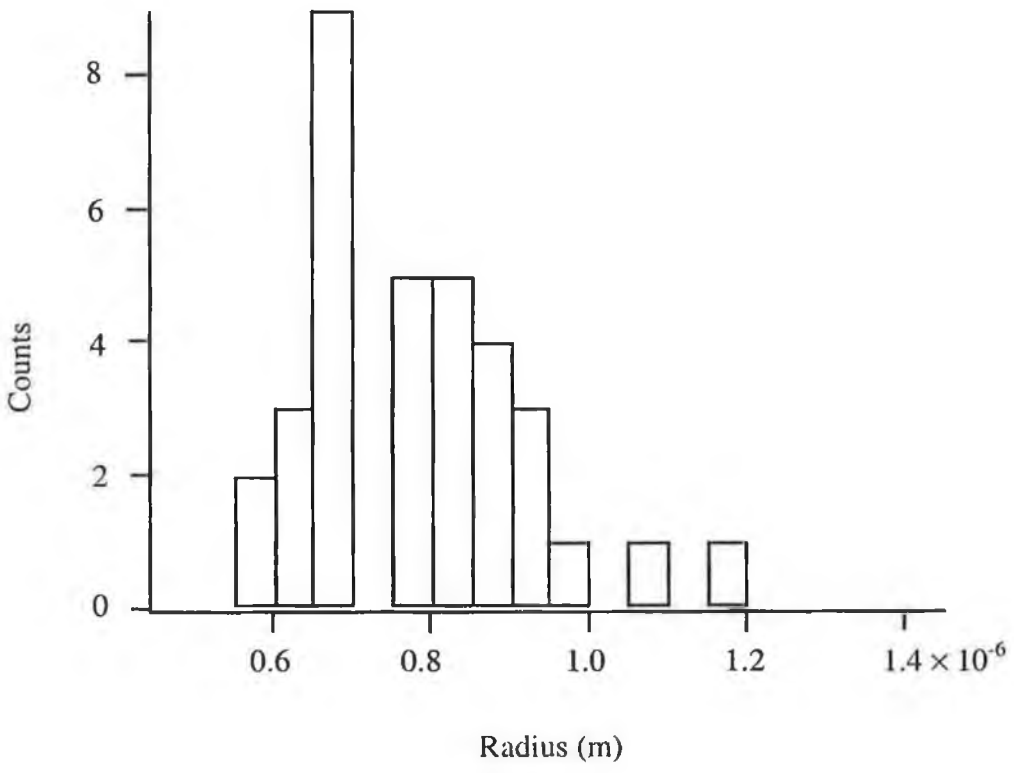

Figure 6.10 *Size distribution for the liposomes in Figure 6.7, calculated using PickPeak analysis programme in IgorPro graphics package.*

Membrane charge density: To calculate the membrane charge density of each individual liposome the basic formula of electrophoresis was used:

$$\mu = \frac{q}{(6 \times \pi \times vis\cos ity \times r)} \qquad (6)$$

Where: q = *charge (coloumbs)*

From the previous calculations we know μ and r. Viscosity is 0.01002 poises (dyna-sec/cm^2), and combining all the constants gives a value of 8.35×10^{-3}.

$$\rho = \frac{8.35 \times 10^{-3}}{(t_m)\sqrt[3]{signal}} \qquad (7)$$

Where: ρ = *density*
t_m =*migration time*
signal = *signal from detector*

Figure 6.11 shows the membrane charge density distribution calculated for the liposomes in Figure 6.7, with the corresponding numbers (counts) of liposomes.

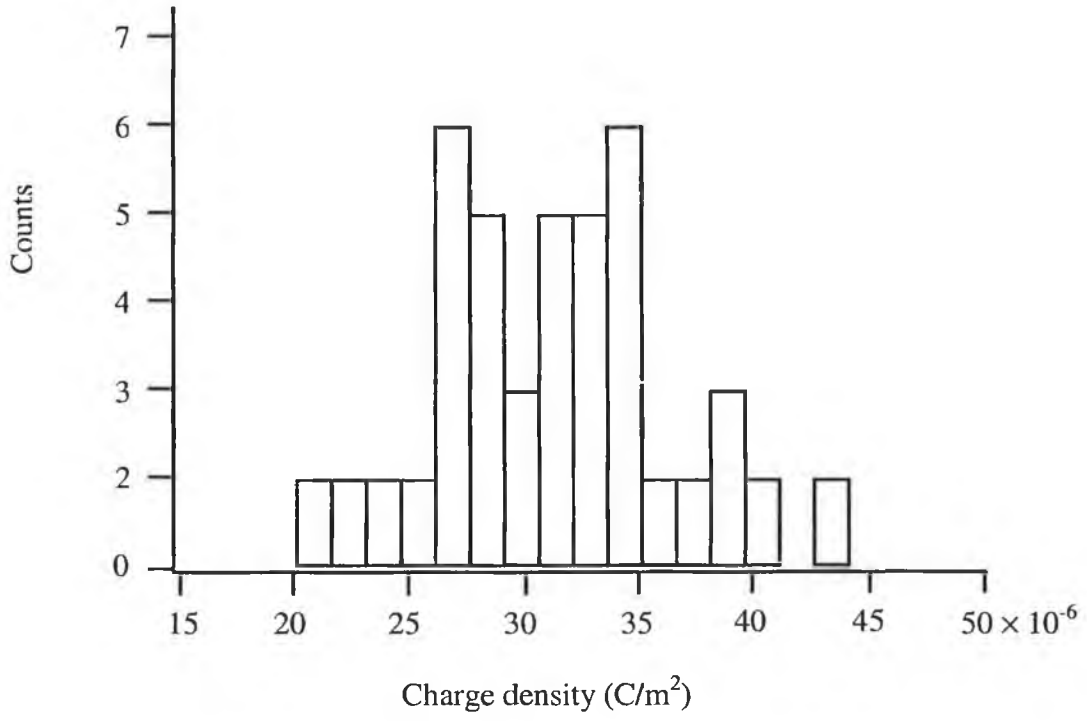

Figure 6.11 *Membrane charge density distribution of liposomes in Figure 6.7, calculated using PickPeak analysis programme in IgorPro graphics package.*

6.3 Discussion

Liposome technology is now well advanced and the physico-chemical properties as well as the fundamental physical and chemical concepts which underly liposome structure, stability and interaction are well established (Lasic and Needham, 1995). They have been used in drug/gene delivery systems for some time (Lasic and Papahadjopoulos, 1998). There are several companies now manufacturing and supplying equipment for liposome production as well as equipment for their characterisation due to the increased use of liposomes in the medical area. Among the different types of methods available for characterisation are extrusion, homogenisation, detergent dialysis, particle size analysis and zeta potential (Woodle and Papahadjopoulos, 1989). Many different methods must be undertaken to fully characterise liposomes. To try and improve this situation several researchers analysed liposomes using capillary electrophoresis. Roberts *et al.,* (1996) published results on liposome behaviour in capillary electrophoresis. In their research, the peak resulting from the population of liposomes was of a broad gaussian nature. Their observations were all based on the entire population of liposomes. It was concluded that there was an overall negative charge on the liposomes. However, the method did not allow for estimation of the charge or its distribution within the liposome population. This is also the case with the other methods reported to date (Tsukagoshi *et al.,* 1998; Radko and Chrambach, 1999). However, the method developed here provides information on the charge of individual liposomes. In studies on the size of the liposomes calculations were made using laser light-scattering particle size distribution and the peak was compared to that from CE analysis. The CE method alone does not provide any information on size (Roberts *et al.,* 1996). In the method reported in this thesis, liposomes are represented by an individual peak that allows the calculation of statistical parameters, including size, on an individual basis for each liposome. This represents a very significant advance in liposome analysis.

Since liposomes have such extensive use in both commercial skin care products and the medical industry, the need for a method to characterise fully liposome preparations is vital for quality control. The method described in this chapter is a major improvement over other current methods attempting to achieve this goal as it gives all the required parameters in the one analysis step. The rational behind for developing this method for liposome analysis was to provide a model for the analysis of cell organelles (also membrane bound vesicles) due to the ability of liposomes to accurately mimic the membrane characteristics and properties of

cells and membrane bound subcellular particles . The results show conclusively that the method and instrument are capable of producing excellent results regarding the analysis of small biological particles.

7 ANALYSIS OF MITOCHONDRIA USING CE WITH POST COLUMN LIF DETECTION

7.1 Introduction

An introduction to cell organelles was given in section 1.4.1 and in section 1.4.2 an examination of the methods used to analyse various organelles, including mitochondria was described. The work presented in this chapter focuses on the analysis of mitochondria using capillary electrophoresis and is based on the method development presented in chapter 6 for the analysis of liposomes as models for organelle analysis.

7.1.1 The Mitochondrion

Mitochondria are small membrane-bound particles found in the cytoplasm of all eukaryotic cells of higher plants and animals. They have a characteristic shape, size, structure and staining properties. The basic structural pattern is an outer membrane enclosing an inner membrane which has 'tube-like' invaginations (cristae) into an inner compartment known as the matrix. The degree of cristae development present in mitochondria varies with different cell types. For example, mitochondria from kidney, heart and skeletal muscle have extensive arrangements of cristae, while mitochondria of fibroblasts and nerve axons have relatively few cristae arrangements. Mitochondria play a critical role in the generation of metabolic energy, in the form of ATP, derived from the breakdown of fatty acids and carbohydrates, in a process known as oxidative phosphorylation (Cooper, 1996).

7.1.2 Origin of mitochondria

Early observations of mitochondria using the light microscope suggested a similarity with bacteria. A comparison between the properties of isolated mitochondria and bacteria revealed many similarities, both structurally and enzymatically. A detailed table of similarities is provided by Tyler, (1992) and give rise to the two main theories about the origin of mitochondria. The one that is commonly accepted is the endosymbiotic theory, which postulates that mitochondria arose from the invasion of aerobic or anaerobic photosynthetic bacteria into ancestral protokaryotic cells. The second theory postulates their existence by compartmentalisation within an ancestral prokaryotic cell (Tyler, 1992).

7.1.3 Functions of the Mitochondrion

The various functions of the mitochondrion are carried out in different locations within it. Each mitochondrion is surrounded by a double membrane system, consisting of the inner and outer membrane. These are separated by the intermembrane space. The numerous folds or cristae of the inner membrane extend into the matrix. Each of these components play a separate functional role, with the matrix and inner membrane representing the major working areas. The mitochondrial genetic system is contained within the matrix, as well as the enzymes responsible for the central reactions of oxidative metabolism following from the breakdown of glucose to pyruvate in the cytosol and its subsequent transport into mitochondria. The inner membrane plays its role in the production of ATP via energy derived from electron transfer reactions involving NADH and $FADH_2$. These reactions are used to create a potential energy difference across the membrane which drives the reactions necessary for ATP production (Reid and Leech, 1980).

7.1.4 Mitochondrial Genetics

Mitochondria contain their own genetic system, which, if the most widely accepted theory about the evolution of mitochondria is correct, has descended from the genome of the original endosymbiotic bacteria that evolved into eukaryotic organelles. The mitochondrial genome is still similar today to that of a bacterial genome, in that it is circular in nature and present in multiple copies per organelle. There is a wide diversity in the size of the mitochondrial genome, ranging from 16kb pairs in the humane mitochondrial genome to approximately 80kb pairs in yeast. Like any other DNA, mitochondrial DNA can be altered by mutations, which can prove deleterious to both organelle and organism. Since almost all of the mitochondria of fertilised eggs are contributed by the oocyte, rather than the sperm, mutations in the mitochondrial DNA are transmitted via the mother.

7.1.5 Intracellular distribution

Although mitochondria are present in all eukaryotic cells, they are not present in a number of fungi and over a thousand species of protozoa. Many of the species of protozoa living in the absence of oxygen have hydrogenosomes instead of mitochondria and these are thought to be derived from mitochondria. Several colourless algae and aquatic moulds also contain no mitochondria (Tyler, 1992). At one extreme 487,000 mitochondria have been found in the giant amoeba cell, and up to 150,000 in the oocytes of some sea urchin eggs (Afzelius, 1957), while at the other, in rat liver, the tissue used most frequently as a source of isolated mitochondria, the number per cell ranges from 500 to 2500. Mitochondria also differ in size. Examination of rat liver cells revealed considerable differences in the size of the mitochondria, despite the identical average size of the cells (Tyler, 1992).

7.1.6 Mitochondrial life cycle

Despite more than one theory on how new mitochondria come to exist, only one theory has withstood the test of time and study. Is it now believed that mitochondria grow and divide to keep pace with cell growth and division. To date the knowledge of the fundamental process involved in this is still incomplete, however, it is understood that growth and division involves the synthesis of a large variety of proteins, lipids, nucleic acids and other components (e.g. enzyme cofactors). The majority of these components are synthesised outside the organelle in the external cytoplasm, and transported inside for assembly at specific sites prior to mitochondrial division. Conclusive evidence for this mechanism was produced in 1963, during experiments with *Neurospora crassa* cells (Luck, 1963). Division takes place in two main stages. The first is the division of the mitochondrial DNA, followed by the division of all other mitochondrial components (mitochondriokinesis). It is known for these two processes to occur at the same time, but in most cases, the DNA division is completed first. The process of division involves the formation of a constriction across the middle of the major axis of the mitochondrion, which gradually deepens and separates the organelle into two roughly equal parts.

7.1.7 Mitochondria and Disease

It is now known that many diseases originate from within the cell, and hence the question as to the location where it all begins to go wrong needs to be answered. Based on what we know about mitochondria, and our understanding of its energy producing operations, it is not surprising that mitochondria should be the first part of the cell to wear out. Respiration is a potentially dangerous process, involving the transfer of electrons from one carrier molecule to another. The electrons' destination is molecular oxygen; in the final reaction the electrons are used to reduce it to water. However, if there is a block in the electron transport chain, or if one component is more active than the next component, the stray electrons can damage the mitochondrion and in doing so can cause damage to other cellular components. Generally the electrons help form reactive oxygen species (ROS), which can damage proteins, DNA, and membranes. Damage to the membranes can short-circuit the charge gradient needed for ATP production, and release pro-apoptotic molecules like cytochrome c that can trigger programmed cell death. Oxidative damage to mitochondrial DNA is linked with Huntington's disease (Polidori *et al.,* 1999). In Parkinson's disease, which represents a genetically heterogeneous group of disorders, a relatively large group of patients are known to possess a functional defect of mitochondrial complex I (the first component of the respiratory chain, located in the inner mitochondrial membrane) (Graeber *et al.,* 1999). Mitochondria are also involved in defects such as mitochondrial myopathy" (indicating muscle involvement) or "mitochondrial encephalomyopathy" (indicating brain and muscle involvement). The mitochondrial encephalomyopathies and myopathies are typically caused by defects in the respiratory chain or the electron transport chain (Hesterlee, 1999).

Due to the role of mitochondria in the development of these diseases, methods capable of analysing both the size and activity of individual mitochondria, as well as the proteins expressed by the mitochondrial genome, may provide valuable contributions to our understanding of the various diseases. This chapter examines both approaches to the analysis of mitochondria, and develops methods for both mass and activity measurements using capillary electrophoresis, as well as investigating the use of capillary gel electrophoresis for analysis of the mitochondrial proteome.

7.2 Analysis of mitochondria by capillary electrophoresis with post column laser-induced fluorescence detection

7.2.1 Analysis of whole cells by fluorescent microscopy

For investigations involving the mitochondrion, there are a number of fluorescent probes available today. Among the most commonly used are nonyl acridine orange, (NAO), rhodamine 123 (Rh123), and 5,5',6,6'-tetrachloro-1,1',3,3'-tetraethylbenzimidazolyl-carbocyanine iodide, (JC-1). NAO is used for the determination of mitochondrial mass, as it binds the lipid cardiolipin found in the mitochondrial membrane in a 2:1 ratio, and its uptake is independent of mitochondrial activity. Rhodamine 123 is a cell-permeable, cationic, fluorescent dye that is readily taken up by active mitochondria without inducing cytotoxic effects. As its uptake is dependent on membrane potential it may be used to measure the activity of mitochondria. The green fluorescent JC-1, 5,5',6,6'-tetrachloro-1,1',3,3'-tetraethylbenzimidazolylcarbocyanine iodide, is also dependent on membrane potential and exists as a monomer at low concentrations or at low membrane potential. However, at higher concentrations (aqueous solutions above 0.1 μM) or higher potentials, JC-1 forms red fluorescent "J-aggregates" that exhibit a broad excitation spectrum and an emission maximum at about 590 nm. Chinese hamster ovary cells (Figure 7.1) were stained with the above dyes and examined by fluorescence microscopy. Figures 7.2 – 7.4 show photographs taken of the cells at different magnifications, 20× and 60×, stained with 10μM NAO, JC-1, and 1μM Rh123.

7.2.1.1 Nonyl acridine orange staining of Chinese hamster ovary cells

Chinese hamster ovary cells were stained with the dye *nonyl acridine orange* (NAO) as outlined in section 2.3.7.1. NAO binds to the cardiolipin content of the mitochondrial membrane, and is well retained in the mitochondria over reasonable time periods (days). It is toxic at high concentrations and binds to all mitochondria, regardless of their energetic state. A sample of the cells were placed on a slide and examined by both light and fluorescent

microscopy at various magnifications. Figure 7.1 shows CHO cells examined by light microscopy prior to labelling and photographed at 20× magnification. For fluorescence, the cells were viewed through a fluorescein longpass optical filter.

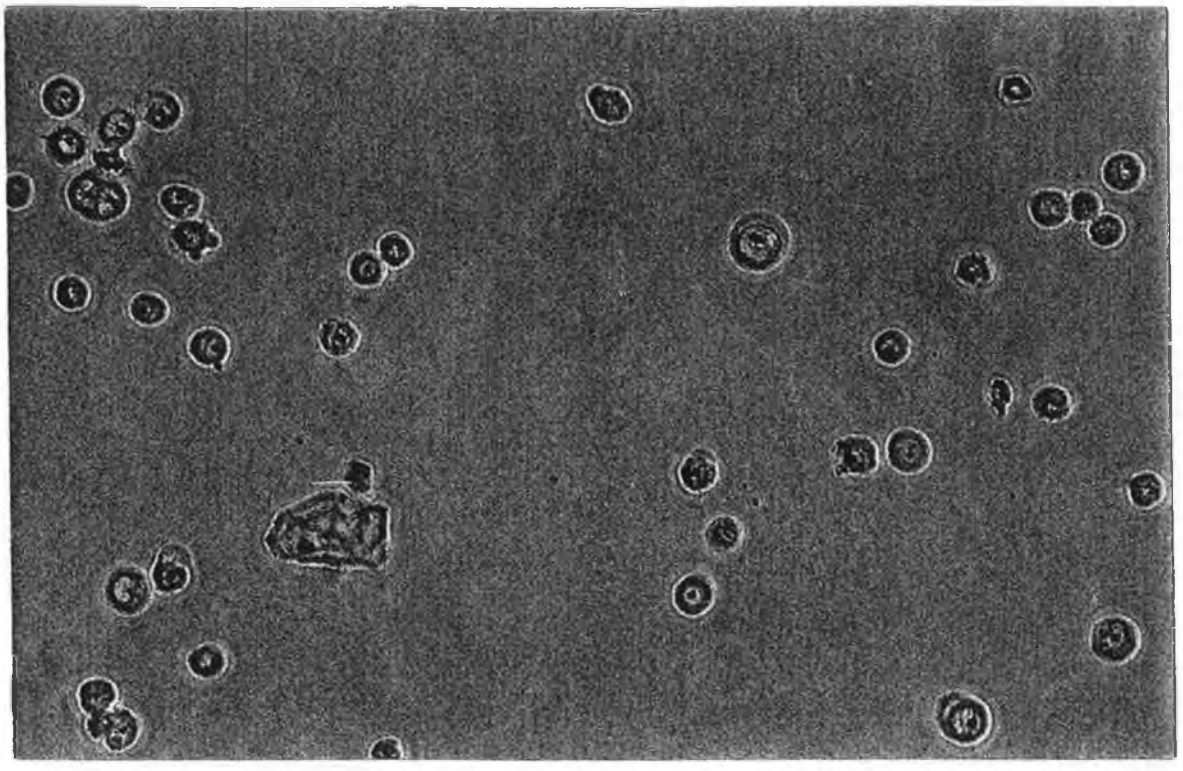

Figure 7.1 *Fluorescent microscopy analysis of unlabelled Chinese hamster ovary cells, photographed under 20× magnification.*

7.2.1.2 Rhodamine 123 and 5,5',6,6'-tetrachloro-1,1',3,3' tetraethylbenzimidazolyl-carbocyanine iodide (JC-1) staining of Chinese hamster ovary cells

Staining with Rhodamine 123 (Rh123) (Figure 7.3) and 5,5',6,6'-tetrachloro-1,1',3,3'-tetraethyl-benzimidazolylcarbocyanine iodide (JC-1) (Figure 7.4), were carried out in the same way as for NAO. Both of these dyes are used for investigations on mitochondrial membrane potential. It is possible to see clearly the live cells and dead cells. As Rhodamine 123 depends on an active mitochondrial membrane potential for its uptake, it will stain only live cells, and hence cells with active mitochondria. This effect is less clear with those cells stained with JC-1.

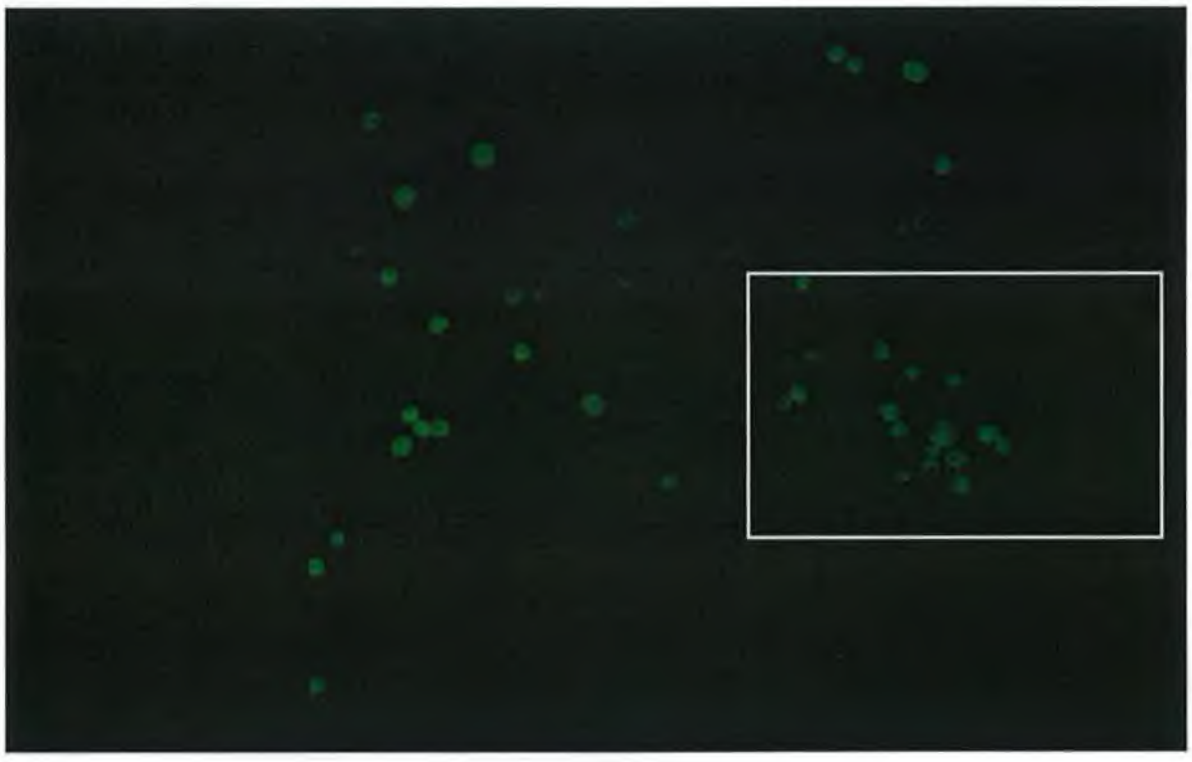

(A)

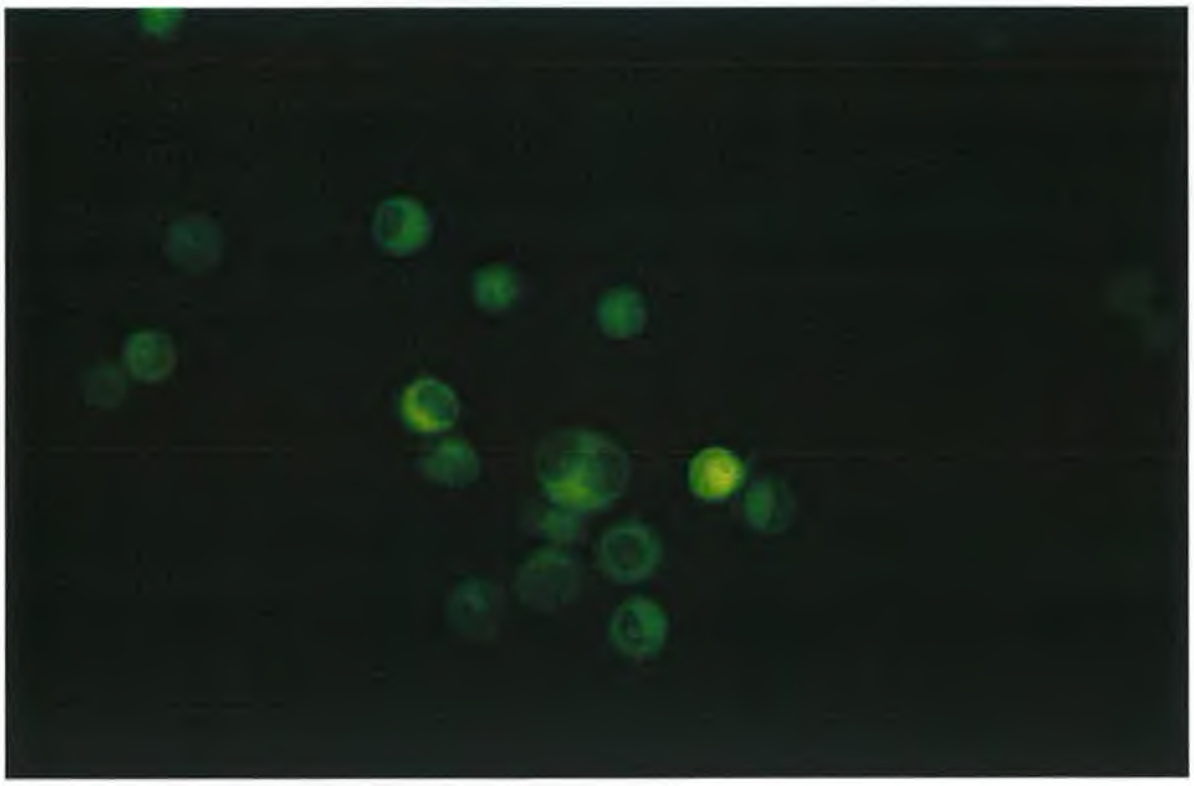

(B)

Figure 7.2 *Chinese hamster ovary cells stained with 10μM Nonyl acridine orange and viewed using a fluorescent microscope.* ***(A)*** *20× magnification and* ***(B)*** *60 × magnification.*

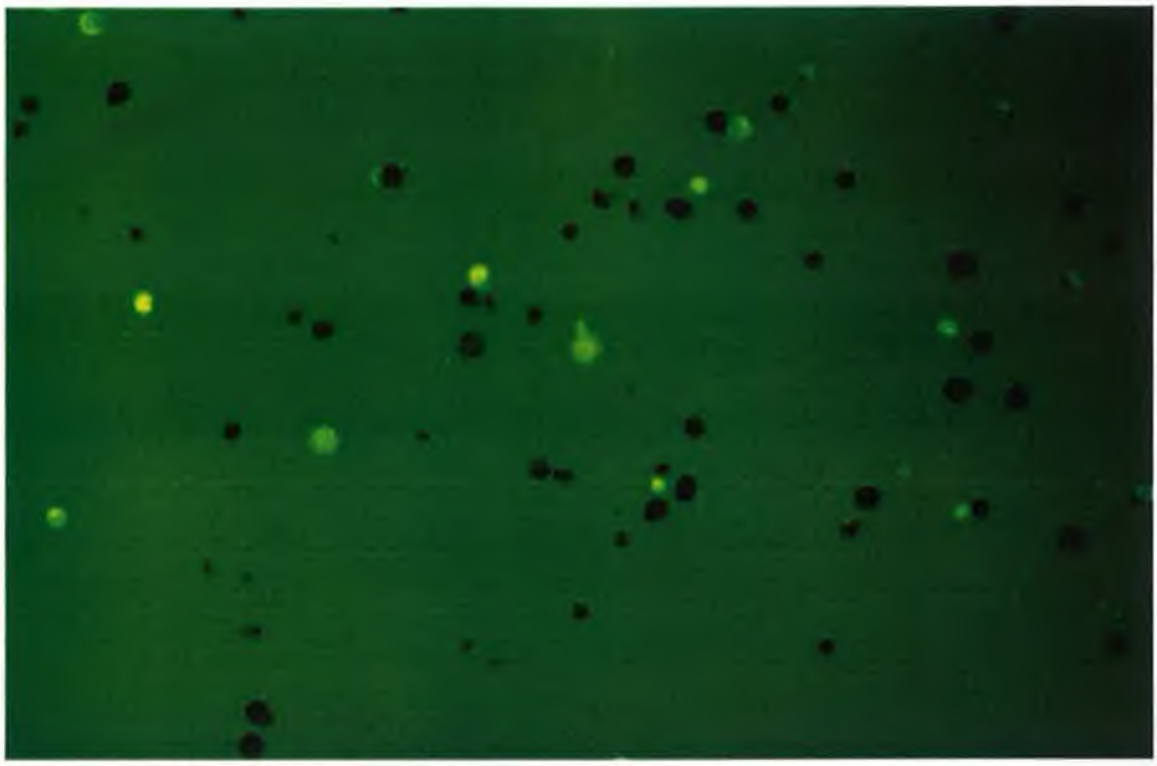

(A)

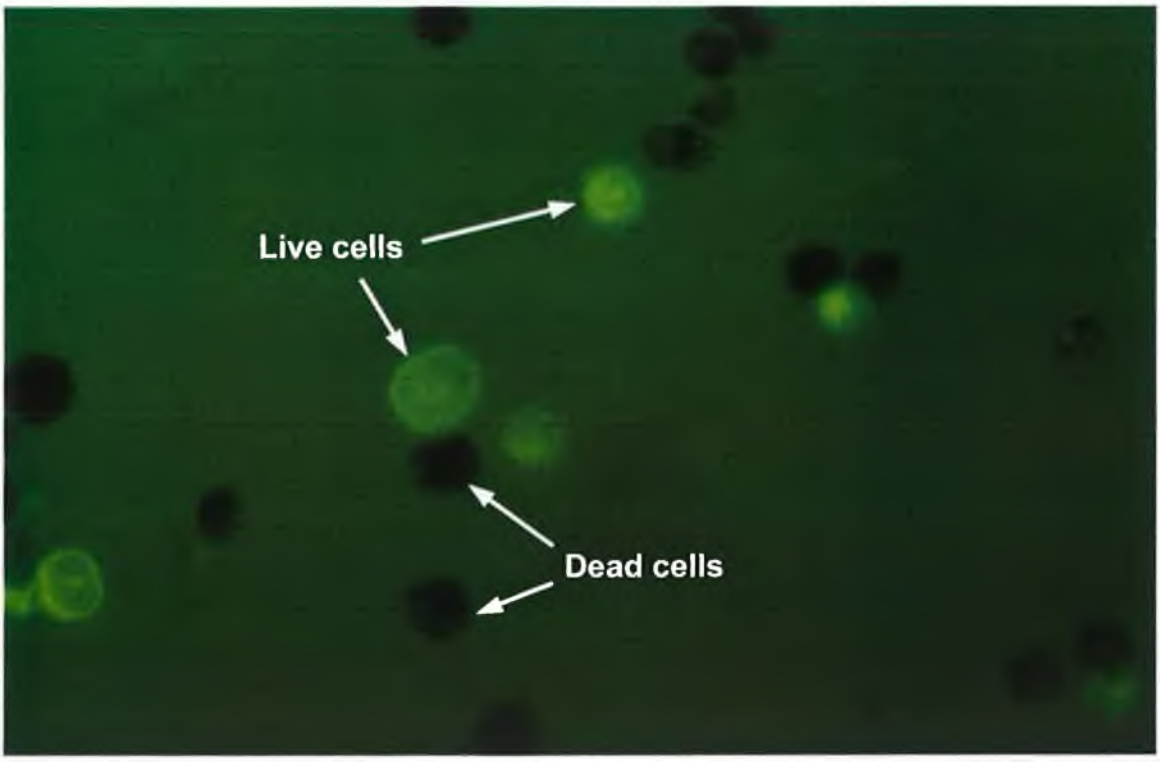

(B)

Figure 7.3 *Chinese hamster ovary cells stained with 1μM Rhodamine 123 and viewed using a fluorescent microscope. (A) 20× magnification and (B) 60 × magnification. Both dead and live cells can be seen.*

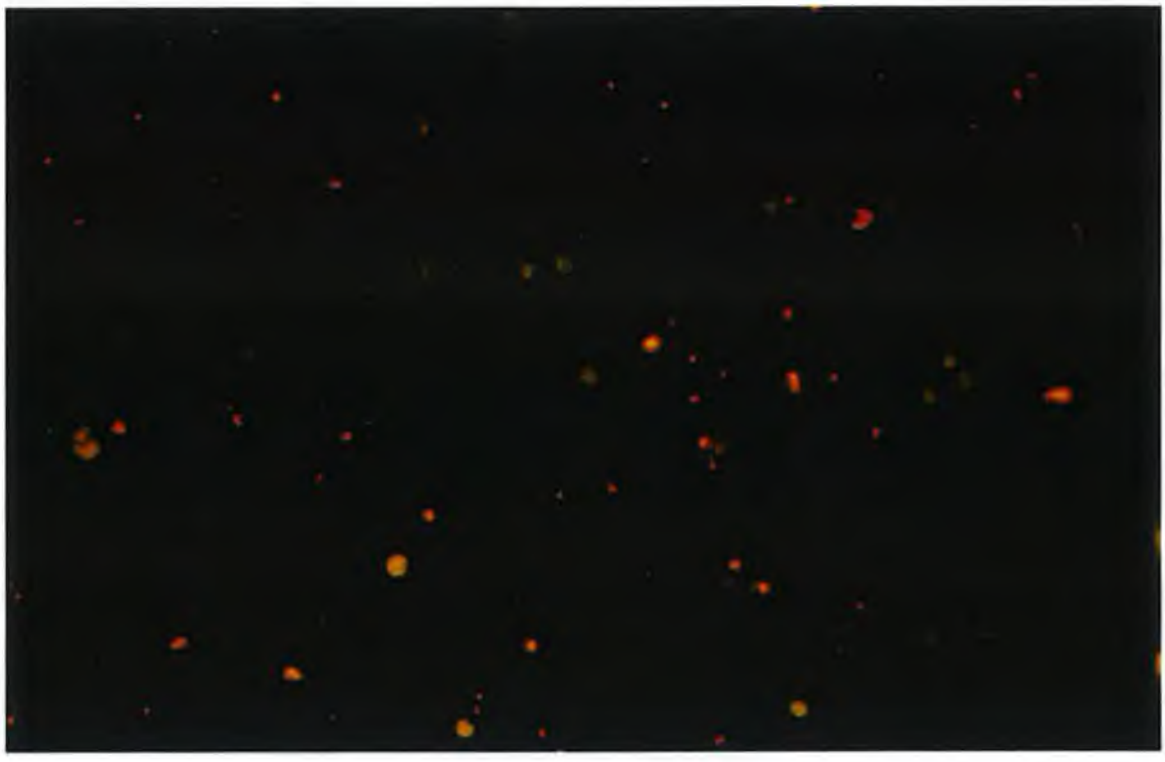

(A)

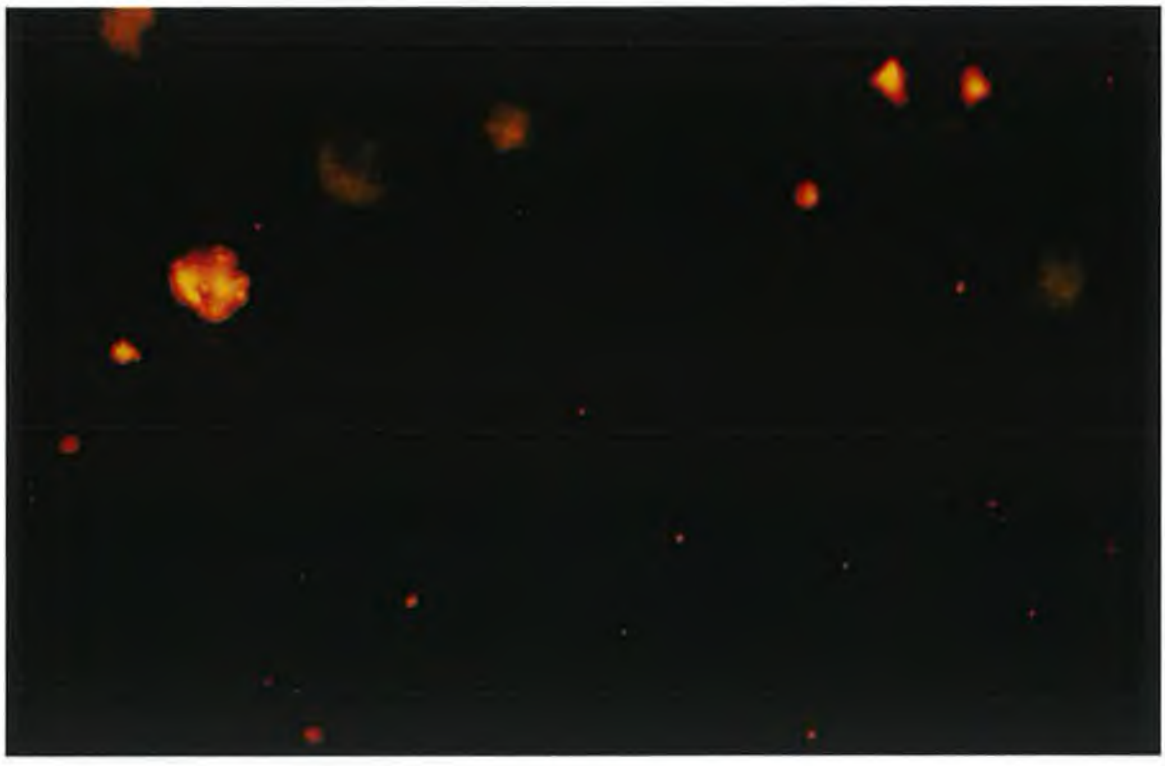

(B)

Figure 7.4 *Chinese hamster ovary cells stained with 10μM JC-1 and viewed using a fluorescent microscope. (A) 20× magnification and (B) 60 × magnification.*

7.2.2 Analysis of whole cells by capillary electrophoresis

Whole hybridoma cells were stained according to the procedure for Chinese hamster ovary cells using NAO stain, and were analysed by capillary electrophoresis. Figure 7.5 shows the results when whole hybridoma cells were analysed by capillary electrophoresis using uncoated capillaries with hydrodynamic and electrokinetic injections.

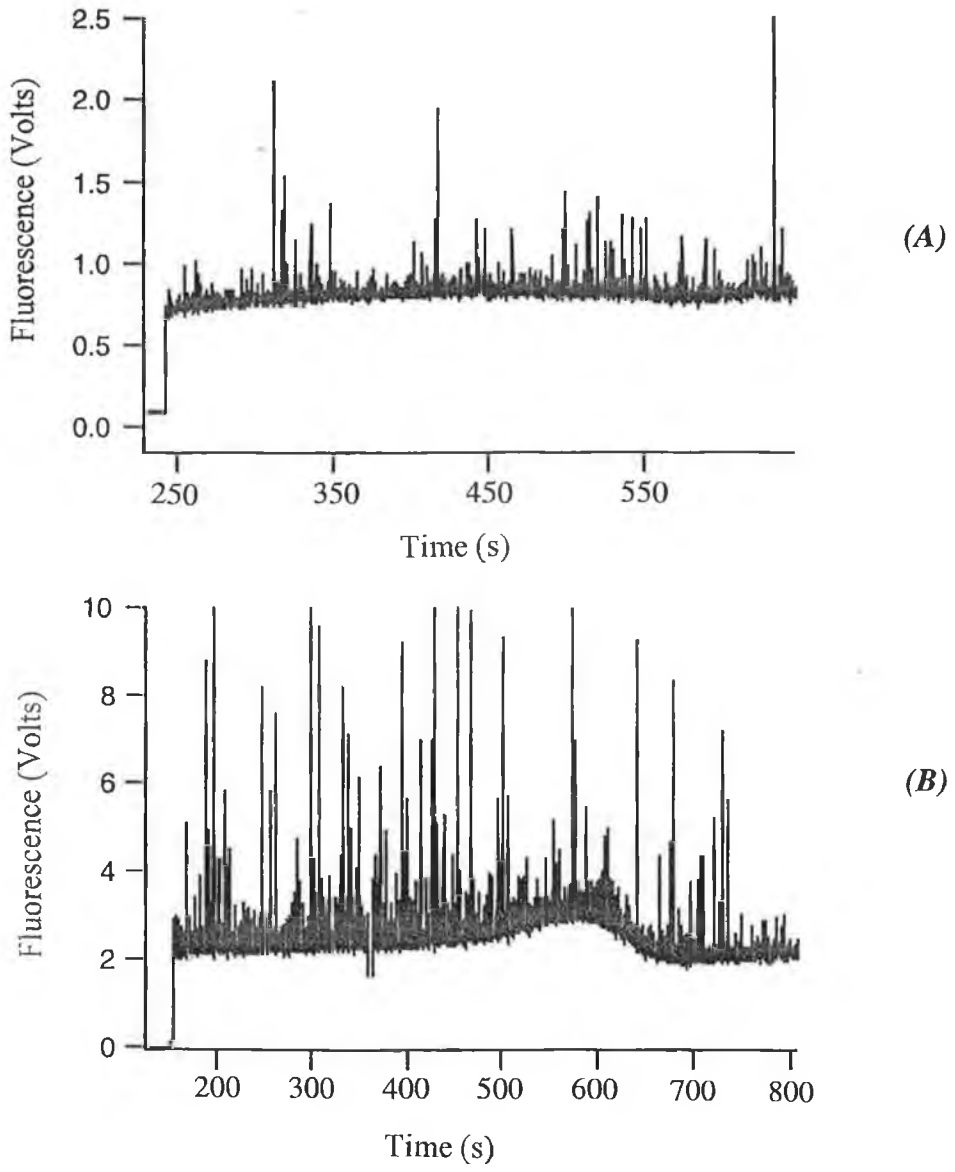

Figure 7.5 *Analysis of whole hybridoma cells by capillary electrophoresis. (A) 30 s electrokinetic injection at 24.8Vcm^{-1}, separation at 200Vcm^{-1}, (B) continuous hydrodynamic injection. Conditions; uncoated fused silica capillary, (40.2cm), separation buffer; 250mM Sucrose, 10mM HEPES, pH 7.5, 0.3×10^{6} cells/ml, PMT 800V with data acquisition at 50Hz. Excitation was at 488nm with detection at 535DF35nm.*

Hydrodynamic injection showed a higher and more intense number of peaks, this could be due to the electric field having a damaging effect on individual cells, thus reducing the signal.

7.2.3 Analysis of isolated mitochondria by capillary electrophoresis

Mitochondria were isolated from Chinese hamster ovary cells as outlined in section 2.3.7.3 and 2.3.7.4 and stained with the relevant dye (NAO or Rhodamine 123). Figure 7.6 shows the tissue homogeniser used for disruption of cells and overlays of the different fractions of Percoll and Metrizamide for ultracentrifugation following homogenisation. The development of mitochondria isolation is detailed in section 7.2.3.1.

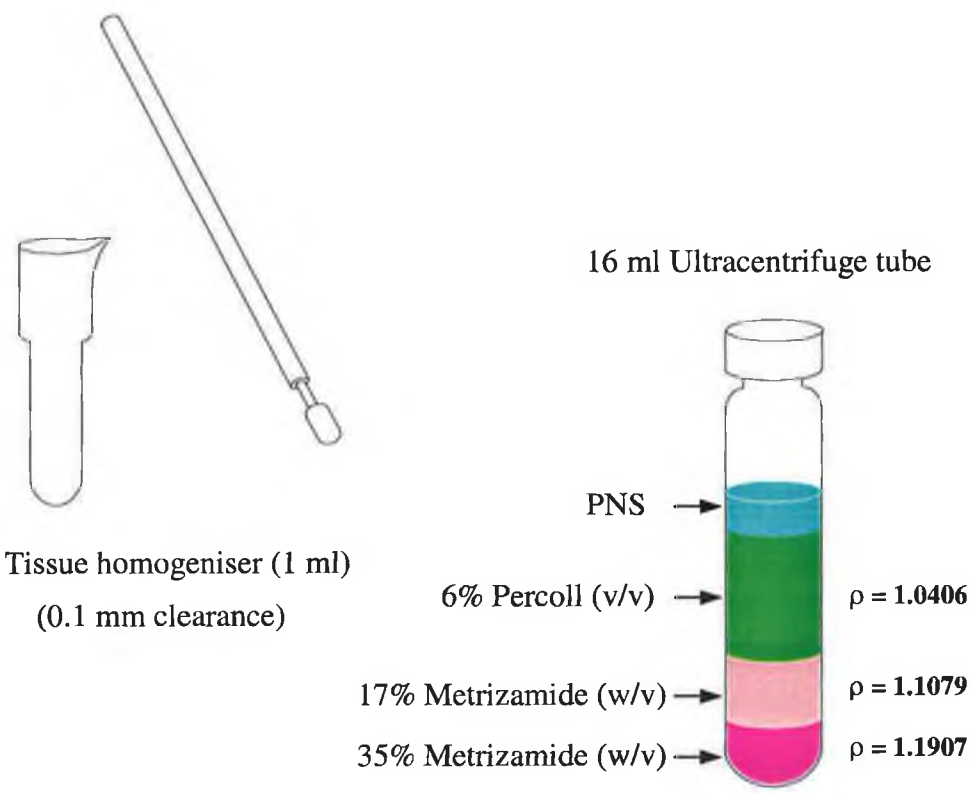

Figure 7.6 *Potter Elvehjem tissue homogeniser used to disrupt cells for isolation of mitochondria, and gradient profile used for ultracentrifugation of postnuclear supernatant (PNS) following cell homogenisation and removal of nuclear fraction.*

7.2.3.1 Development of procedure for isolation of mitochondria

In order to obtain isolated mitochondria, from tissue culture cells, in fractions suitably pure for further studies, the use of density gradient ultracentrifugation was employed. This method was developed by Madden and Storrie (1987) specifically for the preparation of isolated mitochondria from tissue culture cells (CHO's) and was used for the work presented in this chapter. Figure 7.7 shows a flow diagram of the method following staining of the cells for 5 minutes at room temperature with 10^{-6}M NAO or Rhodamine.

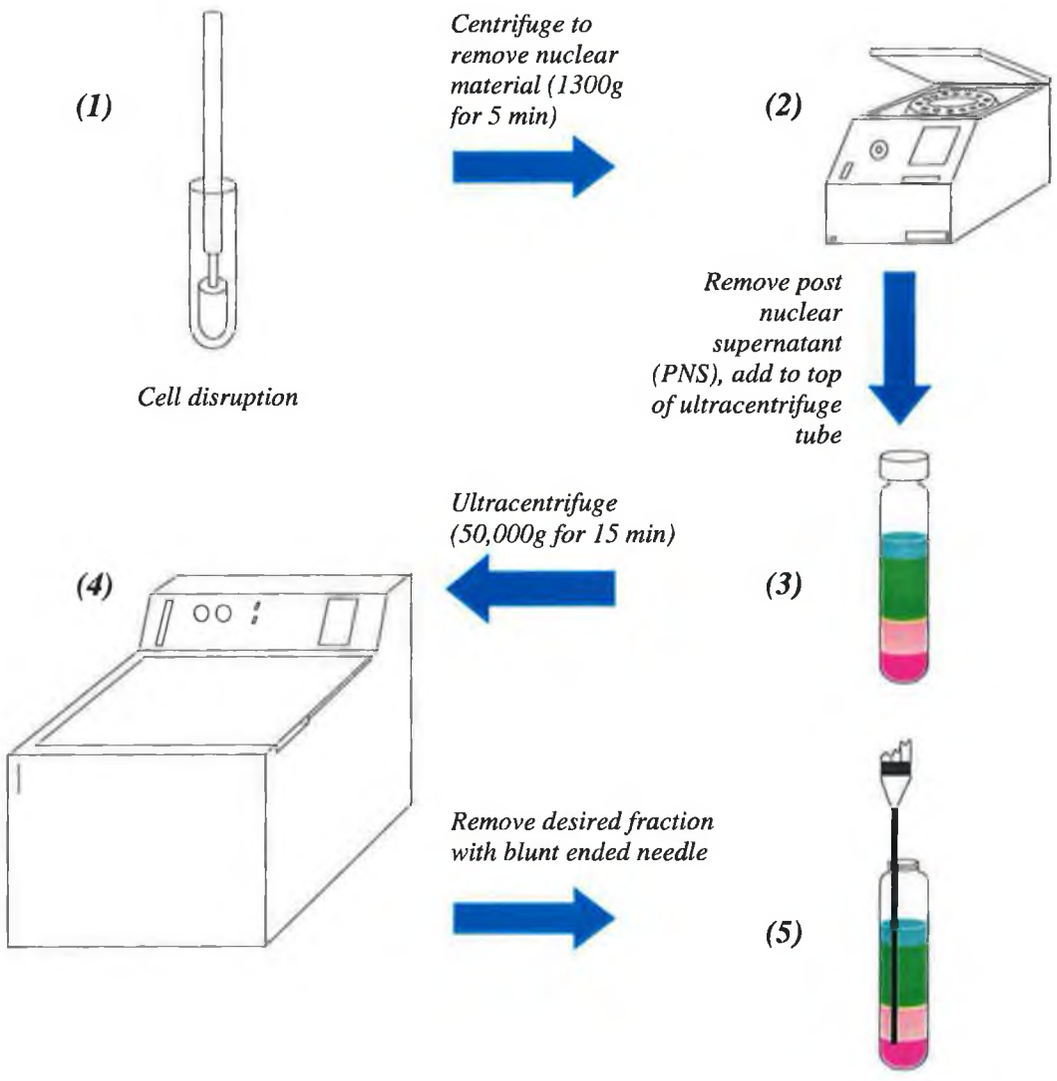

Figure 7.7 *Flow diagram showing sequence of events for isolation of mitochondrial fraction for analysis by capillary electrophoresis with post column laser-induced fluorescence.*

7.2.3.2 Mass measurements using Nonyl Acridine Orange

Uncoated capillaries: For mass measurements, mitochondria were isolated from Chinese hamster ovary cells and stained with nonyl acridine orange as outlined in sections 2.3.7.3 and 2.3.7.4. The fractions were analysed by CE using uncoated fused silica capillaries. Figure 7.8 shows the results obtained. Each peak represents a single mitochondrion and the height is proportional to the amount of dye bound to cardiolipin in the membrane and, hence, the size of the mitochondrion. Unlabelled mitochondria were also analysed to determine if there was any contribution to peak height from scattering (produced when the laser beam strikes a particle/mitochondrion, either labelled or unlabelled). In the blank run, while there are some small peaks, when set against the same scale as the labelled mitochondria electropherogram (Fig. 7.8), the unlabelled mitochondria contribute very little to peak number or height. The absence of a defined window of migration for the mitochondria may indicate a problem of mitochondria continuously interacting with the wall of the capillary throughout the separation. This may be due to interactions between the proteins in the mitochondrial membrane and the capillary wall. This assumption can be made based on the fact that the interactions between proteins and the walls of narrow bore capillaries are well documented. Blank injections consisting only of buffer were made between sample injections, and any peaks observed in the electropherogram would support the conclusions that mitochondria are adhering to the walls of the capillary. Results obtained showed this to be the case, as mitochondria (peaks) were observed in the electropherograms of these blank runs.

The use of the surfactant, digitonin, to try and eliminate these interactions was investigated. Digitonin was chosen over other surfactants (e.g. SDS) because at low concentrations it does not disrupt lipid membranes, a feature of most surfactants. Concentrations of 0.01, 0.05 and 0.1% (w/v) digitonin were tried. However, results were inconclusive with no reproducibility found between repeated injections of the same sample. At all concentrations of digitonin used, there was an accompanying large rise in background, increasing as the digitonin concentration increased. A blank run showed mitochondria eluting from the capillary walls, although in reduced numbers, presumably due to the presence of the digitonin having some effect on sticking. From these results it was clear that the use of coated capillaries to try and eliminate sticking completely would have to be investigated.

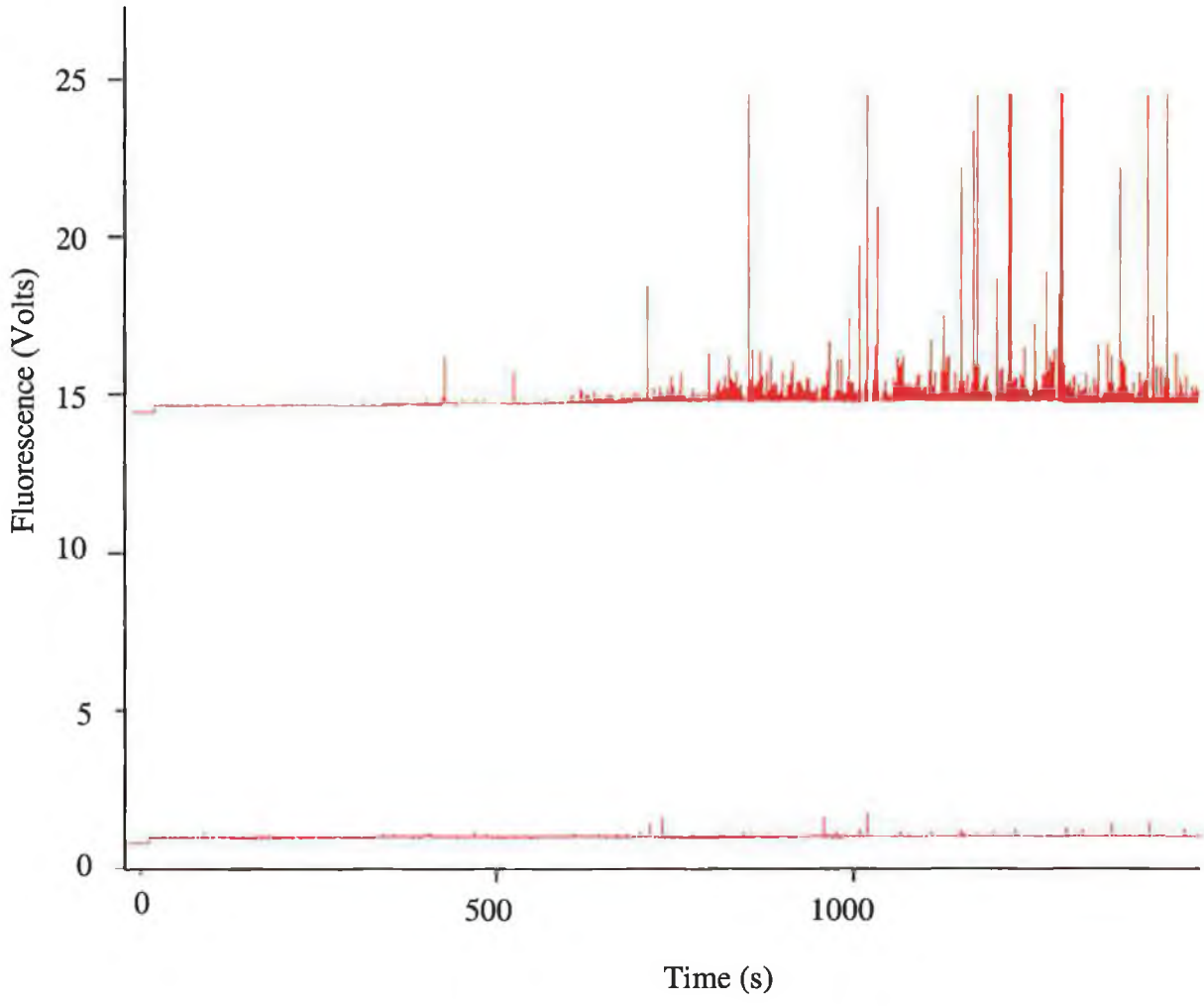

Figure 7.8 *Analysis of isolated mitochondria from Chinese hamster ovary cells. Separation conditions; uncoated fused silica capillary; buffer: 250mM Sucrose, 10mM HEPES, pH 7.5; 5 s injection at 50Vcm^{-1}, separation at 200Vcm^{-1}, PMT 1000V, data acquisition at 50Hz. Mitochondria were stained with 10^{-6}M NAO (upper trace) and analysed unlabelled (lower trace).*

Coated capillaries: A number of capillaries were coated as described in section 2.3.6.2 to attempt to circumvent the problems associated with uncoated capillaries. The results were an improvement with a defined window of migration for the mitochondria (Figure 7.9). Section 7.2.3.3 discusses the advantages of using both coated and uncoated capillaries for analysis of mitochondria.

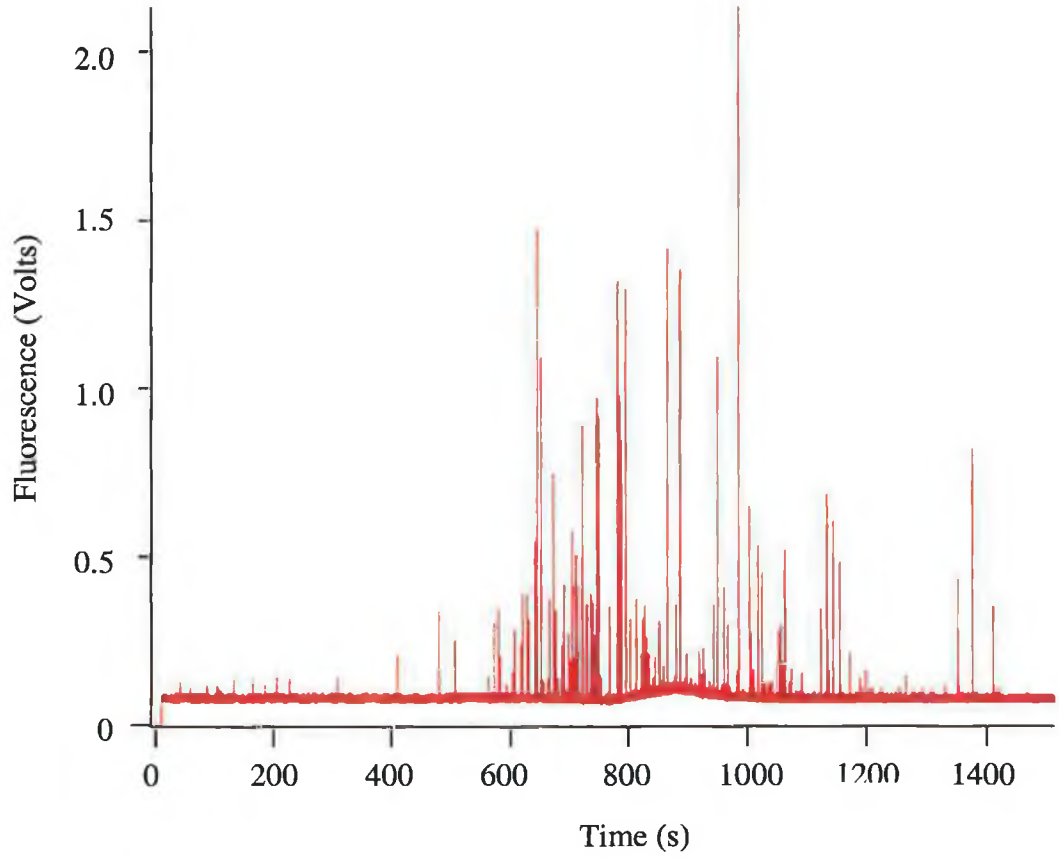

Figure 7.9 *CE separation of nonyl acridine orange-stained mitochondria (final concentration 10^{-6}M) using AAP coated capillaries. Conditions: buffer; 250mM sucrose, 10mM HEPES, pH 7.5, 5 s injection at 52Vcm^{-1}, separation at 200Vcm^{-1}, PMT 1000V, data acquisition at 50Hz. Excitation was at 488nm with detection at 535DF35nm.*

7.2.3.3 Analysis of results from uncoated capillaries

A comparison of electropherograms of mitochondria obtained from both uncoated and coated capillaries is shown in Figure 7.10. When the data is analysed using PickPeaks software analysis, stained mitochondria had mobilities dispersed within a range of 2×10^{-4} cm^2 V^{-1}s^{-1} (90% of all peaks), while the use of a coated capillary demonstrated 90% of all mitochondrial mobility dispersed within a range of 3.6×10^{-4} cm^{2}V^{-1}s^{-1} (Figure 7.10). This mobility dispersion can be used to spread mitochondria elution to obtain analysis of single mitochondria with coated capillaries, while uncoated capillaries can be used to obtain a narrow mobility window.

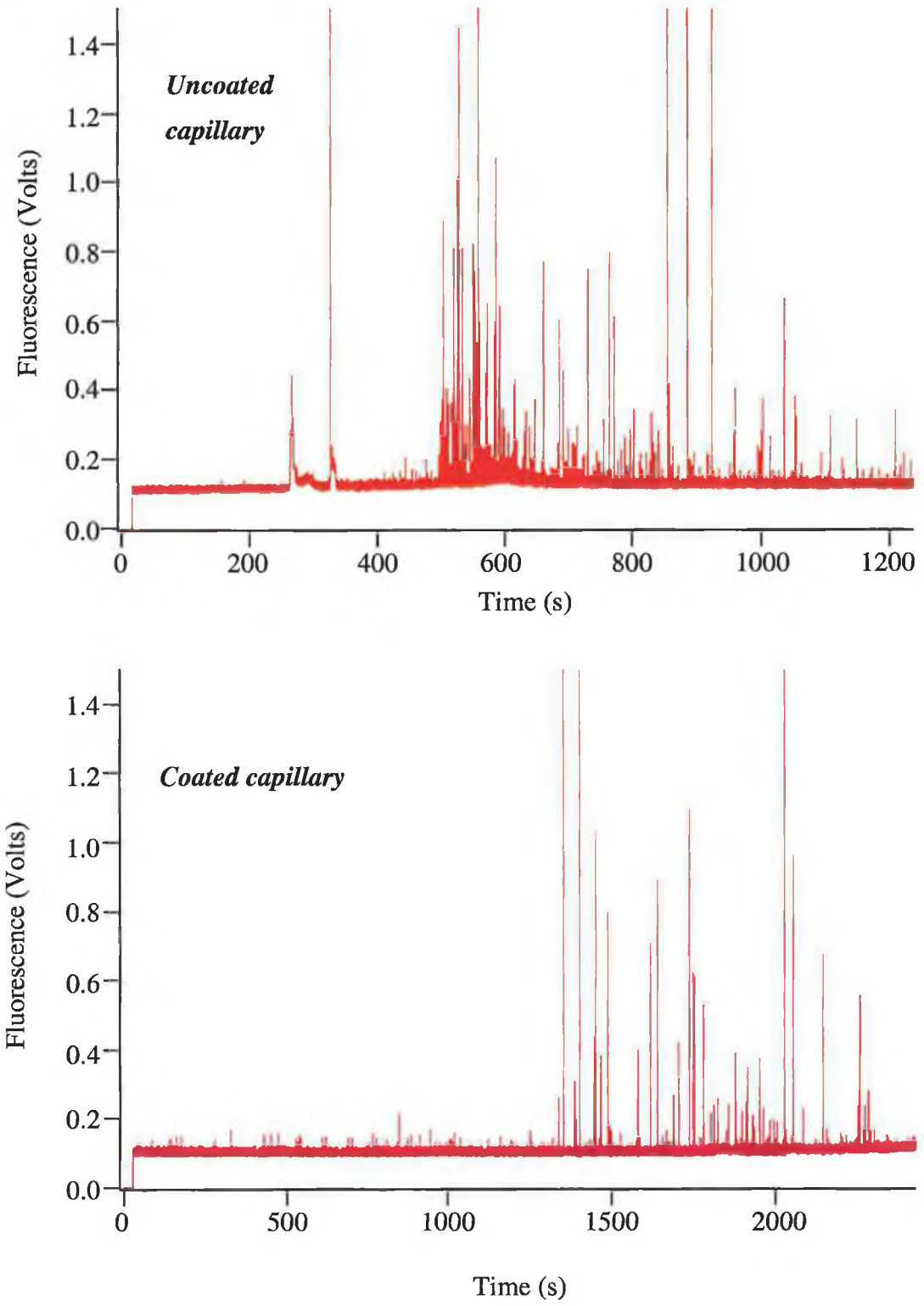

Figure 7.10 *Comparison of electropherograms of mitochondria analysed using uncoated and coated capillaries. Conditions: buffer; 250mM sucrose, 10mM HEPES, pH 7.5, 5 s injection at 52Vcm^{-1}, separation at 200Vcm^{-1}, PMT 1000V, data acquisition at 50Hz. Excitation was at 488nm with detection at 535DF35nm.*

7.2.3.4 Analysis of mitochondrial activity using Rhodamine 123

Rhodamine 123-stained mitochondria were isolated as outlined in section 2.3.7.3 and analysed by CE to investigate the feasibility of carrying out activity measurements in the same manner as for mass measurements, using the dye NAO. Some preliminary results were obtained and Figure 7.11 shows an electropherogram of mitochondria stained with the activity dye, Rhodamine 123 and analysed using an uncoated capillary. The uptake of Rh123 is dependent on membrane potential, and hence each peak represents a single active mitochondrion. The peak height is an indication of the amount of dye present inside, thus giving an indication of its level of activity. A large background rise/peak can be seen at the start of the separation after about 4.1 minutes (250 seconds). This was though to have arisen from dye leaking from the mitochondria due to a loss in membrane potential. This could have occurred due to the electric field applied during the separation possibly disrupting the mitochondrial membrane. Another possibility may be the fact that there were no protease inhibitors present in the isolation medium at this time which could also have resulted in enzymatic damage to the mitochondria from the time of cell disruption and isolation allowing dye to leak from the mitochondria. No results were obtained for coated capillaries. However, this initial investigation shows that the method may be applicable to activity measurements for individual mitochondria, although further investigations are required.

7.2.4 Comparison of different separation voltages for analysis of mitochondria

The effect of the separation voltage on the mobility and separation of the mitochondria was investigated by comparison of two voltages, 200 and 300 Vcm^{-1} to see if the mobility behaviour is consistent for each separation voltage applied. The results were analysed and histograms for mobility were calculated. Figure 7.12 shows the electropherograms obtained for separations at 200 and 300 Vcm^{-1}. Both samples were analysed consecutively from the same fraction, and show that the separation voltage is inversely proportional to migration time (increasing the separation voltage results in a decrease in migration time). The calculated mobilities for both electropherograms along with the average mean, range and mode are shown in Table 7.1.

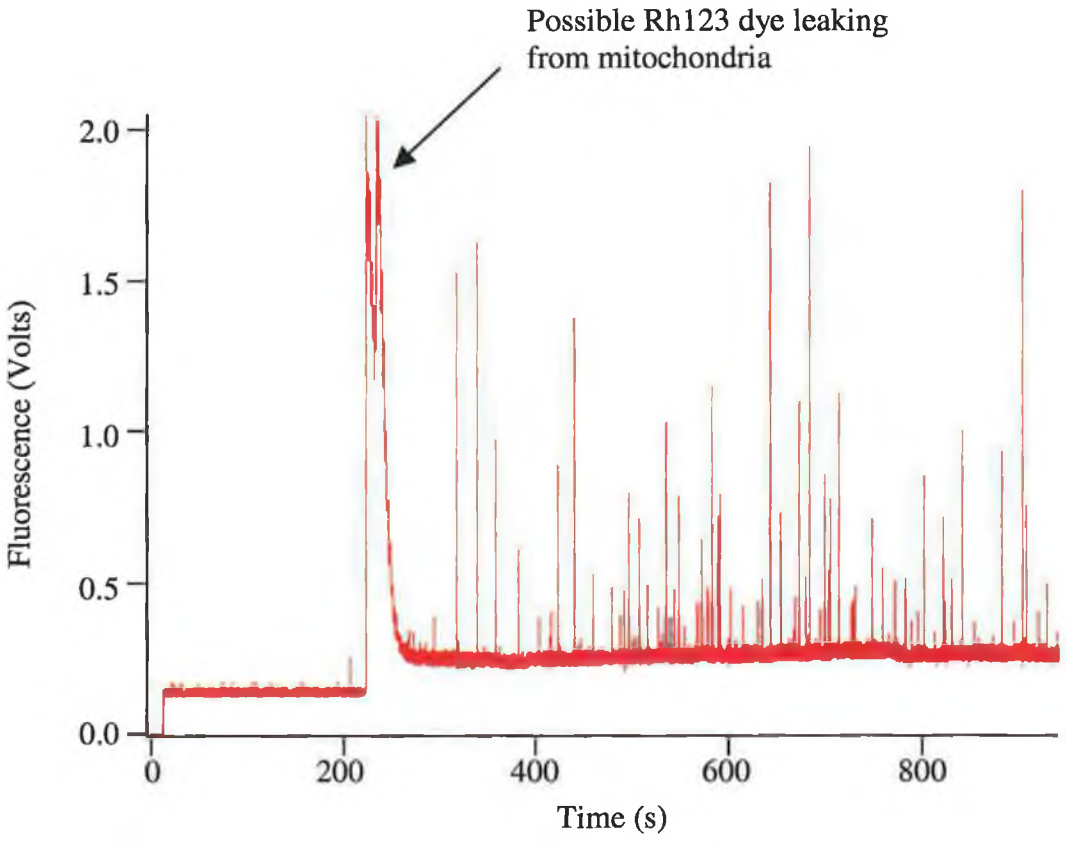

Figure 7.11 *Electropherogram showing Rhodamine 123-stained mitochondria. Conditions: fused silica capillary (uncoated), buffer; 250mM sucrose, 10mM HEPES, pH 7.5; 5 s injection at 52Vcm^{-1}; separation at 200Vcm^{-1}; PMT 1000V, data acquisition at 50Hz. Excitation was at 488nm with detection at 535DF35nm.*

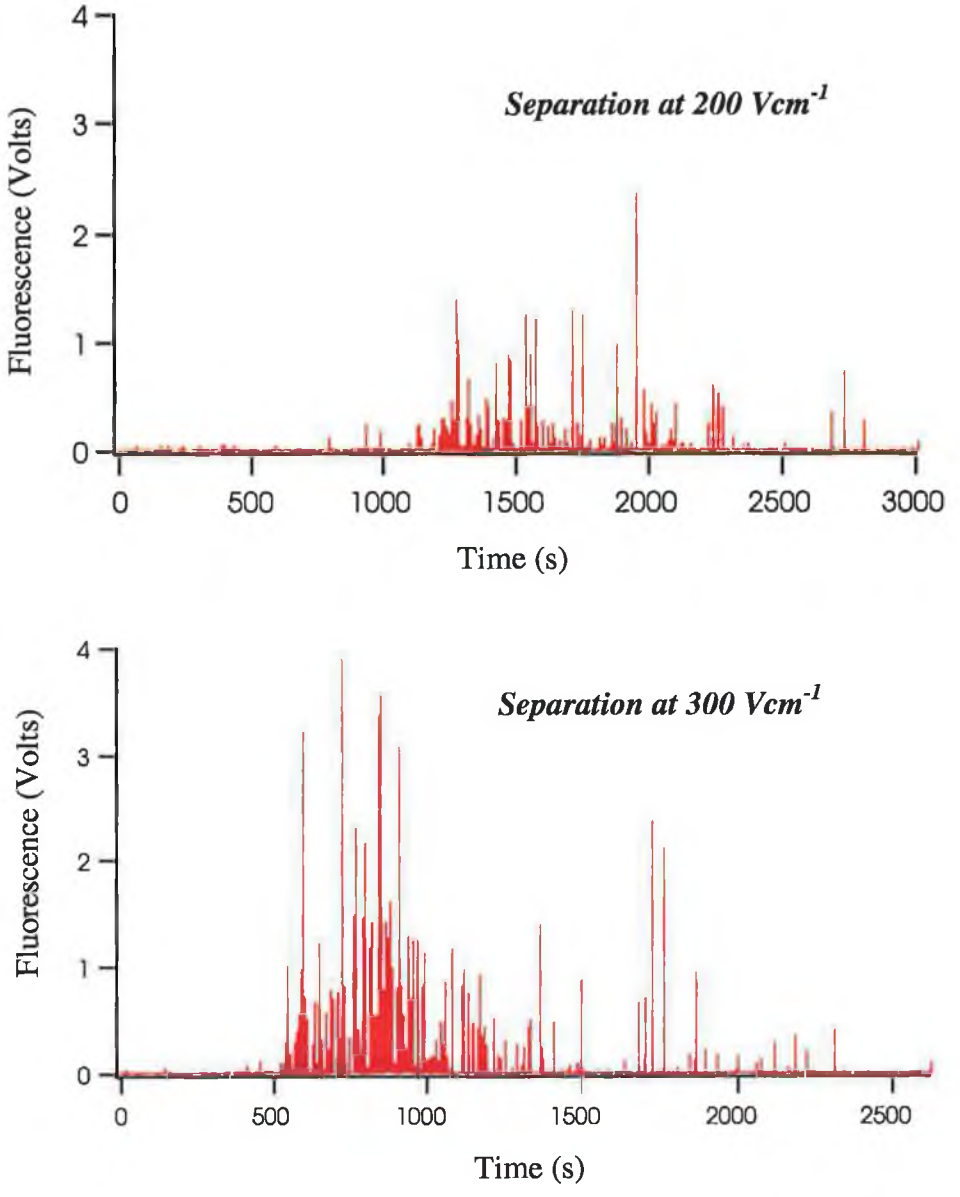

Figure 7.12 *Electropherograms obtained for analysis of the same fraction of mitochondria by CE using two different separation voltages, 200 and 300 Vcm^{-1}. Conditions: buffer; 250mM sucrose, 10mM HEPES, pH 7.5, 5 s injection at 52Vcm^{-1}, separation at 200/300 Vcm^{-1}, PMT 1000V, data acquisition at 50Hz. Excitation was at 488nm with detection at 535DF35nm.*

Mobility	*Separation Voltage ($V\ cm^{-1}$)*	
	200	**300**
Average	2.23×10^{-4}	1.44×10^{-4}
Median	1.50×10^{-4}	1.41×10^{-4}
Range	3.72×10^{-3}	8.35×10^{-4}
Mode	1.50×10^{-4}	1.25×10^{-4}

Table 7.1 *Calculated mobilities for electropherograms shown in Figure 7.12.*

It was expected that the mobility distribution should be the same for both voltage separations, as mobility is independent of capillary length, migration time and applied voltage. However, this was not the case. Figures 7.13 and 7.14 illustrates the two mobility histograms calculated from the electropherograms in Figure 7.12. Large numbers of mitochondria have low mobility at the higher separation voltage, as well as a greater number of more intense events. This may be due to higher electric fields causing polarisation of mitochondria resulting in agglomeration. These agglomerated mitochondria take longer to migrate through the capillary and hence this results in lower mobility values. This is in agreement with the results obtained in chapter 6 (section 6.2.1) for the bead experiments when high electric fields resulted in bead agglomeration. In the case of the liposomes, dilutions of the sample resulted in an increase in electrophoretic mobility and disappearance of intense events in the intensity distribution.

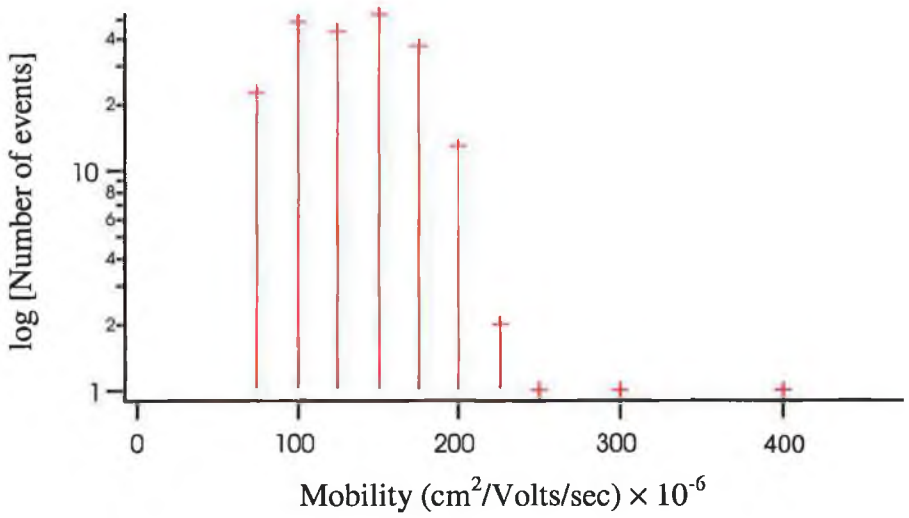

Figure 7.13 *Histogram of mobility distribution for analysis of mitochondria at 200 Vcm^{-1}.*

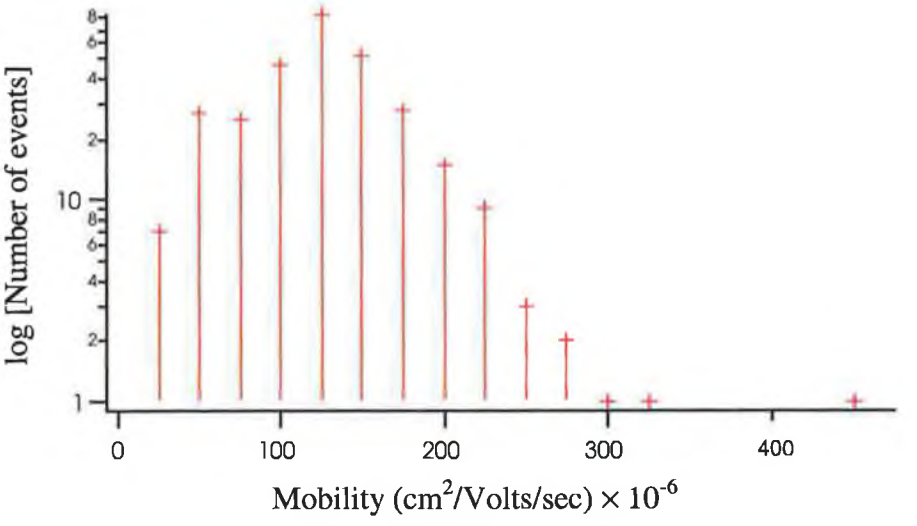

Figure 7.14 *Histogram of mobility distribution for analysis of mitochondria at 300 Vcm^{-1}.*

7.2.5 *Analysis of sample injection reproducibility*

The volume of sample injected into the capillary is varied by changing the injection voltage and the time it is applied to the sample vial. Figure 7.15 shows two electropherograms (A) and (B) obtained from identical injections, with a third identical injection from the same sample (C) shown in Figure 7.17. All three electropherograms should contain the same number of peaks, however following analysis by PickPeaks, the samples were found to have 72, 78, and 127 peaks, respectively. Investigation for error in the injection volume by integration of the area beneath the injection trace in the current plot revealed identical volumes had being injected. It is possible that there may have been 'carry-over' from one injection to the next, despite the use of coated capillaries to try and eliminate the problem of mitochondria adhering to the capillary wall. Analysis of the peak height distribution for all three electropherograms shows the most frequent peak height of about 0.02 volts, with a local maximum at about 0.07 volts in each case (Figures 7.16 and 7.17). A 10 second injection of the same sample expected to have a higher number of peaks, showed only 92 events. However, histogram analysis revealed identical features to samples injected for 5 seconds,

with the most frequent peak height at 0.02 volts with a local maximum at 0.07 volts (Figure 7.18).

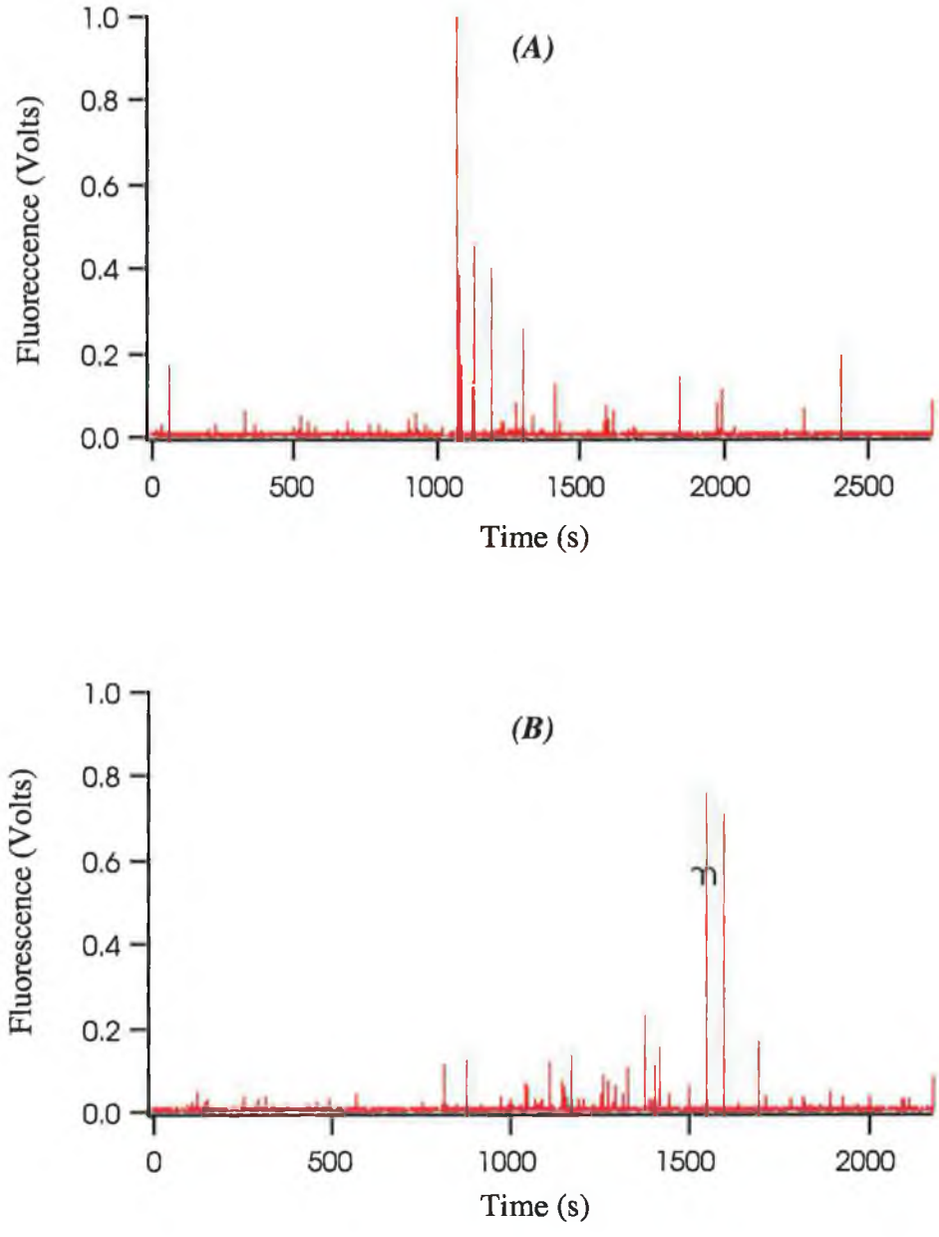

Figure 7.15 *Electropherograms obtained from identical injections of the same sample. Conditions: buffer; 250mM sucrose, 10mM HEPES, pH 7.5, 5 s injection at 50Vcm^{-1}, separation at 200/300 Vcm^{-1}, PMT 1000V, data acquisition at 50Hz. Excitation was at 488nm with detection at 535DF35nm. Histogram analysis of these electropherograms is shown in Figure 7.16.*

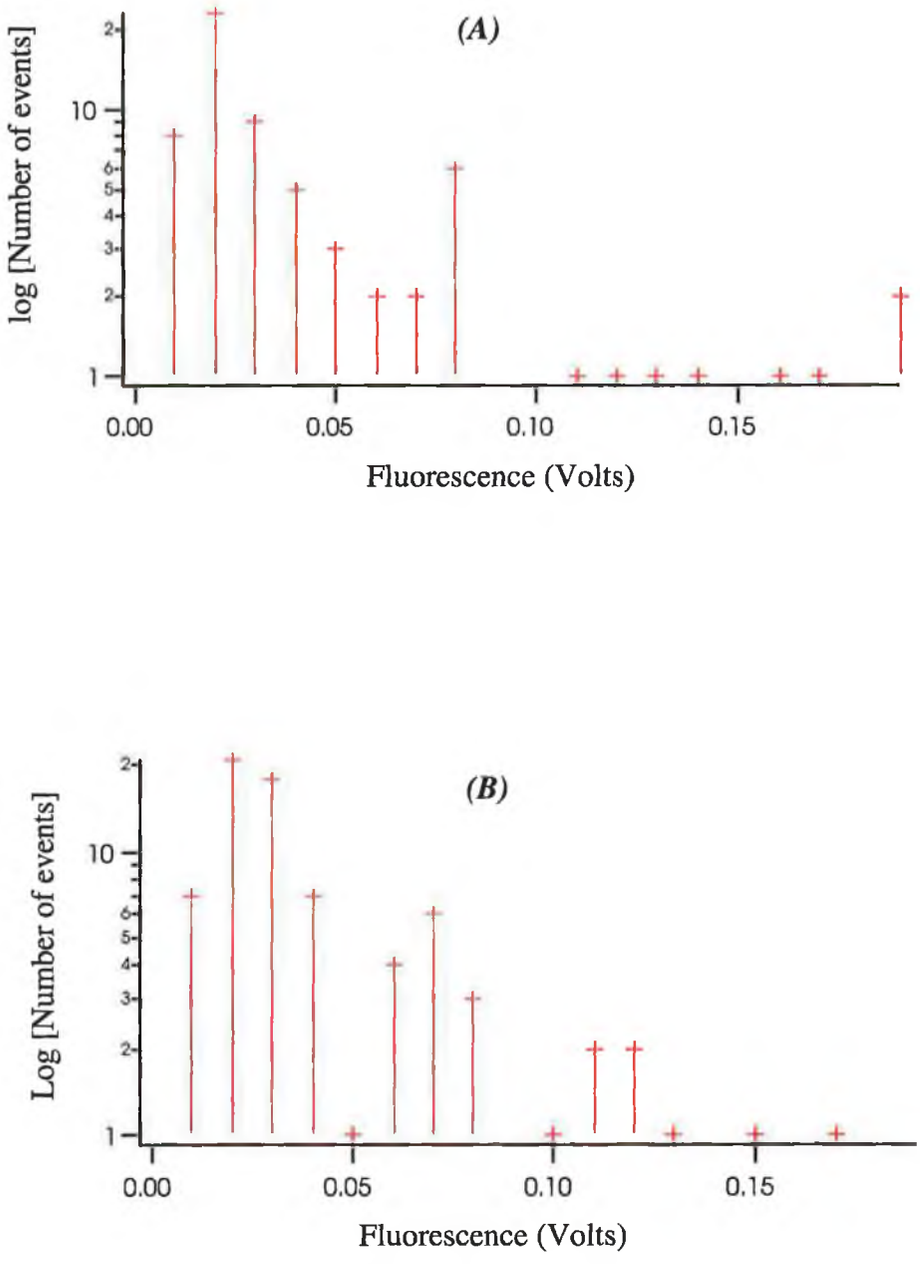

Figure 7.16 *Peak height distribution histograms for electropherograms (A) and (B) in Figure 7.15. The most frequent peak height at 0.02 volts with a local maximum at 0.07 volts can be seen for both injections.*

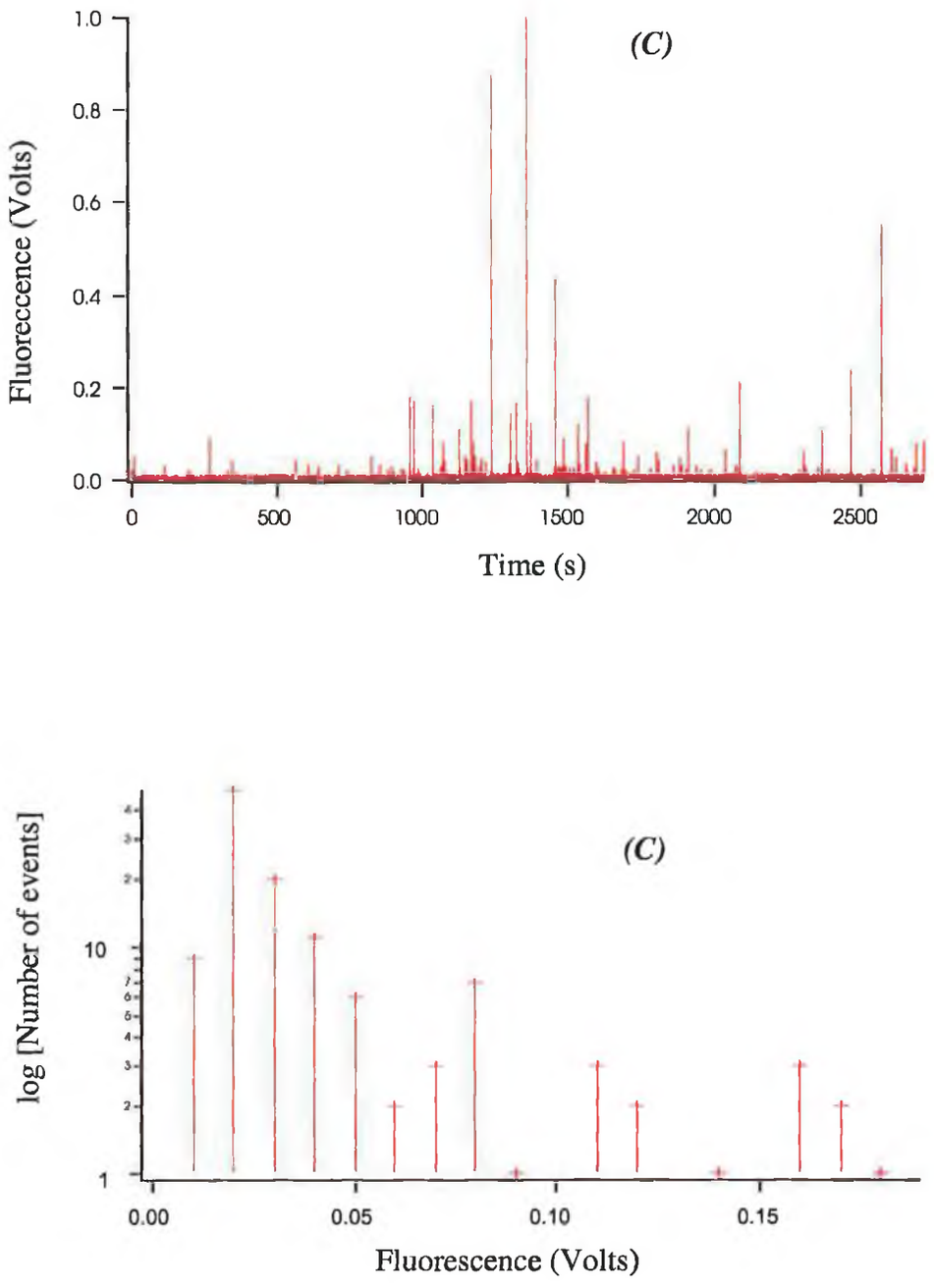

Figure 7.17 *Electropherogram obtained from the third 5 second injection (C) with histogram analysis illustrating most frequent peak height at 0.02 volts with a local maximum at 0.07 volts. Conditions for separation: buffer; 250mM sucrose, 10mM HEPES, pH 7.5, 5 s injection at 50Vcm^{-1}, separation at 200/300 Vcm^{-1}, PMT 1000V, data acquisition at 50Hz. Excitation was at 488nm with detection at 535DF35nm*

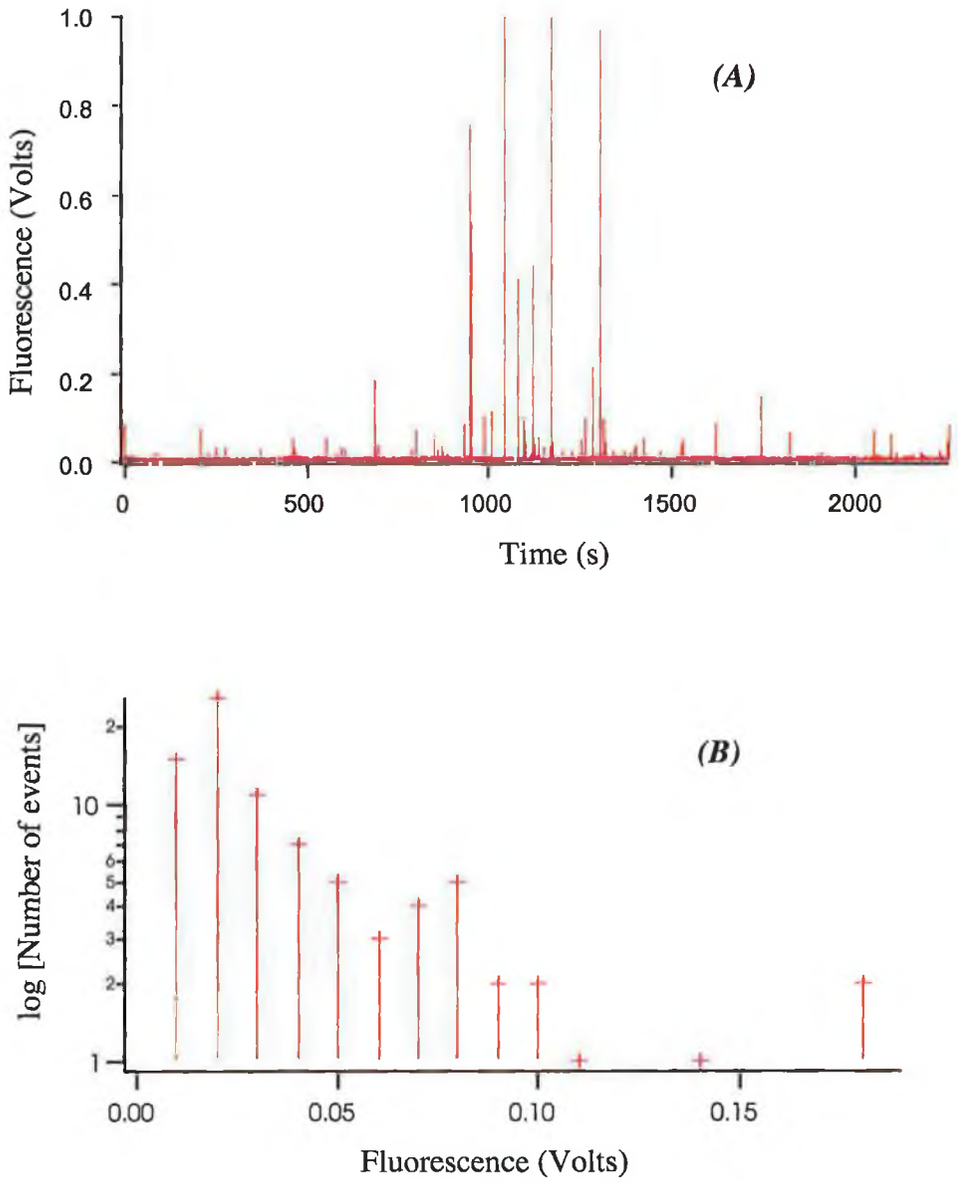

Figure 7.18 *CE electropherogram of a 10 s injection of mitochondria (A), with histogram analysis (B) showing most frequent peak height at about 0.02 volts with a local maximum at about 0.07 volts, identical to that observed for 5 second injections. Conditions for CE separation: buffer; 250mM sucrose, 10mM HEPES, pH 7.5, 5 s injection at 50Vcm^{-1}, separation at 200/300 Vcm^{-1}, PMT 1000V, data acquisition at 50Hz. Excitation was at 488nm with detection at 535DF35nm.*

More investigations are necessary in order to fully explain the inconsistency in the numbers of peaks in the three electropherograms corresponding to identical sample injections. However, it may be possible that there was a lack of homogeneity in the sample, although this is unlikely as the sample is collected from the 17% metrizamide/35% metrizamide (w/v) (M17/M35%) interface, and the density of this is greater or equal to that of the mitochondria. Therefore it is unlikely that any sample settling would occur. The other possibility is that there may be some alterations to the capillary wall with each injection and this may have an effect on the numbers eluting, possibly retaining some mitochondria during the separation. This might explain why the numbers increased from the first to third 5 second sample injection. However, the similarities of peak height distributions suggest that organelle analysis could be carried out even with the variations in the number of peaks for identical injections.

7.2.6 Analysis of mitochondria from different fractions following ultracentrifugation

As outlined in section 7.2.3.1, mitochondria were separated on the basis of their density, with the 17/35% (w/v) interface corresponding to a mitochondrial fraction with no or minimal contamination from other organelles. According to Madden and Storrie (1987) who developed the method, the 6% percoll/17% metrizamide (w/v) (P6/M17%) interface, which is less dense, is expected to contain a higher number of mitochondria than the 17/35% interface. However, this fraction will be contaminated with other organelles of similar density. Analysis of a sample taken from the (P6/M17%) interface stained with NAO, show peak height histograms with distinctly different features than those obtained from analysis of the M17/M35% interface (Figure 7.19). Injection and separation conditions for both were identical. The fact that the histograms display different profiles is an indication that the mitochondria in each fraction have different size profiles. This is as expected as the separation is based on density, and mitochondria with higher protein content (and perhaps differing size) would be expected to separate from mitochondria with less protein content in the membrane. A higher number of peaks in the P6/M17% sample was also observed and this agrees with the reports made regarding the numbers of mitochondria located at each interface. The apparent higher peak values from the P6/M17% fraction may also have a contribution from agglomeration of mitochondria due to the electric field as described earlier.

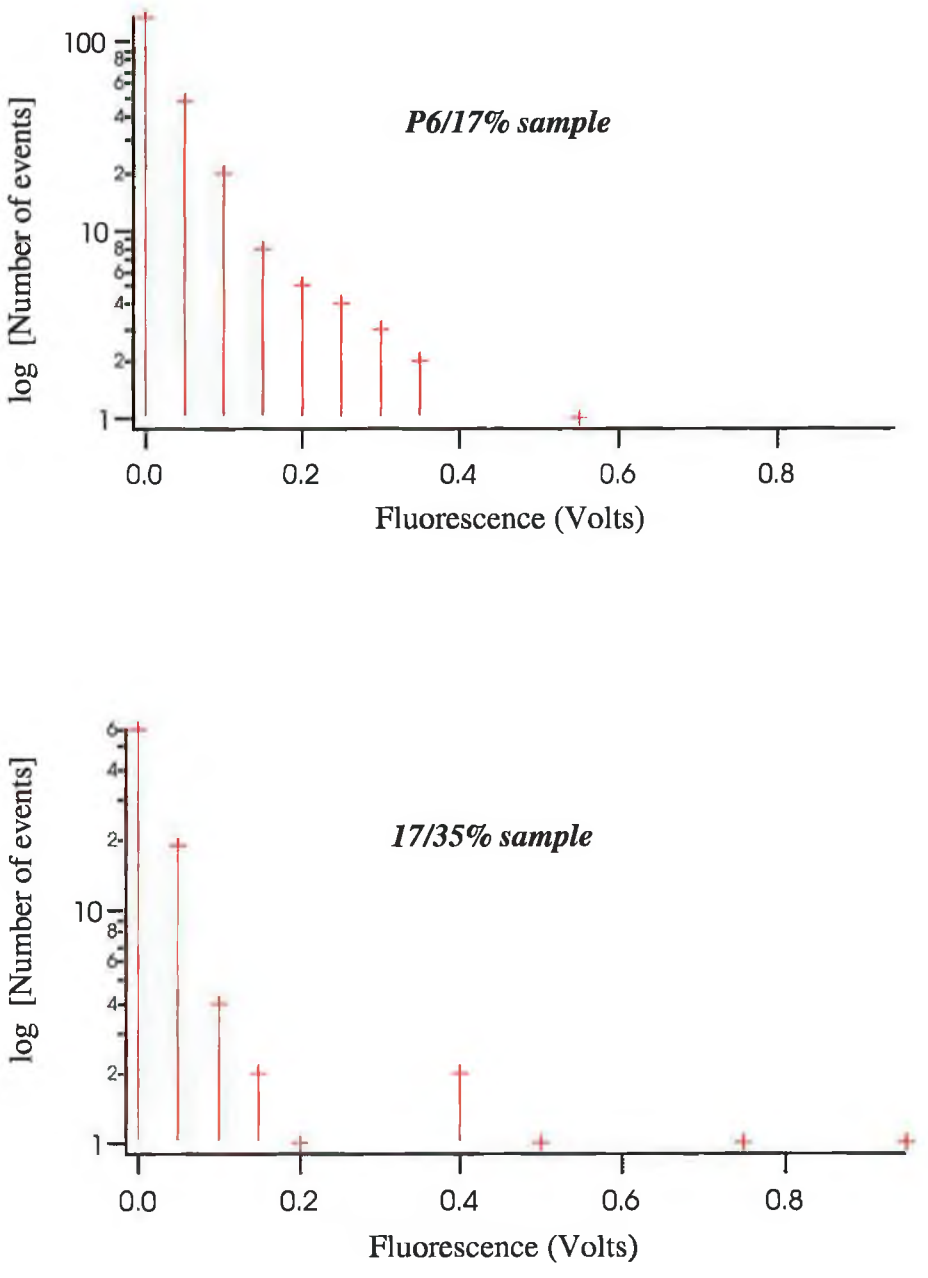

Figure 7.19 *Peak height histogram analysis of electropherograms obtained from analysis of samples taken from the both the P6/M17% interface and the M17/M35% interface. The different profiles of each fraction can be seen corresponding to the different size profiles of the mitochondria, with the P6/M17% sample containing many more mitochondria than the 17/35% sample.*

7.2.7 *Analysis of stability of prepared fractions*

With the preparation of isolated mitochondria from tissue culture cells there may be a problem following the homogenisation process whereby lysosomes, containing many proteases and other potentially harmful enzymes to isolated mitochondria, are also disrupted, releasing enzymes into the homogenate. To circumvent this ultracentrifugation was performed immediately following disruption of the cell. However, as there were no inhibitors added to the homogenate, fractions from the M17/M35% interface, stained with NAO, were analysed three times over a time period of eight hours while stored at room temperature, thus allowing for the possibility of any protease enzymes present in the sample to digest or damage the mitochondria. The effect of this would be no peaks or a reduced number in the electropherograms and a different mobility distribution for any peaks present. However, analysis of peak mobility showed similar trends in all samples (Figures 7.20 and 7.21). Peak numbers for analysis at 0, 4 and 8 hours were 90, 40 and 95, respectively, corresponding to histograms *(A)*, *(B)* and *(C)*.

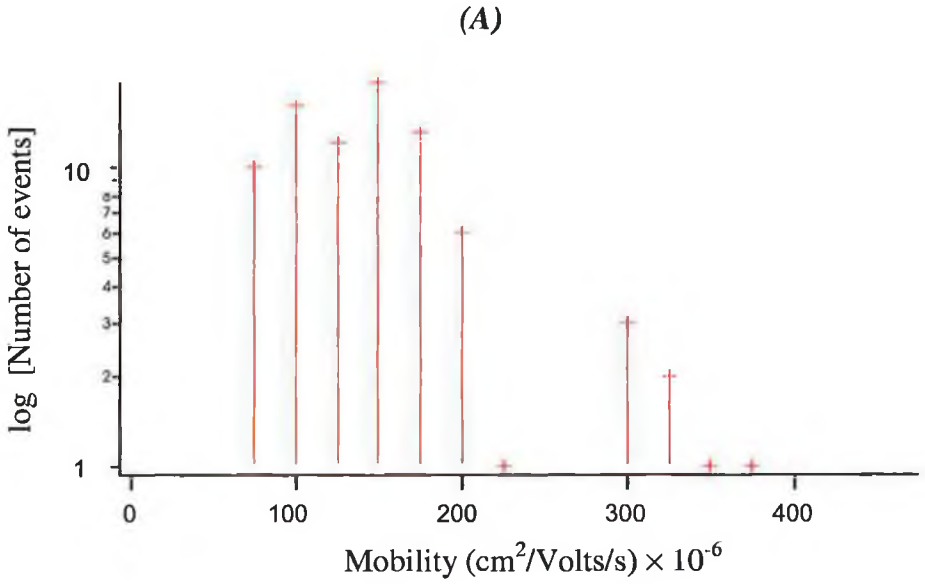

Figure 7.20 *Peak height histogram analysis of stability of mitochondrial fractions prepared by density gradient ultracentrifugation without protease inhibitors added.*

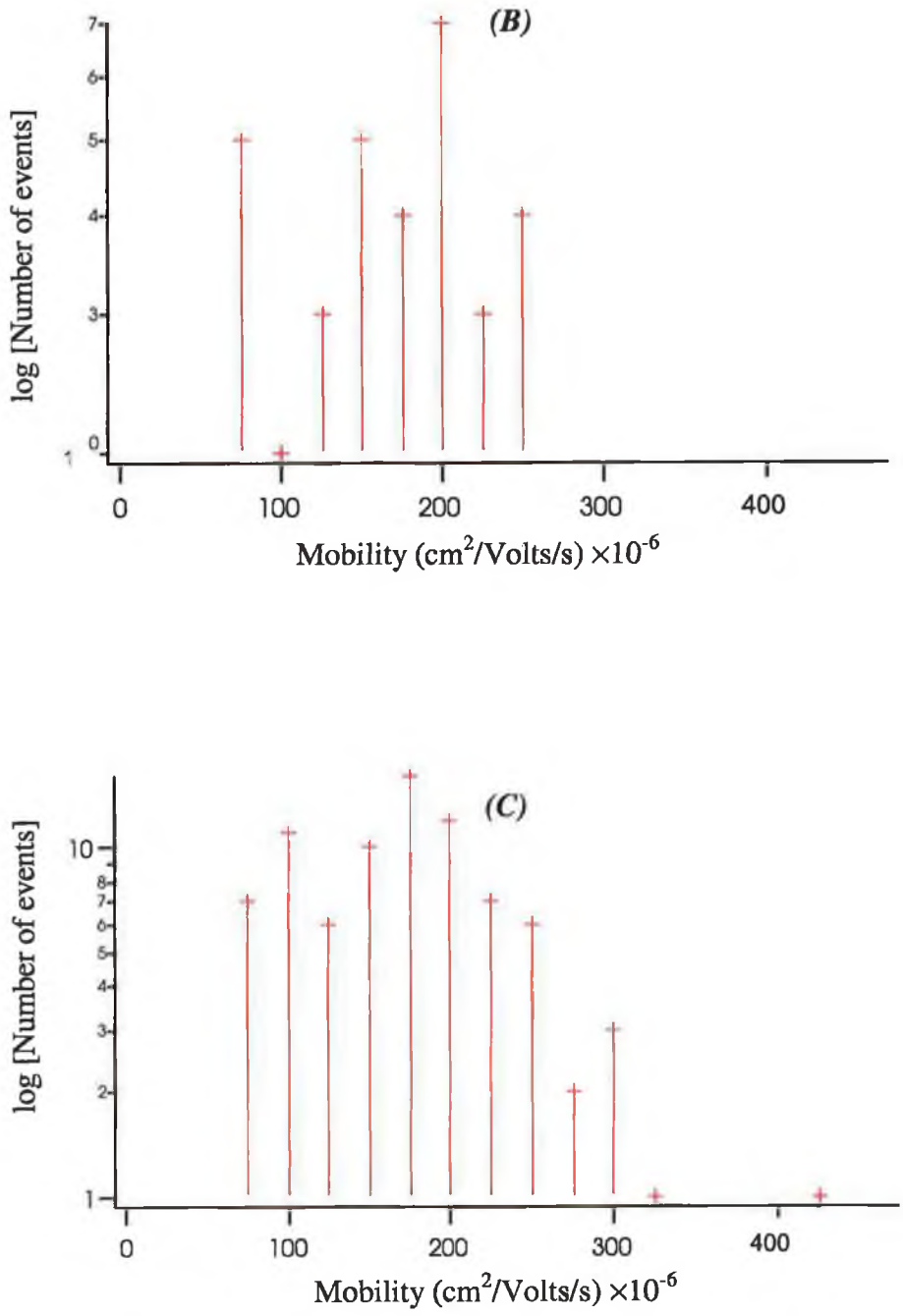

Figure 7.21 *Mobility histogram analysis of mitochondrial fractions prepared by density gradient ultracentrifugation without protease inhibitors added.*

A similar number of peaks (95) in the final electropherogram after 8 hours, compared to the first injection (90), supports the conclusion that the samples are stable and that the mitochondria are not being digested by enzymes released during homogenisation. The mobility histogram distributions are also similar further supporting the idea of intact mitochondria. It also suggests that the ultracentrifugation procedure of isolation for the mitochondria is separating them from potentially harmful enzymes released during cell disruption. This would agree with the theory as it is expected that during ultracentrifugation, the heavier and more dense mitochondria will move towards the bottom of the centrifuge tube, and away from free enzymes that may also be present in the post-nuclear supernatant. These enzymes will remain suspended at the top of the 6% percoll (v/v) medium, and, provided care is taken during removal of the fraction containing mitochondria, should not contaminate the sample.

The methods described so far demonstrate the use of CE in the analysis of whole mitochondria. As outlined in section 7.1.7, however, many disease states of the mitochondrion involve mutations in the genome, and hence in the expression of proteins. As discussed in the introduction (section 1.4.4), the new area of proteomics analyses the proteins expressed by the genome of an organism or cell, or as in the case presented here, the mitochondrial genome. Section 7.3 presents initial investigations into analysis of the mitochondrial proteome using capillary electrophoresis. Various strategies are examined, including the use of coated capillaries, and capillary gel electrophoresis.

7.3 Mitochondrial proteome analysis using capillary electrophoresis

For the analysis of the mitochondrial proteome by capillary electrophoresis, two approaches were investigated. The use of coated capillaries was initially examined, followed by capillary gel electrophoresis. In each case, two sets of fluorescently labelled protein molecular weight markers were analysed; one set labelled with FITC and the other labelled with 3,(2-furoyl) quinoline-2-carboxaldehyde, FQ.

7.3.1 Use of coated capillaries for protein analysis

Due to the problems associated with proteins adhering to the walls of capillaries, the use of coated capillaries for protein separations has become increasingly common (section 4.1.3.3). Here the use of coated capillaries (as used in section 7.2.3.1) was investigated for the separation of six different molecular weight markers (Table 7.2).

7.3.1.1 Analysis of molecular weight markers

FITC-labelled markers were purchased and diluted with water to give the desired concentration prior to analysis, while FQ labelling of markers was carried out as described in section 2.3.8.1. Figure 7.22 (FITC-labelled) and Figure 7.23 (FQ-labelled) show the electropherograms obtained for each set of labelled markers. The separation shows incomplete resolution of the individual proteins in both cases, although there are 5 partially visible peaks for the FITC-labelled markers, none are completely resolved from each other. The FQ-labelled markers showed less resolution, with only three clear peaks, and again, none completely resolved from each other. Investigating the effect of different electric fields (from 200 to 700Vcm^{-1}) and changes in the injection volume showed no improvements on the results. A possible explanation for incomplete resolution of the molecular weight markers can be found in the fact that capillary zone electrophoresis (as performed here) separates components based on mass to charge ratios, and not molecular weight. These markers are manufactured for polyacrylamide gel electrophoresis (SDS-PAGE), which separates based on molecular weight using a sieving matrix. However, due to the nature of the separation process

in CE, differences in the number of labels on the proteins can have a detrimental effect on the separation, producing broad bands for each protein, causing overlap to occur, and hence poor resolution, despite the use of a low concentration of SDS in the buffer. The fact that the FQ-labelled markers show less resolution would agree with this theory, as these were labelled 'in-house' with no control on the number of labels attaching to the different proteins. Its also possible for proteins of different molecular weight to have similar mass to charge ratios, thus having similar mobilities and hence two proteins may elute as a single peak, preventing identification.

Protein	Source	Molecular weight (Da)
Myosin	Rabbit muscle	205,000
β-Galactosidase	*E. coli*	116,000
Albumin	Bovine Serum	66,000
Alcohol Dehydrogenase	Horse Liver	39,000
Carbonic Anhydrase	Bovine Erythrocyte	29,000
Trypsin Inhibitor	Soybean	20,100

Table 7.2 *Protein molecular weight markers analysed by CE.*

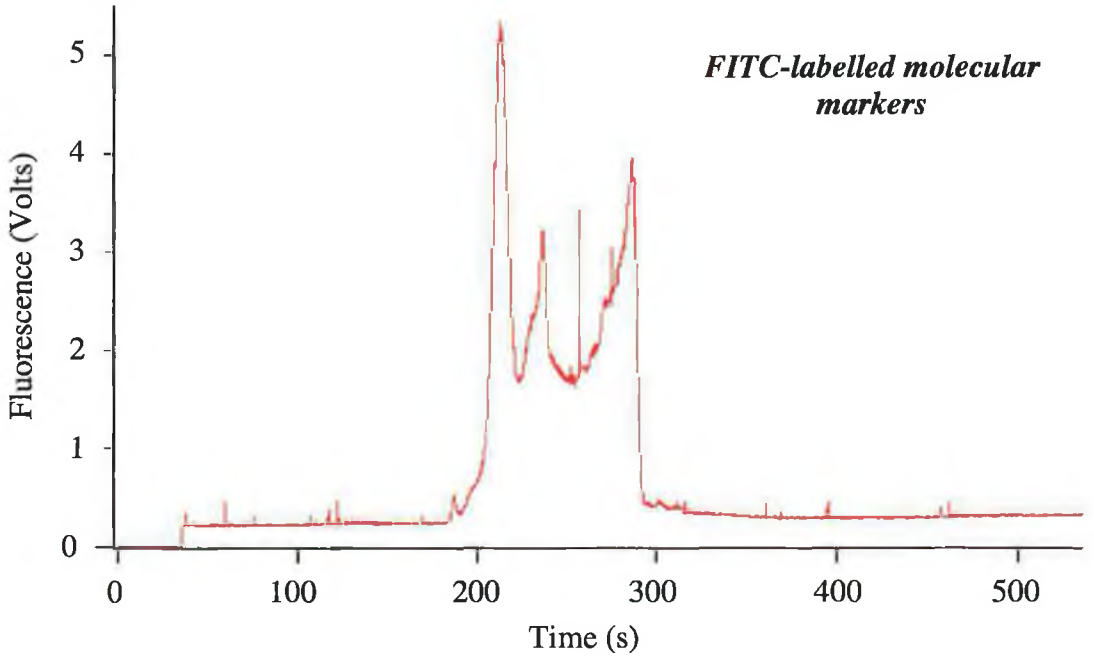

Figure 7.22 *Analysis of FITC-labelled molecular weight markers using coated capillaries. Conditions: AAP coated capillary; buffer: 2.5mM borate, 5mM SDS, pH 9.3; 5 s injection at 100Vcm^{-1}; separation at 200Vcm^{-1}. Excitation was at 488 nm with detection at 535nmDF35nm.*

The electropherogram obtained for the FQ-labelled molecular weight markers illustrates the overlap of the different proteins as they elute. Contained within the electropherogram are the six markers, but it is not possible to resolve them completely as discussed. Despite not achieving complete resolution for the molecular weight markers, it was decided to analyse a mitochondrial protein extract using the coated capillaries.

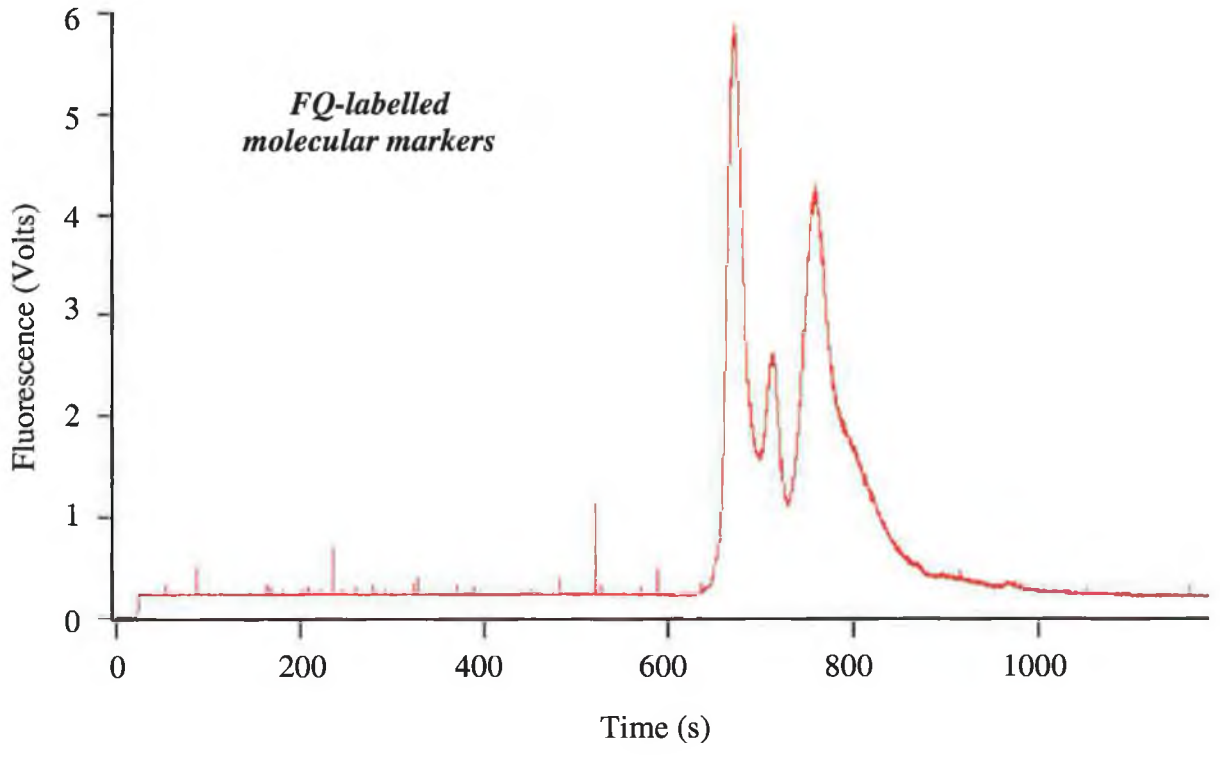

Figure 7.23 *Electropherogram showing separation achieved for FQ-labelled molecular weight markers using coated capillaries. Conditions: AAP coated capillary; buffer: 2.5mM borate, 5mM SDS, pH 9.3; 5 s injection at 100Vcm^{-1}; separation at 200Vcm^{-1}. Excitation was at 488 nm with detection at 635 nm DF35 nm.*

7.3.1.2 CE analysis of mitochondrial protein extract using coated capillaries

Protein was extracted from isolated mitochondria as outlined in section 2.3.8.3 and labelled with FQ according to the procedure detailed in section 2.3.8.1. The resulting sample was analysed by CE and the results are shown in Figure 7.24. While the peaks are resolved from

each other, there are very few, and are at a very low concentration (electropherogram expanded for clarity). The best resolution and peak shape was obtained with an applied electric field of 700Vcm^{-1}. Based on the observations with the molecular FITC- and FQ-labelled molecular weight markers, it is possible that the many proteins contained within the mitochondrial membrane are not resolving using the coated capillaries, accounting for the very few peaks.

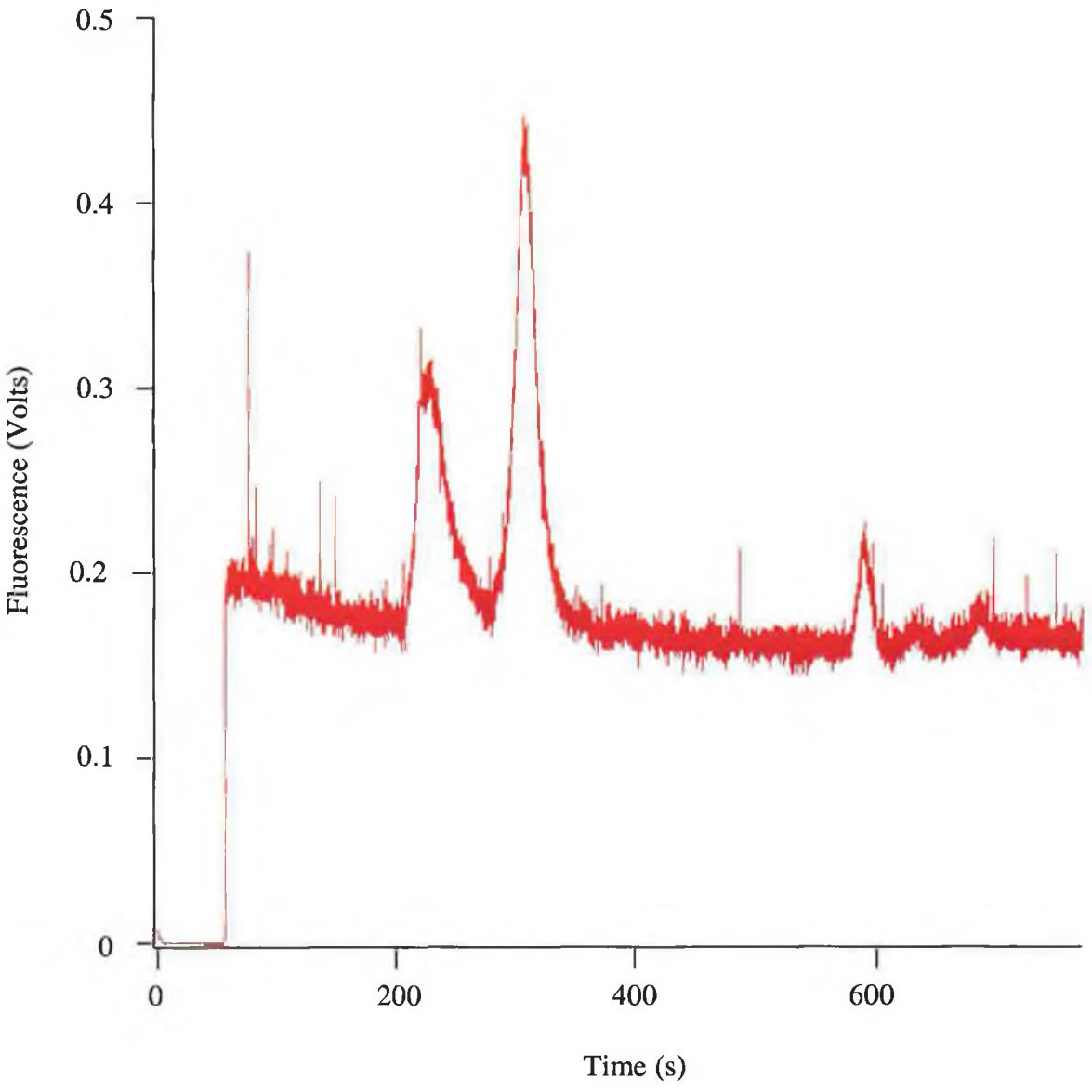

Figure 7.24 *Electropherogram obtained from the analysis of extracted FQ-labelled mitochondrial protein. Conditions: coated capillary; buffer: 2.5mM borate, 5mM SDS, pH 9.3; 30 s injection at 100Vcm^{-1}; separation at 700Vcm^{-1}. Excitation was at 488 nm with detection at 635 nm DF35 nm.*

7.3.2 Capillary gel electrophoresis

As outlined in section 4.1.4.2, capillary gel electrophoresis offers many advantages for analysis of proteins over traditional SDS-PAGE methods, including the application of high voltages resulting in faster analysis times coupled with the ability of quantitative as well as qualitative detection. Here the use of different molecular weight dextrans was investigated to allow the separation to be tailored to the molecular weight markers.

7.3.2.1 Analysis of molecular weight marker standards

A number of different weights of dextrans were tried, with a molecular weight of 185,000Da giving the best resolution for the markers (Figure 7.25), although the FQ labelled markers did not resolve as well as the FITC-labelled markers. Best results were achieved with electric fields of 400Vcm^{-1}. Analysis of FITC-labelled molecular weight markers showed more peaks than expected. A possible explanation for this may again be due to the fact that these markers are manufactured for SDS-PAGE work, and therefore may not be of very high purity. For SDS-PAGE this will not present a problem as only the larger peaks (numbered 1-6, Figure 7.25) would be detected. Its also possible that the smaller peaks observed in the electropherogram only appear with the greater resolving power of capillary gel electrophoresis (due to higher electric fields) which on a SDS-PAGE gel would appear combined with the peak closest, resulting in only six bands on the gel as expected.

In the electropherogram for the FQ-labelled markers, slightly less resolution is observed, again, this could be due to the fact that labelling was carried out 'in-house' with no controls over the labelling process. On the smaller molecular weight proteins, a large number of labels could significantly change the overall molecular weight, possibly affecting the migration time and, in conjunction with different numbers of labels, produce a spread on the peak, similar to that observed for analysis using coated capillaries.

Analysis of individual molecular weight markers would help in optimising the separation at this point, and would provide information on the ability of the gel to separate smaller molecular weight proteins. Table 7.3 shows the individual molecular weight markers, labelled with FQ, which were analysed by capillary gel electrophoresis.

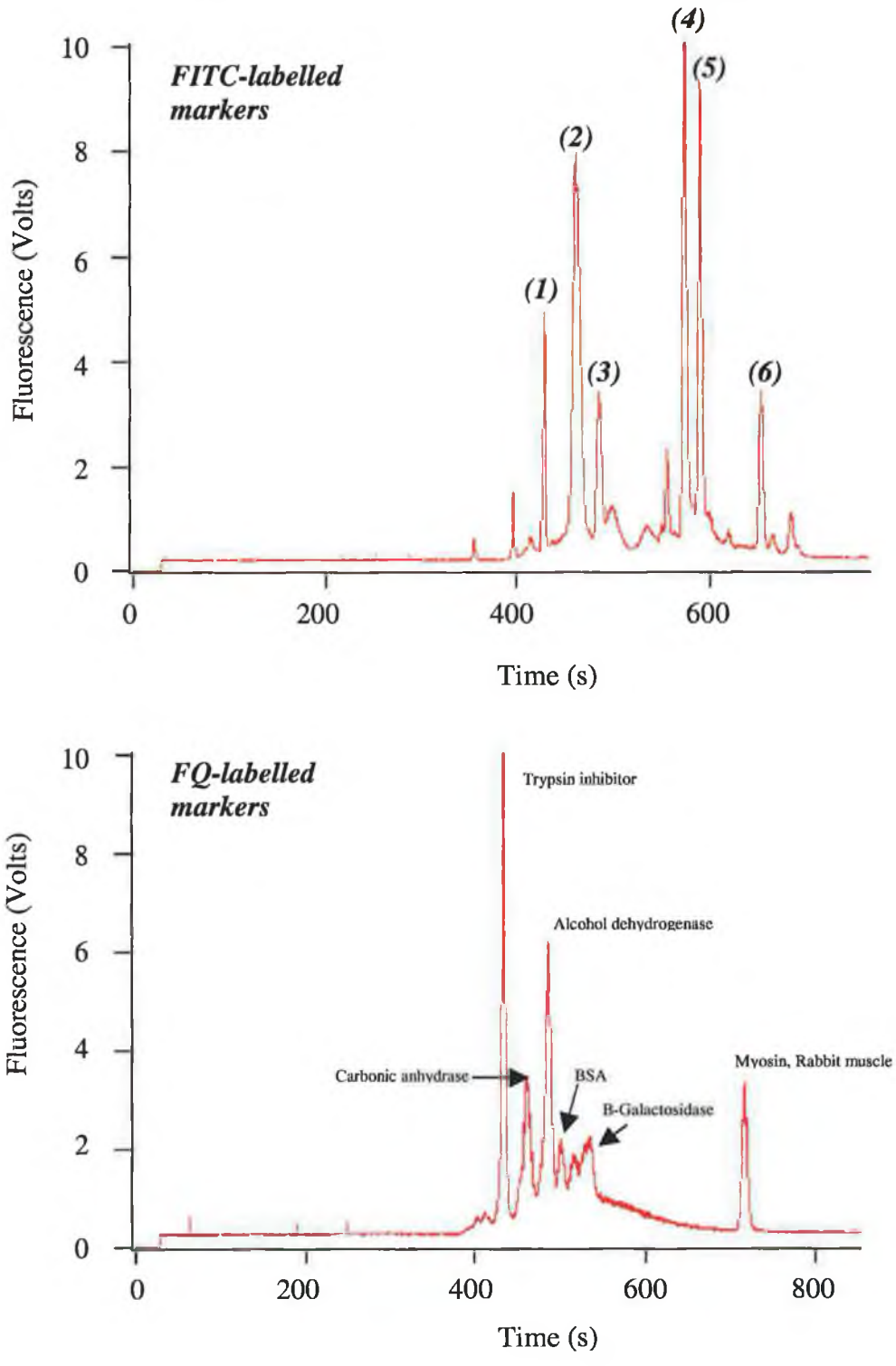

Figure 7.25 *Separation of FITC- (top) and FQ-labelled (bottom) molecular weight markers by capillary gel electrophoresis. Conditions: 5% dextran, 6.7mM SDS, 10mM HEPES, pH 7.5, sheath flow buffer: 10mM HEPES, 6.7mM SDS, pH 7.50. Sample denatured for 5 min at 95^{0}C prior to analysis. Excitation was at 488 nm with detection at 635 nm DF35 nm (FQ-labelled markers), and 535 nm DF 35 nm (FITC-labelled markers).*

Molecular weights for these individual markers ranged from 66,000 for albumin, bovine serum, to 14,200 for α-Lactalbumin, bovine milk. Results are shown in Figure 7.26. While it is expected that the high molecular weight dextran (185,000) will not provide optimum separation for the smaller molecular weight proteins, exactly what separation would be achieved was investigated.

Protein	Source	Molecular Weight (Da)
Albumin,	Bovine Serum	66,000
Ovalbumin	Egg	45,000
Glyceraldehyde-3-Phosphate Dehydrogenase	Rabbit Muscle	36,000
Carbonic Anhydrase	Bovine Erythrocytes	29,000
Trypsinogen	Bovine Pancreas	24,000
Trypsin Inhibitor	Soybean	20,100
α-Lactalbumin	Bovine milk	14,200

Table 7.3 *Individual molecular weight markers FQ labelled and analysed separately*

Analysis of the individual molecular weight markers showed inconsistencies in the migration times of the proteins according to their molecular weight. The most probable cause of this is the sieving gel used was not optimised for proteins in the smaller molecular weight range (14-66kDa). As the separation gel was optimised for the higher molecular weight proteins shown in Table 7.2, this is as expected. A trial run with an extract of mitochondrial protein would be required to first determine the molecular weight range of the proteins before the correct molecular weight sieving matrix could be determined. This was carried out with an extract of protein from isolated mitochondria prepared as before. The result is shown in Figure 7.27.

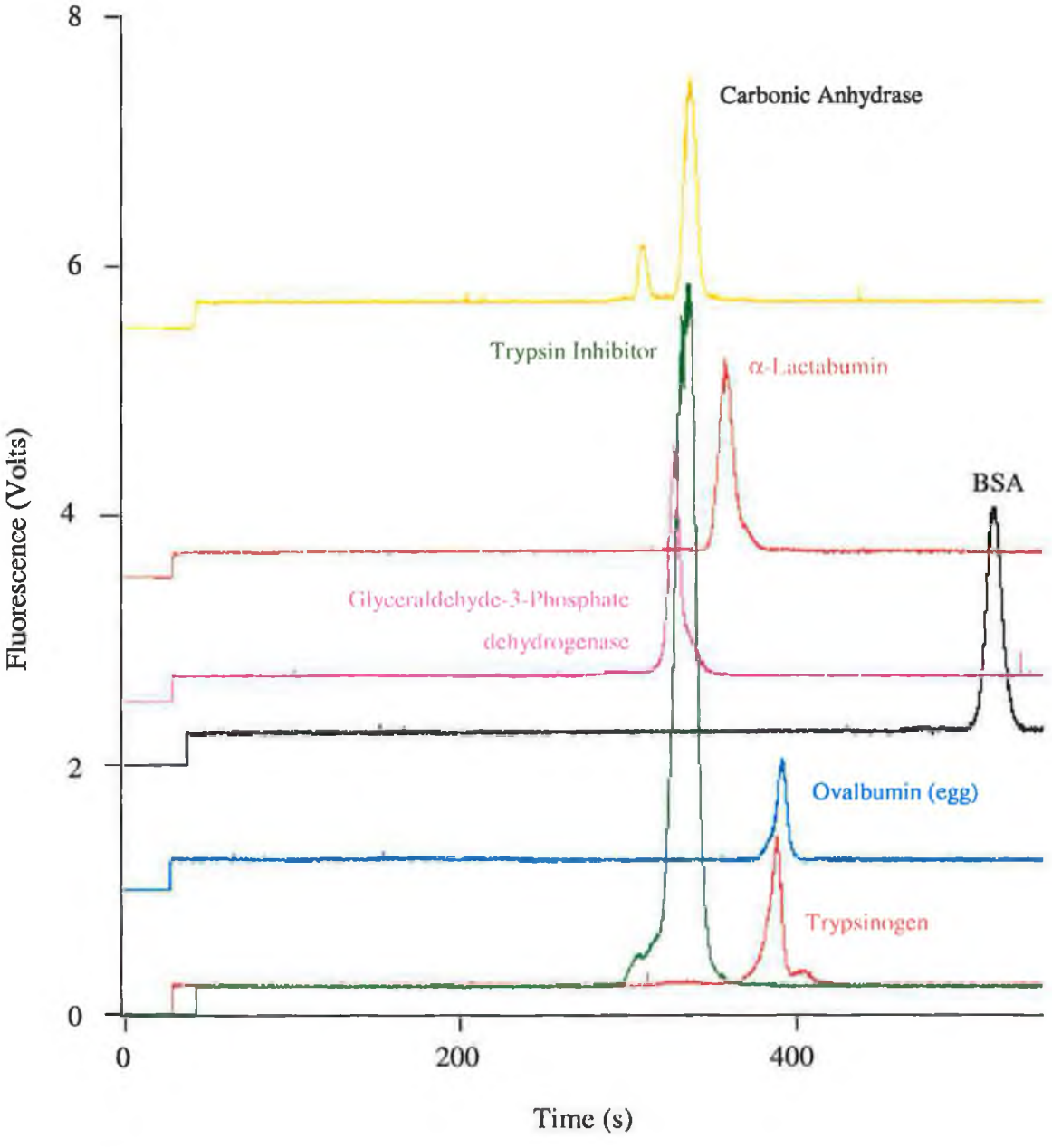

Figure 7.26 *Capillary gel electrophoresis of individually FQ-labelled protein molecular weight markers. Conditions: capillary filled with 5% dextran (MW 185,000), 6.7mM SDS, 10mM HEPES, pH 7.50; sheath flow buffer: 10mM HEPES, 6.7mM SDS, pH 7.50; 10 s injection at 50Vcm^{-1}, separation at 400Vcm^{-1}. Sample denatured for 5 min at 95^{0}C prior to analysis. Excitation was at 488 nm with detection at 635 nm DF35 nm.*

7.3.2.2 Capillary gel electrophoresis of mitochondrial protein extract

Mitochondrial protein was extracted and labelled with FQ as before. Analysis by gel electrophoresis revealed that while peaks corresponding to mitochondrial protein can be seen, resolution was very poor (Figure 7.27). Analysis of relative migration times for both individual and the mixture of molecular weight markers reveal inconsistencies between the migration times and relative molecular weights.

While separation in CGE is primarily based on molecular weight, it is expected that a difference in the number of labels would not have a significant effect on the peak shape and migration time for the larger molecular weight proteins (due to the molecular weight of the label being so small relative to that of the protein), however, this may not be the case for the smaller molecular weight proteins as discussed. From comparison of relative migration times from the electropherogram obtained for the mitochondrial protein extract, with those from the individually labelled molecular weight markers, (Figure 7.26), it indicates that the molecular weights of the proteins present are mostly below 36,000 Da. This would allow for heterogeneity in the labelling of the smaller molecular weight proteins to affect the resolution. The results obtained indicate that a higher molecular weight sieving matrix may give better resolution. These investigations are being carried out.

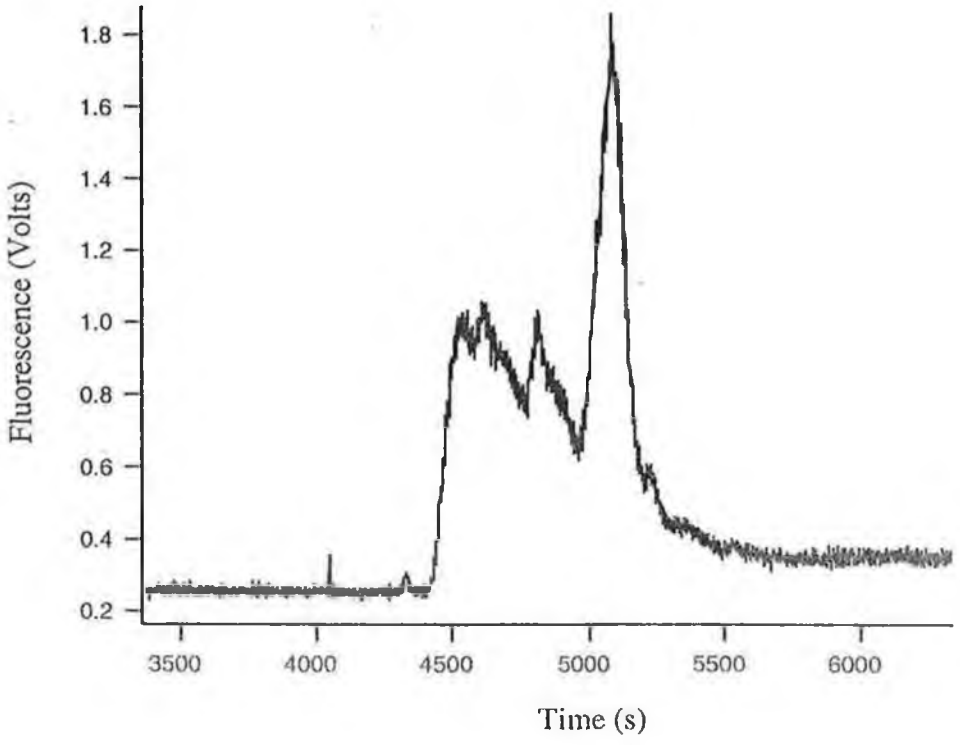

Figure 7.27 *Capillary gel electrophoresis of FQ-labelled mitochondrial protein extract. Conditions: Capillary filled with 5% dextran, (MW 185,000), 6.7mM SDS, 10mM HEPES, pH 7.50. Sheath flow buffer; 10mM HEPES, 6.7mM SDS, pH 7.50; 30 s injection at 50Vcm^{-1}; separation at 400Vcm^{-1}. Sample denatured for 5 min at 95^{0}C prior to analysis. . Excitation was at 488 nm with detection at 635 nm DF35 nm.*

7.4 Discussion

Chapter 6 illustrated the capillary electrophoresis system employed to be an ideal system for analysis of subcellular particles with the analysis of both polystyrene beads and liposomes filled with a fluorescent dye. This chapter examined the application of this method to the analysis of mitochondria following isolation from Chinese hamster ovary cells. Mitochondria play an important role in the the cell providing the energy necessary for life and as discussed in section 7.1.7, also play a critical role in health. There are various methods today used for analysis of the mitochondrion and other organelles (section 1.4.2), but the use of capillary electrophoresis has only recently being applied to this area. A review on the methods and their relative success is given by Radko and Chrambach, (1999). They reported the use of CE for analysis of lipoprotein particles, classified as high (HDL, 7-13 nm diameter), intermediate (IDL, 25-35 nm in diameter), low (LDL, 18-25 nm diameter) and very low (VLDL, 30-80 nm) density lipoproteins using cITP, with the particles separation into 14 well defined zones. However similar to the liposomes analysed by CE (Roberts *et al.,* 1996) (discussed in the same review and chapter 6), there is no information on single particles.

To the date of publication, (February 1999) the authors reported that the sole subcellular particles of some biological relevance analysed by CE were rat liver microsomes, the membrane vesicles formed from isolated rough endoplasmic reticulum in aqueous solutions, with a mean diameter of 150 nm. However, the microsomes, isolated by a similar technique to that used here (density gradient centrifugation) exhibited a broad but single peak in CZE using 150 μm diameter fused silica capillaries internally coated with linear polyacrylamide, similar to that reported by Roberts *et al.* for the liposomes. The results reported here represent the first successful demonstration of the use of capillary electrophoresis for analysis of individual mitochondria. Similar to the results reported in chapter 6 for liposomes, the mitochondrion is visualised as a single peak. Results with the use of NAO demonstrate the applicability of using this as a means of accurately measuring the size of mitochondria, while initial results presented with Rhodamine 123 demonstrate that the method can be used to measure the activity of a single mitochondrion.

The design of the instruments allows for detection of more than one fluorescent probe at the same time. This allows the exciting possibility of measuring both the mass and activity of a single mitochondrion in a single measurement. This would be done with the use of the dye JC-1, as its uptake is dependent on the membrane potential, in conjunction with NAO. As JC-

1 emits fluorescence at a higher wavelength (590 nm) on the formation of red aggregates, due to high mitochondrial membrane potential, collection of emitted fluorescence from both dyes (by use of a dichromatic beam splitter to separate the emissions) would allow mass/activity ratios to be measured for individual mitochondria.

The initial results presented on the analysis of the mitochondrial proteome demonstrate the use of the chromatographic method of CE for an almost entire analysis of a single organelle from a cell. The area of proteomics is rapidly expanding today (section 1.4.4) with projects like the human genome continuing to rely on analysis of both structure and function of genes and gene products (proteins), with detection of changes between normal and diseased states being of paramount importance. In 1990 the US National Cancer Institute (NCI) launched a separate programme to screen more than 60,000 compounds against a panel of 60 human cancer cell lines for determination of potential target molecules and modulators for activity (Patton, 1999). As the mitochondrion is known to be involved in several diseases (section 7.1.7), analysis of the proteome will also provide important information regarding the expression of proteins during the different stages in the life cycle. In conjunction with the methods for analysis of the mitochondrial mass and activity, correlation's can be made between results obtained from these measurements and the type and numbers of proteins expressed by the mitochondrial genome at a given time.

8 CONCLUSIONS

The purpose of this research was to examine chromatographic methods of analysis and their use in biotechnology, concentrating on HPLC and CE. The work focused on the analysis of coumarin metabolism, development of micro-chip based CE immunoassays for a coumarin derivative, warfarin, and an insecticide, parathion, and the use CE in the analysis of subcellular particles. For analysis of subcellular particles liposomes were chosen as the model for the development of the method, and having successfully achieved this, analysis of mitochondria was carried out using a very sensitive unique post-column LIF detection arrangement.

HPLC was used to examine the metabolism of the major human phase I metabolite of coumarin, 7-hydroxycoumarin, in rabbit tissues. The purpose of the examination was to gain more information regarding the metabolic pathways present in rabbit for the phase I metabolite of coumarin. The method was based on a previous HPLC method by Killard *et al.* (1996) with significant improvements made in terms of total run time. This was achieved by altering the gradient elution profile to achieve reductions in the retention time for all components (up to 8 minutes in the case of the internal standard, 4-hydroxycoumarin). The presence of the UDPGT enzyme system responsible for the glucuronidation of 7-hydroxycoumarin and the rate of metabolism for 7-hydroxycoumarin for each of these tissues was determined.

Following on from these conclusions with HPLC, another study using capillary electrophoresis was carried out on rabbit tissue samples. CE with UV detection examined in greater detail the metabolism of 7-hydroxycoumarin, with a study on the breakdown of 7-hydroxycoumarin glucuronide by the enzyme β-glucuronidase. The results of this study provides information on the various organs where glucuronidation occurs in the rabbit, the rates at which it does so, and also details the organs in which breakdown of the glucuronide occurs along with the various rates. From this combined information it is possible to predict where futile cycling (section 1.2.4.3) of the glucuronide may occur.

CE was also applied to analysis of another 7-hydroxycoumarin conjugate, 7-hydroxycoumarin sulphate, via the sulphation pathway. The study examined mouse liver for production of both the glucuronide and the sulphate conjugates. The methodology applied was identical to that used for the glucuronide conjugation and de-conjugation studies of various rabbit tissues, and demonstrated excellent inter- and intra-assay coefficients of

variation for the detection of all three components (7-hydroxycoumarin, 7-hydroxycoumarin sulphate, 7-hydroxycoumarin glucuronide)

Microchip capillary electrophoresis was used to investigate novel approaches towards CE-based immunoassays. After detailed investigations, the use of a labelled drug-protein conjugate and unlabelled antibody for both parathion and warfarin proved the most promising. However, problems arising from the heterogeneity of reagents used in the assays having a detrimental effect on the resolution of both the free drug-protein conjugate and antibody/drug-protein complex, did not allow any accurate quantitation measurements to be made. These observations are in agreement with those reported in the literature (Schmalzing and Nashabeh, 1997) where the use of a polyclonal antibody in an assay for cortisol provided an antibody/antigen complex too broad for quantitation. The authors investigated the differences between using Fab fragments, monoclonal or polyclonal antibodies, with the Fab fragment providing the best resolution and peak shape for the antibody/antigen complex. From the results shown, it is concluded that the use of a drug labelled at a single location would provide the ideal solution in this case. However, as this is not possible for all drugs, a homogenous labelled drug protein conjugate in conjunction with a monoclonal antibody or a Fab fragment prepared from a papain digest of whole monoclonal antibody may also provide enough resolution for quantitation.

In the application of CE to the analysis of subcellular particles, the results obtained for analysis of liposomes as a basis for organelle analysis, demonstrate very well a new level of information available for the first time using CE. The unique design of the CE instrument allowed for detection of single events corresponding to individual liposomes. Never before has this level of detail on an individual liposome basis being reported for CE. While the method sets out to define the parameters for analysis of cellular organelles, it has demonstrated its use as an excellent method for the complete characterisation of liposomes which may be manufactured for use in the medical industry. The method demonstrates detection of single events corresponding to individual mitochondria when applied to the analysis of mitochondria, following purification from Chinese hamster ovary cells. This also represents the first reported analysis of mitochondria by CE. The ability to stain mitochondria with various dyes (NAO, Rh123 and JC-1) will allow measurements on mass and activity of individual mitochondria to be made using this method.

Mitochondrial proteome analysis on solvent extracted mitochondrial protein by capillary gel electrophoresis with the same instrument showed initial results, with proteins in the molecular weight range around 35,000Da confirmed to be present in the mitochondrial membrane. The results however, illustrated that the gel needed to be optimised towards the smaller molecular weight proteins, and not the larger (66,000 – 205,000 Da) molecular weights as was the case here, before any meaningful conclusions can be made. Unfortunately, as the research visit to the University of Minnesota was at an end, there was no time to complete this work.

In summary, capillary electrophoresis along with HPLC, has shown themselves to be extremely versatile tools for analysis in analytical biotechnology, with the above examples of drug molecules, cells and subcellular particles representing two extremes of size experienced by the analytical scientist. The work required an intimate understanding of the theory of chromatography and the problems and obstacles encountered when working with both small molecules and large particles. In addition, the work has made a significant contribution to the understanding of phase II metabolism of coumarin and provided results on a new level of detail and precision for analysis of both liposomes and mitochondria using CE, thus allowing for analysis of all organelles by capillary electrophoresis.

9 REFERENCES

Afzelius, B. A., (1957) Electron Microscopy of Sea Urchin Eggs. *Slmqvist and Wiksell, Upsalla, Sweden.*

Alberts, B., Bray, D., Lewis, J., Raff, M., Roberts, K. and Watson, J. D., (1989) Intracellular sorting and the maintenance of cellular compartments, In "Molecular Biology of the Cell (2nd edition), Garland Publishing Inc., New York, USA, *pp 405-479.*

Atamna, I. Z., Issaq, H. J., Muschik, M. and Janini, G. M., (1991) Optimisation of resolution in CZE: combined effect of applied voltage and buffer concentration. *J. Chromatogr., 588: 315.*

Bangham, A. D., (1981) In: "Liposomes: from physical structure to therapeutic applications", Knight, C. G., (Ed), Elsevier, Amsterdam, New York.

Bangham, A. D., Standish, M. M. and Watkins, J. C., (1965) Diffusion of univalent ions across the lamellae of swollen phospholipids. *J. Mol. Biol., 13: 238-241.*

van den Berg, A. and Lammerick, T. S. J., (1998) Micro Total Analysis Systems: Microfluidic aspects, Integration Concept and Applications, In "Microsystem Technology in Chemistry and Lifesciences", Manz, A., Becker, H., (Eds), Springer-Verlag, New York, Heidelberg, Berlin. *pp. 21-49.*

van der Bery, A. and Gerveld, P., (1995) Micro Total Analysis Systems, Kluwer Academic Publishers, Dordrecht, Netherlands.

Biblingmeyer, B. A., (1992) Overview of modern liquid chromatography, In "Practical HPLC: Methodology and Applications", John Wiley and Sons, New York, USA. *pp. 1-27.*

Bogan, D. P., Keating, G. J., Reinartz, H., Duffy, C. F., Smyth, M. R. and O'Kennedy, R., (1997) Analysis of coumarins, In "Coumarins - Biology, Applications and Mode of Action". O'Kennedy, R and Thornes R.D. (Eds), John Wiley and Sons Ltd., Chichester, England, *pp 267-302.*

Bogan, D.P. and O'Kennedy R., (1996) The simultaneous determination of coumarin, 7-hydroxycoumarin and 7-hydroxycoumarin-glucuronide in human plasma and serum by high-performance liquid chromatography. *J. Chromatogr., **686**: 267-273.*

Bogan, D. P., Thornes, R. D., Teigtmeier, M., Schafer, E. A. and O'Kennedy, R., (1996a) The direct determination of 7-hydroxycoumarin and 7-hydroxycoumarin glucuronide in urine by capillary electrophoresis. *Analyst, **121**: 243-247.*

Bogan, D. P., Deasy B. and Smyth M. R., (1996b) Interspecies differences in coumarin metabolism in liver microsomes examined by capillary electrophoresis. *Xenobiotica, **26 (4)**: 437-445.*

Bogan, D.P., Killard A. J., and O'Kennedy R., (1995) The use of capillary electrophoresis for studying the *in vitro* glucuronidation of 7-hydroxycoumarin. *J. Cap. Elec. **2(5)**: 241-245.*

Bogan, B. P., Deasy B., O'Kennedy R., Smyth M. R. and Fuhr U., (1995a) Determination of free and total 7-hydroxycoumarin in urine and serum by capillary electrophoresis. *J. Chromatogr. B, Biomed. Appl., **663**: 371-378.*

Braithwait, A. and Smith, F. J., (1985) High Performance Liquid Chromatography, In "Chromatographic Methods", Chapman and Hall, London and New York, *pp. 212-290.*

Bratten, C. D. T., Cobbold, P. H. and Cooper, J. M., (1997) Micromachining sensors for electrochemical measurement in subnanolitre volumes. *Anal. Chem., **69**: 253-258.*

Briceno, G., Change H. Y., Sun X. D., Schulz P. G. and Xiang X. D., (1995) A class of cobalt oxide magnetoresistance materials discovered with combinatiorial synthesis. *Science, **270**: 273-274.*

Brishammar, S., Hjerten, S., and Hofsten, B. V., (1961) Immunological precipitation in agarose gels. *Biophys. Acta, **53:** 518-523.*

Brown, J. A., Novak, E. K., Takeuchi, K., Moore, K., Medda, S. and Swank, R. T., (1987) Lumenal location of the microsomal β-glucuronidase-egasyn complex. *J. Cell Biol. **105**: 1571-1578.*

Brown, P. R., (1989) In "High Performance Liquid Chromatography", Brown, P. R. and Hartwick, R. A., (Eds), John Wiley and Sons, New York, *pp. vii-ix.*

Bushey, M. M., and Jorgenson, J. W., (1989) Capillary electrophoresis of proteins in buffers containing high concentrations of zwitterionic salts. *J. Chromatogr., **480**: 301-310.*

Campos, C. C. and Simpson, C. F., (1992) Capillary electrophoresis, *J. Chromatogr. Sci., **30:** 53-58.*

Carchon, H. and Eggermont, E., (1992) Capillary electrophoresis. *American Laboratory, January, 67-72.*

Carchon, H. and Eggermont, E., (1989) Automation and data management in isotachophoresis. *Anal. Chim. Acta, **219**: 247 – 256.*

Casley-Smith, J. R. and Casley-Smith J. R., (1986) High Protein Odemas and the benzo-pyranones, JB Lippencott Company, Sydney, Australia.

Carrazon, J. M. P., Vergara, A. G., Garcia, A. J. R. and Diez, L. M. P., (1989) Determination of coumarins by voltammetric techniques in micellar and emulsified media. *Anal. Chim. Acta, **216**: 231-242.*

Clarke, D. J. and Burchell, B., (1994) The uridine diphosphate glucuronosyltransferase multigene family: function and regulation, In "Conjugation-Deconjugation Reactions in Drug Metabolism and Toxicity", Kauffman F. C, (Ed.), Springer-Verlag, New York. *pp 3-29.*

Chapman, D., (1984) Physiochemical properties of phospholipids and lipid-water systems, In: "Liposome technology, Volume I: Preparation of liposomes", CRC Press Inc., Boca Raton, Florida, USA. *pp. 1-18.*

Chiari, M., Nesi, M. and Righetti, P. G., (1996) Surface modification of silica walls: A review of different methodologies, In "Capillary electrophoresis in Analytical Biotechnology", Righetti, P. G. (Ed), CRC Press, New York, USA. *pp. 1-36.*

Chiem, N. and Harrison, D. J., (1997) Microchip-based capillary electrophoresis for immunoassays: Analysis of monoclonal antibodies and theophylline. *Anal. Chem., **69**: 373-378.*

Cholerton, S.C., Idle, M.E., Vas, A., Gonzalez, F. J. and Idle, J. R., (1992) Comparison of a novel thin-layer chromatographic-fluorescence detection method with a spectrofluorimetric method for the determination of 7-hydroxycoumarin in human urine. *J. Chromatogr., **575**: 325-330.*

Cole, R. O., Hiller, D. L., Chwojdak, C. A. and Sepaniak, M. J. (1996) Evaluation of extended light path capillaries for use in capillary electrophoresis with laser-induced fluorescence detection. *J. Chromatogr. A, **736**: 239-245.*

Consden, R., Gordon, A. H., and Martin, A. J. P., (1944) Qualitative analysis of proteins: Partition chromatographic method using paper. *Biochem. J., 38: 224-232.*

Cooper, G. M., (1996) Bioenergetics and Metabolism, In "The Cell: A Molecular Approach", Sinuaer Associates, Sunderland, England. *pp. 389-421.*

Cossarizza, A., Ceccarelli, D. and Masini, A., (1996) Functional heterogeneity of an isolated mitochondrial population revealed by cytofluorometric analysis at the single organelle level. *Exp. Cell Research, **222 (1)**: 84-94.*

Dale, G. and Latner, A. L., (1969) Isoelectric focusing of proteins in acrylamide gels followed by electrophoresis. *Clin. Chem. Acta, **24**: 61-67.*

Davis, B., (1964) Disc electrophoresis II – Method and application to human serum proteins. *Ann. N. Y. Acad. Sci., **121**: 404.*

Deamer, D. and Bangham, A. D., (1976) Large volume liposomes by an ether vapourisation method. *Biochim. Biophys. Acta, **443**: 629-632.*

Deasy, B., Bogan, D. P., Smyth, M. R., O'Kennedy, R. and Fuhr, U., (1995) Study of coumarin metabolism by human liver microsomes using capillary electrophoresis. *Anal. Chim. Acta., **310**: 101-107.*

De Kanter, R., Olinga ,P., De Jager, M. H., Merema, M. T., Meijer, D. K. F. and Groothius, G. M. M., (1999) Organ slices as an *in vitro* test system for drug metabolism for human liver, lung and kidney. *Toxicology in Vitro, **13 (4-5)**: 737-744.*

Dempsey, E., O'Sullivan, C., Smyth, M.R., Egan, D., O'Kennedy, R. and Wang, J., (1993) Differential pulse voltammetric determination of 7-hydroxycoumarin in human urine. *J. Pharm. & Biomed. Anal., **11(6)**: 443-446.*

DeVries, M. H., Groothius, G. M. M., Mulder G. J., Nquyen, H. and Meijer, D. K. F., (1986) Secretion of the organic anion harmol sulphate from liver into blood. *Biochem. Pharmacol., **34**: 2129-2135.*

Dussossoy, D., Carayon, P., Belugou, S., Feraut, D., Bord, A., Goubet, C., Roque, C., Vidal, H., Combes, T., Loison, G. and Casellas, P., (1999) Co-localisation of sterol isomerase and sigma$_1$ receptor at endoplasmic reticulum and nuclear envelope level. *Eur. J. Biochem., **263 (2)**: 377-385.*

Dutton, J. G., (1991) Glucuronidation of Drugs and Other Compounds, CRC Press, Pocock House, 235 Southwark Bridge Rd., London, SE1 6LY, UK.

Effenhauser, C. S., (1998) Integrated Chip-Based Microcolumn Separation systems, In "Microsystem Technology in Chemistry and Life Sciences", Manz, A. and Becker, H. (Eds), Springer-Verlag, New York, *pp. 52-81.*

Effenhauser, C. S., Paulus A., Manz A. and Widmer H. M., (1994) High speed separation of antisense oligonucleotides on a micromachined capillary electrophoresis device. *Anal. Chem., **66**: 2949-2953*

Effenhauser, C. S., Manz, A. and Widmer, H. M., (1993) Glass chips for high speed capillary electrophoresis: Separation with submicrometer plate heights. *Anal. Chem., **65**: 2637-2642.*

Egan, D. and O'Kennedy, R., (1992) Rapid and sensitive determination of coumarin and 7-hydroxycoumarin and its glucuronide conjugate in urine and plasma by high performance liquid chromatography. *J. Chromatogr. B,Biomed. Appl., **582**: 137-143.*

Egan, E., O'Kennedy, R., Moran, E., Cox, D., Prosser, E. and Thornes, R. D., (1990) The pharmacology, metabolism, analysis and applications of coumarin and coumarin related compounds. *Drug Metab. Rev., **22 (5)**: 503-529.*

Ehrengerg, B., Montana, V., Wei, M. –D., Wuskel, J. P. and Loew, L. M., (1988) Membrane potential can be determined in individual cells from the Nernstein distribution of cationic dyes. *Biophys. J., **53**: 785-794.*

Evangelista, R. A. and Chen, F. T., (1994) Analysis of structural specificity in antigen antibody reactions by capillary electrophoresis with laser induced fluorescent detection. *J. Chromatogr. A, **680**: 587-593.*

Evans, R. R. and Relling, M. V., (1992) Automated high-performance liquid chromatographic assay for the determination of 7-ethoxycoumarin and umbelliferone. *J. Chromatogr., **578**: 141-145.*

Fodor, S. P. A., Read, J. L., Pirrung, M. C., Stryer, L., Lu A. T. and Solas, D., (1991) Light directed, spatially addressable parallel chemical synthesis. *Science, **251**: 767-773.*

Foffani, A., (1953) Polarographic kinetic studies on coumarins. *Atti Accad. Nazl. Lincei, Rend., **14**: 418-423.*

Gamache, P., Ryan, E. and Acworth, I. N., (1993) Analysis of phenolic and flavanoid compounds in juice beverages using high-performance liquid chromatography with coulometric array detection. *J. Chromatogr., **635**: 143-150.*

Godovac-Zimmermann, J., Soskic V., Poznanovic S. and Brianza F., (1999) Functional proteomics of signal transduction by membrane receptors. *Electrophoresis, **20 (4-5)**: 952-961.*

Goffeau, A., (1997) Molecular fish on chips. *Nature, **385**: 202-203.*

Graeber, M. B., Grasbon-Frodl E., Abell-Alef P. and Kosel S., (1999) Nigral neurons are likely to die of a mechanism other than classical apoptosis in Parkinson's disease. *Parkinsonism and Rel. Dis., **5**: 187-192.*

Grigg, G. W., (1977) Genetic effects of coumarins. *Mutat. Res. **47**: 161-181.*

Gschwendtner, A., Hoffmann-Weltin Y., Mikuz G. and Mairinger T., (1999) Quantitative assessment of bladder cancer by nuclear texture analysis using high resolution image cytometry. *Modern Pathology **12 (8)**: 806-813.*

Guasch, R. M., Guerri C. and O'Connor J. –E., (1995) Study of surface carbohydrates on isolated Golgi subfractions by fluorescent-lectin binding and flow cytometry. *Cytometry, **19 (2)**: 112-118.*

Harmala, P., Vuorela H., Rahko E. L. and Hiltunen R., (1992) Retention behaviour of closely related coumarins in thin-layer chromatographic preassays for high performance liquid chromatography according to the "PRISMA" model. *J. Chromatogr., **593**: 329-337.*

Harrison, D. J., Fluri, K., Sieler, K., Fan, Z., Effenhauser, C. S. and Manz, A., (1993) Micromachining a minaturised capillary electrophoresis-based chemical analysis system on a chip. *Science, **261**: 895-897*

Harrison, D. J., Manz, A., Fan, Z., Ludi, H. and Widmer, J. M., (1992) Capillary electrophoresis and sample injection systems integrated on a planar glass chip. *Anal. Chem.*, ***64**: 1926 – 2642*

Hawthorne, S.B., Krieger M.S. and Miller D.J., (1988) Analysis of flavour and fragrance compounds using supercritical fluid extraction coupled with gas chromatography. *Anal. Chem., **60**: 427-477.*

Helmholtz, H. Z., (1879) About electrical interfaces (translated title). *Annal. Phys. Chem., 7: 337-339.*

Heeren, F., Verpoorte E., Manz A. and Thormann W., (1996) Micellar electrokinetic chromatography: Separations and analysis of biological samples on a cyclic planar microstructure. *Anal. Chem., **68**: 2044-2048.*

Hermann, T., Wersch G., Uhlemann E. –M., Schmid R. and Burkovski A., (1998) Mapping and identification of corynebacterium glutamicum proteins by two dimensional gel electrophoresis and microsequencing. *Electrophoresis, **19 (18)**: 3217-3221.*

Hesterlee, S., (1999) Mitochondrial myopathy: an energy crisis in the cells. Quest, **6** (4) *(http://www.mdausa.org/publications/Quest/q64mito.html)*

Hiller, D. L. and Cole, R. O., (1995) Short column gradient elution HPLC for the rapid determination of 7-ethoxycoumarin metabolites in liver slice incubates. *Anal. Biochem., **227**: 251-254.*

Hirata, Y. and Novotny, M., (1979) Techniques of capillary liquid chromatography. *J. Chromatogr. **186**: 521-528.*

Hjerten, S., (1987) Carrier-free zone electrophoresis, displacement electrophoresis and isoelectric focusing in a high performance electrophoresis apparatus. *J. Chromatogr., **403**: 47 – 61.*

Hjerten, S., (1967) High performance electrophoresis. *Chomatogr. Rev., **9**: 122-127.*

Huang, C., (1969) Studies on phosphatidylcholine vesicles , formation and physical characteristics. *Biochemistry, **8**: 344-347.*

Hubin, N. and Noethe, L., (1993) Active optics, adaptive optics and laser guide stars. *Science **262**: 1390-1394.*

Huntingdon Life Sciences, (1996) ^{14}C-Coumarin. Dermal absorption in man. Project number RIF 30/943257. Report to RIFM.

Indahl, S.R. and Scheline, R.R., (1971) The metabolism of umbelliferone and herniarin in rats and by the rat intestinal microflora. *Xenobiotica, **1(1)**: 13-24.*

Ishii, J., (1978) A study of high performance liquid chromatography. I. Development of technique for miniaturisation of high performance liquid chromatography. *J. Chromatogr. **144**: 157-168.*

Issaq, H. J., Atamna, I. Z., Muschik, G. M. and Janini, G. M., (1991) The effect of electric field strength, buffer type, and concentration on separation parameters in capillary zone electrophoresis. *Chromatographia, **32**: 155-161.*

Jacobson, S. C., Hergenroder, R., Koutney, L. B. and Ramsey, J. M., (1994) Effects of injection schemes and column geometry on the performance of microchip electrophoretic devices. *Anal. Chem., **66**: 1107-1113.*

Jacobson, S. C., Hergenroder, R., Moore, A. W. and Ramsey, J. M., (1994a) Precolumn reactions with electrophoretic analysis integrated on a chip. *Anal. Chem., **66**: 4127-4132.*

Jacobson, S. C., Koutny, L. B., Hergenroder, R., Moore, A. W. and Ramsey, J. M., (1994b) Microchip capillary electrophoresis with a post column integrated reactor. *Anal. Chem., **66**: 3472-3476.*

Jirovetz, L., Buchbauer, G., Jäger, W., Woidich, A. and Nikiforov, A., (1992) Analysis of fragrance compounds in blood samples of mice by gas chromatography, mass spectrometry, GC/FTIR and GC/AES after inhalation of sandalwood oil. *Biomed. Chromatogr., **6**: 133-134.*

Jorgenson, J. W. and Lukacs, K. D., (1981) Zone electrophoresis in open tubular glass capillaries. *Anal. Chem., **53**: 1298-1302.*

Kauffman, F. C., (1994) Regulation of drug gonjugate production by futile cycling in intact cells. In "Conjugation-Deconjugation Reactions in Drug Metabolism and Toxicity", Kauffman F. C, (Ed.), Springer-Verlag, New York, Heidleberg, Berlin. *pp 245-255.*

Killard, A. J., Bogan, D. P. and O'Kennedy, R., (1996) The analysis of the glucuronidation of 7-hydroxycoumarin by high performance liquid chromatography. *J. Pharm. Biomed. Analysis, **14**: 1585-1519.*

Kim, E., Xia, Y. and Whitesides, G. M., (1995) Polymer microstructures formed by moulding in capillaries. *Nature, **376**: 581-584.*

Kitagawa, H. and Iwaki, R., (1963) Coumarin derivatives for medicinal purposes. XVII Pharmalogical studies on coumarin derivatives having biological activity. *J. Pharm. Soc. Japan, 83: 1124-1128.*

Knox, J. H., (1980) Theoretical aspects of liquid chromatography with packed and open small bore columns. *J. Chromatogr. Sci., **18**: 453-461.*

Knox, J. H., (1982) Introduction, In "High performance liquid chromatography". Edinburgh University Press, Knox, J. H., (Ed). *pp. 1-29.*

Kolin, A., (1954) Separation and concentration of proteins in a pH field combined with an electric field. *J. Chem. Phys., **22**: 1628-1269.*

Kolin, A., (1954) Erratum: Separation and concentration of proteins in a pH field combined with an electric field. Correction. *J. Chem. Phys., **22**: 2099.*

Koutny, L. B., Schmalzing, D., Taylor, T. A. and Fuchs, M., (1996) Microchip electrophoretic immunoassay for serum cortisol, *Anal. Chem, **68**: 18-22.*

Krumdieke, C. L., Dos Santos, J. E. and Ho, K., (1980) A new instrument for the rapid preparation of tissue slices. *Anal. Biochem., **104**: 118-123.*

Kumar, A., Abbott, N. A., Kim, E., Biebuyck, H. A. and Whitesides, G. M., (1995) Patterned self assembly monolayers and meso scale phenomena. *Acc. Chem. Res., **28**: 219-226.*

Kung, L. and Roberts, R. C., (1999) Mitochondrial pathology in human schizophrenic striatum: A postmortem ultrastructural study. *Synapse **31 (1)**: 67-75.*

Lake, B. G., (1999) Coumarin metabolism, Toxicity and Carcinogenicity: Relevance for Human Risk Assessment. *Fd. Clin. Toxicol., **37 (4)**: 423-453.*

Lamiable, D., Vistelle, R., Trenque, D., Fay, R., Millart, H. and Choisy H., (1993) Sensitive high preformance liquid chromatographic method for the determination of coumarin in plasma. *J. Chromatogr., **620**: 273-277.*

Lasic, D. D. and Needham, D., (1995) Stealth liposomes: A prototypical biomaterial. *Chem. Rev., **95**: 2601-2628.*

Lasic, D. D. and Papahadjopoulos, D., (1998) General Introduction, In: "Medical applications of liposomes", Lasic, D. D. and Papahadjopoulos, D., (Eds), Elsevier Publications, Amsterdam, The Netherlands. *pp. 1-14.*

Lauer, H. H. and M^{c}Manigill, D., (1986) Capillary zone electrophoresis of proteins in untreated fused silica tubing. *Anal. Chem., **58**: 166-170.*

Law, B., Malone, M. D. and Biddlecombe, R. A., (1996) Enzyme-linked immunosorbent assay (ELISA) development and optimisation, In: "Immunoassay: A practical guide", Law, B., (Ed) Taylor and Francis Ltd, London, England, *pp. 127-149.*

Lee, Y., Haung, T. –S., Yang, M. -L., Huang, L. –R., Chen, C. –H. and Lu, F. –J., (1999) Peroxisome proliferation, adipocyte determination and differentiation of C3H10T1/2 fibroblast cells induced by humic acid: Induction of PPAR in diverse cells. *J. Cell. Physio., **179 (2)**: 218-225.*

Loew, L. M., Tuff, R. A., Carington, W. and Fay, F. S., (1993) Imaging in five dimensions: time dependent potentials in individual mitochondria. *Biophys. J. **65**: 2396-2407.*

Lovell, D. P., van Irsel, M., Walters, D. G., Price, R. J. and Lake, B. G., (1999) Genetic variation in the metabolism of coumarin in the mouse liver. *Pharmacogenetics, **9 (2)**: 239-250.*

Luck, D. J. L., (1963) Genesis of mitochondria in *Neurospora crassa. Proc. Natl. Acad. Sci. USA, **49**: 233-240.*

Lusis, A. and Paigen, K., (1977) Mechanisms involved in the intracellular localisation of mouse glucuronidase. In "Isoenzymes: Current topics in biological and medical research, Vol. 2", Rattazzi, M. C., Scandialos, J. G., Whitt, G. S., (Eds), Liss, New York, USA. *pp. 63-106.*

Macko, V. and Stegemann, H., (1969) Mapping of potato proteins by combined electrofocusing and electrophoresis. Identification of varieties. *Hoppe-Seyler's Z. Physiol. Chem., **350**: 917-922.*

Macouillard-Poulletier de Gannes, F., Belaud-Rotureau, M. -A., Voisin, P., Leducq, N., Belloc, F., Canioni, P. and Diolez, P., (1998) Flow cytometric analysis of mitochondrial activity in situ: Application to acetylceramide-induced mitochondrial swelling and apoptosis. Cytometry, ***33 (3)**: 333-339.*

Madden, E. A. and Storrie, B., (1987) The preparative Isolation of Mitochondria from Chinese Hamster Ovary Cells. *Anal. Biochem., **163 (2)**: 350-357.*

Maftah, A., Ratinaud, M. H., Dumas, M., Bonte, F., Meybeck, A. and Julien, R., (1994) Human epidermal cells progressively loose their cardiolipins during ageing without change in mitochondrial transmembrane potential. *Mech. of Age. and Develop., **77 (2)**: 83-96.*

Mathews, C. K. and van Holde, K. E., (1990) Encoding and expression of genetic information in eukaryotes, In "Biochemistry", The Benjamin Cummings Publishing Company, Inc., CA, USA. *pp 996-1034.*

Matsubara, N. and Terabe, S., (1996) Miceller electrokinetic chromatography in the analysis of amino acids and proteins, In "Capillary electrophoresis in Analytical Biotechnology", Righetti, P. G. (Ed), CRC Press, New York, USA. *pp. 156-182.*

Meineke, I., Desel, H., Kahl, R., Kahl, G. F. and Gundert-Remy, U., (1998) Determination of 2-hydroxyphenyl acetic acid (2HPAA) in urine after oral and parenternal administration of coumarin by gas liquid chromatography with flame ionisation detection. *J. Pharm. Biomed. Analysis, **17 (3)**: 487-492.*

Mikkers, F. E. P., Everaerts, F. M. and Verheggen, T. P. E. M., (1979) High performance zone electrophoresis. *J. Chromatogr. **169**: 11-20.*

Moreau, W. M., (1988) Semiconductor lithography: Principals and Materials, Plenum Press, New York.

Nakajima, S. and Kawazu, K., (1980) Coumarin and euponin, two inhibitors for insect development from leaves of *Eupatorium japonicum. Agric. Biol. Chem. **44**: 2893-2899.*

Nashabeh, W. and El Rassi, Z., (1991) Capillary Zone Electrophoresis of proteins with hydrophilic fused silica capillaries. *J. Chromatogr., **559**: 367-383.*

O'Farrell, P. H., (1975) High resolution two-dimensional electrophoresis of proteins. *J. Biol. Chem., **250**: 4007-4021.*

Ohta, T., Watanabe, K., Moriya M., Shirasu, Y. and Kada, T., (1983) Antimutagenic effects of coumarin and umbelliferone on mutagenesis induced by 4-nitroquinoline 1-oxide or UV irradiation in *E. coli. Mutat. Res. **117**: 135-138.*

Orlov, Y. E., (1988) Determination of coumarin in sweet clover herbage by a polarographic method. *Khimiya Prirodnykh Soedinenii, 1: 131-132.*

Pasquali, C., Fialka, I. and Huber, L. A., (1999) subcelluar fractionation, electromigration analysis and mapping of organelles. *J. Chromatogr B, Biomed. Appl., 722: 89-102.*

Patton, W., (1999) Proteome analysis II. Protein subcellular redistribution: Linking physiology to genomics via the proteome and separation technologies involved. *J. Chomatogr. B, Biomed. Appl., 722: 203-223.*

Pearce, R., Greenway, D. and Parkinson, A., (1992) Species differences and interindividual variation in liver microsomal cytochrome P 450 2A enzymes: Effects on coumarin, dicoumarol, and testosterone oxidation. *Arch. Biochem. Biophys., 298: 211-225.*

Pelkonen, O., Raunio, H., Rautio, A. and Pasanen, M., (1997) The metabolism of coumarin, In "Coumarins: Biology, Applications and mode of action, O'Kennedy, R., Thornes, R. D, (Ed's), John Wiley and Sons Ltd., Chichester, England. *pp. 67-92*

Perrot, M., Saglicco, F., Mini, T., Monribot, C., Schneider, U., Schevchenko, A., Mann M., Jeno P. and Boucherie, T., (1999) Two dimensional gel protein database of Saccharomyces cerevisiae (update 1999). *Electrophoresis, 20 (11): 2280-2298. (http://www.ibgc.u-bordeaux2.fr/YPM)*

Polidori, M. C., Mecocci, P., Browne, S. E., Senin, U. and Beal, M. F., (1999) Oxidative damage to mitochondrial DNA in Huntington's disease parietal cortex. *Neuroscience Lett., 272: 53-56.*

Poole, S.K., Daly, S.L. and Poole, C.F., (1993) A thin layer chromatographic method for determining the authenticity of natural vanilla extracts. *J. Planar Chromatogr., 6(2): 129-137.*

Qin, D., Xia, Y., Rodgers, J. A., Jackman, R. J., Zhao, X. and Whitesides, G. M., (1998) Microfabrication, Microstructure and Microsystems, In "Microsystem Technology in Chemistry and Life Sciences", Manz, A. and Becker, H., (Eds), Springer-Verlag, New York, Berlin Heidelberg. *pp. 3-19.*

Radko, S. P. and Chrambach, A., (1999) Capillary Electrophoresis of subcellular-sized particles. *J. Chromatogr. B., Biomed. Appl., 722: 1-10.*

Raymond, D. E., Manz, A. and Widmer, H. M., (1994), Continuous sample pretreatment using a free flow electrophoresis device integrated on a silicon chip. *Anal. Chem., 66: 2858-2865.*

Reeves, J. P. and Dowben, R. M., (1970) Water permeability of phospholipid vesicles. *J. Membr. Biol., 3: 123-126.*

Reid, R. A. and Leech, R. M., (1980) Biochemistry and Structure of Cell Organelles, Blackie, Glasgow and London.

Reinke, L. A., Moyer, M.J. and Notley, K. A., (1986) Diminishes rates of glucuronidation and sulphation in perfused rat liver after chronic ethanol administration. *Biochem. Pharmacol., 35: 439-447.*

Rickard, E. C., Strohl, M. M. and Nielson, R. G., (1991) Correlation of electrophoretic mobilities from capillary electrophoresis with physiochemical properties of proteins and peptides. *Anal. Biochem., 197: 197-207.*

Rief, O. W., Lausch, R., Scheper, T. and Freitag, R., (1994), Fluorescein isothiocyanate labelled protein G as an affinity ligand in affinity/immunocapillary electrophoresis with fluorescent detection. *Anal. Chem., **66**: 4027-4033.*

Ritschel, W. A., Grummich, K. W., Kaul, S. and Hardt, T. J., (1981) Biopharmaceutical parameters of coumarin and 7-hydroxycoumarin. *Pharmaz Ind., **43**: 271-276.*

Roberts, M. A., Locascio-Brown, L., MacCrehan, P. and Durst, R. A., (1996) Liposome Behaviour in Capillary Electrophoresis. *Anal. Chem., **68**: 3434-3440.*

Rodriguez-Diaz, R., Zhu, M. and Wehr, T., (1997) Strategies to improve performance of capillary isoelectricfocusing. *J. Chromatogr. A, 772: 145-160.*

Roy Chowdery, J., Novikoff, P., Roy Chowdery, N. and Novikoff, A. B., (1985) Distribution of UDP-glucuronyltransferase in rat tissue. *Proc. Natl. Acad. Sci. (USA), **82**: 2990-2994.*

Runkel, M., Tegtmeier, M. and Legrum, W., (1996) Metabolic and analytical interactions of grapefruit juice and 1,2-benzopyrone in man. *Eur. J. Clin. Pharmacol. **50 (3)**: 225-230.*

Sabe, L., Andritsch, I., Mangoud, A., Awad, S., Khalifa, A. and Krishan, A., (1999) Flow cytometric analysis of estrogen receptor expression in isolated nuclei and cells from mammary cancer tissues. *Cytometry **36 (2)**: 131-139.*

Salamero, J., Sztul, E. S. and Howell, K., (1990) Exocytic transport vesicles generated *in vitro* from the *trans*-Golgi network carry secretory and plasma membrane proteins. *Proc. Natl. Acad. Sci. (USA), **87**: 7717-7721.*

Saoine, T. O., (1964) Naturally occurring coumarins and related physiological activities. *J. Pharm. Sci., **53**: 231-264.*

Sazuka, T., Yamaguchi, M. and Ohara, O., (1999) Cyano2Dbase updated: Linkage of 234 protein spots to corresponding genes through N-terminal microsequencing. *Electrophoresis, **20 (11)**: 2160-2171. (http://www.kazusa.or.jp/tech/sazuka/cyano/proteome.html)*

Schena, M., (1996) Genome analysis with gene expression microarrays. *Bioassays, **18**: 427-431.*

Schmalzing, D. and Nashabeh, W., (1997) Capillary Electrophoresis based immunoassays: A critical review. *Electrophoresis, **18**: 2184-2193.*

Schmalzing, D., Nashabeh, W., Fuchs, M., (1995) Solution phase immunoassay for determination of cortisol in serum involving capillary electrophoresis. *Clin. Chem., **41(9)**:1403-1406.*

Schwer, C. and Kenndler, E., (1991) Electrophoresis in fused silica capillaries: the influence of organic solvents on the electroosmotic velocity and the ξ potential. *Anal. Chem., **63**: 1801-1807.*

Sharifi, S., Christoph Michaelis, H., Lotterer, E. and Bircher, J. (1993) Determination of coumarin, 7-hydroxycoumarin, 7-hydroxycoumarin glucuronide and 3-hydroxycoumarin by HPLC. *J. Liq. Chromatogr., **16 (6)**: 1263-1278.*

Shimura, K. and Karger, B. L., (1994) Affinity probe electrophoresis: analysis of recombinant human growth hormone with a fluorescent labelled antibody fragment. *Anal. Chem., **66**: 9-15.*

Skoog, D. A., Holler, F. J. and Nieman, T. A., (1998) Separation techniques, In "Principles of instrumental analysis", Harcourt Brace College Publishing, Philadelphia, Sydney, Tokyo. *pp. 673-795.*

Smeraldi, C., Berardi E. and Porro D., (1994) Monitoring of peroxisome induction and degradation by flow cytometric analysis of Hansenula polymorpha cells grown in methanol and glucose media: cell volume, refractive index and FITC retention. *Microbiology, **140 (11)**: 3161-3166.*

Snyder, L. R., Glajch, J. L. and Kirkland, J. J., (1988) Difficult separations: The use of other separation variables and procedures, In "Practical HPLC method development", John Wiley and Sons, New York, USA, *pp 123-152.*

Sond, M. I., Iwata, K., Yamada, M., Yokoyama, K., Takeuchi, T., Tamiya, E. and Karube, I., (1994) Multisample analysis using an array of microreactors for an alternating current field enhanced latex immunoassay. *Anal. Chem., **66**: 778-781.*

Stegemann, H., (1970) Protein mapping in polyacrylamide and its application to genetic analysis in plants. *Agnew. Chem. (Internat. Ed.), **9**: 643.*

Steinegger, E. and Hansel, R., (1992) Pharmakognosie, Julius Springer, Berlin. *pp 376-382*

Swank, R. T., Novak, E. K. and Zhen, L., (1994) Genetic regulation of the subcellular localisation and expression of glucuronidase. In "Conjugation-Deconjugation Reactions in Drug Metabolism and Toxicity", Kauffman F. C, (Ed.), Springer-Verlag, New York, H. *pp 131-160.*

Terebe, S., Otsuka, K. and Ando, T., (1985) Electrokinetic chromatography with micellar solution and open tubular capillary. *Anal. Chem., 57: 834 – 841.*

Terry, S. C., Jerman, J. H. and Angel, J. B., (1979) A gas chromatographic air analyser fabricated on a silicon wafer. *IEEE Trans Electron Devices, **EC-26**: 1880.*

Thomas, C. A., Garner, D. L., DeJarnette, J. M. and Marshall, C. E., (1998) Effect of cryopreservation on bovine sperm organelle function and viability as determined by flow cytometry. *Biology of Reproduction, **58 (3)**: 786-793.*

Thompson, R.D. and Hoffmann, T.J., (1988) Determination of coumarin as an adulterant in vanilla flavouring products by high-performance liquid chromatography. *J. Chromatogr., **438:** 369-382.*

Tiselius, A., (1937) A new apparatus for electrophoretic analysis of colloidal mixtures. *Trans. Faraday Soc., **33**: 524-528.*

Tsukagoshi, K., Okumura, Y. and Nakajima, R., (1998) Migration behaviour of dyestuff-containing liposomes in capillary electrophoresis with chemiluminescence detection. *J. Chromatogr. A, **813 (2)**: 402-407.*

Tyler, D., (1992) A century of mitochondrial research, In "The Mitochondrion in Health and Disease", VCH Publishers, New York, N.Y., USA. *pp 1-38.*

Verheggen, T. P E. M., Beckers, J. L. and Everaerts, F. M., (1988) Simple sampling device for isotachophoresis and capillary zone electrophoresis. *J. Chromatogr. **452**: 615-622.*

Vesterburg, O., (1969) Synthesis and isoelectric fractionation of carrier ampholytes. *Acta Chem,. Scand., **23:** 2653-2666.*

Virtanen, R., (1974) Zone electrophoresis in a narrow bore tube employing potentiometric detection. *Acta. Polytechnica Scand., **123:** 1-7.*

Walmsely, A. R., Batten, M. R., Lad, U. and Bulleid N. J., (1999) Intracellular retention of procollagen within the endoplasmic reticulum is mediated by prolyl 4-hydroxylase. *J. Biol. Chem., **274 (21):** 14884-14892.*

Walsh, J. S., Patenella, J. E., Halm, K. A. and Facchine, K. L., (1995) An improved HPLC assay for the assessment of liver slice metabolic viability using 7-ethoxycoumarin. *Drug Met. and Disp., **23(8):** 869-874.*

Walstrom, A., Persson, K. and Rane, A., (1989) Metabolic interaction between morphine and naloxone in human liver – a common pathway of glucuronidation? *Drug Met. and Disp., **17:** 218-220.*

Weinberg, D.S., Manier, M. L., Richardson, M. D. and Hailbach, F. G., (1993) Identification and quantification of coumarin, phthalide, and sesquiterone compliance markers in an umbelliferous vegetable beverage. *J. Agric. Food Chem., **41:** 48-51.*

Weinmann, I., (1997) History of the development and applications of coumarin and coumarin related compounds, In: "Coumarins: Biology, Applications and mode of action", O'Kennedy, R., Thornes, R. D, (Ed's), John Wiley and Sons Ltd. Chichester, England. *pp 1 – 22.*

Weinshilboum, R. and Otterness, D., (1994) Sulphotransferase enzymes, In "Conjugation-Deconjugation Reactions in Drug Metabolism and Toxicity", Kauffman F. C, (Ed.), Springer-Verlag, New York, Heidleberg, Berlin. *pp 45-78.*

Wieland, T. and Fisher, E., (1948) Electrophoresis onto filter paper. *Naturwissenschaften, **35:** 29-30.*

Wilkins, M. R., Gasteiger E., Sanchez J. –C., Bairoch A. and Hochstrasser D. F., (1998) Two dimensional gel electrophoresis for proteome projects: The effects of protein hydrophobicity and copy number. *Electrophoresis, **19 (8-9)**: 1501-1505.*

Willard, H. H., Merritt, L. L., Dean, J. A. and Settle, F. A., (1988) High performance liquid chromatography: theory and instrumentation, In "Instrumental methods of analysis". Seventh edition. Wadsworth Publishing Company, Belmont, California, USA. *pp 580-613.*

Woodle, M. C. and Papahadjopoulos, D., (1989) Liposome preparation and size characterisation. *Meth. Enzymol., **171**: 193-217.*

Wu, S. and Dovichi, N. J., (1989) High sensitivity flourescence detector for fluorescein isothiocyanate derivitives of amino acids separated by capillary zone electrophoresis. *J. Chromatogr., **480:** 141-155.*

Xia, Y., Kim, E., Zhao, X-M., Rodgers, J. A., Prentiss, M. and Whitesides, G. M., (1996) Complex optical surfaces formed by replica moulding against elastomeric masters. *Science, **273**: 347-349.*

Yamada, H., Watanabe, K., Saito, T., Hayashi, H., Niitani, Y., Kikuchi, T., Ito, A., Fujikawa, K. and Lohmander, L. S., (1999) Esculetin (dihydroxycoumarin) inhibits the production of matrix metalloproteinases in cartilage explants, and oral administration of its prodrug, CPA-926, suppresses cartilage destruction in rabbit experimental osteoarthritis. *J. Rheumatol., **26 (3)**: 654-662.*

Yamazaki, H., Tanaka, M. and Shimada, T., (1999) Highly sensitive high-performance liquid chromatographic assay for coumarin 7-hydroxylation and 7-ethoxycoumarin *O*-deethylation by human liver cytochrome P450 enzymes. *J. Chromatogr. B, Biomed. Appl., **721 (1)**: 13-19.*

Zimmerman, C. L., Ratna, S., Leboeuf, E. and Pang, K. S., (1991) High performance liquid chromatographic method for the direct determination of 4-methylumbelliferone and its glucuronide and sulphate conjugates. Application to studies in the single pass *in situ* perfused intestine-liver preparation. *J. Chromatogr. B, Biomed Appl.,* ***563****: 83-94.*

10 APPENDIX

Single event analysis using IgorPro™, Apple Macintosh version.

Procedure: PickPeaks

This procedure was used to analyse all data files collected for analysis of liposomes and mitochondria on the CE instrument. The programme allows for the representation of the current and signal plots from the instrument and manipulates these waves to correct for background. The procedure will then count the number of peaks (events) above a set threshold for the sample and produce histograms showing both the distribution of fluorescence intensity and mobility of peaks in the sample. The threshold represents the fluorescence value that is used to guarantee that a peak is a real event rather than noise. Five times the standard deviation of the background guarantees that only 1% of the peaks are false positives. This value is larger than the limit of detection (three) and smaller than the conventional limit of quantitation (ten). Further calculations (membrane charge distribution, radius) were made using the results from the above programme input into the equations derived, and calculated in IgorPro.

Preparation prior to using PickPeaks.

1. Wave scaling change must be done prior to the subsequent steps.
2. Based on the background noise (Std. Dev.) estimate the threshold for peak detection. The suggested value is 5x(Std. Dev.). This value is called THR1 in PickPeaks.
3. Duplicate the wave for analysis (i.e. run0x) TWICE. Names to use are run0x**C** and **Migtime**.
4. Subtract the background by using the command line. (i.e. type run0xC=run0x- X).
5. Equate Migtime=x by using the command line.

Use of PickPeaks.

1. In Igor, **OPEN** procedure **PickPeaks**, hide the procedure do not kill.
2. Type in the command line PickPeaks(run0xC,Migtime,THR1). Use the actual names and values for THR1).
3. Make new table and look at Peakwave and Timewave. They contain the information on the migration time and the intensity for each peak. The number of points+1 represents the number of peaks.

Representation of results.

1. Duplicate Peakwave as PeakHisto, MobiHisto, Mobi, Size, SizeHisto, Density, and DensityHisto. Waves that do not end in Histo will contain calculations. Waves whose names end in Histo will represent histograms.
2. For Calculations, type equations and values in command line after simplifying equations. For example: Mobi=0.2/Timewave
3. For Histogram representation use the option with the same name under **Analysis.** Select the destination wave to be the one that has the "Histo" ending in its name. The source wave is the equivalent name without "histo" ending. Number of bins is 20. Bin width estimate to include all points or best representation of distribution.
4. Make graphs and choose bars for representation.

PickPeak Function. Igor Pro.

```
| Version 1.01, 990414


#pragma rtGlobals=1



| PickPeaks(fluorescence, Migtime,thr1)
|     Selects single-event peaks in electropherogram
|     Creates X and Y waves that represent single events.
|     Creates waves Peakwave and Timewave for events above threshold
(thr1).

Function PickPeaks(fluorescence, Migtime, thr1)
      Wave fluorescence
      Wave Migtime
      Variable thr1

      variable/D numPoints
      variable/D p = 0
      variable/D t=0
      variable/D w = 1
      variable/D val, val_1

      numPoints = numpnts(fluorescence)

      Duplicate/O fluorescence Peakwave
      Duplicate/O Migtime Timewave



      do
                  | checking every point for peaks about thr1


            if (fluorescence[p]< thr1)
                  DeletePoints t, 1, Peakwave, Timewave
```

```
        p += 1
    Else

                do

                if (fluorescence[p]<fluorescence[p+1])
                                                |Is there an
                                                 event?
                    DeletePoints t, 1, Peakwave, Timewave

                else
                    Peakwave[t]=fluorescence[p] |assign maximum
                    Timewave[t]=Migtime[p]      |assign time for
                                                 maximum
                    t+=1
                                                |increase peak
                                                 counter
                endif
                    p += 1
                while (fluorescence[p-1]<fluorescence[p])

                do
                if (fluorescence[p]>fluorescence[p+1])
                |is this position still part of the event?
                    DeletePoints t, 1, Peakwave, Timewave
                    p += 1
                    endif

                while (fluorescence[p]>fluorescence[p+1])


    endif


while (p<numPoints+1)

End
```

Formulae

Calculation of buffer concentrations from stock solutions:

$$V_1C_1 = V_2C_2$$

Coefficient of variation calculations:

$$C.V = \frac{S.D.}{mean} \times \frac{100}{1}$$

Rate of reaction:

$$Rate\ of\ reaction = slope \div [protein] \div molecular\ weight$$

Where: *slope* = slope of the linear portion of the graph

[*protein*] = protein concentration of the organ (Table 3.1)

Molecular weight = molecular weight of 7-HCG (338.14)

Electrophoretic mobility (μ) of a charged molecular species:

$$\mu = q/6\pi\eta r$$

Where:

q = the charge on the particle

η = the viscosity of the buffer

r = the stokes radius of the particle

Percentage precision:

Percentage accuracy:

$$\frac{\textit{calculated result} \times 100}{\textit{nominal result}}$$

Limit of detection:

$$LOD = \frac{3\delta}{h} \times amount\ (moles)$$

δ = *standard deviation of baseline (100 times width of peak)*

h = h_{inj} - h_{sip}

h_{inj} = *peak height for injection, time"t"*

h_{sip} = *peak height for siphoning, time "t"*

amount calculated from injection volume(equations 2 and 3)

Sensitivity:

$$\frac{S_2 - S_1}{C_2 - C_1}$$

S_2 = signal from second injection
S_1 = signal from first injection
C_2 = concentration of second injection
C_1 = concentration of first injection

Electrophoretic mobitity:

$$\mu = \frac{L^2}{V \times t_m} \quad (1)$$

Where:

μ = *mobility*
L = *length to detector*
V = *separation voltage*
t_m = *migration time*

Number of moles injected into capillary:

$$moles = V_{inj} \times c \quad (2)$$

where

$$V_{inj} = V_{cap} \frac{t_{inj}}{t_m} \times \frac{V_{inj}}{V_{CE}} \quad (3)$$

V_{inj} = *injection volume*
c = *concentration (molarity)*
V_{cap} = *volume of capillary*
t_{inj} = *injection time*
v_{inj} = *injection voltage*
v_{CE} = *separation voltage*

Radius of liposomes:

$$r = \sqrt[3]{\frac{3}{4}\frac{k_1(signal)}{1000\pi}} \qquad (5)$$

Where:

r = *radius of liposome*

$k_1 = \frac{1}{t \times c}$

Signal = *signal from detector*

π = *3.14*

c = *concentration (moles/l) of fluorecsein used to label liposomes.*

t = *transfer function of detector*

Liposome membrane charge:

$$\mu = \frac{q}{(6 \times \pi \times vis\cos ity \times r)} \qquad (6)$$

Where:

q = *charge (coloumbs)*

r = *radius (of liposome)*

$$\rho = \frac{8.35 \times 10^{-3}}{(t_m)\sqrt[3]{signal}} \qquad (7)$$

Where:

ρ = *density*

t_m = *migration time*

signal = *signal from detector*